CRANFIELD UNIVERSITY

Douglas Clive Wagstaff

The Stability of Novel Energetic Materials and Associated Propellants

COLLEGE OF DEFENCE TECHNOLOGY

DEPARTMENT OF ENVIRONMENTAL AND ORDNANCE SYSTEMS

PHD THESIS

CRANFIELD UNIVERSITY

COLLEGE OF DEFENCE TECHNOLOGY

DEPARTMENT OF ENVIRONMENTAL AND ORDNANCE SYSTEMS

PHD THESIS

2004 - 2005

Doug Wagstaff

The Stability of Novel Energetic Materials and Associated Propellants

Supervisor : Dr J.M.Bellerby

June 2005

Abstract

A study into the degradation of crystalline Hydrazinium Nitroformate (HNF) in isolation has been carried out alongside studies into HNF / polyNIMMO propellant degradation. The contribution of gas / solid autocatalysis in the degradation of the crystalline phase has been determined to be very low. Studies via GC-MS analysis do suggest that the presence (and eventual release) of the crystal impurity, isopropyl alcohol, is a more significant contributor to the eventual autocatalytic breakdown of the crystal matrix. Investigations into the chemical compatibility of HNF with nitrosated and nitrated derivatives of 2NDPA and pNMA indicated that the reaction of HNF is most rapid with N-NO-2NDPA. This reaction between HNF and N-NO-2NDPA is proposed to be the principal route to rapid propellant degradation in 2NDPA stabilised propellant systems.

Analysis of a range of polyNIMMO / HNF propellants has allowed development of a hypothesis for this family of propellant compositions over a range of temperatures. The data has indicated that the degradation of polyNIMMO / HNF propellants is a complex process involving a number of interrelated and interdependent reactions. It appears that a significantly different reaction scheme dominates at 80°C compared to either 60°C or 40°C.

The incorporation of a 1% anhydrous sodium sulphite + 1% pNMA mixed stabiliser system has shown promise for use in propellant formulations up to temperature of 80°C. Some level of success in stabilisation has also been achieved using very high levels of pNMA within the propellant formulation.

Acknowledgements

I would like to acknowledge the contribution that a number of people have made to the completion of this thesis. Without their help I am sure that the study would have not have progressed as far as it has.

At ROXEL (UK Rocket Motors)

My thanks go out to John Ayris and Martin Sloan, who have alternated the role of being my boss over the past 7 years but have never shown the urge to terminate the stability project (even when things were not going so well and I consistently failed to spend my research budget!).

Thanks also go to Mike Keeton (now retired), Celina Parker and their staff in the main laboratories at ROXEL who have all expressed a great degree of patience / understanding whilst waiting for me to finish this program of work. A special mention goes out to Aftab Ahmad, Jennie Keal and Ann-Marie Say who carried out much of the DSC analysis to assess potential gas / solid reactions.

At RMCS

Many thanks to John Bellerby for his support and advice during the conception and eventual development of this project. Also to Anjum Agha and Phil Gill for technical support, and Marjorie, Maggie and Jenny for advice and training on the laboratory equipment. Finally, my thanks go to Dean Sayle who showed that computational chemistry is so much more than just the art of producing pretty pictures.

List of Contents

List of Tables

List of Figures

(ix)

(xiv)

Glossary

2NDPA	2-nitrodiphenylamine
ADN	Ammonium Dinitramine
ANF	Ammonium Nitroformate
AP	Ammonium Perchlorate
CL20	Hexanitrohexaazaisowurtzitane
DBTDL	Dibutyl-tin-dilaurate
HCl	Hydrogen Chloride
HNF	Hydrazinium Nitroformate
HNOx	Acids associated with oxides of nitrogen
HTPB	Hydroxy terminated polybutadiene
HZ	Hydrazinium Ion
IPA	Isopropyl Alcohol (Propan-2-ol)
Isp	Specific Impulse
MeCN	Acetonitrile
NF	Nitroform
NOx	Oxides of Nitrogen
NO-2NDPA	N-Nitroso-2-Nitrodiphenylamine
NO-pNMA	N-Nitroso-4-nitro-methylaniline
ONO2	Nitrate Ester Group
pNMA	Para-Nitromethylaniline
RMM	Relative Molecular Mass
RT	Retention Time
THF	Tetrahydrofuran

1 Introduction

This thesis deals with assessment and investigation of the stability of a number of potential future propellant ingredients with respect to their possible incorporation into tactical rocket motors. In general terms, propellant stability relates to the changes which occur in either single ingredient or propellant properties over time under different environmental conditions. These changes can occur to affect physical properties (e.g. mechanical) or chemical properties (e.g. loss of oxidiser) of the propellant formulation under changing storage conditions of temperature, humidity or mechanical stress. For the purpose of this thesis, the term "propellant stability" will be limited to the chemical changes which may occur in a propellant formulation within its anticipated service life (equivalent to 15 years ambient storage).

Previous studies [1] [2] on propellants containing some of the novel ingredients to be investigated have suggested that the stability of the proposed propellant formulations is such that it would give significantly less than the required service life (15 years). The results of this study have confirmed this position. However, the longevity of the propellants investigated has been increased as a result of work undertaken during this study. Even with these improvements, the propellant formulations still do not fulfil in-service requirements for tactical systems. However, greater understanding of the propellant degradation mechanisms and methods of control have been achieved which may act as the base for any future studies.

Chapter 1 gives an overview of the present state of scientific understanding of the novel energetic materials hydrazinium nitroformate (HNF) and poly (3-nitratomethyl-3-metyloxetane) (polyNIMMO) with specific emphasis on their ageing characteristics. Chapter 2 details practical investigations into HNF degradation chemistry especially an investigation of possible presence of gas / solid autocatalysis. The chapter also details studies of chemical incompatibility of HNF with nitrated derivatives of the common rocket propellant stabilisers 2-Nitrodiphenylamine (2NDPA) and para-nitro-methyl aniline (pNMA). Chapter 3 builds on the conclusions from Chapters 1 and 2 and applies it to the ageing characteristics of a series of polyNIMMO based, HNF loaded propellants. An overall correlation of analytical data from propellant ageing studies and recommendations for further study is given in Chapter 4.

An improved understanding of the stability of next generation propellant was the academic goal of this thesis with the commercial goal being the production of a new form of rocket propellant which fulfils tactical requirements. The first part of this objective has been fulfilled but the development of a fully compliant, tactical system has not been possible during these studies. However, the oxidiser HNF does show promise for use within commercial (civilian) propulsion or ground based strategic missile systems.

1.1 Next Generation Propellant Ingredients: Research Drivers

Philbin [1] suggests that the performance limits for double base (nitrocellulose / nitroglycerine based) propellant systems have almost been reached and that composite propellant systems (typically ammonium perchlorate / rubber based) suffer from smoke and signature problems. This view is shared by the majority of the rocketry community [3] and has resulted in the major drivers for development of next generation propellants into tactical and strategic missile systems to be :-

1)   substitution of propellant components that contribute low levels of energy
        and / or adversely affect propellant combustion characteristics with higher
        energy alternatives,

2)   reduction of the environmental impact of post firing residues and exhaust
        gases both in short term (i.e. immediate toxicity) and long term (e.g. effect on
        ecological systems),

3)   production of propellant formulations which increase the stealth of any missile
        system to which they are attached by reduction of smoke or plume signature, and

4)   reduction in motor vulnerability to in-service threat (e.g. bullet impact or
        unplanned fast or slow heating).

Investigation into the novel materials chosen for this study fall into all of these categories and so incorporation is hoped to lead to wide ranging improvements in any propellant produced.

The term "energetically inert" is sometimes applied to the low energy materials in category (1). This relates to the inability of their reaction during combustion to liberate gaseous products or energy at a sufficiently rapid enough rate to contribute in a positive way to the overall propellant burn. Obviously, the majority of materials have the ability to contribute an energy change into a burning reaction (either positive or negative) but the rates / quantities of energy release and gassification during the burning reaction are the critical factors within propellant technology. The value of the changes outlined in item (1) to rocketry is that by replacement of inert materials with energetic materials, a future propellant with an increased "energy density" can be prepared. The term energy density means that, in a specified volume, the explosive formulation has more chemical energy within its bond structure available to the burning reaction than within conventional propellants. Generally, pursuit of high energy density propellants requires the use of chemicals with high physical density and high heats of formation, formed solely of hydrogen, carbon, oxygen and nitrogen atoms. The use of energetic binders to replace inert ones also allows a reduction in solids loading without the loss of performance but with potential improvements in motor vulnerability [4]

The main target of item (2) has been the removal of oxidisers containing chlorine and those ballistic modifiers and metal alloys that contain heavy metals such as cadmium or lead and heavy metal salts. The most common chlorine containing oxidiser is ammonium perchlorate (AP) which has been used for many years [5]. On combustion, AP produces hydrogen chloride (HCl) gas. HCl is thought to be a contributor to ozone depletion and the greenhouse effect within the atmosphere of the Earth [3]. When it is considered that each US Space Shuttle launch ejects in the region of 7 - 8 tonnes of HCl into the atmosphere, any reduction was seen as being beneficial. However, this level of atmospheric pollution is minor compared to the production of greenhouse gases by industry or natural processes (eg volcanoes). [6] [7] [8] As a consequence, although a major driver in the 1990s, the issue of removing HCl for environmental reasons is of only minor importance today. More importantly than helping to improve the environment, from a tactical missile perspective, the minimisation of HCl formation leads to a reduction in secondary smoke formation (caused by nucleation of HCl with aerial moisture) formed from any rocket motor efflux [9]. This reduction potentially improves the stealth and ease of guidance of any missile system incorporating the novel propellant formulation. Some motor designs have been produced which "neutralise" HCl production by the incorporation of either magnesium or sodium ions within the propellant formulation but these have been found to be unsatisfactory. [6] [8] On ignition

the magnesium or sodium ions convert the HCl from AP combustion into magnesium or sodium chloride, both of which are less polluting than HCl. However, the systems suffer from losses in performance and the production of secondary smoke. These are due to the magnesium or sodium ion species failing to contribute energy or gaseous products to the combustion process but producing solid products on cooling away from the propellant plume. These neutralising formulations show that it is more desirable to initially remove the HCl-producing species from the formulation rather than try to mitigate against its effects after combustion.

1.2 Materials For Investigation

1.2.1 HNF : Hydrazinium Nitroformate

HNF (alternatively called hydrazinium nitroformate, hydrazine nitroform, amino ammonium nitroformate and hydrazine trinitromethanide [10]) is an oxidiser with the potential for formation of clean burning propellants (i.e. no chlorine atoms are present in the structure). Figure 1 shows the chemical structure of the material.
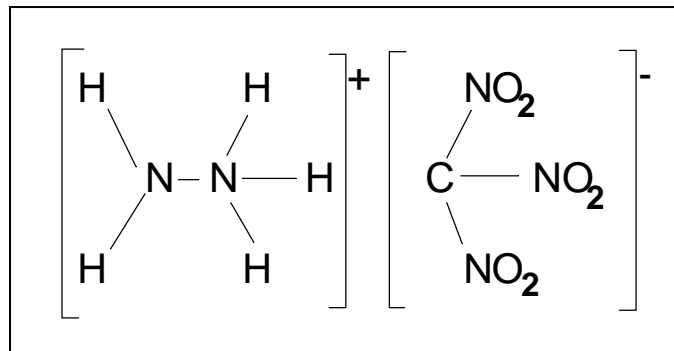
Figure 1 : Structure of HNF

Theoretical calculations of HNF based propellants show that they are superior to alternatives based on materials such as ammonium dinitramine (ADN) or hexanitrohexazaisowurtzitane (CL20) and far superior to traditional ammonium perchlorate (AP) / hydroxy terminated polybutadiene (HTPB) formulations. Figure 2 shows theoretical performance values (based on specific impulse, Isp, against solids loading) for HNF propellants compared to other potential propellant systems. The higher the value of Isp, the more desirable the propellant. From the figure, it can be seen that HNF is the most desirable for next generation propellant research based on specific impulse considerations.
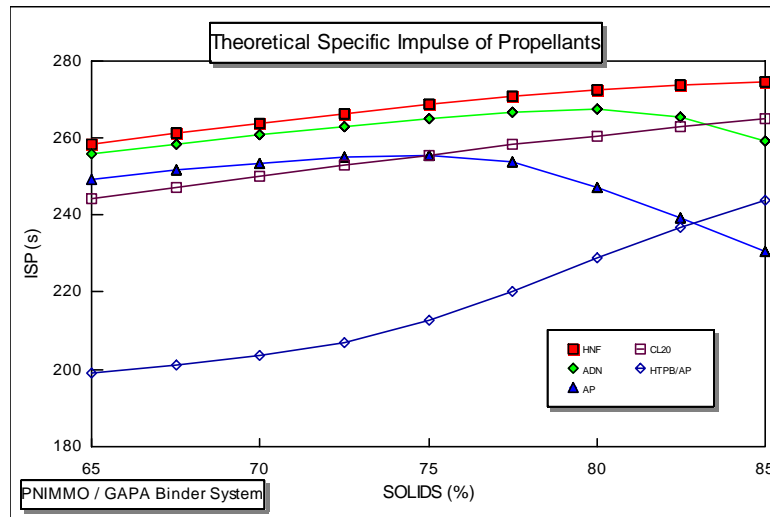
Figure 2 : Theoretical Performance Graphs For Next Generation Materials [11]

However, burn rate characteristics of solid HNF propellants have been shown to be undesirable with high pressure exponent values [12] and also poor chemical stability [1] [2] [13] [14] [15] being reported. These problems will need to be overcome if widespread use of the material is to be undertaken. More recently, studies into the use of HNF in liquid monopropellant systems have shown further promise for use of the material [16] [17] [18] [19] [20] [21] and this may be a more viable method for incorporation of HNF in future systems.

HNF is a golden yellow, crystalline solid with a single polymorph being evident. The crystals generally have large length to diameter (L/D) ratios after recrystallisation and therefore a needle-like appearance. The material was initially synthesised in the 1950s [10] from the direct reaction of hydrazine and nitroform but poor stability was achieved for the product formed, possibly due to the presence of impurities. This needle-like structure is not well suited to solids packing within propellant formulations [22] and so morphological improvements are required. More recently, [15] [23] [24] [25] [26] [27] [28] work undertaken in the Netherlands has lead to significant improvements in both synthesis and crystallisation techniques and some propellant development work has been carried out. These in turn have led to allied improvements in chemical stability. A prilling method for the material has also been patented [29] that may also be expected to further reduce impurities. Other centres of study are Japan [30][31] , India [32] [33] [34] [35] , USA [29] [36] [37] [38] [39] and China [40] .

Various patents [29] [31] [41] [42] [45] [46] have been issued relating to the production and refinement of HNF. Veltmans et al [43] and Schoyer [44] give details of the character of each of the early grades of HNF commercially available and highlight many of the difficulties associated with the development of the material. More recently, Veltmans et al [28] have proposed a sonocrystallisation method based on the application of ultrasound to the HNF liquor during cooling. The crystals formed by this sonocrystallisation method are proposed to have an improved crystal morphology to those of the earlier grades. Veltmans et al [28] have suggested that a reduction in particle size of HNF leads to a lowering of DSC onset of decomposition and also an increase in the gas volume evolved during vacuum thermal stability (VTS) testing suggesting reduced stability. However, the sonocrystallised material shows unexpectedly good thermal stability for the particle size, which suggests that the effect of reduction in particle size might not be driven solely by surface area effects. In a separate paper, Veltmans et al [47] further discuss the sonocrystallisation method and suggests that frequencies which result in less nucleation based on crystal cavitation during formation lead to the most stable crystals. This may have resulted in a reduction in impurities within the crystals which would be expected to aid overall stability.

Some difficulties with transport due to high sensitiveness to friction were initially encountered which limited the level of world-wide research applied to the Netherlands produced product. Methods of phlegmatisation [2] failed to provide a commercially viable product as there were problems with achieving dephlegmatisation when the product arrived at the customer. However, a transport hazard classification (1.1D) has been awarded [48] for the pure material which will increase the opportunities for research in the future. Other direct methods of desensitisation prior to transportation (eg as detailed by Cesaroni et al [49]) have also been described and show promise.

Overcoming the various difficulties associated with HNF is one of the greatest challenges within propellant development but the material offers the greatest possible benefits if these challenges can be overcome.

1.2.2 PolyNIMMO

PolyNIMMO is an energetic nitrated oxetane polymer with the formal chemical name poly(3-nitratomethyl-3-methyloxetane) [50]. Its structure is shown in Figure 3 where X and Y are either continuation of the polymeric chain or terminating groups (principally either di- or tri-hydroxy groups)
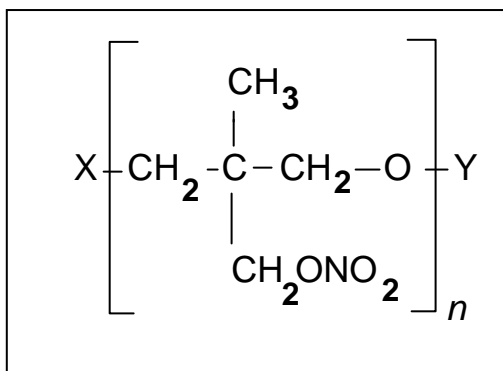
Figure 3 : Structure of polyNIMMO

Bunyan et al [51] have shown that the prepolymer comprises of both linear and cyclic forms. Within the cyclic form, the polymerisation factor, n, can reach a value of up to 20 before X and Y react together to terminate polymerisation.

A wide range of oxetane based explosives have been developed and investigated [52] [53] [54] [55] [56] but polyNIMMO has been identified as one which has promising properties for use as a propellant binder when crosslinked with isocyanate cure systems. Pilot scale manufacture started within the UK in the early 1990s [57] and continues to this day. As a consequence, much work has been undertaken within the UK to assess the viability of this material [58] [59] [60] but the material has also been produced at Thiokol and Aerojet within the USA [61].

The nitrate ester linkage (-ONO_2) within the polymer side chain imparts energy to the polymer but is also a likely source of chemical degradation [62]. The uncured material is a high viscosity liquid with a yellow, transparent colour and slight odour [60] [63]. In propellant technology, the material is planned for use as a polymeric support for energetic solid fillers. This polymeric

support could act as a replacement for the non-energetic polymer hydroxy terminated poly butadiene (HTPB) which is used extensively in composite propellant systems throughout the world [64]. The polyNIMMO material is also anticipated to reduce propellant vulnerability against accidental but violent stimulation [57] [65] [66] [67].

The benefits of using polyNIMMO, in addition to its improved energy density compared to HTPB, is that energetic plasticisers such as glycidyl azide polymer (azide derivative) (GAP A) or butane triol trinitrate (BTTN) are fully miscible with the polymer [68]. This plasticiser incorporation allows further increases in energy density by use of these plasticisers whilst improving low temperature mechanical properties. HTPB has shown limited miscibility with energetic plasticisers and this restricts the maximum specific impulse achievable for a plasticised HTPB binder. [68]

The main disadvantage of utilising polyNIMMO is that the mechanical properties of the cured polymer are significantly inferior to HTPB over a wide temperature range (even when plasticised). For example, unplasticised di or tri functional polyNIMMO polymers crosslinked with trifunctional isocyanates form hard, transparent, yellow rubbers with a glass transition point (Tg) of approximately - 2 to -30°C dependent on polymer grade and cure system [57] [62] [65]. Use of plasticisers may lower this Tg value to between -45 and -50°C but the plasticised polymers formed are weak at elevated temperatures [68]. Compare this against plasticised HTPB with a glass transition of ~ -60°C and acceptable propellant properties over a wide operating temperature range and polyNIMMO can be seen to still have considerable improvements to be made. PolyNIMMO exhibits faster cure than HTPB at equivalent catalyst levels which may, in part, also contribute to its undesirable mechanical properties. [57] [62] These high glass transition point values limit polyNIMMO to use in land and sea launched systems (which require Tg value of ~ -35°C) and excludes its use in air launched systems (which require Tg values of ~ -60°C). [67] In order to extend the platforms upon which the propellants could potentially be deployed, some work has been carried out to assess prepolymer copolymerisation between polyNIMMO and HTPB [69] but work is still progressing on this method of improvement of polyNIMMO mechanical properties. A second disadvantage of polyNIMMO compared to HTPB is that the introduction of the bulky nitrated sidechains increases polymer viscosity. This increased viscosity presents difficulties in wetting any solids within a propellant formulation which in turn

results in added deterioration of mechanical properties [67]. Further optimisation on the functionality of polyNIMMO and its processing will be required to improve these poor mechanical properties.

Another consideration with the future incorporation of polyNIMMO into propellant technology is the cost of the material. HTPB is widely used in different industries and as a result is significantly cheaper than polyNIMMO. If adopted for future research, polyNIMMO will be solely a propellant ingredient resulting in no "economy of scale" price advantages. As such it will require to show significant advantages over current, in-service formulations to justify its incorporation [62].

Interestingly, Cumming [58] has highlighted that the choice of energetic binder type has little effect on propellant performance. This suggests that of all the potential propellant component changes available (ie in oxidisers, plasticiser or binders), binder selection may be driven more keenly by other factors (i.e. mechanics) rather than just propellant performance.

1.3 Nitrate Ester Degradation and Stabilisation

1.3.1 Nitrate Ester Degradation

The nitrate ester group (-C-O-NO$_2$) is perceived to be the primary centre of degradation within the polyNIMMO molecule [62] via loss of NOx and HNOx species. This mechanism of degradation is encountered within many types of explosive material, most importantly Nitrocellulose and Nitroglycerine. Because of the importance of these explosives, investigation into the chemical breakdown of the nitrate ester group has been widely studied. [70] [71] [72] [73] [74] [75] The degradation follows a general scheme as detailed in Figure 4.

This series of reactions lead to autocatalytic breakdown of the nitrate ester parent molecule. Control of the reaction sequence to minimise autocatalysis has been the focus of numerous studies [76-90]. The accepted method for removal of NOx and HNOx from explosive degradation is via the use of a series of basic, substituted amines or ureas to preferentially react with any acidic species evolved as a result of nitrate ester degradation. Figure 5 shows a series of materials that have shown promise for use as chemical stabilisers.

$$RCH_2\text{-}O\text{-}NO_2 \longrightarrow RCH_2O^{\bullet} + NO_2 \quad (a)$$

$$RCH_2\text{-}O\text{-}NO_2 + RCH_2O^{\bullet} \longrightarrow RCHO_2H + RCHO + NO_2 \quad (b)$$

$$RCH_2O^{\bullet} + NO_2 \longrightarrow RCHO + HNO_2 \quad (c)$$

$$RCH_2O^{\bullet} + RCH_2O \longrightarrow RCHO_2H + RCHO \quad (d)$$

$$RCH_2OH + 2NO_2 \longrightarrow RCHONO_2 + HNO_2 \quad (e)$$

$$RCH_2O^{\bullet} \longrightarrow R^{\bullet} + HCHO \quad (f)$$
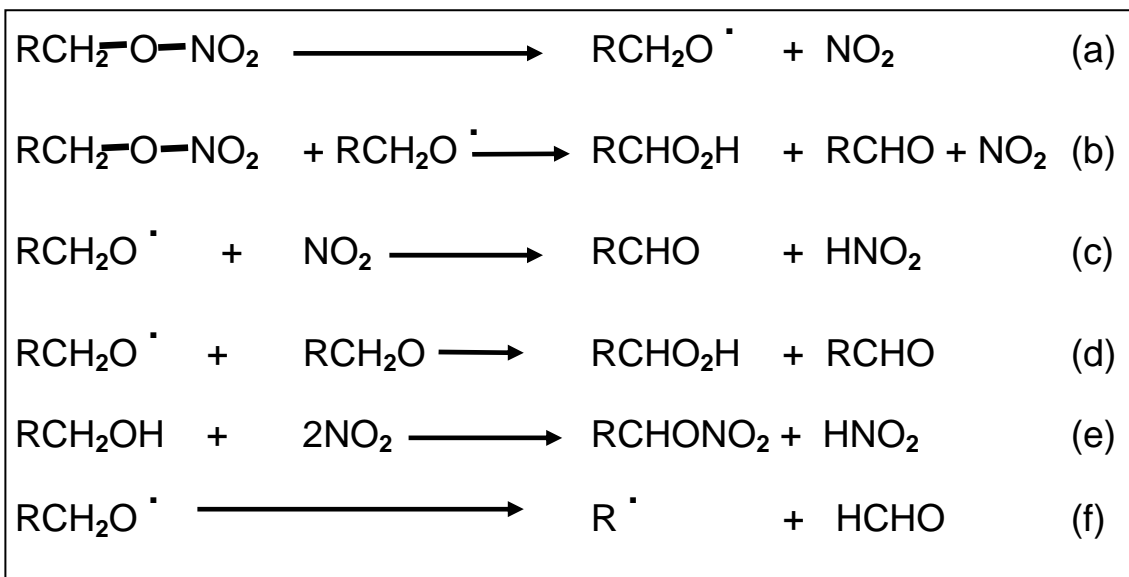
Figure 4 : Nitrate Ester Degradation Proposed by Jeffrey et al [75]

For this study into HNF and polyNIMMO degradation, 2-Nitrodiphenylamine (2NDPA) and para Nitromethylaniline (pNMA) have been chosen as stabilisers.
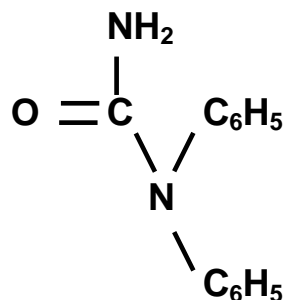
**Diphenyl urea
(Akardite I)**
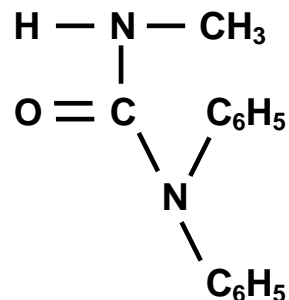
**Methyldiphenylurea
(Akardite II)**
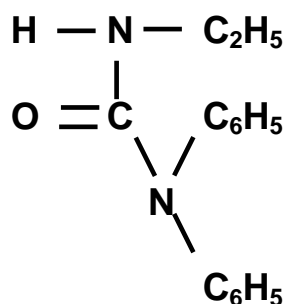
**Ethyldiphenylurea
(Akardite III)**
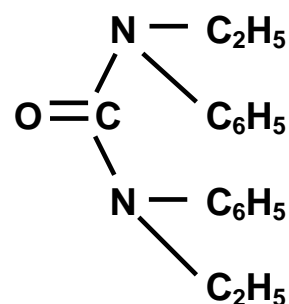
**Diethyldiphenylamine
(Centralite I)**
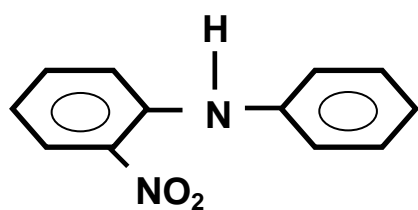
**2- Nitrodiphenylamine
(2NDPA)**
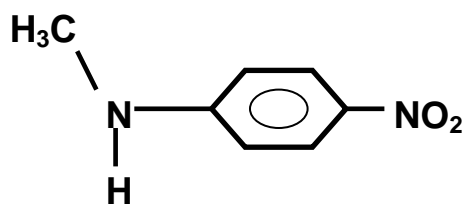
**para-Nitromethylaniline
(pNMA)**

Figure 5 - Chemical Stabilisers for Nitrate Ester Explosives

1.3.2 Reaction of pNMA and 2NDPA

Various detailed studies of the pNMA / 2NDPA stabiliser reaction with the degradation products of nitrate ester explosives have been carried out. A general reaction scheme for each stabiliser is shown in Figures 6 and 7. Different authors detail subtle differences between the reaction schemes and products depending on reaction conditions and the analytical technique applied. However, there is general agreement that reaction is via N-nitrosoation followed by rearrangement to C-nitration. The reader is directed to Volk [77]. Bohn [78] [81] , Curtis [79] , Sammour et al [82-89] and Apatoff [76] for more detailed reviews of reaction schemes.

2NDPA → N-Nitroso-2NDPA →

2, 4'-Dinitrodiphenylamine →

N-Nitroso-2,4'-dinitrodiphenylamine →

2,4,4'-Trinitrodiphenylamine →

N-Nitroso-2,4,4'-trinitrodiphenyamine →

2,2',4,4'-Tetranitrodiphenylamine →

N-Nitroso-Tetranitrodiphenylamine →

2,2',4,4',6 – Pentanitrodiphenylamine →

N-Nitroso-2,2',4,4',6 – Pentadiphenylamine →

2,2',4,'4,6,6' - Hexanitrodiphenylamine
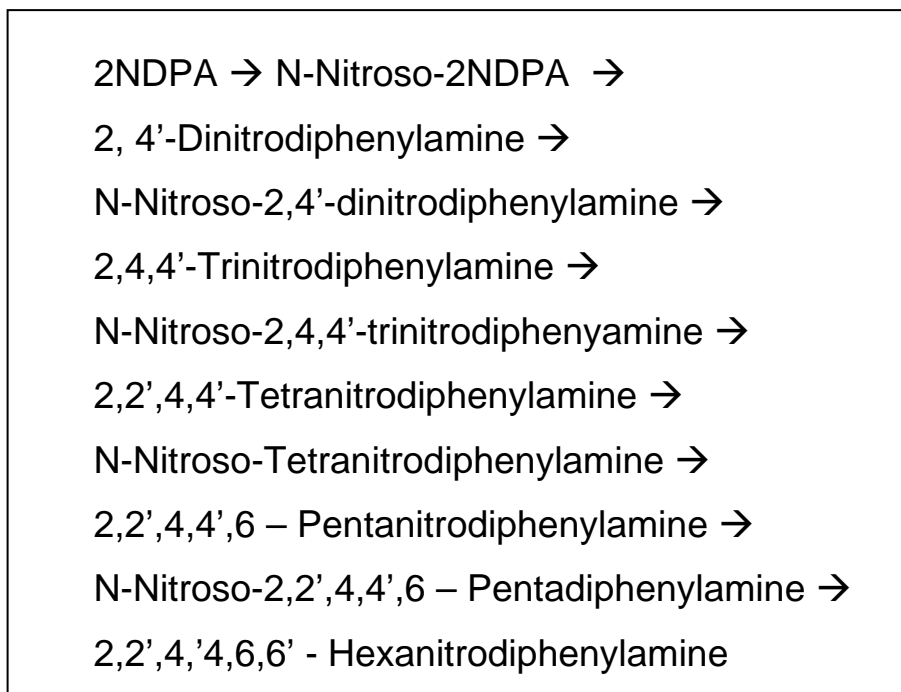
Figure 6 - Reaction of 2NDPA With Degradation Products of Nitrate Ester Decomposition [76] [77]

pNMA → N-Nitroso-pNMA →

N-Nitro-pNMA →

Ortho, para - dinitromethyl aniline
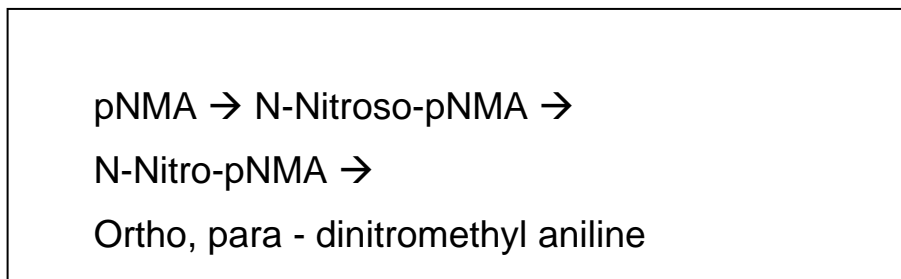
Figure 7 - Reaction of pNMA With Degradation Products of Nitrate Ester Decomposition [85]

1.4 Material Specific Chemistry
1.4.1 Overview of Degradation of polyNIMMO

A detailed investigation of the ageing character of polyNIMMO prepolymer was undertaken by Kemp et al [91]. They suggest that during pyrolysis at a number of temperatures, polyNIMMO prepolymer forms both lower (due to backbone splitting) and higher (due to increased polymerisation / crosslinking) molecular weight species. They also suggest that the course of the reaction (ie to split backbone or to crosslink) is driven via an aerial oxidation reaction. When aerial oxygen is available, chain scission is the dominant reaction. However, if aerial oxygen becomes depleted (eg during ageing in a sealed vessel) this reaction subsides and cross linking reactions become dominant. They suggest that during the oxidation reaction a formate ester is formed via chain cleavage. This reaction is shown in Figure 8. They also suggest that a long lived radical species is encountered during the ageing process and suggest that this is a nitroxide formed via the reaction

$$R \cdot + NO_2 + R' \rightarrow R-N(-O\cdot)-R' \qquad \text{(Reaction R1)}$$
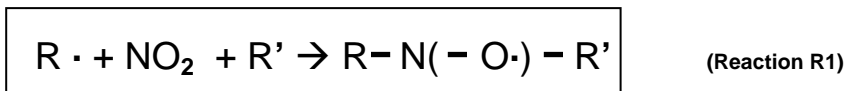
This reaction requires the interaction of two highly reactive radical species which initially appears unlikely. However, the mobility of any radical within the polyNIMMO matrix will be reduced due to the high viscosity of the material. Because of this reduced mobility and the sequential nature of polymeric breakdown in any location where the decomposition has started, there is a potential increase in the probability of this type of reaction occurring. Kemp et al also detail that, after ageing at 130°C and subsequent cooling, paraformaldehyde condensed upon the cooler areas of the storage vessel. They attribute this paraformaldehyde formation to the "standard" decomposition reaction of nitrate esters associated with loss of NOx species. Although they tried to determine the source of the formaldehyde within the polymer structure, they could not unequivocally attribute the formaldehyde formation to either side chain or main chain degradation. This suggests that the two reactions (ie oxidation or denitration) may be occurring simultaneously within the polymer sample during storage.

Manelis [62] investigated the mechanical and chemical breakdown of isocyanate cured polyNIMMO at elevated temperatures and concluded that the decomposition of the nitrate ester grouping on the polymer backbone was the major cause of chemical degradation. This degradation agrees with the accepted mechanism of nitrate ester breakdown detailed in Section 1.3 to form NOx species; this appears to confirm the work of Kemp et al, that, once aerial oxidation reactions have finished, liberation of NOx is the driving reaction. Manelis also undertook his ageing at a lower temperature than Kemp which would be expected to reduce oxidation reactions and promote loss of NOx species. Again, this appears to show agreement concerning the degradation mechanism. Addition of a denitration stabiliser (2NDPA) to protect against denitration products (i.e. NOx) significantly reduced the rate of nitrate ester breakdown and retarded the associated chain scission during storage. This appears to confirm that the rate determining step for the degradation of the cured polymer is the intramolecular cleavage of the nitrate ester $O-NO_2$ bond. Analysis of nitrated 2NDPA derivatives after being incorporated into polyNIMMO and stored at 60°C appears to show that their formulation has proceeded via the expected mechanism of N-Nitrosation followed by rearrangement and finally ring nitration.[62] However, a reduction in polymer backbone breakdown is also seen with 2NDPA addition, suggesting that the material may also act as an antioxidant against peroxide formation [62].

Bunyan et al [51] state that the volume of gas evolved during Vacuum Thermal Stability (VTS) testing of polyNIMMO is similar in magnitude to that of nitrocellulose and significantly less than nitroglycerine.   The lower NO_2 content of polyNIMMO compared to nitroglycerine is likely to be the source of this improved VTS result. This result appears to confirm the work of Manelis [62] which suggested that the breakdown of the nitrate ester $(C-O-NO_2)$ group was the source of polyNIMMO breakdown. Following denitration, the reaction products preferentially attacked the polymer backbone leading to chain scission at the polyether linkage. It is likely that this reaction runs concurrently with the oxidation initiated reaction shown in Figure 8.

Bunyan [51] and Kemp et al [91] all state that the gaseous products evolved from polyNIMMO during storage at between 70 and 100°C were similar although the magnitude of gaseous evolution was much greater at 100°C. The principal product detected was nitrogen with lesser products in the order of CO_2, N_2O, CO and NO. No reaction mechanism for the production of these products was given. Overall, there appears to be general agreement about the mechanism by which polyNIMMO decomposes. The competing mechanisms of peroxide formation with chain

scission and denitration of the nitrate ester side chain exist at all temperatures but both are temperature and environment (i.e. sealed or unsealed storage) dependent.
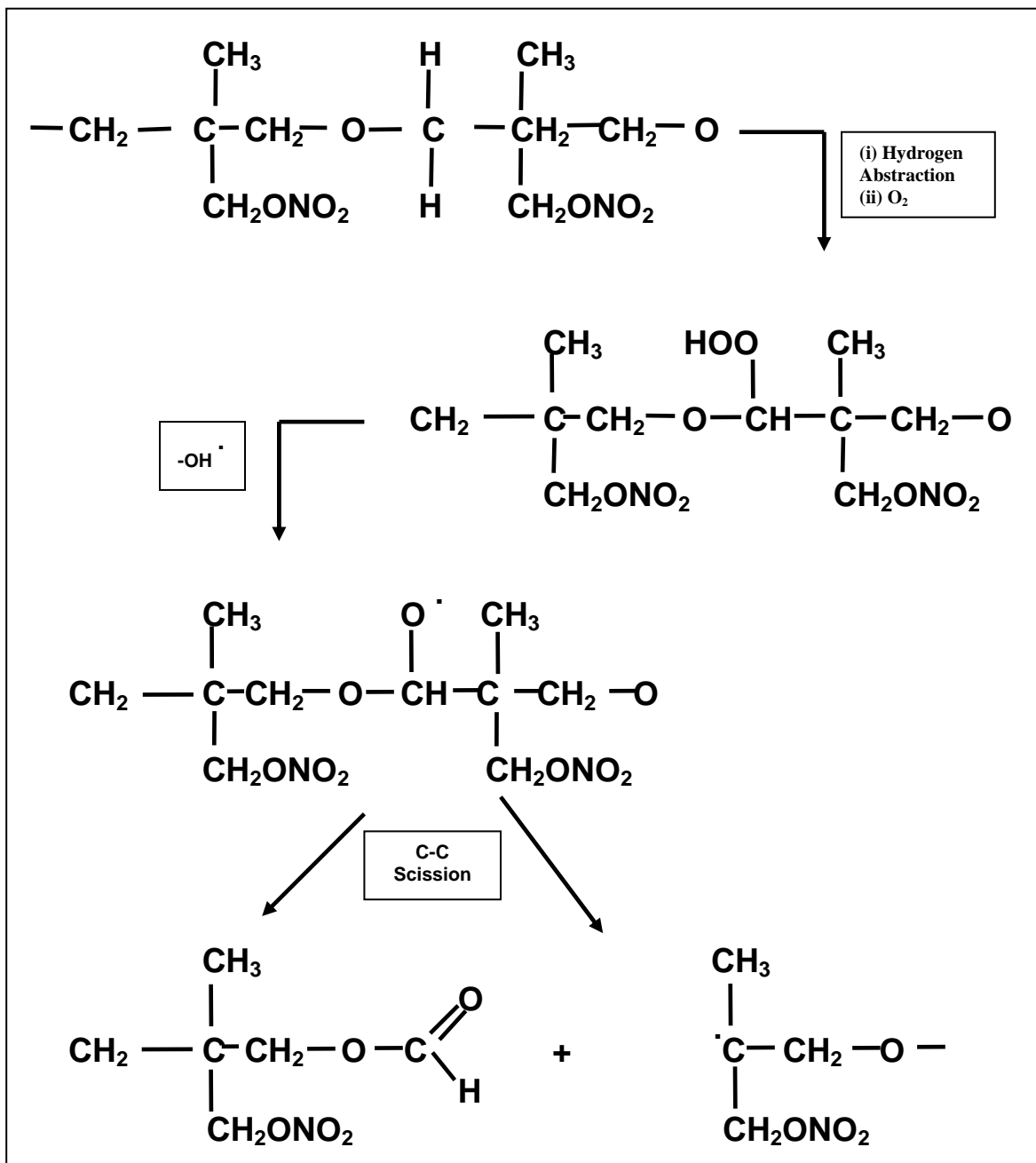
Figure 8 : PolyNIMMO Degradation During Ageing [91]

1.4.2 Overview of Chemistry of HNF

1.4.2.1 Molecular Structure

In many ways, HNF is an unusual salt of nitroform. The majority of nitroform salts decompose at or just above room temperature but HNF has increased thermal stability compared to many nitroform derivatives [41] [93]. This increased stability has been attributed to an extension of the area of charge delocalisation within the HNF molecule or the HNF crystal structure and extensive hydrogen bonding.

Dickens [94] [95] undertook some of the earliest studies of the HNF crystal structure in 1967 and 1970. He concluded that there was extensive hydrogen bonding present within the HNF crystal lattice with 8 units in the unit cell. Dickens also concluded that the nitroformate anion is non-planar within the HNF crystal and that the "precise (crystal) geometry is dependent on environment". The CN_3 framework of the nitroformate ion ($C(NO_2)_3^-$) (also called the "trinitromethanide ion") may be planar but the N_2C-NO dihedral angles are between 4 and 74°. This wide dihedral angle is attributable to the low energy barrier to -NO_2 rotation (typically in the range of 0.3 - 0.8 kJ mol^{-1}). Dickens reports that one of the nitro groups is significantly twisted out of the plane of the CN_3 structure. This may allow some degree of freedom of position of the oxygens of the NO_2 group relative to the CN_3 framework, possibly helping to explain the improved stability of this particular nitroformate structure. Dickens' papers show a graphical depiction of the unit cell. The hydrazinium ions ($N_2H_5^+$) present within the cell are hydrogen bonded to neighbouring nitroformate ions with two main hydrazinium orientations being suggested. One form has the hydrogen atoms of the $N_2H_5^+$ ion staggered and the other has the hydrogen atoms of the ion eclipsed.

The torsion of the nitroformate group in HNF is observed in various other nitroformate crystals (e.g. rubidium [96] or potassium [97] salts) and these salts have a variety of crystal forms. This might suggest that HNF would also show this tendency. Williams and Brill et al [98] state that following storage at 77°C and subsequent infrared analysis, the N-N stretching doublet at 955-971 cm^{-1} in the HNF crystal spectrum broadened reversibly to a single absorbance. This change

from doublet to singlet was taken as evidence of increasing torsional disorder and the authors suggest that this might be accompanying a solid - solid transition. This may give support to the consideration of HNF crystal form variation, possibly due to rotation of the NO_2 groups around the central CN_3 group or alternatively redistribution of hydrogen bonds. However, no enthalpy change was detected by DSC, suggesting that any enthalpy change (if present) was thermally neutral. Visual inspection of HNF crystals after storage at 80°C often show an increased opacity which suggests that some crystal disorder may be induced during the storage period [99]. Although no discussion of different HNF crystal forms has been found within the literature, the possibility of different crystal forms cannot be discounted.

The anion hydrogen bonding has been shown to affect the density of HNF (theoretically 1.86 - 1.89 g/cm^3) [98] and a measured density of 1.872 has been reported [2]. The density is seen to vary with the different crystallisation technique used to recover the HNF from the parent liquor, presumably due to crystal orientation effects. EVAP(oration) grade exhibited a lower density than COOL (crystallised) grade, this being explained as due to the increased porosity of the EVAP grade HNF [2].

1.4.2.2 HNF Elevated Temperature Storage.

A number of studies [12] [98] [100] [101] have been undertaken into the assessment of HNF decomposition under self-sustained combustion / decomposition but limited studies have been carried out at temperatures below this autoignition point ($\sim$ 125°C). As a consequence, the stability of HNF during slow decomposition at lower temperatures is not well understood. Pearce [92] carried out the determination of permanent gases evolved from HNF after storage at 40, 50 and 60°C under air and concluded that increases in N_2O and CO_2 are observed during storage with no observed increase in N_2 occurring. He states that the evolution of CO_2 appeared "erratic" and attributed this erratic nature to a possible reaction with hydrazine or a hydrazine derivative. This is not unexpected as routine detection of carbon dioxide by, for example Draeger tube, relies on the CO_2 / N_2H_4 reaction [102] ie

$$CO_2 + N_2H_4 \rightarrow NH_2.NH.COOH$$ **(Reaction R2)**

Further stop flow studies continuing the initial work of Pearce were undertaken by Veltmans et al [28] detailing GC-MS investigations of ageing HNF at 40, 60, 70 and 80°C. The results appear to confirm the primary product of degradation at all temperatures to be N_2O. However, at $< 60°C$ the level of degradation was very small even after considerable ageing. Degradation at 70°C was evident after 70 hours storage with a rapid rate of increase of N_2O production beyond 80°C. Associated with this more rapid N_2O evolution at this temperature, both CO_2 and N_2 are observed. Throughout the whole storage period at 70°C there was a slow increase in water production. Schmidt [103] details the gas phase reaction of hydrazine with oxygen as :-

$$N_2H_4 + O_2 \rightarrow N_2 + 2H_2O$$
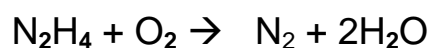
(Reaction R3)

This may also help elucidate the source of the water and nitrogen detected by Bellerby et al [104] [105] during their ageing studies. At 80°C, degradation was rapid from the outset with N_2O being the major product and N_2, CO_2 and water being the minor contributors.

Bellerby et al [104] propose the reaction

$$3N_2H_5^+.C(NO_2)_3 \rightarrow 2NH_4^+.C(NO_2)_3 + 3N_2O + H_2O + NH_4^+HCO_2$$
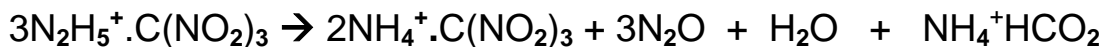
(Ammonium Formate)

(Reaction R4)

for the evolution of the products. They also suggest that the loss of the hydrazinium ion occurs at a faster rate than loss of the nitroformate ion. They suggest that this is due to formation of nitrous acid where three hydrazinium ions react with one nitroformate ion to liberate 3 nitrous acid molecules on route to formation of ammonium formate.

Bellerby and Blackman [105] show other detailed graphs of gaseous evolution from HNF at 70°C. They state that after 200 hours storage, HNF crystals become aggregated. This appears to coincide with a plateau on the graph showing evolution of water within the sample. Presumably some degree of water adsorption occurred at this point. However, ageing of HNF in humid environments has suggested that HNF has a hygroscopic point of 94% (which means that water is not taken up until the humidity is greater than this value). [43] This appears to suggest that water adsorption onto fresh HNF would be unlikely to occur but this does appear to be the most likely explanation of Bellerby's work. Some studies of the hydrated hydrazinium ion [106] suggest that, if

solvation was to occur, that a comparatively weak acid might be formed. Formation of an acid, even a weak acid, would at first glance, be expected to destabilise any remaining HNF. However, this does not appear to have occurred within these test samples. An explanation of this may possibly be related to the importance of water on crystal form which is reported by Zee[23] during HNF production. He found that preparation of HNF in an anhydrous reaction media leads to no improvement (and occasionally a decrease in) the purity of the product formed. This was unexpected as water was thought to act to destabilise HNF as an impurity and had been detailed to do so by Brown et al[107]. However, further studies by Zee found that it was necessary to have a small proportion of proton transferring medium to catalyse salt formation (and produce a purer product). This was the action which water provided (the use of lower alcohols (C_1 - C_6) also served this purpose). Without the use of "wet" hydrazine, the product formed has a melting range of ~ 58 - 70 °C whereas a "wet" hydrazine starting material raised this melting point to ~ 115°C. This shows the importance of the proton transfer medium to the final properties of the product and the formation of a strong acid may aid stability. A patent by Brown et al[107] appears to confirm that an acidic species aids HNF stability but recent attempts by the author at replication of this patent data have been unsuccessful. This may also be related to the adsorption of water within the HNF ageing study.

Bellerby and Blackman[105] detail a slight reduction in oxygen content after 100 hours of HNF storage at 70°C during ageing. This reduction may again be a consequence of formation of water via reaction R3 detailed above. However, they confirm that the principal products of elevated temperature storage are N_2O with CO_2 and N_2. These authors[105] continued the HNF ageing study by assessing the H-NMR spectrum of fresh and partially aged HNF. The unaged material showed peaks at 3ppm and 7ppm which were assigned to the NH_2 and NH_3^+ groups within the hydrazinium group respectively. After ageing they identified both water and the NH_4^+ ion to be present within the partially aged HNF sample. Strong ageing of HNF leads to the loss of crystalline form and the formation of a slurry. ^{1}H-NMR assessment of this slurry showed the loss of both NH_2 and NH_3^+ groups and the presence of solely the NH_4^+ species. This was further confirmed by N-NMR spectroscopy. This study appears to confirm the possible formation of ammonium nitroformate (ANF) during the ageing process which was originally suggested by Koroban et al[108] (reaction (e) in Figure 9). Rapid heating rate experiments such as those by Brill et al[98] also identified ANF as a solid residue. The other decomposition products observed during HNF ignition also appear to agree with Bellerby and Blackman with N_2O, CO, H_2O and

$HC(NO_2)_3$ (i.e. nitroform) being observed. The presence of nitroform was not noted within the lower temperature trials and this suggests that a different reaction mechanism is in action at the higher heating rates. Similarly, N_2H_4 was detected by Brill et al [98] but not by Bellerby, the compound existing for only a very short time period within the high rate heating experiment. This short observation time can be attributed to the high reactivity of the hydrazine molecule but also suggests that the initial step during high rate decomposition includes proton transfer from the hydrazinium ion. The decomposition of hydrazinium diperchlorate ($N_2H_6(ClO_4)_2$) detailed by Pai Verneker et al [109] suggests that dissociation of the molecule is driven by proton transfer to form hydrazinium perchlorate and perchloric acid ie
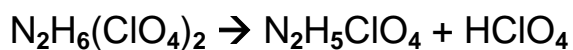
$$N_2H_6(ClO_4)_2 \rightarrow N_2H_5ClO_4 + HClO_4$$ (Reaction R5)

This suggests that proton transfer is a significant reaction mechanism within hydrazinium salts. However, they suggest that at low temperatures proton transfer is unlikely due to the low rate of decomposition observed and that solid state ionic diffusion is dominant at lower temperatures. This would suggest that this reaction is possibly too high energy to occur at lower heating rates. Brill [98] suggested that the overall reaction of HNF under very rapid heating was :

$$2HNF \longrightarrow 2ANF + N_2 + H_2$$ (Reaction R6)

suggesting a bimolecular reaction scheme. Koroban [108] suggested a range of potential reactions within the HNF ageing process; these are shown in Figure 9. He also suggests a trimolecular route towards the formation of ANF but quotes an unbalanced reaction equation. Possibly, a reaction course incorporating a combination of bi- and tri- molecular processes leads to the overall stoichometry predicted by Brill. The work of Bellerby et al [104] [105] most closely aligns with reaction (e) of Koroban's work but has also balanced the stoichometry.

However, Koroban's research [108] into HNF storage at 100°C, appears to point to a much wider range of chemical species being evolved during ageing than observed by Bellerby or Brill. However, this would be expected to be the case due to the higher reaction temperature (compared to Bellerby) but longer time frame (compared to Brill) being used to dissociate the molecule. Although interpretation is hampered by a language barrier, chemical equations detailed within the text, suggest the possible formation of N_2H_4, N_2H_2, NH_3, NO_2, N_2O_4, HNO_2, H_2O and N_2O via

various complex reaction schemes but it is unclear whether all of these species were actually detected during their testing. These reactions are shown in Figure 9.

$$2N_2H_4 + N_2H_5C(NO_2)_3 \longrightarrow H_2C(NO_2)_2 + HNO_2 + 2N_2H_3^{\cdot} + N_2H_4 \quad (a)$$

$$\longrightarrow N_2H_4\text{-}HON{=}C(NO_2)_2 + 2N_2H_3^{\cdot} + H_2O \quad (b)$$

$$2N_2H_3^{\cdot} \longrightarrow N_2 + 2NH_3 \quad (c)$$

$$N_2H_5^{+} + HNO_2 \longrightarrow H_2N\text{-}NHNO + H_2O + H + NH_4^{+} + N_2O \quad (d)$$

$$3N_2H_5C(NO_2)_3 \longrightarrow 2NH_4C(NO_2)_3 + 2H_2O + N_2 + 2N_2O + [CNO_2H_3] \quad (e)$$

$$NH_4^{+} + HNO_2 \longrightarrow H^{+} + N_2 + 2H_2O \quad (f)$$

$$C(NO_2)_3^{-} + HNO_2 \longrightarrow CH(NO_2)_2^{-} + N_2O_4 \quad (g)$$
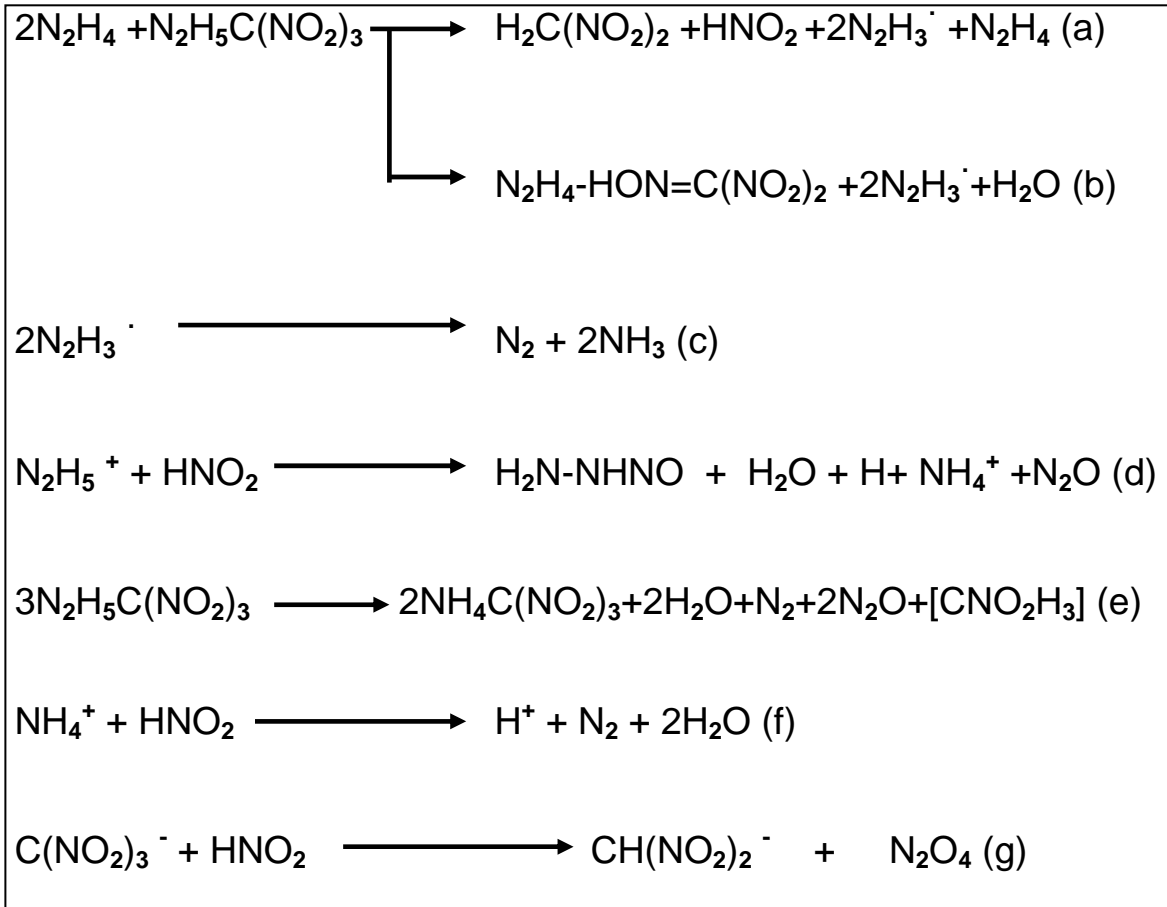
Figure 9 : Proposed Chemical Reactions During HNF Ageing [108]

The differences between the conclusions of Koroban [108] , Brill [98] and Bellerby [104] are proposed to be due to the different test regimes employed. Koroban did continuous monitoring studies at 100°C whereas Bellerby undertook stopflow studies at a range of temperatures. Brill in turn heated the sample "instantaneously" to its decomposition point. These differences result in additional thermal breakdown reactions of the HNF molecule (when stored at higher temperature) and various intermolecular reactions between products in the gaseous state modifying species detected in the post storage residues (in stop flow monitoring). Interestingly, this effect of rate of energy deposition into the HNF molecule is further highlighted by Brill [98] .When heated rapidly

to > 260°C, carbon dioxide is also observed within the gaseous degradation products of HNF. Increasing the maximum heating temperature promotes the formation of CO_2 along with NO. It is suggested that the reaction may follow the path

$$HNF \longrightarrow 2NO + CO_2 + 2H_2O + 3/2\,N_2 + \tfrac{1}{2}\,H_2$$
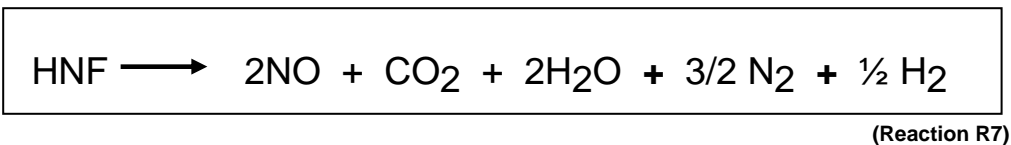
(Reaction R7)

The different storage conditions help to elucidate the order of bond cleavage at different rates of energy deposition and thus may aid interpretation of the overall reaction course.

Assessment of HNF in sealed and unsealed environments highlight that samples in sealed environments degrade at a higher rate than those in unsealed environments [110]. This possibly suggests some degree of autocatalysis in the degradation of the HNF molecule where preliminary degradation species re-attack other HNF molecules within the bulk material. Vacuum thermal stability testing of HNF highlights this acceleration of degradation rate during storage with the total gas volume measured showing exponential growth during storage. Hordijk et al [111] suggests that the use of HNF is hampered by its own instability and this autocatalysis may be a reflection of this instability. However, Vacuum Thermal Stability (VTS) data [110] for HNF gas evolution during ageing generally gives the profile shown in Figure 10. This shows an initial rapid evolution of gaseous products followed by a near plateau region. Following this plateau, autocatalysis eventually starts to occur. This storage profile is more exaggerated at increased storage temperature. The first rapid increase is often attributed to solvent or impurity loss [91] but this has still to be confirmed.
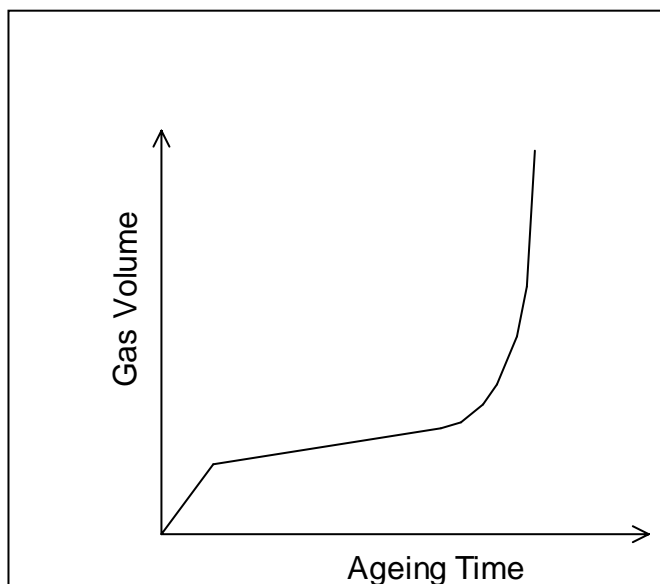
Figure 10 : Typical Plot of HNF Vacuum Thermal Stability Test Result [28]

The author has previously proposed [99] that the degradation or crystal deformation which drives the start of the autocatalytic reaction in HNF does not occur at temperatures below 80°C and that this temperature may act as a "barrier" beyond which the autocatalytic species started to be evolved. However, the crystal disorder detailed by Brill et al [98] at 77°C indicates that significant changes do occur within the crystal structure during storage at this temperature. Possible routes to autocatalysis / degradation were the subject of further investigation during this study. All degradation studies of HNF suggest that the overall decomposition of HNF is a complex series of reactions, some sequential, some running in parallel. As such, identification of acceptable thermal / chemical stabilisers or inhibitors is likely to require a complex chemical solution. In addition to the complexity of reaction, many of the reaction products are likely to be temperature dependent, potentially short lived and change with storage environment. This again complicates the identification of a single stabiliser species to cover all potential reaction variants.

1.4.2.3 HNF Stabilisation

Early investigations into HNF based propellants based on unsaturated carboxyl terminated hydrocarbon (CTPB) binders suggested that the incorporation of nitroguanidine in the 2-20%Wt range into the mixture improved the overall longevity of the formulation [112]. The patent covering this also suggests that the presence of double bonds within the binder structure and their interaction with the HNF molecule is the source of chemical breakdown. It also suggests the use

of triethylene melamine as a preferential curing agent for the system. The addition of either ethyl centralite or 2-nitrodiphenylamine (2NDPA) into the formulation to act against denitration were seen to accelerate the deterioration of the propellant formed. This detrimental effect of 2NDPA has also been seen in other studies [113]

Comparison of cyanoguanidine with nitroguanidine showed that cyanoguanidine, although slightly improving the overall propellant stability compared to unstabilised systems, did not improve the stability to such an extent as nitroguanidine. It was proposed that, due to the structural differences between the cyano and nitro derivatives, that the nitramino (-NHNO$_2$) group was the critical moiety for stabilisation. However, ethylene dinitramine (containing two of these groupings) was not effective in stabilising the propellant formulations. This suggests that the action of the stabilising species is not simply chemical moiety based. Replication of these results on more recent (i.e. purer) batches of HNF failed to highlight a positive effect of nitroguanidine addition. [110] This lack of replication suggested that the action of nitroguanidine may differ from the mechanism proposed in the patent (e.g. it is possible that, due to the age of the patent and so the lower purity of HNF involved, the action was possibly acting against HNF impurities and not directly against HNF degradation).

Schoyer [44] suggests that both magnesium sulphate and calcium carbonate can help inhibit the initial decomposition of HNF but have little or no effect once the initial degradation has occurred (i.e. they have no effect on reducing autocatalysis).   This appears to overlap with the work of Jago [113] who patented a method of HNF stabilisation within nitrocellulose matrices using salts of the Group IIa metals (ie Be, Mg, Ca, Ba, Sr). Although he could not offer details of the method by which stabilisation occurred, he suggested that counter ions such as sulphate, bisulphate, sulphite, bisulphite, nitrate , nitrite, phosphate, hydrogen phosphate, carbonate, bicarbonate, chloride, acetate, oxalate, tartrate, lactate or benzoate helped to stabilise the NC portion of the formulation and the cation stabilises the HNF. The stabilising effect of nitrocellulose alone on HNF has been observed by the author although once degradation occurs, the sample gives a response that is both rapid and quite violent. The action of the metal ion may be similar to that proposed by Groves [114] who investigated and patented the interaction of alkali metal co-ordination compounds with hydrazine as potential oxidisers. It may be that the high reactivity of HNF leads to the formation of a "bridging" molecule which extends the charge delocalisation within HNF and thus aids stability by reducing charge mobility.

Brown et al [107] suggest the introduction of a small proportion of acid into pure HNF to aid stability. They suggest that the addition of either oxalic, picric, phosphoric acids or phosphorus pentoxide all contribute to improved HNF life. Attempts to duplicate the effects of oxalic acid addition [64] showed that there was a reduction in gas volume and this was taken by Brown to indicate improved stability. However, the HNF present was severely degraded during testing suggesting a high degree of solid / solid (ie non-gaseous) reaction. Therefore the assignment of "improved stability" by Brown is proposed to be inappropriate.

In a separate patent [115] Brown suggests that the use of zinc oxalate, zinc chloride and mercurous and mercuric oxalate are all beneficial to the ageing characteristics of HNF. However, Rice [116] suggests that the use of these particular stabilisers is more suitable to positively influencing the impact sensitiveness of the material rather than its chemical stability. He suggests that the use of the anhydrides of carboxylic acids gives a significant improvement in chemical stability but does not table any data.

Overall, identification of a chemical stabiliser for HNF has not yet been successfully achieved. Much of the early work was hampered by the use of impure (and lower stability) HNF and / or ignored the effect of the stabiliser on the HNF present. The HNF development work being undertaken in the Netherlands is continuing to improve the purity of the material produced but further studies into the area of stabilisation will be required.
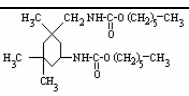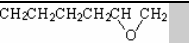
1.4.2.4 Assessment of Functional Groups on HNF

Marshall [117] of Nobel Enterprises carried out an assessment of HNF reaction against various functional groups. Although providing no comments on data analysis, he has kindly agreed that this data can be reproduced and disclosed within this thesis and it is shown in Table 1. The two sets of analytical data show different aspects of HNF reactivity. Due to the high heating rate used within the DSC method (although not specified, typically 5 or 10K/min), generally only reactions with a high probability * of occurrence with HNF are observed. This is because any low probability * reactions generally cannot become established before sample ignition occurs.

Once ignition does occur, binary mixtures may show an effect on the dynamic decomposition process (ie by sharpening or broadening the decomposition exotherm) but this is often more closely associated with the heat flow characteristics of the additive during the decomposition

than true sample reactivity. For example, where an additive is close to its melting point, the energy released during HNF decomposition is transferred to the additive to promote melting. The exotherm peak temperature is therefore detected later on the DSC trace and appears retarded to higher temperatures. This shift in exothermic peak temperature does not indicate an improvement in stability etc but is solely a characteristic of the test method. As a consequence, changes in exotherm peak temperature values are not always indicative of a change in decomposition mechanism. A similar situation can be observed for melting points.

* In a complex chemical system, the formation of products can be viewed as a probabilistic distribution ranging from the most likely to the least likely products. For example, within many organic reactions, the high yield products have a higher probability of formation than the other by-products. By manipulation of test conditions, the "probability" of a product being formed can be modified (generally to facilitate increased production of the target product). Within a dynamic, rapidly changing system such as dynamic high rate DSC of HNF, the processes that are the most facile, energetically favourable and irreversible are likely to dominate as other "marginal" reactions do not have sufficient time to establish themselves before the material has decomposed. In steady state conditions, all reactions can be allowed to come to an equilibrium position as experimental time is not the driving force and so all reactions possible at any given temperature can occur. In the terms of this thesis, "high probability" is used to describe reactions that are facile, energetically favourable, and irreversible (or have high values of equilibrium constant); low probability reactions are those reactions that are less facile but are still energetically favourable and irreversible.

Test Material	Formula	DSC of 1/1 Mix with HNF (Cool grade)				Vacuum Stability 48 Hours at 60°C		
		Minor Exo (Onset) (°C)	HNF Melt (°C)	Main Exo Onset (°C)	Main Exo Peak (°C)	Test material (ml/g)	1/1 Mix with HNF (Cool Grade) (ml/g)	Contribution of Reaction (ml/g)
HNF	$N_2H_5C(NO_2)_3$		131	132	134	0.53	-	-
1-Hexanol	$CH_3CH_2CH_2CH_2CH_2OH$		132	133	135	0.11	0.11	- 0.21
2-Hexanol	$CH_3CH_2CH_2CH_2CH(OH)CH_3$		133	134	136	0.31	0.4	- 0.02
1,2-Hexandiol	$CH_3CH_2CH_2CH_2CH(OH)CH_2OH$		-	120	150	0.1	9.24	8.93
1-chloro-2-propanol	$CH_3CH(OH)CH_2Cl$		128		133	0.34	1.47	1.04
IPDI/1-hexanol product			130	131	133	Not Tested		
1,2 Epoxyhexane	$CH_2CH_2CH_2CH_2CH\ CH_2$ O	83	132	133	135	Removed after 21 hrs Storage		Incompatible
Hexanoic Anhydride	$CH_3CH_2CH_2CH_2CH_2C(O)OC(O)CH_2CH_2CH_2CH_2CH_3$		135	137	139	0.2	0.65	0.28
Ethylhexanoate	$CH_3CH_2CH_2CH_2CH_2C(O)OCH_2CH_3$		128	129	132	0.04	0.18	-0.11
Hexanoic Acid	$CH_3CH_2CH_2CH_2CH_2CH_2COOH$		133	134	136	0.55	1.07	0.53
Hexanoyl Chloride	$CH_3CH_2CH_2CH_2CH_2CH_2COCl$	80 to 140 irregular	-	140	153	2.66	3.57	1.98
Hexanal	$CH_3CH_2CH_2CH_2CH_2CHO$		-	40	66	Not Tested		
3-Hexanone	$CH_3CH_2CH_2C(O)CH_2CH_3$		-	131	155	0.22	15.9	15.53
1-Chlorohexane	$CH_3CH_2CH_2CH_2CH_2CHCl$		134	135	137	2.22	1.53	0.15
1-aminohexane	$CH_3CH_2CH_2CH_2CH_2CH_2NH_2$		-	110	138	19	14.4 (14 Hrs)	Incompatible
Dihexylether	$CH_3CH_2CH_2CH_2CH_2CH_2OCH_2CH_2CH_2CH_2CH_3$		129	130	132	1.91	1.23	0
Trans-5-decene	$CH_3CH_2CH_2CH_2CH_2CHCHCH_2CH_2CH_2CH_3$		133	134	136	0.56	0.5	-0.03
2-ethylhexylnitrate	$CH_3CH_2CH_2CH_2CH(CH_2CH_3)CH_2ONO_2$		130	131	134	Not Tested		

Items marked in grey show high degree of reaction with HNF

Table 1 : Reaction of HNF With Various Functional Groups [117]

From the DSC data in Table 1, it can be observed that 1,2-hexandiol, hexanal and 1-aminohexane all show significant changes in test data from the HNF control. This suggests that the reaction between HNF and these materials is a high probability event, leading to widespread sample decomposition; this indicates that the functional groups are most likely chemically incompatible with HNF. Slightly less obvious in terms of reaction are 1,2-epoxyhexane and hexanoyl chloride, both of which show minor exotherms before HNF decomposition. In these samples, onset and peak exotherm data is similar to that of the control (although hexanoyl chloride appears to retard peak decomposition). The low level events observed suggest that the reactions are low probability events that fail to propagate into the bulk material. This implies that the first series of high probability reactions may lead to autocatalytic breakdown reactions whereas the second fail to propagate widespread decomposition.

Vacuum stability analysis is better suited to identifying both high and low probability events due to the longer contact times involved. It also allows improved quantification of any effect via the evolved gas measurement. From the data given, there are indications that 1-aminohexane and 1,2-hexanediol still exhibit significantly inferior data to the HNF control; this confirms the detrimental nature of these test samples on HNF stability. Vacuum stability data also suggests that the items that gave low probability reactions by DSC (ie 1,2-epoxyhexane and hexanoyl chloride) both have more extensive reactions during this test. This indicates that these reactions are more significant than proposed by DSC.

For the alcohols tested, the mono-hydroxyl forms appear to show some degree of reduction in vacuum stability evolved gas volume compared to HNF. This may suggest that the samples are beneficial in reducing HNF degradation but could also be indicative of a "gas free" degradation mechanism occurring or possibly the dissolution of gaseous products or solid HNF into the test liquid; either of these effects would reduce the level of decomposition detected. The data given also shows the secondary alcohol to have inferior "stabilising" properties compared to the primary alcohol. The trial of a 1,2-diol analogue shows this to be significantly chemically incompatible with HNF, liberating a large quantity of gas during testing. As HNF and gas solubility within each of the alcohols would be expected to be similar, the poor result of the 1,2-diol appears to strengthen the observation that the mono-hydroxy alcohols aid stability of the alcohol / HNF mixture via chemical interaction rather than a physical solvation effect. This proposal is further reinforced during substitution of the hydroxy group in the α position of the diol with a chlorine atom. This leads to the level of incompatibility to be significantly reduced compared to the diol structure but is still evident. The compatibility of the chlorine group with HNF appears good (viz 1-chlorohexane result) and so the likely explanation for the VTS change is due to the reduction of hydroxyl groups (although shortening the molecule chain length may have also possibly contributed). The relative increase in evolved gas volume for the 1-chloro-2-propanol result (compared to 1-chlorohexane or 2-hexanol results) may suggest that the increased reaction is due to the added electronegativity of the terminal α group influencing the reactivity of the ß-hydroxy group. The very high gas volume achieved from the 1,2-diol suggests that the 1,2 substitution pattern is significant. This may suggest that where two reactions sites which are available for bonding are adjacent, that this orientation is especially detrimental to HNF stability. Dickens [94] [95] predicted extensive hydrogen bonding within the HNF structure and Groves [114] proposed that the formation of coordination compounds were useful in the stabilisation of hydrazine. Extending these conclusions by Dickens and Groves, the reactivity of the hydroxyl group and its distortion of the electron distribution or the formation of hydrogen bonding onto or from

the HNF structure may be an important factor in HNF reactivity. This distortion of the electron distribution may in turn lead to the formation of a coordination compound as proposed by Groves or lead to redistribution of charge over a wider structure (with the possibility of either "stabilisation" or decomposition dependent on the level of distortion of the electron distribution over the molecular structures).

Schmidt [103] details that "one of the pronounced features in hydrazine and derivatives is the presence of hydrogen and lone pair electrons on the same molecule. Hydrogen bonding contributes significantly to the material properties". Combining this with the extension of hydrogen bonding observed by Dickens [94] [95], it does not seem unreasonable to assume that some degree of hydrogen bonding will be encountered within at least some aspects of HNF reactivity.

A combination of hydrogen bonding and electron cloud distortion may be the source of the differing levels of reaction between different functional groups. The level of distortion or hydrogen bonding of any acceptor group would then determine whether pseudo stabilisation or degradation occurs. For example, Figure 11 shows a series of hypothetical schemes for HNF reaction with a range of different molecular structures. Although indicated for the hydrazinium ion, similar schemes could be drawn for the nitroformate ion. In each structure, the dotted line shows the hypothetical distortion of the electron cloud around the HNF structure due to the presence of the second reactant (possibly resulting in hydrogen bonding but this is not intrinsic to the hypothesis).
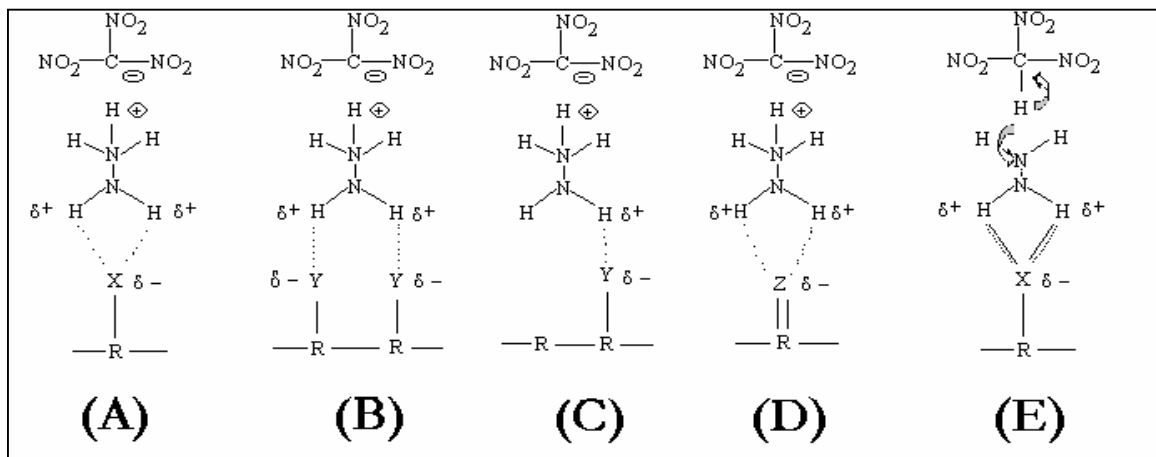
Figure 11 – Hypothetical Hydrogen Bonding Schemes In HNF Chemical Reactions

By distortion of the electron distribution within any of the hypothetical bonding schemes it is proposed that the distortion will affect the nitroformate to hydrazinium ion attraction, due to changes in the spatial distribution of electrons within the "coordination" structure formed. This distortion can then lead to either weakening or strengthening of the ionic bond due to

changes in the overall polarity.   In all cases, the group X, Y or Z is proposed to lead to distortion or extension of the electron cloud within the HNF structure. However, the effect this distortion makes is different in each case. In scheme A, the electronegativity of X leads to distortion but with the potential for formation of a small delocalised electron ring structure. In B, distortion is encouraged by a pair of adjacent groups which again has potential for ring formation but over a wider range. For scheme C, a single bond is formed and so the formation of a ring structure is not possible. Although single bond formation is likely to be less desirable than ring formation, single bond formation may be preferable to hypothesis (D) where a ring structure is formed but the electron density of the R=Z bond is higher than the R-X in hypothesis (A). Finally, in hypothesis (E) the H-X bond is such that it leads to a disruption of the Hydrazinium / Nitroformate bond and widespread breakdown of the HNF molecule (although hypothesis (E) is drawn with a single moiety (X) it could have easily have been drawn with a doublet of groups as in hypothesis (B)). Within any distortion of the electron distribution over any adduct formed between HNF and a secondary species, the relative level of the distortion may be hypothesised to affect whether stabilisation, no reaction or disruption of HNF occurs. Any distortion that may occur would be expected to affect the Hydrazinium / Nitroformate bond by affecting the overall ionic character of the bond. From studies by Pai Vernchar [109] and Tang [36], hydrogen transfer between ions containing the hydrazinium ion is a possible reaction course for HNF breakdown although perceived to be a high temperature reaction during their studies on hydrazinium perchlorate. The lower thermal stability of HNF may reduce the temperature at which this may occur. If transfer was to occur, the species formed (ie hydrazine and nitroform) would be expected to be highly reactive. Hypothesis (E) shows a route to hydrogen transfer via excessive distortion of the electron cloud over the adduct formed. Here the electron cloud becomes distorted over the new NHXR bond such that the N_2H_4-X bond is preferential to the Hydrazinium / Nitroformate bond. Cleavage would then occur at the hydrazine / nitroform boundary via hydrogen transfer. This is where chemical incompatibility would be detected. The other extreme of interaction is where the distortion of the electron cloud leads to an improvement in overall stability by strengthening the Nitroform / Hydrazinium attraction.

The chemical incompatibility observed for aldehyde groups in Marshall's data [117] suggests that either the lack of potential leaving group is an important missing component or that the reaction leads to the extreme case of HNF degradation (given in hypothesis (E)) due to excessively strong bond formation. However, although the electronegativity of the aldehyde and ketone carbonyl groups would be expected to be similar, they show significantly different rates of reaction with HNF with the ketone group showing a much less severe reaction. This suggests that added stabilisation of any intermediate via the electron releasing properties of

the carbon backbone is an added important contributor to the reactivity. This added stabilisation of any intermediate is likely to be important in reducing the strength of the C=O - ---- H bond (and thus reducing strain on the N_2H_5----- $C(NO_2)_3$ linkage, so safeguarding the HNF molecule), due to reduction in any induced polarity.

Within a secondary carbocation, two aliphatic chains are available to stabilise the reaction intermediate whereas within a primary carbocation, only one group is available. This in turn affects the relative reactivity of each group. Cassario et al [118] detail a reaction for aldehydes and amines as shown in Figure 12.
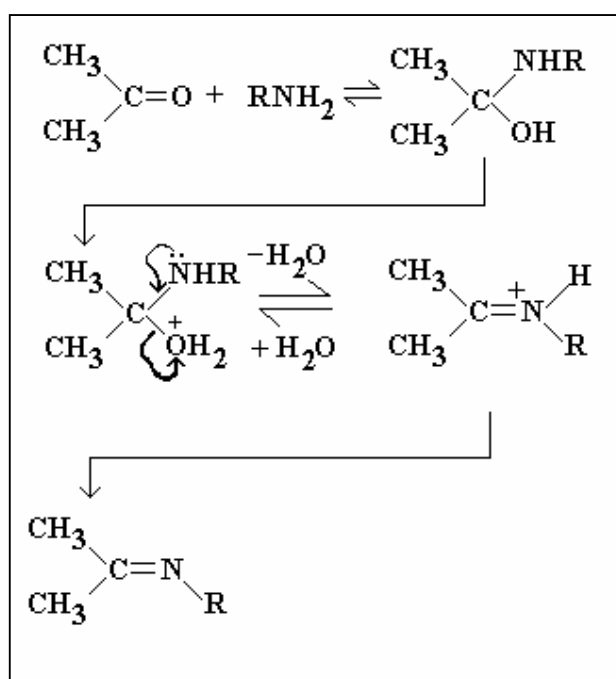
Figure 12 : Reaction of Carbonyl groups with amines [118]

In addition to the stabilisation of the carbocation intermediate, for an aldehyde, step 1 of the reaction in Figure 12 would form an intermediate
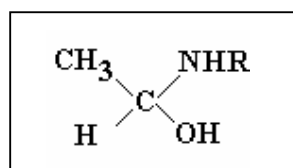
that would potentially more easily facilitate release of water from the intermediate structure (and thus make the transformation more energetically desirable). In addition to the reaction

course given in Figure 12, Schmidt [103] details the formation of both hydrazones and azines from the reaction of hydrazine with carbonyl groups; these are shown Figure 13 . Although the formation of azines would initially be unlikely within HNF due to the nitroformate ion requiring extensive rearrangement, it suggests a possible reaction which may lead to competition at the hydrazinium / nitroformate ion boundary.

$$R_2CO \quad + \quad H_2NNH_2 \longrightarrow R_2C{=}N{-}NH_2 \ + \ H_2O$$
Hydrazone

$$2R_2CO \quad + \quad H_2NNH_2 \longrightarrow R_2C{=}N{-}N{=}CR_2 \ + 2H_2O$$
Azine
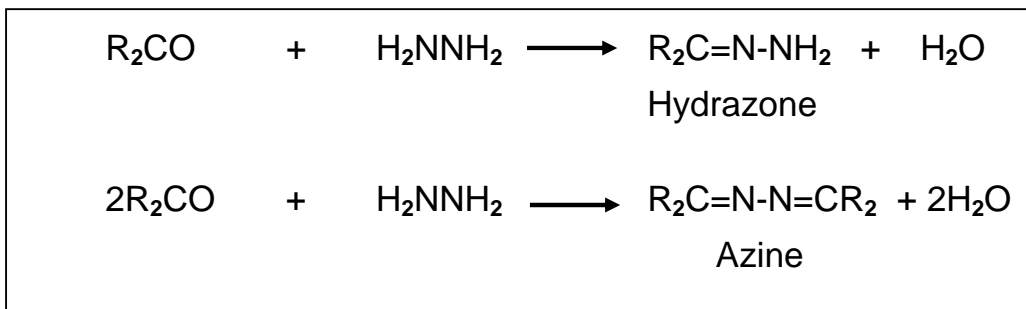
Figure 13 : Carbonyl Reaction with Hydrazine [103]

In addition, for liquid carbonyl compounds, improved stability of the ketone compared to aldehyde structure might also be related to the keto-enol equilibrium observed within the ketone class. The enol form of the ketone (if formed) would allow a greater degree of stabilisation (as observed in the primary alcohol and carbonyl data) whilst still allowing extension of the hydrogen bonding structure. Formation of the enol form would likely require a degree of solvation of HNF (to allow acid catalysis to assist enol formation), but previous studies [110] have highlighted the susceptibility of HNF to degradation during solvation. The enol-keto transition is shown in Figure 14 with arrows indicating the possible release of electrons from neighbouring groups on the carbon chain backbone.
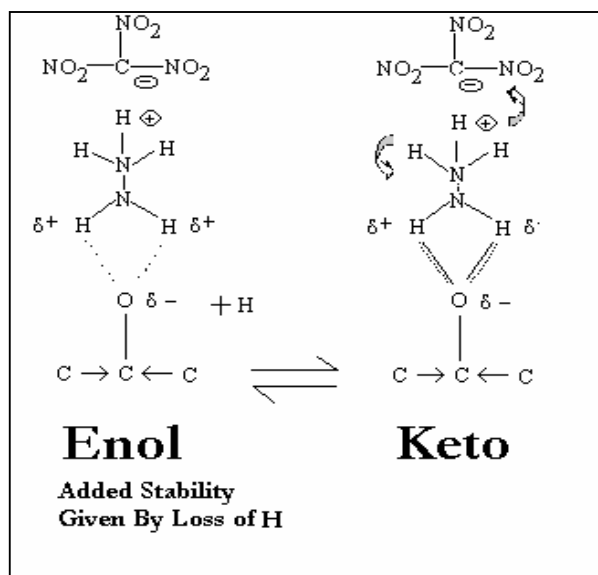
Figure 14 – Enol – Keto Tautomerism In Ketone Containing Compounds And Its Possible Affect On HNF Stability

In the keto form, HNF degradation via proton transfer is more likely compared to reaction in the enol form. The hexanone used within the trials is a liquid at room temperature and so enol / keto transitions are viable as a potential reaction course during elevated temperature storage ageing.

The differences between ketone and aldehyde reactivity with HNF highlights the possible effect of an extended molecular structure modifying charge delocalisation on any intermediate formed. The apparent differences between the compatibilities of the 1 and 2-hydroxy alcohols may also be related to the ability to delocalise the charge over any intermediate structure. However, in that situation, the terminal hydroxy position is superior to the β position in reducing reaction with HNF. This does not agree with the hypothesis of electron release from the carbon chain where a secondary intermediate would provide a great degree of stability. This suggests a steric effect is occurring or reaction is determined by the ease of release of hydrogen from the O-H structure. Further study would be required to investigate this effect.

Overall, various factors are proposed to affect the balance position between incompatibility and stabilisation including :-

1) Electronegativity of the reactive group on the secondary material and the resulting strength of electron cloud distortion
2) Stabilising effect of internal molecular structure of secondary material (eg electron releasing properties of carbon chain to which reactive pendent group is attached)
3) Possible ease of elimination of a small molecule in preference or in addition to adduct formation (eg loss of NO_2 from $RC-ONO_2$ in preference to formation of a H-O-H bond structure with the hydrazinium ion)
4) Possible stabilisation provided by ring formation

For a pendent group X-Y bonded at position Co on a carbon chain structure Cn --- Co --- Cm with chain electron releasing properties ΔHn and ΔHm, a hypothetical relationship can be written as :-

$$\Delta H_{total} = \Delta H \text{ (X-Y Cleavage)} - [n \times \Delta H \text{ (“Hydrogen Bond” Formation)}] + \text{Resonance Energy from Ring structure (if present)} + \Delta Hn + \Delta Hm$$

Where **n** is the number of bonds (hydrogen or otherwise) formed with ΔHf of these bonds likely to be closely related to the ability of the molecular structure to attract electrons. The relative value of this ΔH_{total} compared to the strength of the $[N_2H_5]^+$ $C[NO_2]_3^-$ bond would be expected to determine whether distortion of the electron cloud distribution would initiate HNF breakdown or pseudo stabilisation ie

If $\Delta H_{Total} > \Delta H_{Cleavage}$ Nitroformate / Hydrazinium Ion $\rightarrow$ Degradation of HNF

If $\Delta H_{Total} < \Delta H_{Cleavage}$ Nitroformate / Hydrazinium Ion $\rightarrow$ No Reaction or Possible Stabilisation

The stabilisation of the reaction intermediate from Figures 11A to 11E gives some level of elucidation of the effect of carbonyl groups and aids explanation of the results from the carboxyllic acid, ester or acid anhydride groups. All of these functional groups have potentially "reactive" oxygen groups available but show comparatively little reaction with HNF. This is proposed to be due to the reduction in the overall electron attraction of the molecule compared to the pure carbonyl structure. Within the carboxyllic acid, ester, and acid anhydride samples it is proposed that if reaction occurs, it is limited by charge delocalisation over the molecular bond structures. Table 1 does not give VTS data for the nitrate ester group although this would have been a valuable data point.

Similar arguments serve to explain the other results in Table 1 ie for hexonyl chloride, dihexylether and trans-5-decene. In hexanoyl chloride more extensive breakdown of HNF is observed than the carboxyllic acid as the chloride atom cannot distribute charge as effectively due to its lower electron affinity than an oxygen atom. In the ether structure, hydrocarbon chains reduce the dipole on the oxygen, reducing reactivity and also allowing hydrogen bonding to occur without hydrogen atom transfer or disruption of the hydrazinium / nitroformate bond. In the alkene structure, no reaction is observed as it is proposed that there is no tendency towards hydrogen transfer from the HNF structure. It is possible that within this structure, there is a degree of stabilisation provided by the alkene group as evidenced by the slight reduction in liberated gas during VTS testing. This stabilisation may be due to non-destructive, weak hydrogen bonding occurring in the structure.

From this hypothesis, for possible alkene stabilisation, it is possible to envisage a structure where the C-C bond is a multiple bond (ie an alkene or alkyne) and the higher electron density may aid formation of a ring structure via pendent groups eg in 2,3-dihydroxybut-2-ene and release of hydroxyl hydrogens (shown in Figure 15).
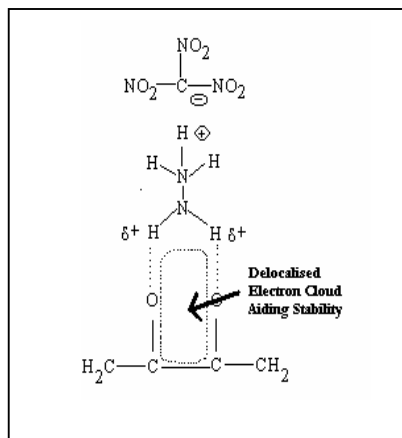
Figure 15 – Hypothetical Reaction Between HNF and 2,3-Dihydroxybut-2-ene

However, within this structure, the charge delocalisation might also cause the H-O hydrogen bonding to be excessively strong, potentially leading to cleavage of the nitroformate / hydrazinium ion bond.

For any secondary material it is proposed that, if charge delocalisation is possible but the electronegativity / dipole of the system is too high, full charge / proton transfer may occur leading to widespread breakdown of the HNF present. If charge delocalisation of the intermediate is possible and the dipole of the system is not too strong, it is proposed that covalent or hydrogen bonding may occur without breakdown of HNF. If this can occur with an associated elimination of a small molecule then this is beneficial for the overall longevity of the mixture.

If the interpretation of the data in Table 1 is correct, then it would be expected that HNF propellant longevity would be highly dependent on sample solid acidity / basicity and liberated water.

2 Studies of Crystalline HNF

The literature review given in Chapter 1 highlights various aspects of the ageing characteristics of crystalline HNF. Further investigation of crystalline HNF was thought to be beneficial to more closely elucidate some of its ageing behaviour and reactions. Increased focus onto the possibility of autocatalytic breakdown of HNF with its primary gaseous decomposition and also studies into potential interaction between crystalline HNF and common rocket motor chemical stabilisers were thought the most beneficial areas for study.

The following investigations were undertaken :-

1) Assessment of HNF purity and identification of contaminants by H-NMR
2) Semiquantitative assessment of gaseous products evolved from HNF during elevated temperature storage by use of selective colorimetric reagents.
3) Assessment of possible catalysis of solid HNF via interaction with gaseous HNF degradation products
4) Chemical compatibility analysis of HNF with 2NDPA, pNMA and nitrated derivatives of the two stabilisers by DSC
5) Study of gas/ solid interaction of HNF by GC-MS.

Results for these trials would then be combined to aid elucidation of an extended reaction course. The combination of a range of observations from analytical techniques to elucidate an overall reaction course is common within the explosive industry; Volk et al [120] , Petrzilek et al [121] and Bohn [122] [123] give typical examples.

2.1 Material Supply

2.1.1 HNF Samples

The sample of HNF chosen for the majority of this study was EVAP grade (Batch E9) purchased from APP bv, Klundert, The Netherlands. A small body of work was also undertaken on S/NS grade S13 and an "Improved Stability" grade Batch 23. After discussion with APP, initial concerns about degradation of the sample over the duration of this study were allayed. More recently, Schoyer et al [119] have shown from kinetic studies that "at normal room temperature, HNF can be safely stored for 100s of years" which confirms that ambient storage of the material should not change its chemical reactivity.

2.1.2 2NDPA, pNMA and Nitrated Derivatives of 2NDPA and pNMA

Samples of the chemical stabilisers 2NDPA and pNMA were supplied by ROXEL (Rocket Motors UK) Limited from production lots. Nitrated and Nitrosated derivatives of the stabilisers were supplied by the Laboratory Services Department at ROXEL (Rocket Motors UK) Limited from their stock of HPLC standards.

2.1.3 Hydrazine Scavengers

A number of active species (hydrazine, nitroform, nitrous oxides, ammonia etc) had been identified during the literature review as potential degradation products of HNF. Of these, hydrazine was perceived to be the most reactive and therefore a product requiring control. Audrieth and Ackerson [124] detail various potential stabilisers for aqueous hydrazine; it was proposed that these may have some applicability in reducing further hydrazine reactions if evolved from HNF. These materials were to act as hydrazine scavengers to remove the reactive species from the reaction vessel. By comparison of the recommended scavengers with the Merck catalogue [125] to assess availability, the materials shown in Table 2 were identified for assessment.

Sodium Sulphide Na_2S
Sodium Thiosulphite $Na_2S_2O_3$
Anhydrous Sodium Sulphite Na_2SO_3
Ammonium Carbonate $(NH_4)_2CO_3$
Sodium Thiocyanate $NaSCN$
Ammonium Peroxodisulphate $(NH_4)_2S_2O_8$
Quinol
Di-n-butylamine $(CH_3CH_2CH_2CH_2)_2NH_2$

Table 2 : Potential Hydrazine Scavengers For use in HNF Propellant Development

2.2 HNF Purity Analysis - ^{1}H-NMR Analysis of HNF EVAP Grade Batch E9

2.2.1 Experimental and Discussion

Analysis of EVAP grade HNF (Batch E9) was undertaken in solution using a Bruker ^{1}H-NMR Spectrometer DP x 250 at a solution concentration of 0.1g/10ml at a temperature of 300K. Samples were dissolved in Deuterated Dimethylsulfoxide for analysis with testing being undertaken over a frequency Sweep 0 - 4990 Hz against a standard of Tetramethylsilane over the 0-10ppm range. Figure 16 shows the initial ^{1}H-NMR spectrum.
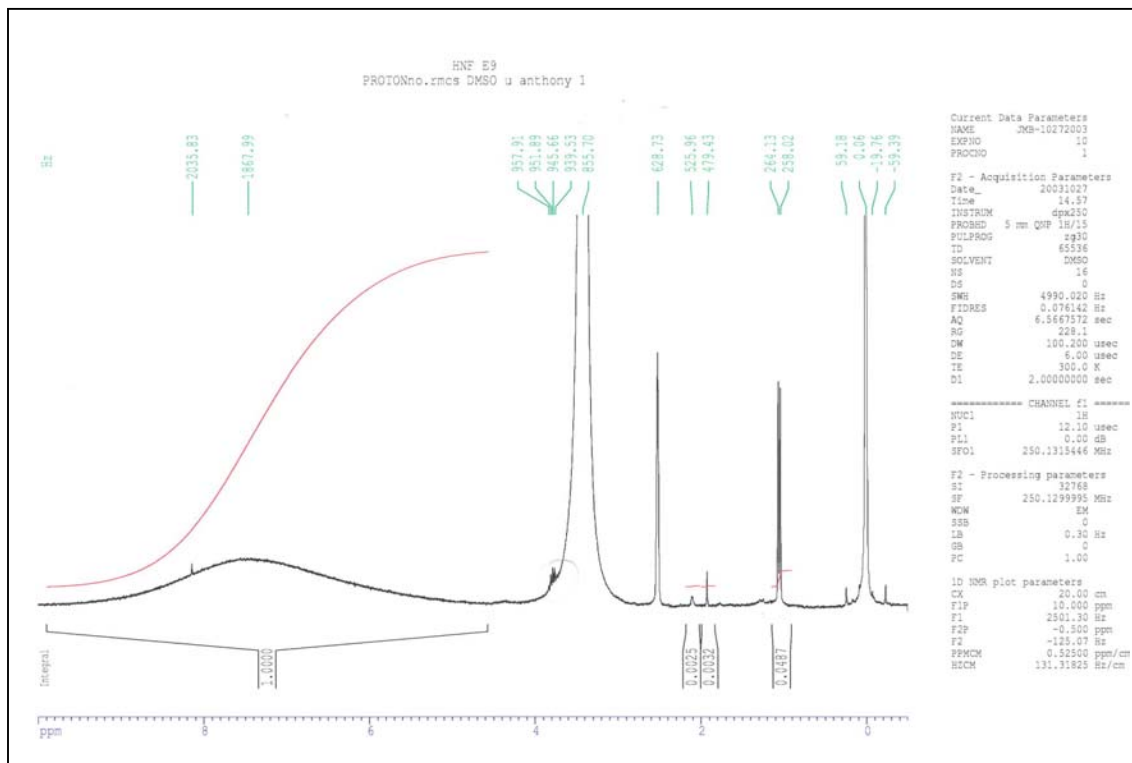
Figure 16 – H-NMR of HNF EVAP Batch E9 in Deuterated DMSO

From Figure 16, the sample response for the NH_3 group of HNF is observed as a wide peak centred at 7.4ppm. The second HNF peak attributable to NH_2 (and possibly water) is centred at 3.5ppm. However, there are also a number of smaller peaks observed in the 0.0 – 3.5ppm range. Expansion of the spectrum in this region is shown in Figure 17. The peak centred at 2.5ppm has been attributed to an impurity of non-deuterated DMSO present within the deuterated DMSO solvent. The second doublet of peaks at 1.1 and 1.05ppm is attributed to an impurity in Isopropyl Alcohol (IPA). The source of this IPA was attributed to the HNF sample under analysis and so was identified as the primary impurity retained from the manufacturing process.
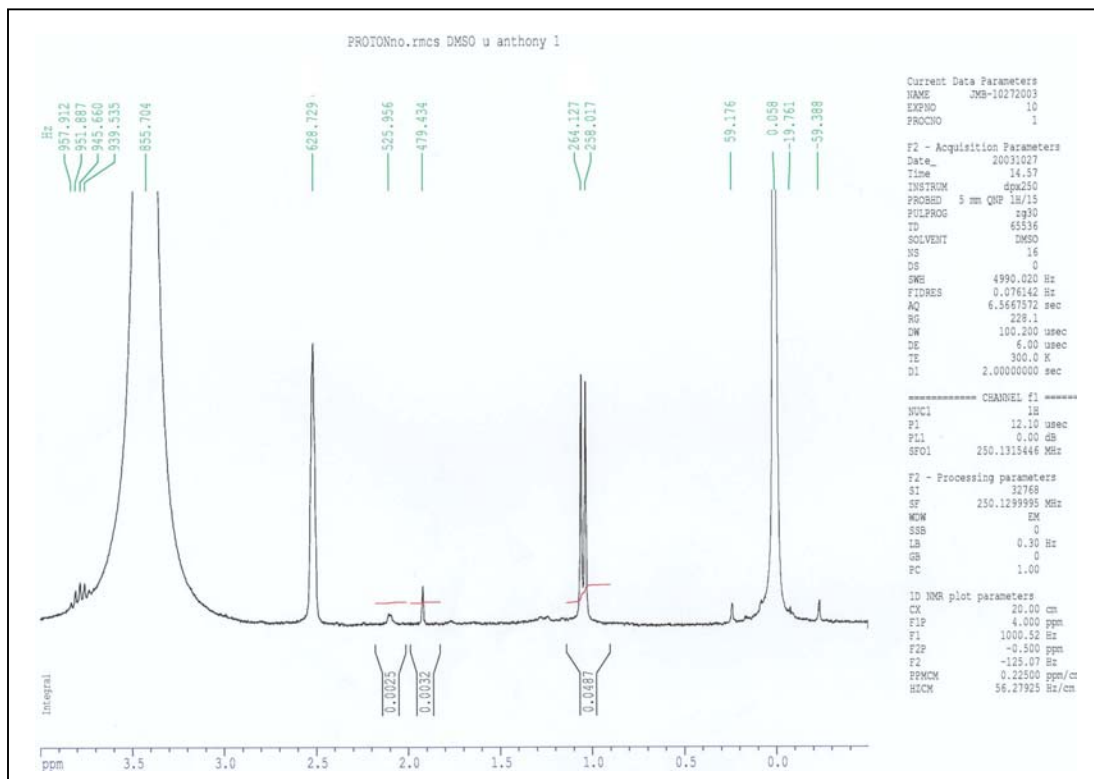
Figure 17 – Expansion of ^{1}H-NMR spectrum over 0 – 3.5ppm range

2.3 GASTEC Detector Tube Gas Analysis

2.3.1 Introduction

A consideration that has to be applied to any study into degradation chemistry is the possible effect of continued reaction of primary degradation species to form further products.   If further reaction does occur to remove the primary degradation species, then the concentrations of species determined at any time during any ageing period reflect the secondary reaction rather than the primary degradation course. This further reaction of degradation products can come from a number of sources. The most prevalent is due to the formation of a highly reactive product during the initial stages of chemical breakdown which in turn then reacts with other species in the test matrix. A second source is due to reaction of a reactive species during the analytical phase of the program (eg on-column reaction in GC-MS) or potentially non-detection of an analyte by a specific analytical method.

Within crystalline HNF degradation, the formation of hydrazine and nitroform via cleavage of the ionic bond structure must be viewed as a potential reaction course. Koroban [108] suggests that this is a possible route to the degradation of HNF. However, GC-MS work by Bellerby et al [104] and Pearce [92] have failed to detect hydrazine or nitroform directly during their studies,

possibly due to recombination of the analytes during either storage or analysis phases or possibly because the analytes are not liberated during ageing. Pearce [92] does detail that the carbon dioxide levels detected during his storage trial is "erratic" and suggests that this is due to the direct reaction of hydrazine with carbon dioxide (as given in Reaction R2) . However, more direct assessment of whether hydrazine was liberated (or not) was thought beneficial.

To this end, HNF samples stored at 60°C were assessed via the use of a series of colorimetric detection tubes sourced from DETECTAWL [102] under the trade name "GASTEC tubes". The use of these tubes was chosen in preference to GC in order to minimise gaseous recombination or decomposition reactions which might be observed during GC either pre- or post- injection onto the column. It had previously been established via discussion with Bellerby et al that the GC apparatus chosen to undertake gas analysis could not successfully separate and detect HNO_3, NO_2 and N_2H_4. For the storage trials, 0.25g samples of EVAP grade HNF were weighed into 10ml vials. A pierced septum cap was crimp fitted to the vial and the septum seal pierced sufficiently to allow introduction of the GASTEC tube whilst maintaining a tight seal. Samples were stored at 60° C in an air circulating oven. The tubes chosen for analysis were :-

     a)   Carbon Monoxide

     b)   Ammonia

     c)   Carbon Dioxide

     d)   Nitric Acid

     e)   Nitrogen Dioxide

     f)   Amines (non-specific)

     g)   Nitrogen Oxide (NO)

     h)   Hydrazine

as these analytes were thought to be the most likely to be formed from primary degradation reactions in HNF. No N_2O or nitroform tube was available so, although proposed to be a major product of HNF degradation, it was not possible to assess these species during the trials. The control sample for the trials was produced using an empty glass tube. Following storage, HNF samples were reweighed and mass loss during storage assessed. The experimental setup is as shown in Figure 18
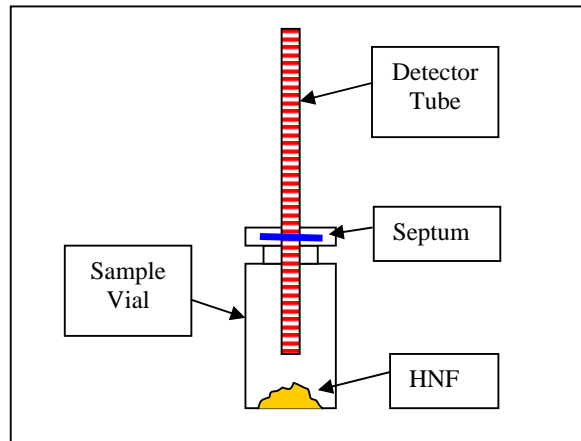
Figure 18 - Analytical Arrangement for GASTEC Detector Tube Analysis

2.3.2 Results and Discussion

The majority of the HNF samples aged visibly in similar ways with very little change in colour / form during storage. Some very light aggregation at the end of the storage period was the only evidence of ageing in most samples. However, the sample connected to the CO detector tube initially formed a small number of red / brown droplets on the inner walls of the sample vial and the HNF slowly discoloured during the test to a grey / yellow colour. This apparent breakdown of HNF during this trial indicates that the introduction of the GASTEC tube has adversely affected the HNF test sample stability. Work presented by Bellerby [104] has showed that the level of carbon monoxide liberated is very low during elevated temperature storage. This suggests that the high level of CO detected during the GASTEC tube trials is due to an interference effect (most likely between hydrazine and potassium palladosulfite $(K_2Pd(SO_3)_2)$ of the detector tube [126]). As such, although an additional colorimetric reaction is evident, it is proposed to be due to a secondary reaction or interferences and is not part of the HNF decomposition.

Figures 19 to 21 show the same test data on extended range axes for each of the HNF test samples up to 98 hours storage. Each sample detector tube continued to function throughout storage with the exception of the HNO_3 tube that became saturated at 25ppm after 72 hours storage. As a consequence, HNO_3 production might continue beyond the levelling off shown.
.
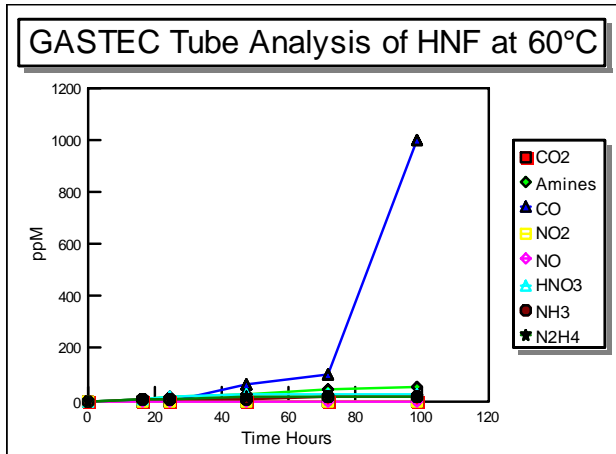
Figure 19 : Overall Gas Evolution Data from HNF at 60°C
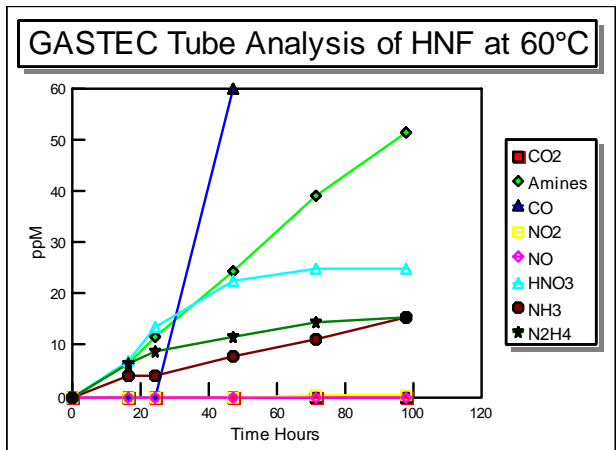
Figure 20 : Expanded Range Graph of Gas Evolution from HNF at 60°C
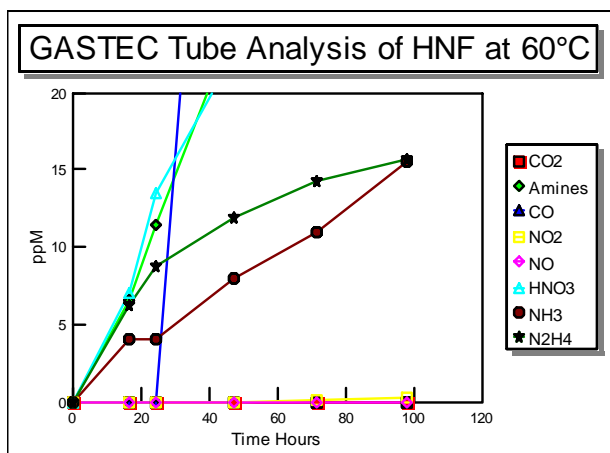
Figure 21 : Expanded Range Graph of Gas Evolution from HNF at 60°C

Figures 19-21 show some results for the species detected. These can be summarised as :-

1)   No detection of both CO_2 and NO during storage

2)   Total amine measurement does not total the sum of the ammonia tube + hydrazine tube measurements.

3)   The CO measurement suggests that the evolution of CO does not occur until after 24 hours storage but beyond this storage time CO is the major degradation species detected. However, as detailed above, this is proposed to be due to a chemical interference from another species reacting with the colorimetric reagent.

4)   Hydrazine evolution occurs comparatively rapidly in the early stages of storage but the rate of evolution decreases over time.

5)   Detection of HNO_3 and Amines is observed at similar rates prior to saturation of the HNO_3 detector tube.

6)   Evolution of total amines, HNO_3 and possibly NH_3 appears at a constant rate during storage.

A number of different reaction types can be hypothesised to be encountered during the trial and can be summarised as :-

1)   HNF thermal degradation forms gaseous products and the GASTEC detector reagent causes no shift of decomposition equilibrium due to the removal of gas from the vial

2)   HNF thermal degradation forms gaseous products that are modified in the rate of evolution (i.e. accelerated or decelerated) due to removal of gaseous products by reaction with the GASTEC colorimetric reagent.

3)   Reagents within the GASTEC tube volatilise and permeate into the HNF vial leading to either no reaction or a positive or negative effect on HNF degradation due to the GASTEC reagent chemical reactivity.

4)   HNF degradation products recombine within the vial to form secondary gaseous products which are either undetected or produce spurious results

2.3.3 Mass Loss From HNF Samples During GASTEC Tube Studies

Table 3 details the measured gaseous concentration and mass loss from the test samples.

GASTEC Tube	% Mass Loss	Average Mass Loss (%)	Mean Measured ppm	RMM of Analyte	Mean ppm / RMM	Molecular Ratios of Mass Losses
CO_2	7.94	7.4	0	44	0	0
CO_2	6.95					
NH_3	0.92	0.85	13	17	0.76	1.9
NH_3	0.78					
NO	7.55	7.8	0	30	0	0
NO	8.1					
N_2H_4	1.01	1.3	15.63	32	0.49	1.2
N_2H_4	1.64					
Amines	1.29	1.2	58	----	----	
Amines	1.1					
HNO_3	2.01	1.85	25	63	0.4	1
HNO_3	1.7					
NO_2	7.29	7.16	0.3	46	0	0
NO_2	7.04					
Control	1.38	1.48				
Control	1.57					
CO	14.35	14.68	1000	28	35.7	89 (XS)
CO	15					

Table 3 : Ratio Of Mass Losses From HNF During GASTEC Tube Assessment (Shaded Area Is Proposed To Be Due To A Contamination Or Colorimetric Interference).

Relating the mass loss data to the GASTEC tube measurements, a number of reaction hypotheses were tested :-

1)   If mass loss of sample was ~ 1.5% (ie the same as the HNF control sample) and the GASTEC tube read 0 ppm then the analyte was not present and no effect on HNF degradation has occurred. From the data in Table it can be seen that no stored sample showed this reaction condition.

2)   If mass loss from sample was ~1.5% and GASTEC tube read > 0 ppm then the analyte was potentially present and analyte removal did not alter HNF decomposition mechanism. Also, the contents of GASTEC tube did not appear to react with HNF. No sample stored showed this reaction condition exactly although the HNO_3 tube did show some degree of this type of reaction.

3)   When mass loss was > 1.5% and the GASTEC tube read 0 ppm then it suggested that the volatilisation of the tube content accelerated HNF decomposition. The results from the CO_2, NO and NO_2 tube trials suggest that this occurred within these storage samples. A secondary proof of the detrimental effect of hydrazine on HNF stability is that the CO_2 tube utilises hydrazine in its colorimetric detection. Liberation of this hydrazine gave a reduced stability of the HNF present with in the test vial.

4)   When mass loss was > 1.5% and the GASTEC tube read > 0 ppm then the removal of the analyte potentially accelerated HNF decomposition or the volatilisation of the tube contents accelerated HNF decomposition. The CO tube sample showed this type of reaction course. However, CO liberation was only observed to occur after a lengthy storage period suggesting that tube contents (and its associated reaction with HNF) was not responsible for the CO liberation. However, the observation that droplets of liquid are seen solely within this test sample highlighted that some additional reaction was occurring in this test sample compared to the others.

5)   Mass loss < 1.5% and tube reading > 0 ppm. The removal of this species from the reaction vessel (or conversely, the presence of the GASTEC tube contents) potentially improved the stability of the stored HNF. Ammonia, hydrazine and amines tubes all showed this type of reaction.

All of these reaction courses are complicated by competing reactions and interferences on the GASTEC colorimetric species. However, in a simplistic assessment, the results suggest that autocatalysis may occur due to the presence of amine based species whereas HNO_3 removal has little effect on stability.

The final column of Table 3 relates the measured ppm value to the RMM of the analyte. From these data, a molar ratio of HNF degradation species is suggested. If the previous assumptions are applied (e.g. that no interferences except CO are observed) then the ratio of species potentially evolved during the initiating degradation process is proposed to be :-

$$1 \text{ } HNO_3 : 1.2 \text{ } N_2H_4 : 1.9 \text{ } NH_3 : + \text{ An Unidentified Amine}$$
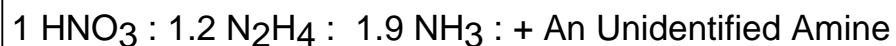
(Reaction R8)

These results were normalised to :-

$$[N_2H_5] \, [C(NO_2)_3] \quad 1HNO_3 : 1N_2H_4 : 2NH_3 : + \text{Unidentified Amine}$$
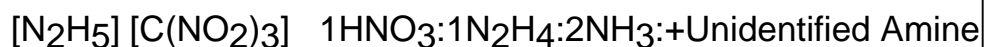
From Figures 19 to 21, it appears that the liberation of HNO_3, N_2H_4 and NH_3 are concurrent. For concurrent liberation to occur, and for decomposition products to follow the ratio given, the degradation is unlikely to be unimolecular. This agrees with the work of Brill [98], Bellerby [104] and Koroban [108], all of which suggest a di- or tri-molecular decomposition scheme.

The presence of hydrazine does help elucidate some possible secondary effects within the ageing profile. Schmidt [103] details various oxidation mechanisms for hydrazine; these are :-

$$N_2H_4 \longrightarrow NH_3 + N_2$$
$$\searrow N_2 + N_2H_4$$
$$\searrow HN_3 + NH_3$$
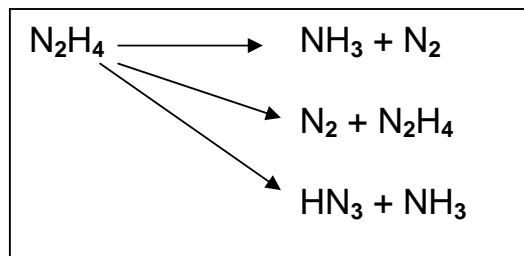
Each of the oxidation reactions progresses via the formation of a concatenated Nitrogen intermediate, all of which have amine groups within their structure. The structures suggested by Schmidt are :-

$$H_2N\text{-}NH\text{-}NH\text{-}NH_2$$
$$H_2N\text{-}N=N\text{-}NH_2$$
$$HN=N\text{-}NH\text{-}NH$$
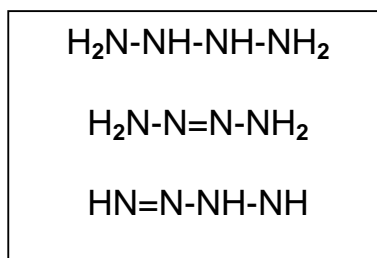
The oxidation schemes help explain the ammonia detected during these trials and also the Nitrogen detected by Bellerby [105] and Pearce [92] during their HNF ageing studies. The differences between the total amine levels detected by GASTEC analysis and the values of the sum of the ammonia and hydrazine tubes may be related to the detection of one or more of the reaction intermediates of the hydrazine reduction. Schmidt also details the gas phase reaction of hydrazine with oxygen as :-

$$N_2H_4 + O_2 \longrightarrow N_2 + 2H_2O$$
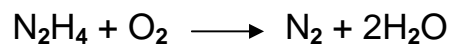
This may also help elucidate one source of water as detected by Bellerby et al during their ageing studies [105] . However it is also possible that a second reaction detailed by Schmidt [103] between hydrazine and nitrogen-containing oxidisers is the source of water production (especially within the final propellant formulations where HNOx and NOx species will be present).

$$N_2H_4 + HONO \longrightarrow HN_3 + 2H_2O$$
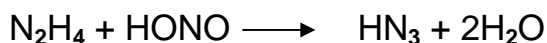
Liberation of nitrous acid during HNF degradation has been suggested by Bellerby et al [104] as an important reaction step during the thermal decomposition of HNF. Overall, the high reactivity of hydrazine with itself and other species does suggest its presence within the HNF sample would be detrimental to sample longevity.

However, the presence of HNO_3 appears unlikely within the degradation as no other researcher has detailed detection of this analyte. Closer inspection of the colorimetric reagent tube highlighted that the it functioned via reaction with a Hammett indicator:-

4-Phenylazodiphenylamine+Nitric Acid→ Red Purple

ie a non-specific reaction for any acidic species [126] . The hydrazine scheme degradation given above gives a reaction course via the formation of hydrazoic acid (HN_3) and it is proposed that this may be the acidic species detected during by the HNO_3 tube the analysis.

From the limited trial data achieved within the trial, the ageing of HNF at 60°C is hypothesised to be characterised by :-

HNF → Hydrazine → Amine Intermediate → Ammonia + Nitrogen + Hydrazoic Acid
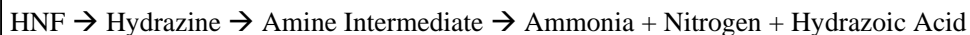
Hydrazoic acid would then be expected to react further via reaction R15 to form nitrogen, nitrogen oxides and water [127] .

$$HN_3 + xO_2 \longrightarrow H_2O + \quad Y$$

If $x = 0.5$, $Y = 3/2\ N_2$

If $x = 1.0$, $Y = 3/2\ N_2O$

If $x = 7/2$, $Y = 3NO$

If $x = 13/2$, $Y = 3NO_2$

If $x = 13/2$, $Y = 3/2N_2O_4$

<div align="right">
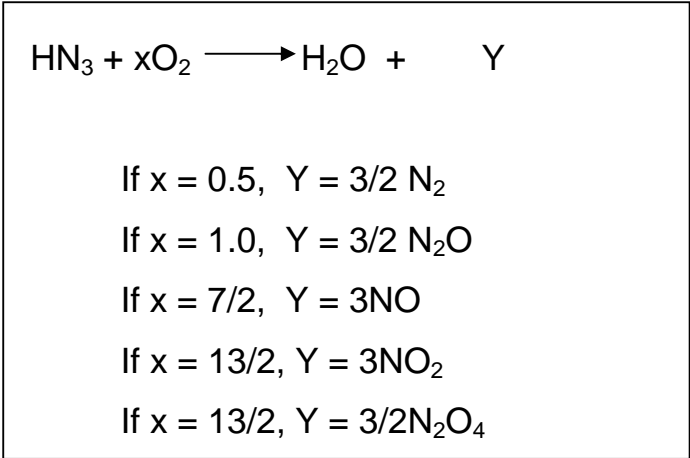
(Reaction R15)

</div>

Overall, this suggests an underlying thermal degradation scheme for HNF of

$$HNF \longrightarrow N_2H_4 + \quad NH_3 + \text{Unidentifed Amine}$$

with $+ O_2$ branch giving $N_2 + H_2O$ and $+ HONO$ branch giving $HN_3 + H_2O$.

<div align="right">
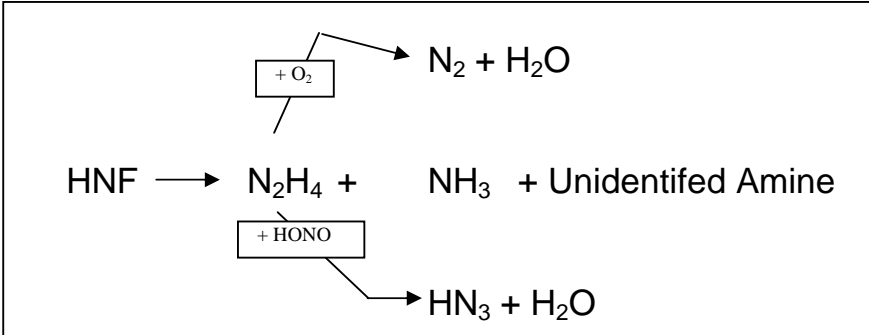
(Reaction R16)

</div>

2.4 DSC Analysis to Assess Potential Gas / Solid Catalysis of HNF Degradation

2.4.1 Introduction

Previous trials [110][111] have indicated some degree of autocatalysis in the decomposition of HNF during ageing. In order to elucidate the level of autocatalysis present, a series of HNF samples were analysed by DSC to assess the effect of gaseous degradation products on HNF stability. Assessment of 3 HNF grades (EVAPoration Grade Batch E9, Solvent / Non-Solvent Grade Batch S13, and the new "Improved Stability" grade batch HNF-23) were carried out over a range of heating rates, both in sealed (unpierced) and open (ie without lids) DSC pans. Samples were also assessed in the form that they were originally received and also after dry grinding. Assessment of the sample results in terms of the exothermic peak temperature and exotherm peak integration (assigned to enthalpy of decomposition) were carried out.

2.4.2 Experimental

Approximately 0.7mg of HNF was analysed using a Mettler TA-4000 with STAR^e thermal analysis system and tested following the various thermal profiles detailed in Table 4. Prior to initiation of the thermal ramp, a 2 minute settling time was undertaken at the lowest part of the ramp to allow temperature equilibration. All analyses were undertaken in a stagnant air atmosphere utilising Mettler DSC pan type 1, sealed and unpierced (for sealed sample trials) or pan type 1 unsealed (ie with no lid) for unsealed sample trials. Control and post analysis data assessment was undertaken using the Mettler STAR^e semi-automatic data assessment system.

2.4.3. Results and Discussion

Table 4 shows details of the various thermal profiles chosen for investigation; Table 5 shows results of the analysis in each of the test regimes. Figures 22 to 28 show the results in graphical form.

Pretreatment	**Sample Confinement**	**Heating rate (K/Min)**
None	Open Pan	0.1
		1
		10
		20
None	Sealed, Unpierced Pan	0.1
		1
		10
		20
Ground	Open Pan	0.1
		1
		10
		20
Ground	Sealed, Unpierced Pan	0.1
		1
		10
		20

Table 4 – Test Conditions for DSC Solid / Gas Catalysis

Pretreatment	Sample Confinement	Heating rate (K/Min)	Pan Type	Trace Ref	Peak Temp (°C)	Exotherm Integration (J / g)
HNF E9	As Received	0.1	Open	8.205	114	1468
HNF S13	As Received	0.1	Open	8.222	112	1351
HNF-23	As Received	0.1	Open	8.201	114	1256
HNF E9	As Received	0.1	Sealed	8.209	109	4339
HNF S13	As Received	0.1	Sealed	8.224	108	3868
HNF-23	As Received	0.1	Sealed	8.196	113	856
HNF E9	Ground	0.1	Open	8.243	113	3750
HNF S13	Ground	0.1	Open	8.266	115	1136
HNF-23	Ground	0.1	Open	8.277	114	1360
HNF E9	Ground	0.1	Sealed	8.250	108	4231
HNF S13	Ground	0.1	Sealed	8.270	108	3699
HNF-23	Ground	0.1	Sealed	8.278	108	4060
HNF E9	As Received	1	Open	8.207	125	1663
HNF S13	As Received	1	Open	8.240	123	1467
HNF-23	As Received	1	Open	8.197	123	1373
HNF E9	As Received	1	Sealed	8.208	123	3436
HNF S13	As Received	1	Sealed	8.242	122	3477
HNF-23	As Received	1	Sealed	8.198	123	3048
HNF E9	Ground	1	Open	8.248	123	1440
HNF S13	Ground	1	Open	8.268	123	1522
HNF-23	Ground	1	Open	8.275	123	1447
HNF E9	Ground	1	Sealed	8.249	123	3325
HNF S13	Ground	1	Sealed	8.269	123	3343
HNF-23	Ground	1	Sealed	8.276	124	3413
HNF E9	As Received	10	Open	8.204	142	1711
HNF S13	As Received	10	Open	8.241	139	1708
HNF-23	As Received	10	Open	8.199	139	1889
HNF E9	As Received	10	Sealed	8.206	142	2205
HNF S13	As Received	10	Sealed	8.226	150	3226
HNF-23	As Received	10	Sealed	8.200	141	2754
HNF E9	Ground	10	Open	8.246	139	1867
HNF S13	Ground	10	Open	8.253	141	1615
HNF-23	Ground	10	Open	8.273	140	1831
HNF E9	Ground	10	Sealed	8.247	142	2500
HNF S13	Ground	10	Sealed	8.267	141	2951
HNF-23	Ground	10	Sealed	8.274	142	2828
HNF E9	As Received	20	Open	8.202	144	1932
HNF S13	As Received	20	Open	8.223	144	2294
HNF-23	As Received	20	Open	8.194	143	1546
HNF E9	As Received	20	Sealed	8.203	145	2371
HNF S13	As Received	20	Sealed	8.225	150	1979
HNF-23	As Received	20	Sealed	8.195	150	2399
HNF E9	Ground	20	Open	8.244	145	2658
HNF S13	Ground	20	Open	8.251	143	1648
HNF-23	Ground	20	Open	8.271	145	1869
HNF E9	Ground	20	Sealed	8.245	149	1440
HNF S13	Ground	20	Sealed	8.252	149	3061
HNF-23	Ground	20	Sealed	8.272	149	2985

Table 5 : HNF Decomposition Data

The following trends were determined from the Figures 22 – 28 :-

2.4.3.1 Trends in DSC Peak Temperature Data

1) From Figure 22 the nearer horizontal the data, the less variation is present between sample grades. It can be observed that peak temperature was generally similar for all sample grades within any set of test conditions.
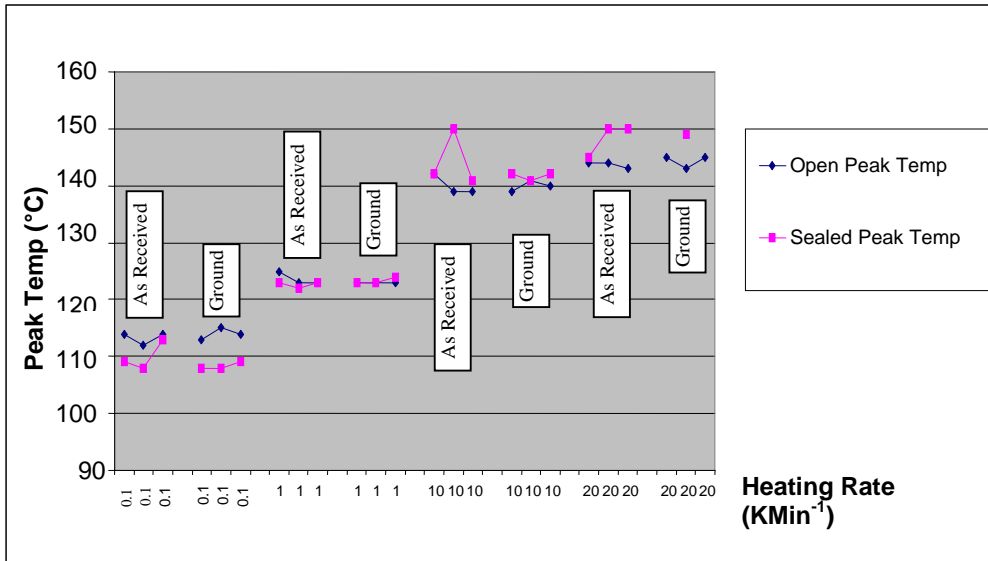
Figure 22 – Variation in HNF Mean Peak Decomposition Temperature With Heating Rate (Left to Right Across Each Data Set Order of Grades for Data is EVAP, S/NS, Improved Stability)

2) Figure 22 also suggests that there was a change in peak temperature at the extremes of testing conditions between open and sealed conditions. At the lowest heating rate (0.1K/min) sealed samples show a lower peak temperature value compared to open samples. At 20K/min, the reverse is apparent with sealed samples showing higher peak values compared to the open pans.

3) From Figures 22 and 23, as the heating rate is increased, there is a shift towards higher values for the decomposition peak temperature. This is a characteristic of the test method and is due to the changes in the rate of energy deposition into the sample; higher heating rates lead to an increase in the hysterisis observed between the measured (cell) temperature and the actual (sample) temperature, appearing to shift thermal events to higher temperatures.
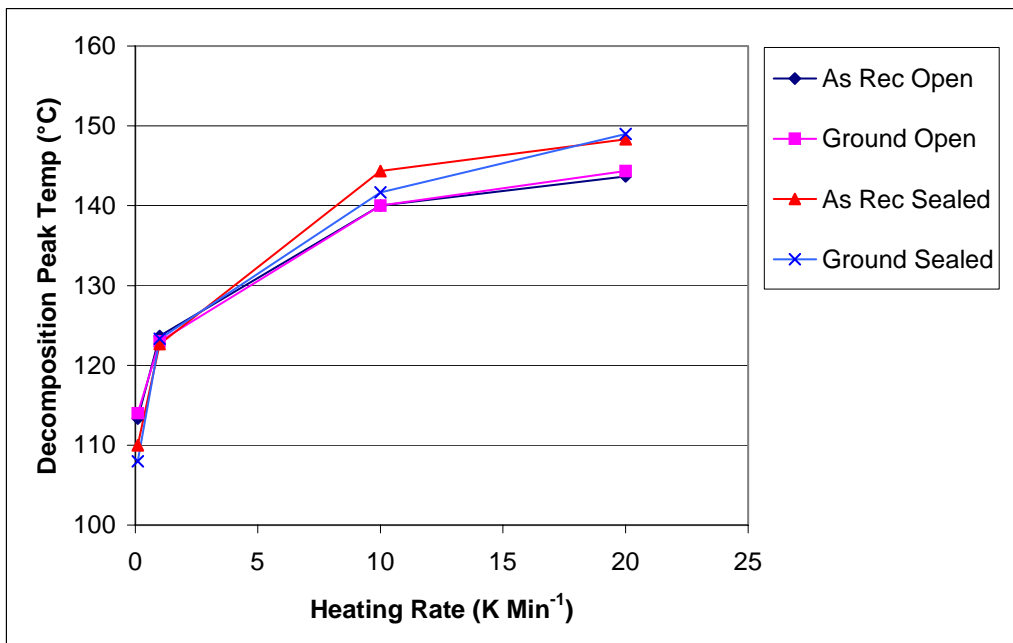
Figure 23 – Variation in HNF Mean Peak Decomposition Temperature With Heating Rate
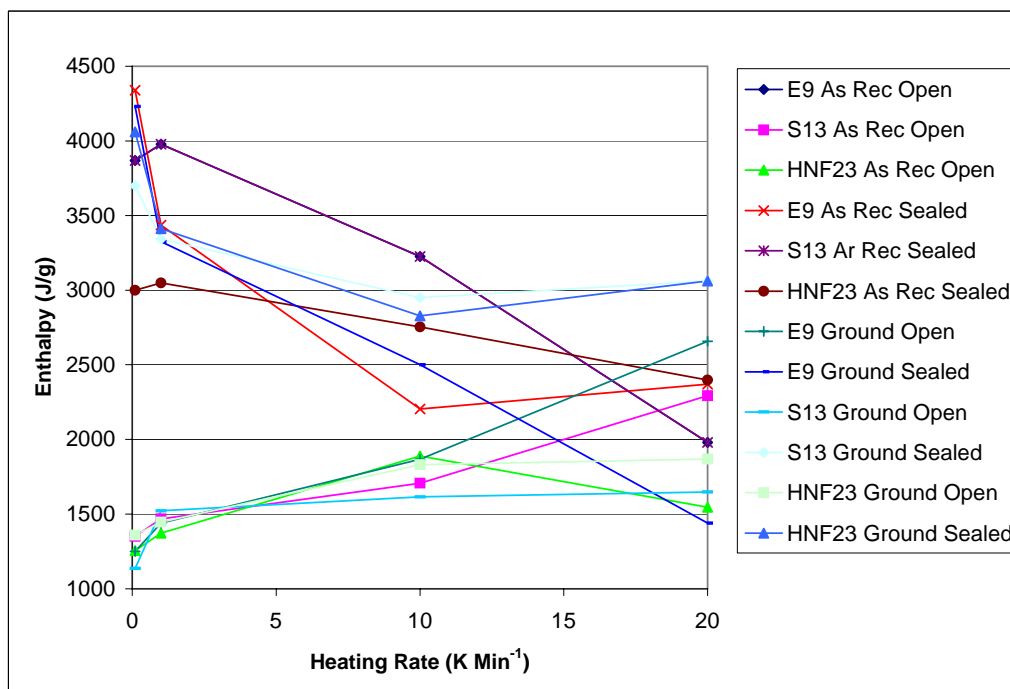
Figure 24 – Variation In Decomposition Enthalpy With Sample Type and Test Conditions
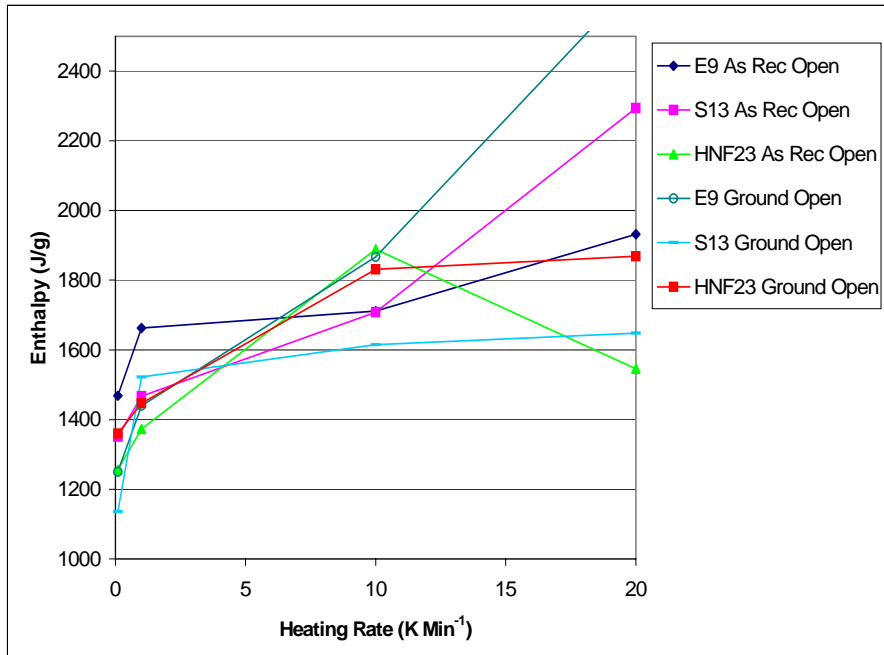
Figure 25 – Variation in HNF Decomposition Enthalpy With Heating Rate – Open Pan Samples
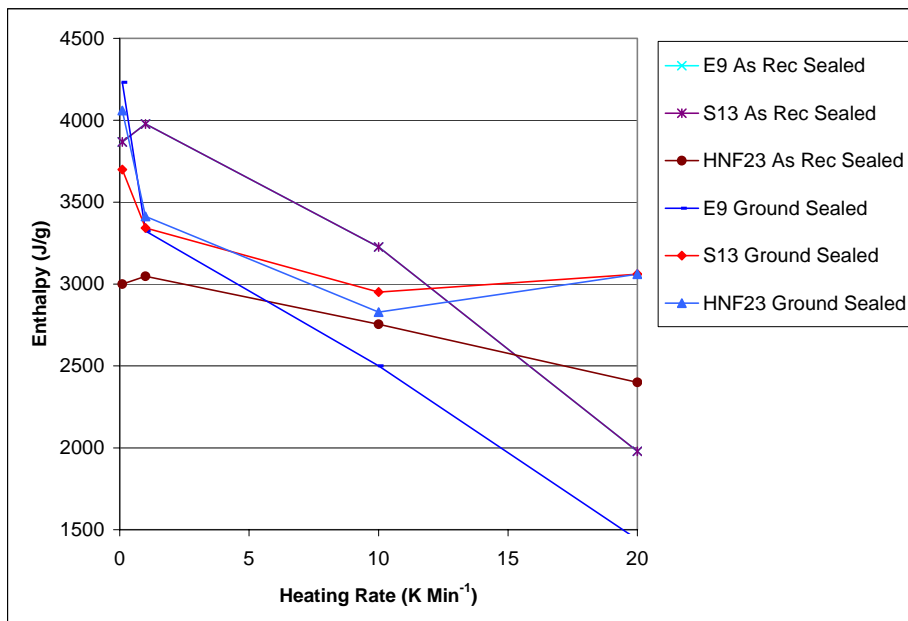
Figure 26 – Variation in HNF Decomposition Enthalpy With Heating Rate – Sealed Samples
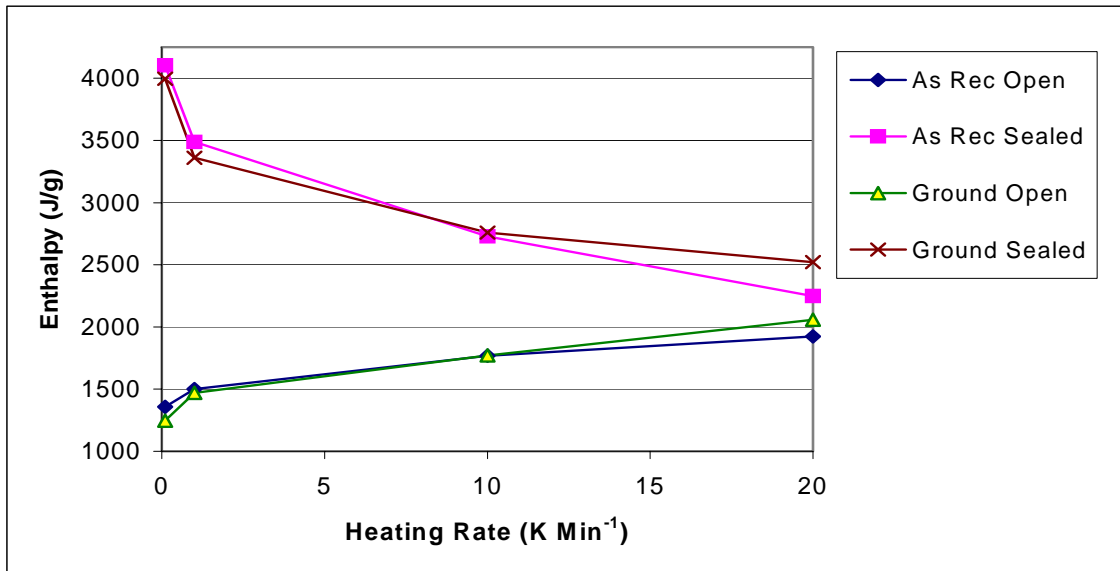
Figure 27 – Mean HNF Decomposition Enthalpy Values for Sealed and Open Conditions for HNF in Ground and As Received Conditions
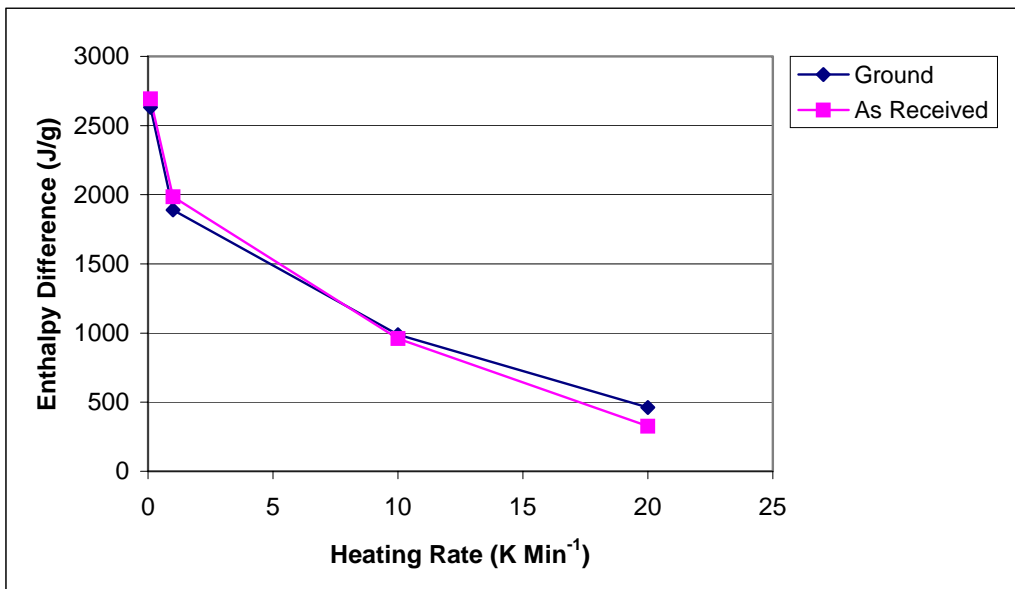
Figure 28 – Mean Differences in Enthalpy of Decomposition for HNF in Sealed and Open Conditions During DSC Analysis

Although not shown on Figures 22 to 28, increased heating rate leads to detection of an initial endothermic event being observed immediately prior to the decomposition endotherm. This can be seen on Figures 29-32 for HNF undergoing heating at 20K min⁻¹.

Figure 29 - HNF S13 As Received 20K/min – Open Pan
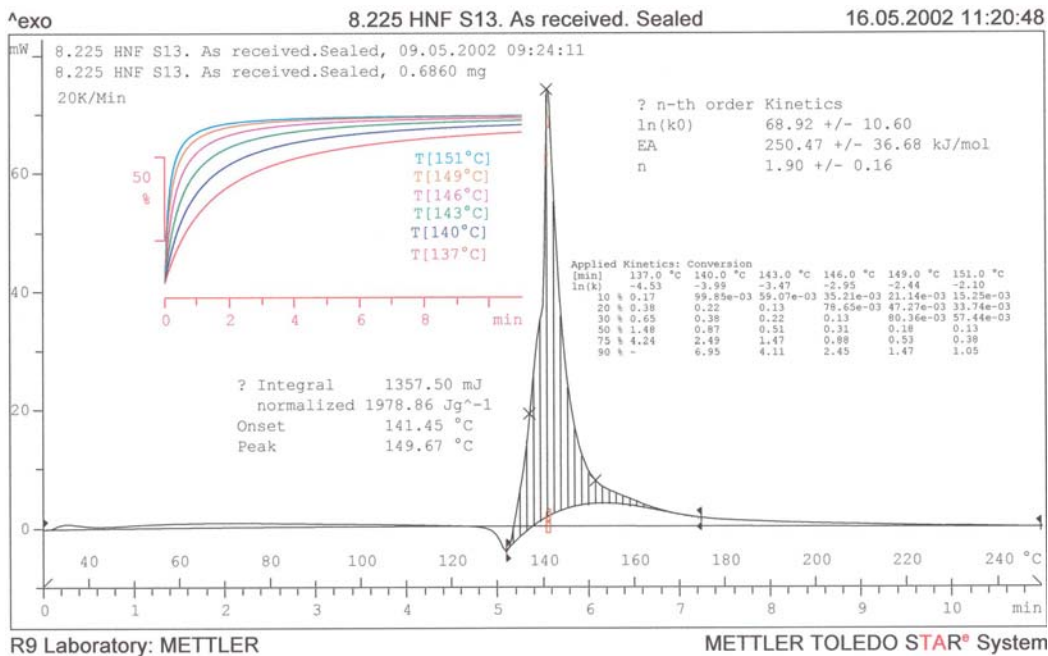
Figure 30 - HNF S13 As Received 20K/min – Sealed Pan
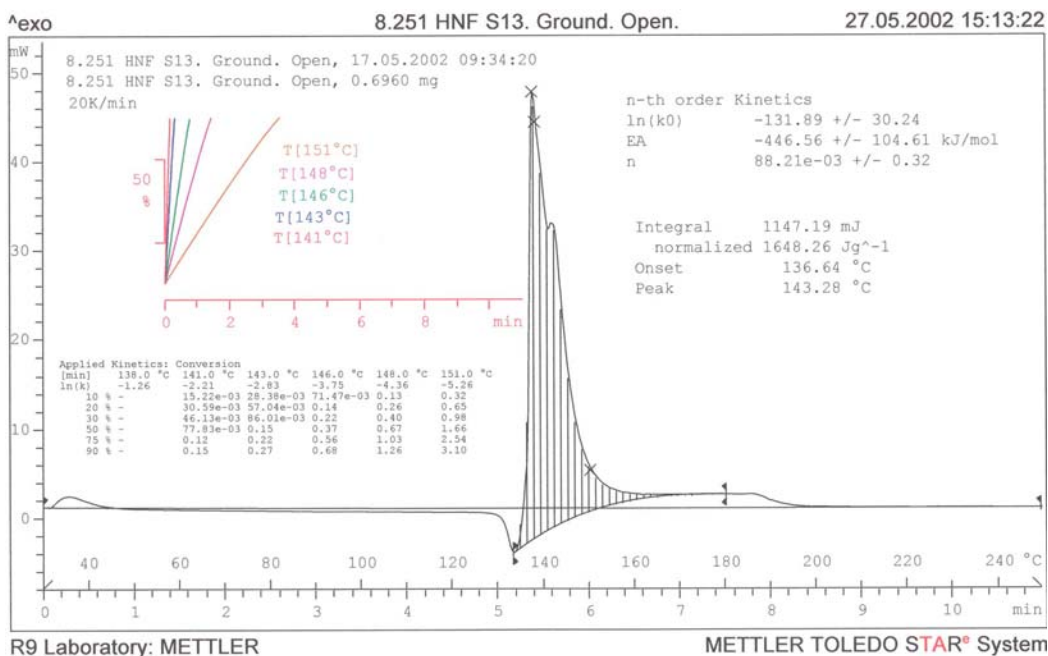
Figure 31 - HNF S13 Ground 20K/min – Open Pan

This endotherm is generally attributed to the presence of a melting endotherm or a solid / gas initiating reaction. The endotherm is not observed at lower heating rates as the slower rate of change of the endothermic event being more easily compensated for by the test equipment. This loss of endotherm can be seen on Figures 33-35.
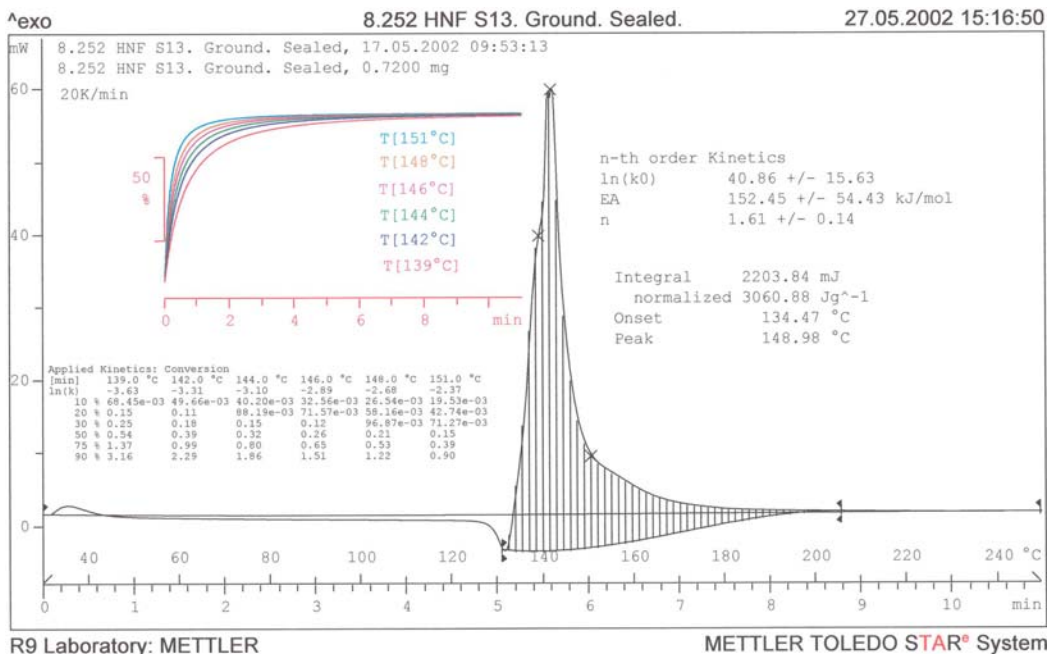
Figure 32 - HNF S13 Ground 20K/min – Sealed Pan

From Figures 22 and 23, there appears to be little difference between responses from samples in the ground or as received state.

2.4.3.2 Trends in Enthalpy Data

1)   From Figure 24, it is observed that there is a separation of the test samples into two groups; one from open samples and one from sealed samples (with the open pan samples showing lower enthalpy values)

2)   Figures 25 and 26 suggest that at many heating rates there is a lower degree of spread in enthalpy values in open conditions compared to sealed conditions.

3)   There are some differences observed between enthalpy values between different grades of HNF within any one set of test conditions. This is proposed to reflect an experimental error term. The spread of data is accentuated at higher heating rates which is indicative of an accentuation of experimental error. It may possibly be indicative of a change in reaction mechanism but the source of any variation is unclear.

4   Figure 27 shows the mean data for each set either, open, sealed, ground or as received. The data suggests that there was comparatively little change in mean enthalpy values achieved by grinding. This is confirmed in Figure 27 that shows the differences between mean enthalpy values for all samples in the two conditions, ground and as received. The similarity of the traces suggests that the differences between the data sets is near constant over the heating rate range.

2.4.3.3 – Overall Discussion of DSC Data

For a gas / solid or solid / solid reaction scheme for HNF degradation to be autocatalytic, the simplified reaction scheme below would be required to be occurring during storage.

Initiation   A $\longrightarrow$ B + C At Rate 1 and Enthalpy $\Delta H1$

Propagation B + A $\longrightarrow$ B + D At Rate 2 and Enthalpy $\Delta H2$

Catalysis

A = Initiation Species B = Reactive gaseous product   C and D = Unreactive Solids
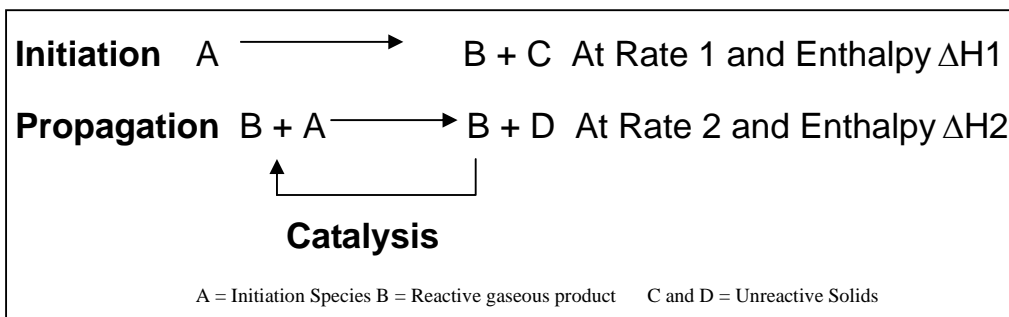
In this reaction scheme, the concentration of B is the driving force if Rate 2 > Rate 1 (where Rate 1 is the rate of thermal decomposition of the species A)

If however a self-limiting reaction was to be occurring but still with liberation of a reactive species B, the simplified reaction course would follow the reaction scheme :-
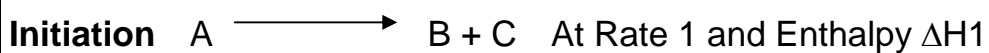
Initiation   A $\longrightarrow$ B + C   At Rate 1 and Enthalpy ΔH1

Propagation   B + A $\longrightarrow$ D   At Rate 2 and Enthalpy ΔH2

A = Initiation Species B = Reactive gaseous product   C and D = Unreactive Solids

In this reaction scheme, the concentration of A is the driving force for the reaction, regardless of the reaction rate of either initiation or propagation steps. Thus liberation of B would lead to increased decomposition of A via the propagation step but would not lead to any further decomposition until the initiation reaction was undertaken again.

The test data shows that ground samples show little or no difference in thermal profile from samples that are tested in the "As Received" state. This initially suggests that catalysis (if present) is not affected by surface area. This would suggest that any gas / solid reaction that may be occurring in the sample pans does not significantly catalyse sample decomposition. The apparent lack of sensitivity to surface area effects suggests that, if catalysis does occur within HNF decomposition, it is more likely to be occurring within a condensed phase.

The differences observed between sealed and unsealed conditions aids the interpretation of the contribution of any gas / solid interaction. However, the test data is complicated by the differences in peak profile for the two test conditions. The main trends that can be observed in the thermal traces are a general decrease in sample peak temperature (as shown in Figure 23) and an enthalpy trend either upwards (Sealed Conditions) or downwards (Open Conditions) (Figure 27) with heating rate. These trends are general artefacts of the instrumental design and operation. Adams and Wagstaff [128] showed that this reduction of measured decomposition temperature was observed with a range of energetic materials; the HNF decomposition profile (shown in Figure 23) mirrors these studies. The trend is explained by the relative rate of energy deposition into the sample at different heating rates. However, even with consideration of this instrumental effect, there does appear to be some very slight difference between the decomposition peak temperature for items at 0.1K/min between the open pan and sealed conditions. This reduction in peak temperature initially appears to indicate that there is a degree of gaseous catalysis associated with the HNF degradation (ie retention of gaseous products changes the decomposition mechanism

therefore leading to decomposition at a lower temperature). However, it is difficult to assign this unequivocally. It is possible that the differences between peak temperatures is attributable to the different energy densities present in the samples (ie the retention of gaseous species leads to a relatively higher energetic system than the open pan system). This lower level of energy available is proposed to lead to a retardation of breakthrough of any activation energy barrier thus moving detection to relatively higher temperatures. The enthalpy differences observed between sealed and open conditions (and the energy available within the sample pan) are attributable to either :-

1) associated with energy losses due to the liberation of gaseous products, removing energy from the system on rapid diffusion thus modifying enthalpy changes in open environments, or

2) a change in reaction course to a higher energy decomposition

For a change in reaction course to occur and to be dependent on the retention of gaseous products, the products must contribute to the enthalpy of decomposition. This is best achieved if the gases retained within the pan were available for further reaction / decomposition (eg reactive heteroatomic molecules such as hydrazine but not "inert" gases such as nitrogen). Retention of these products (and their availability to contribute to the overall decomposition) would be expected to modify the measured enthalpy values; this would suggest that conclusion 2 above may be valid. Interestingly, the closer convergence of enthalpy values with heating rate (Figure 24) between open and sealed pans suggests that there is greater overlap in enthalpy values at higher heating rates. This would suggest that any contribution of energetic gaseous products is lessened within these samples. This would suggest a reaction course as shown in Figure 39.

At lower heating rates, gaseous products are present for some considerable time within the sample pan prior to decomposition (ie if the gaseous products only occurred close to the decomposition temperature, they would not have time to be lost by open pan samples. At 20K/min, gaseous products do not have time to form immediately prior to decomposition and thus the decomposition enthalpy is similar from both sealed and open conditions). This long contact time for low heating rate samples in sealed conditions would suggest that these products do not have a catalytic effect on decomposition.

Comparison of the 0.1K/min thermal traces (Figures 33 to 38) does show an interesting additional effect. In sealed conditions (Figures 34, 36 and 38), it can be observed that the front of the decomposition peak is not a smooth curve but shows a plateau region, whereas the peak is smooth on the open pan variants (Figure 33, 35 and 37). This plateau region is also seen on samples analysed at 1K min^{-1}.. This plateau region suggests an additional reaction mechanism is occurring within the sealed samples, which is not occurring in open conditions. This additional process then superimposes itself onto the smooth change observed in the open pan analogues. It can be seen that this additional reaction does not start at the peak temperature but has a long period of initiation. For example, Figures 35 (Open) and 36 (Sealed), show that the exothermic reaction starts at ~99°C before peaking at 112.3 and 107.9°C respectively. At a heating rate of 0.1K/min, this equates to a contact time of 130 min and 90 min of pre-reaction respectively. This may suggest that the reaction may not be true autocatalysis but be a self-limited reaction. If gas / solid catalysis was occurring, the high temperature and close proximity to the decomposition temperature involved in the test environment, would be expected to force this reaction to occur rapidly. Reaction would then be expected to lead to a rapid decomposition via an accelerating rate of decomposition. The traces do show an accelerating rate of decomposition (shown by the exponential rate curve front of the exothermic peak) but appears comparatively slow. This suggests that any reaction is a self limiting reaction scheme.
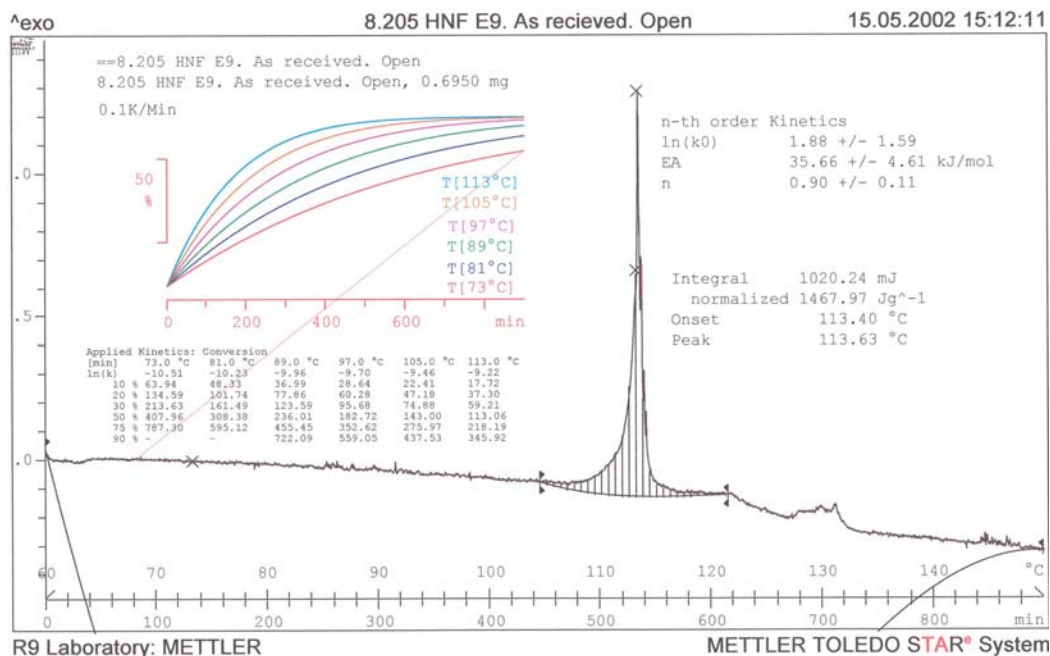
Figure 33 – HNF E9 As Received 0.1K/min – Open Pan

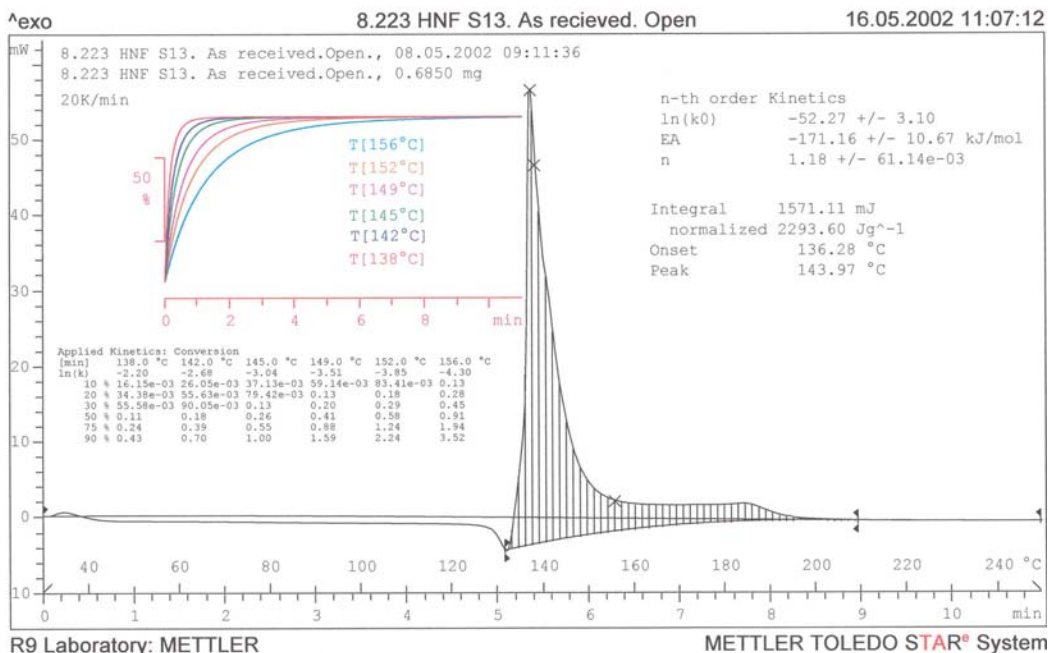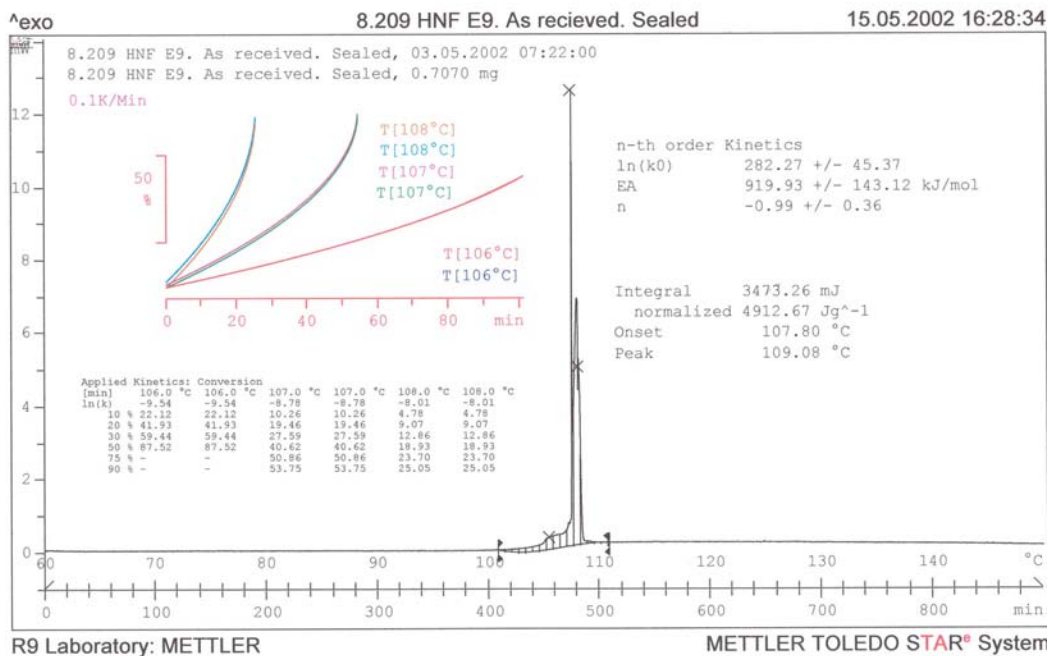Figure 34 - HNF E9 As Received 0.1K/min – Sealed Pan
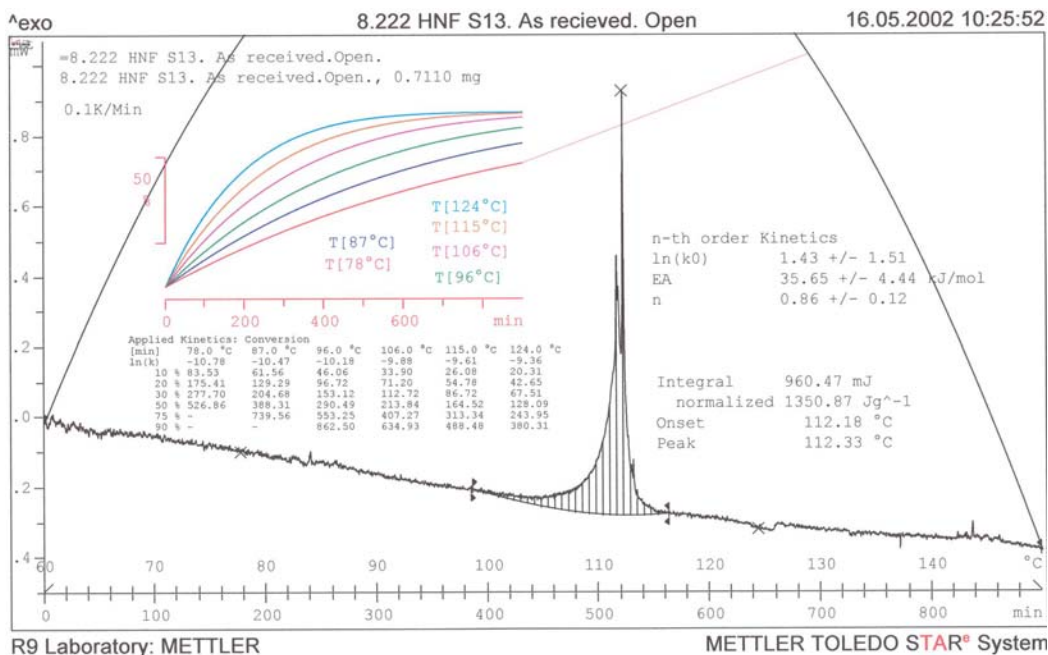
Figure 35 - HNF S13 As Received 0.1K/min – Open Pan
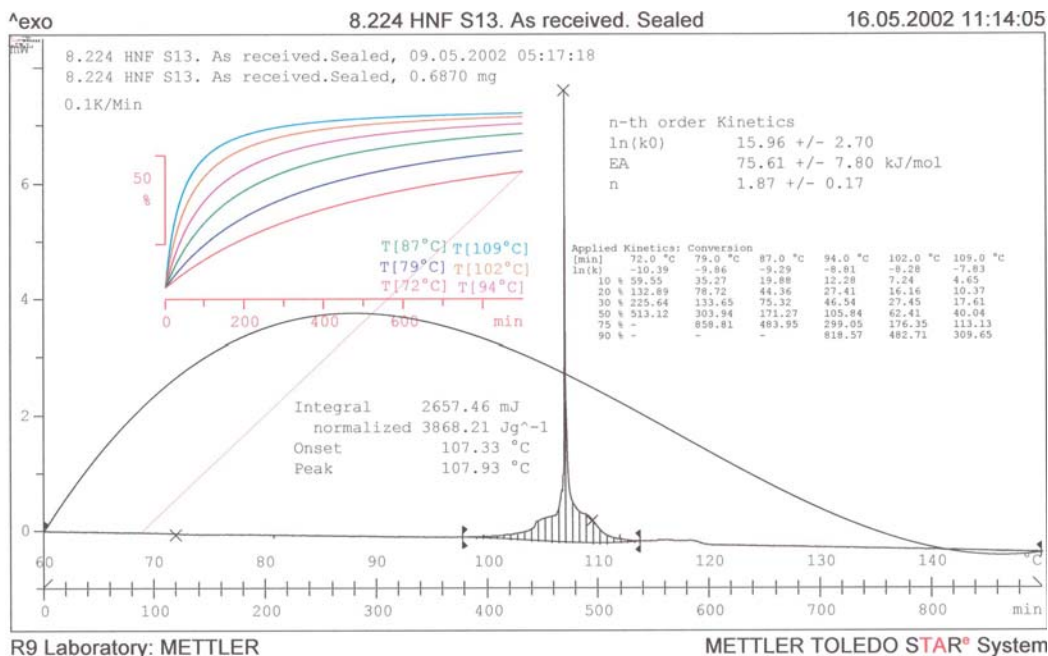
Figure 36 - HNF S13 As Received 0.1K/min – Sealed Pan
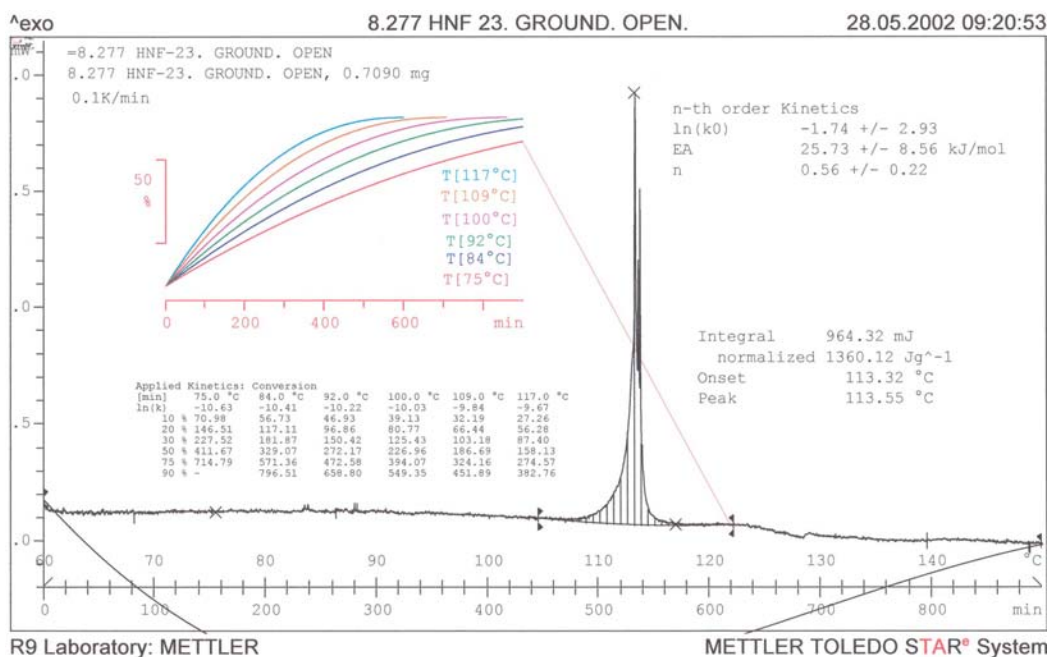
Figure 37 - HNF 23 Ground 0.1K/min – Open Pan
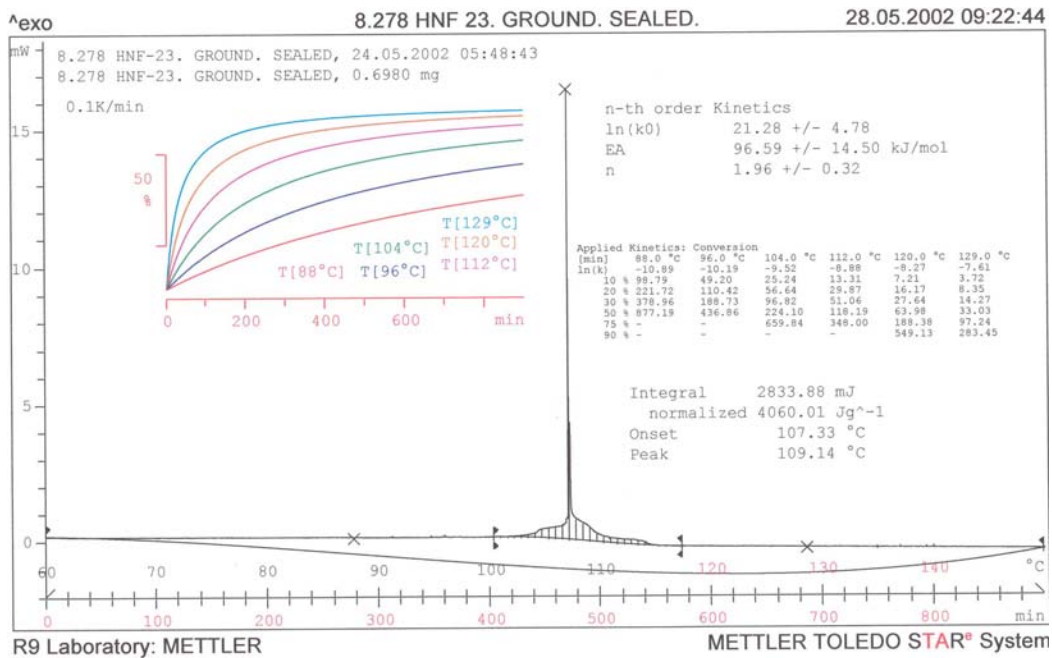
Figure 38 - HNF 23 Ground 0.1K/min – Sealed Pan
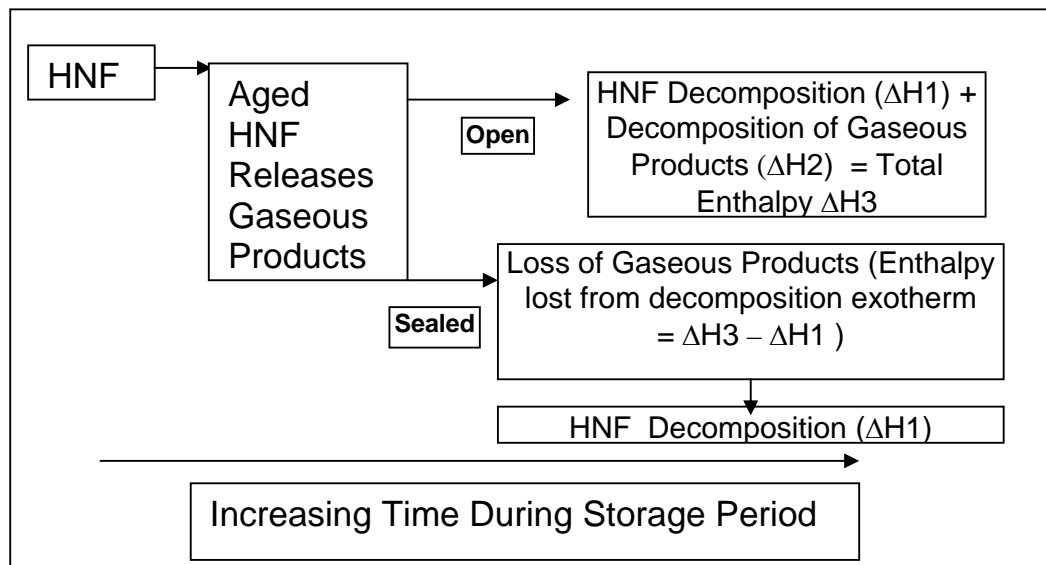
Figure 39 – Schematic of HNF Decomposition Under Sealed and Open DSC Pan Conditions

In the sealed samples, immediately prior to the plateau region, there is an area of rapid energy change that would equate to autocatalysis. Within the sealed environment, the plateau is proposed to be due to the superimposition of an endothermic event on the decomposition exotherm. It is proposed that it is not that the decomposition has slowed but that the exothermic energy of the decomposition is being redirected to undertaking an overall endothermic process. Figure 40 shows the proposal.
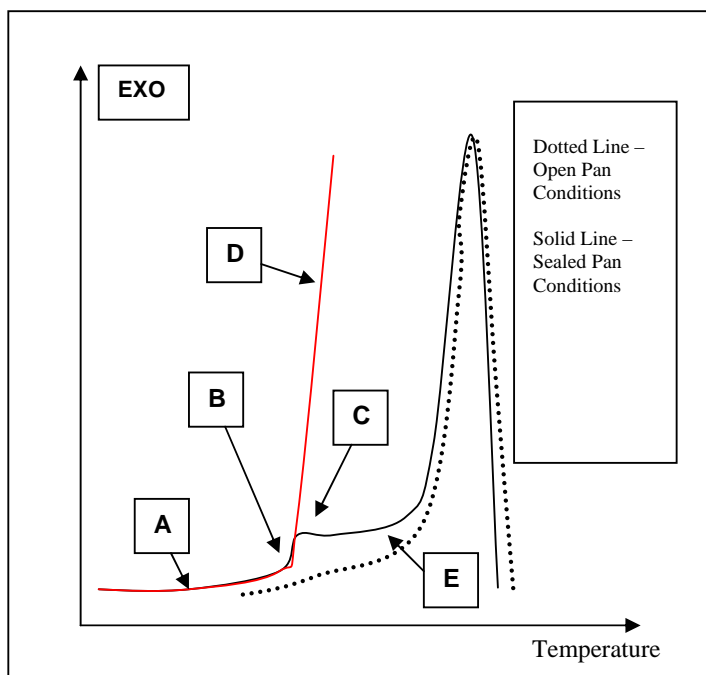
A = Onset of thermally induced decomposition, regardless of sealed or unsealed conditions

B = Start of large scale exothermic decomposition due to catalysis. Simultaneous start of a large scale endothermic event.

C = Hypothetical position where reaction course can diverge. Towards point D, reaction progresses without interference from any competing endothermic event. Towards point E, the exothermic rate of energy liberation and endothermic energy "trapment" are at near equal rates thus resulting in an overall energy change of near zero.

E = At point, exothermic energy liberation reaction is in excess of endothermic event (possibly the endothermic event has come to completion) and an overall exothermic energy change is detected.

Figure 40 - Hypothetical DSC Trace at Low Heating Rate for HNF

From the assessment of enthalpy and peak temperature it is proposed that :-

1) Gaseous products from HNF degradation do affect the mechanism of decomposition of HNF but do not catalyse the decomposition reaction

2) The gaseous products have a secondary effect on the heat flow characteristics of the samples.

2.4.4 Overall Conclusions From DSC Studies Into HNF Autocatalytic Degradation

At low heating rates, decomposition of HNF is initiated long before large scale HNF decomposition occurs. This suggests that the degree of interaction between gaseous degradation products liberated early in the decomposition and the residual solid HNF is comparatively benign in terms of accelerating solid decomposition. There is also very little effect of particle size or HNF grade on the decomposition rate. This again is taken as evidence that any autocatalysis that might be present within the decomposition due to gas / solid interaction is low, non-existent or restricted to late within the decomposition process. There is a shift in decomposition peak temperature to lower values in sealed conditions that, in itself, would indicate a gaseous catalytic effect. However, there is also an apparent associated decrease in decomposition enthalpy detected in the open pan samples. This enthalpy change is proposed to reflect loss of energy from the system due to loss of gaseous species but is proposed to not show any degree of catalysis. Overall, the data suggests that, although the gaseous products from HNF decomposition do play a part in the overall HNF decomposition in sealed conditions, the contribution towards gas / solid catalysis appears low or non-existent. The effect of HNF grade or particle size appears low although the level of experimental error associated with DSC analysis does complicate data interpretation

2.5 DSC Compatibility Testing of HNF with Nitrated Derivatives of 2NDPA and pNMA
2.5.1 Introduction

Chemical incompatibility of 2NDPA and HNF had been suggested previously by Jago [113] . However, it was unclear whether this chemical incompatibility was also to be encountered within nitrated derivatives of 2NDPA or pNMA. Analysis of HNF with a range of nitrated derivatives of 2NDPA and pNMA was undertaken to elucidate the degree of reactivity further.

2.5.2 Experimental

Analysis was undertaken using a Mettler TA-3000 with TA-72 Graphware. The thermal profile chosen for analysis was from 100- 130°C at a ramp rate of 1K/min in a stagnant air environment. Approximately 7mg of HNF was analysed in a 1:1 mixture with the derivative and tested using Mettler DSC pan type 1 sealed and unpierced. A thermal equilibrium settling period of 2 minutes was applied prior to initiation of the heating cycle.

2.5.3 Results and Discussion

Figures 41-52 show the DSC traces associated with the trials. From the test data, assessment of peak onset and peak exotherm was undertaken. Changes in these values were taken as being indicative of changes within the HNF decomposition mechanism or decomposition rate due to the presence of the derivative. Table 6 shows test results for these trials.

Trial Reference	Sample Name	Onset of Exotherm (°C)	Peak Temperature of Exotherm (°C)	Enthalpy (J/g)
1001	HNF Control	117.7	128.1	989
1005	HNF Control	117.9	127.5	770
1002	HNF + N-NO-2NDPA	See discussion below		
1003	HNF + 2,2'-DNDPA	114.7	Sample moved from sensor	
1004	HNF + N-NO-pNMA	108.2	120.5	1222
1006	HNF + N-NO-2NDPA	See discussion below		
1007	HNF + 2NDPA	114.8	123.9	1111
1008	HNF + 2,4-DNDPA	116.7	125.8	326
1009	HNF + 2,4-DN pNMA	116.8	125.9	467
1015	HNF + 2,4'-DNDPA	116.4	126.3	410
1016	HNF + 4,4'-DNDPA	116.2	121.4	142
1017	HNF + 2,2',4-TNDPA	117.3	126.4	253

Table 6 – DSC Analysis of HNF and pNMA and 2NDPA Nitrated Derivatives

The results in Table 6 show that the majority of derivatives cause no significant modification to the onset or peak temperatures of HNF degradation. The comparatively low heating rates applied were chosen to accentuate both medium and large scale chemical incompatibilities. Although there is variation within the test data, the majority is proposed not to be directly associated with material chemical incompatibility. A general shift of peak temperature to lower temperatures throughout the dataset for all samples compared to the control   is observed but this shift is proposed to reflect changes to the decomposition mechanism of HNF and so is not directly indicative of chemical incompatibility between HNF and the nitrated derivative. Any compound exhibiting this thermal profile is proposed not to cause premature decomposition of HNF, but possibly does influence the HNF decomposition mechanism after thermal induced initiation, effectively "sharpening" the decomposition by accelerating the reaction.

The samples that are proposed to show true chemical incompatibility (ie those that chemically destabilise HNF solely by being in contact) are :-

N-NO-2NDPA - Highly Incompatible

N-NO-pNMA - Incompatible but not to the same degree as the 2NDPA analogue

2,2'-DNDPA - Possibly exhibits mild incompatibility but data unclear

2NDPA - Possibly exhibits mild incompatibility but data unclear

It can be observed that the enthalpy values achieved for the material that are proposed to be chemically incompatible with HNF are significantly higher that those of the "compatible" derivatives. This is likely to be due to the coupling effect of the incompatible derivatives encouraging complete decomposition of HNF and being consumed in the reaction. In compatible samples, energy is likely dissipated from the HNF decomposition exotherm into endothermic processes associated with the derivatives within the sample pan (eg melting or volatilisation). These processes change the rate of energy release observed, thus giving an apparent reduction in overall measured enthalpy. Post heating, visible inspection showed that "incompatible" derivatives gave blackened residues whereas compatible ones gave red / orange residues. This suggests that the incompatible derivatives have contributed more directly to the overall decomposition and been oxidised to carbon residues in the process. The use of sealed pans (a pseudo adiabatic situation) can also complicate data assessment by the timing of the rupture of the hermetic seal. In the extreme case, movement of the sample from the sensor is observed and gives a distinctive thermal profile eg as seen in Figure 45. Rupture can lead to rapid loss of elevated temperature gaseous species from the pan that then changes the thermal character of the overall "adiabatic" condition. A second complication is that it is possible for the sensor to "top out" on high levels of energy liberation and this might have occurred on some traces (eg Figures 45 and 47   both of which show "blunted" peak exotherms).
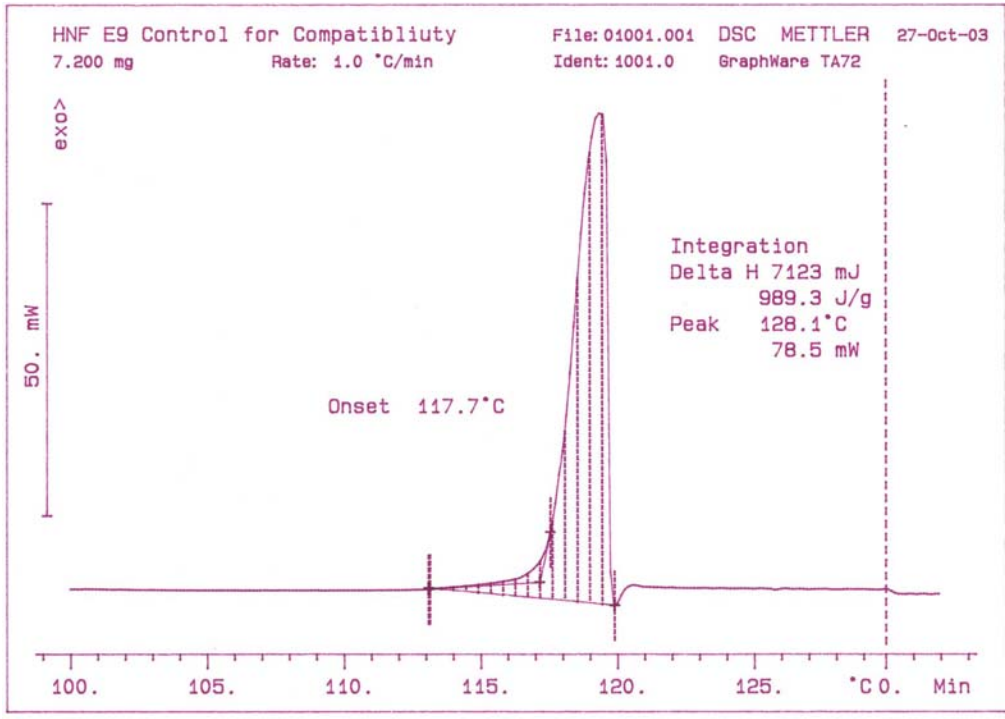
Figure 41 – DSC Trace Ref 1001 – HNF Control Sample
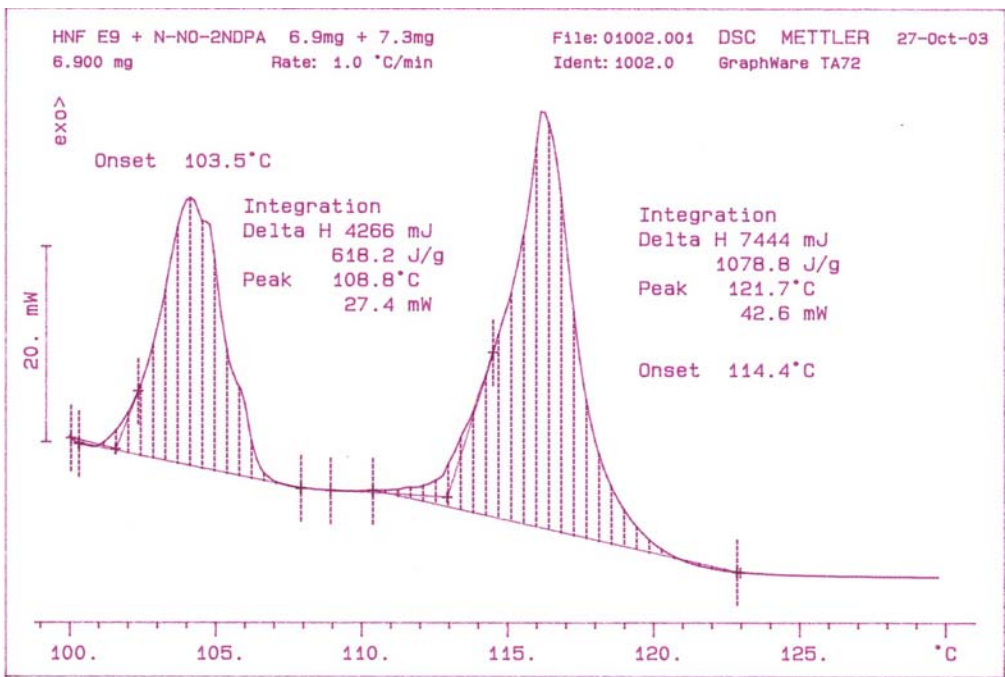
Figure 42 – DSC Trace Ref 1002 – HNF + N-NO-2NDPA
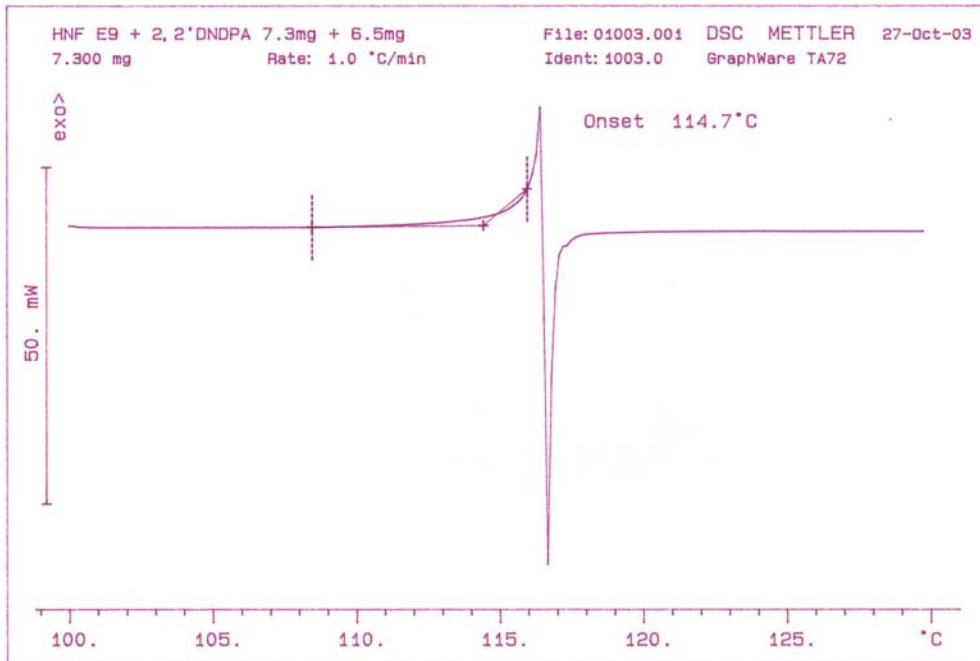
Figure 43 – DSC Trace Ref 1003 – HNF + 2,2'DNDPA
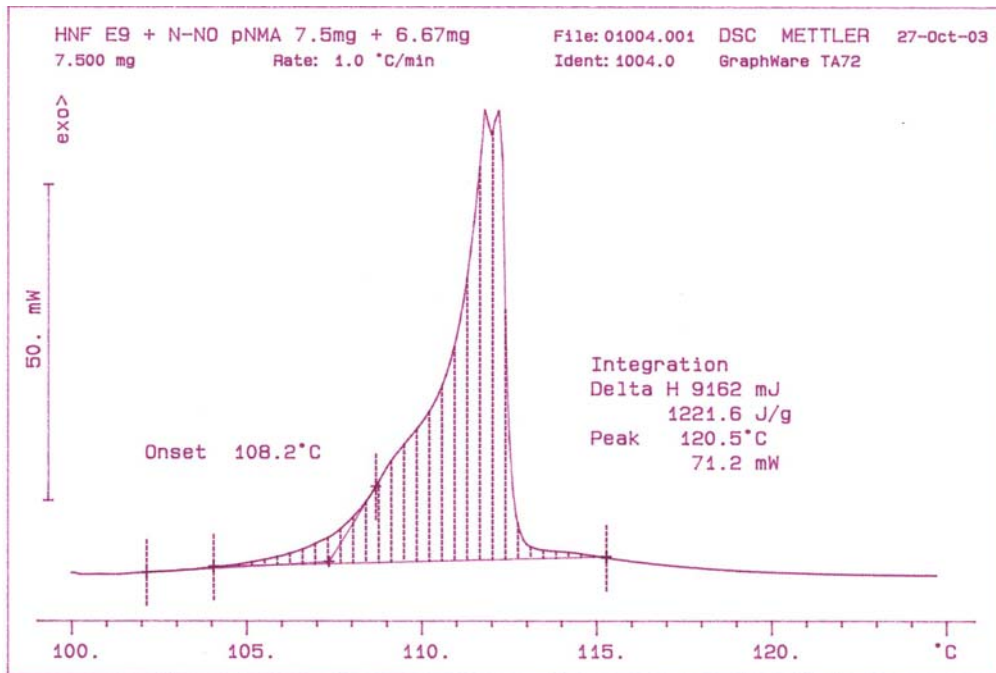
Figure 44 – DSC Trace Ref 1004 – HNF + N-NO pNMA
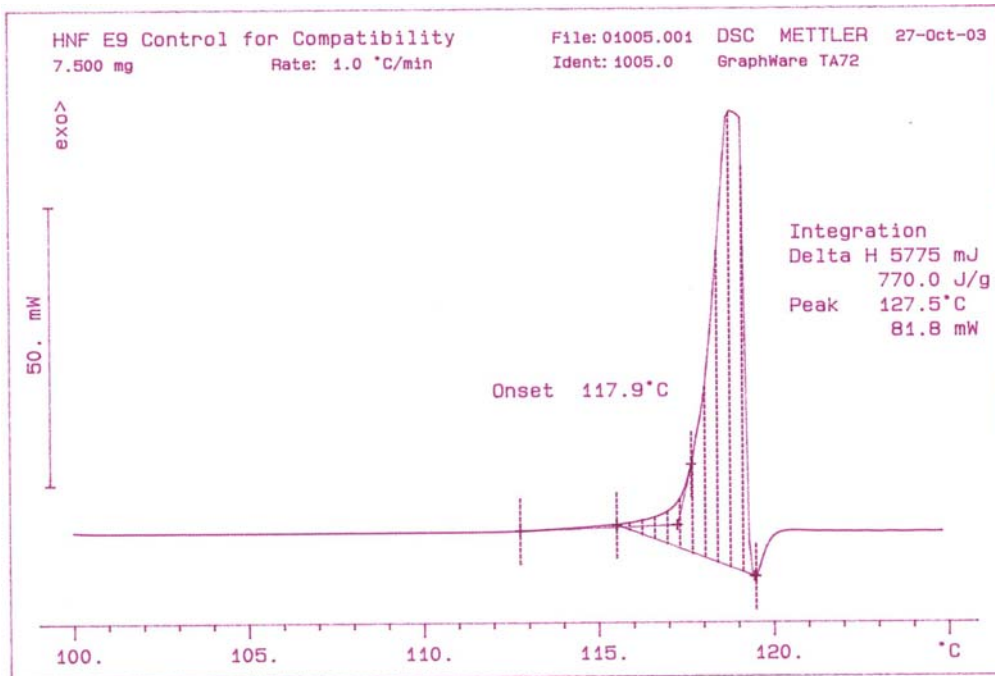
Figure 45 – DSC Trace Ref 1005 – HNF Control
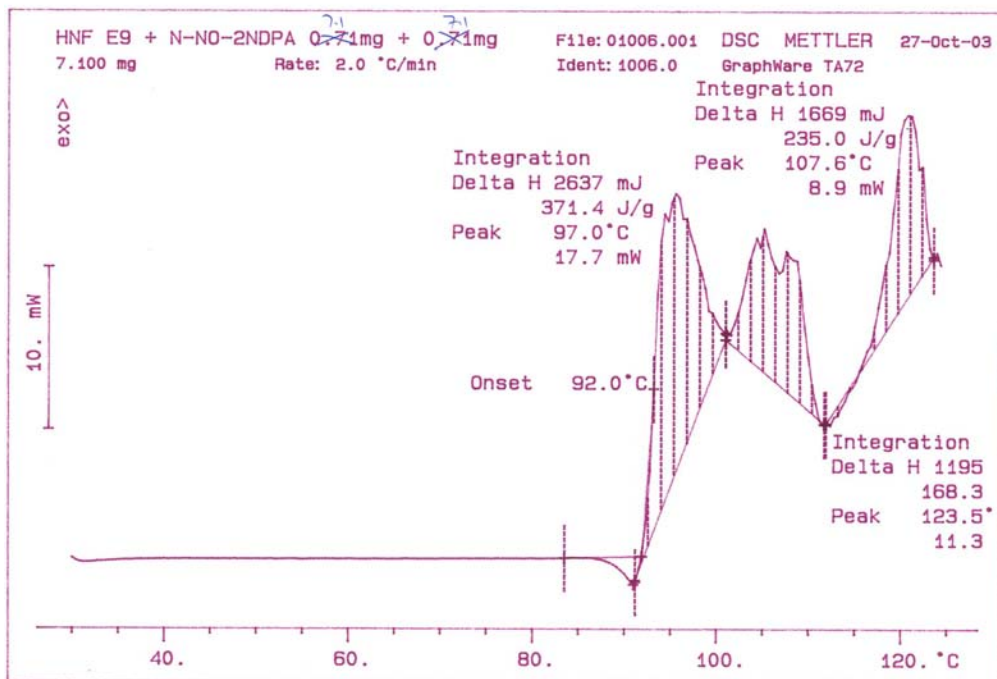
Figure 46 – DSC Trace Ref 1006 – HNF + N-NO-2NDPA
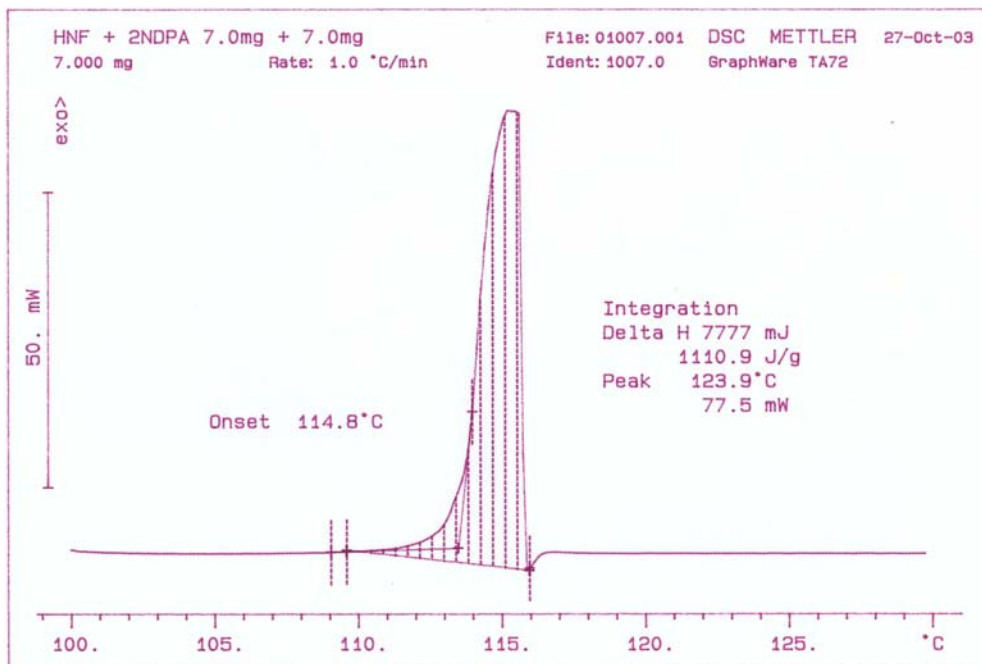
Figure 47 – DSC Trace Ref 1007 – HNF + 2-NDPA
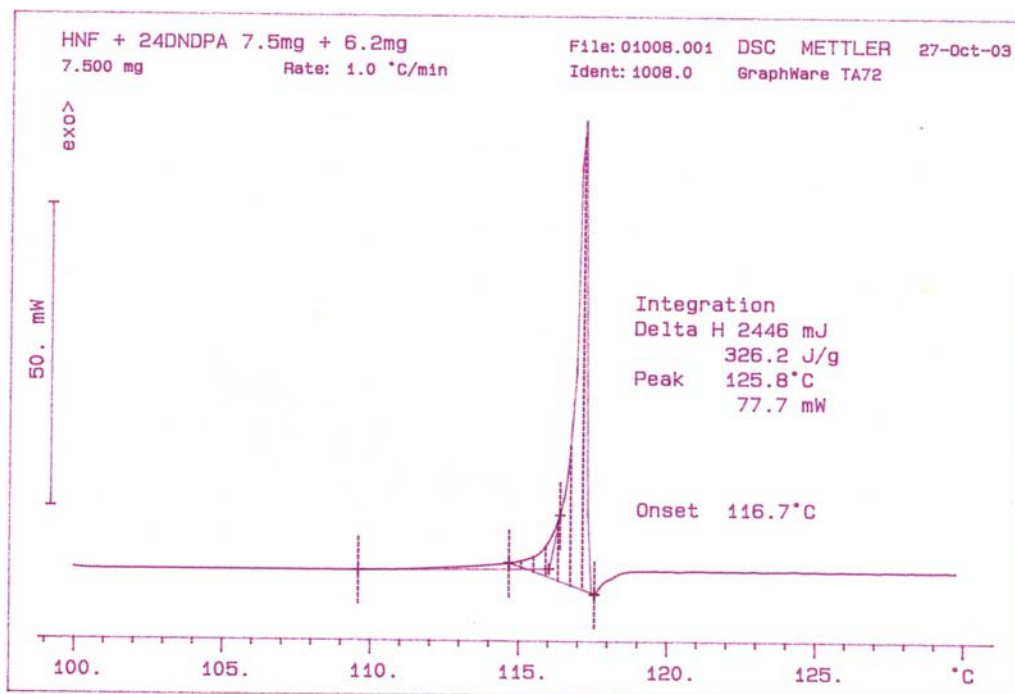
Figure 48 – DSC Trace Ref 1008 – HNF + 2,4-DNDPA
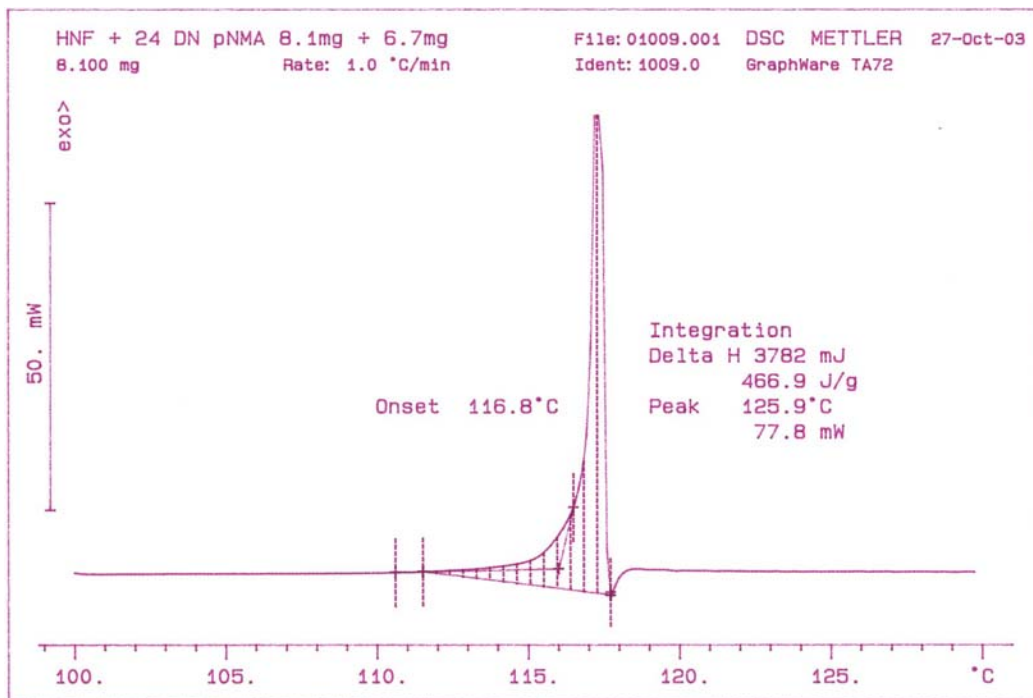
Figure 49 – DSC Trace Ref 1009 – HNF + 2,4- DNMA
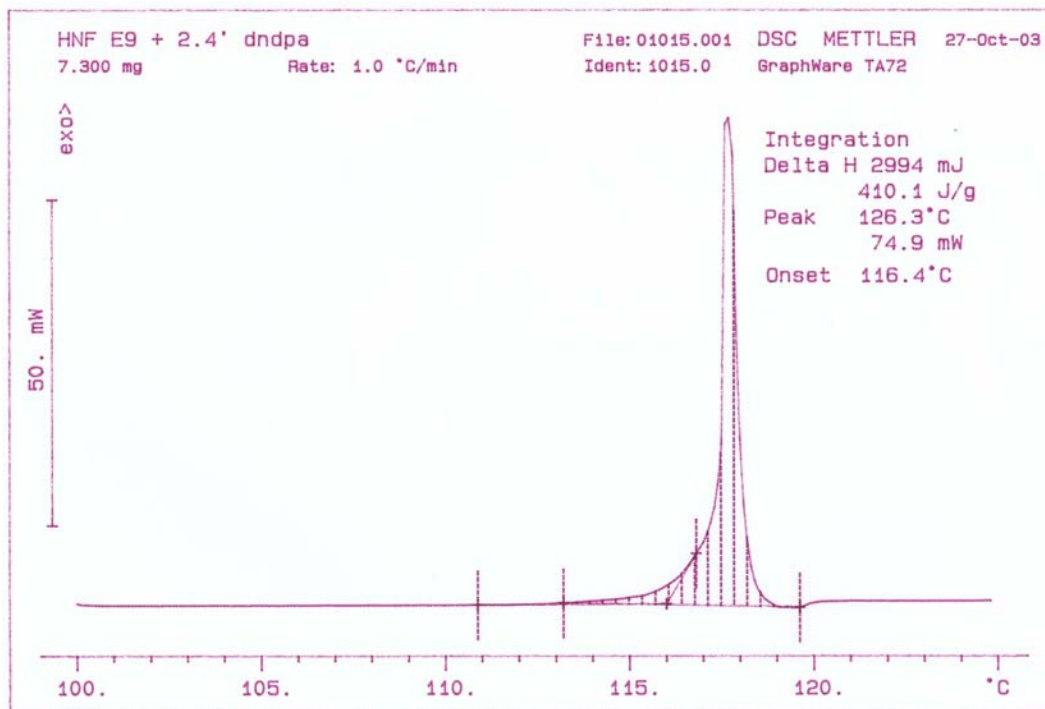
Figure 50 – DSC Trace Ref 1015 – HNF + 2,4'DNDPA
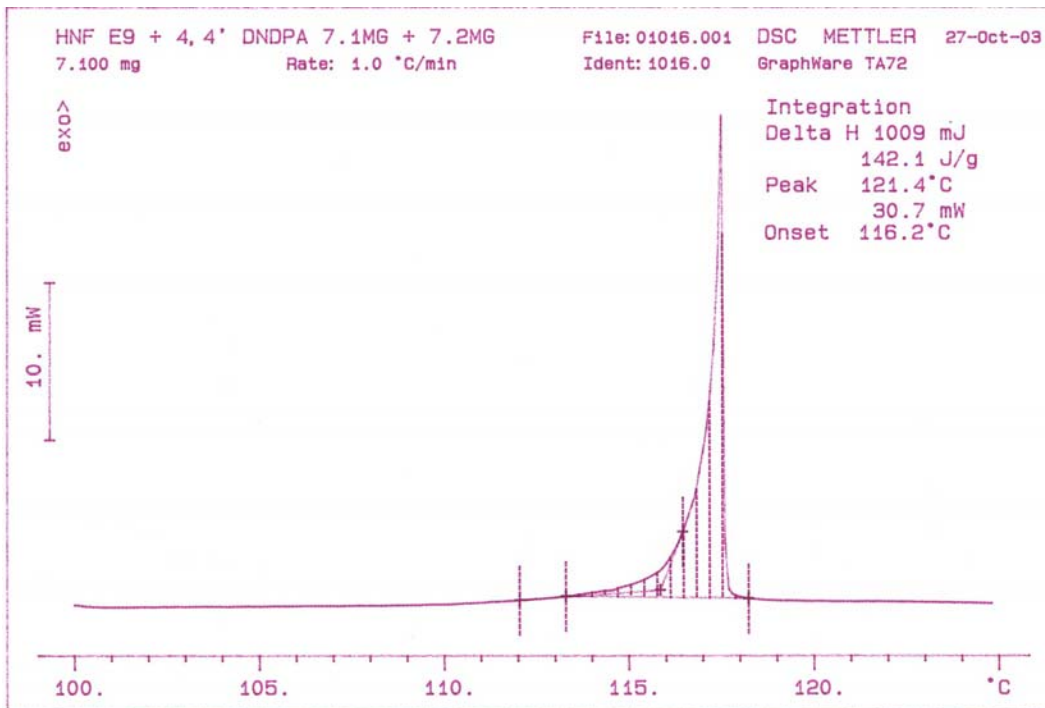
Figure 51 – DSC Trace Ref 1016 – HNF + 4,4'-DNDPA
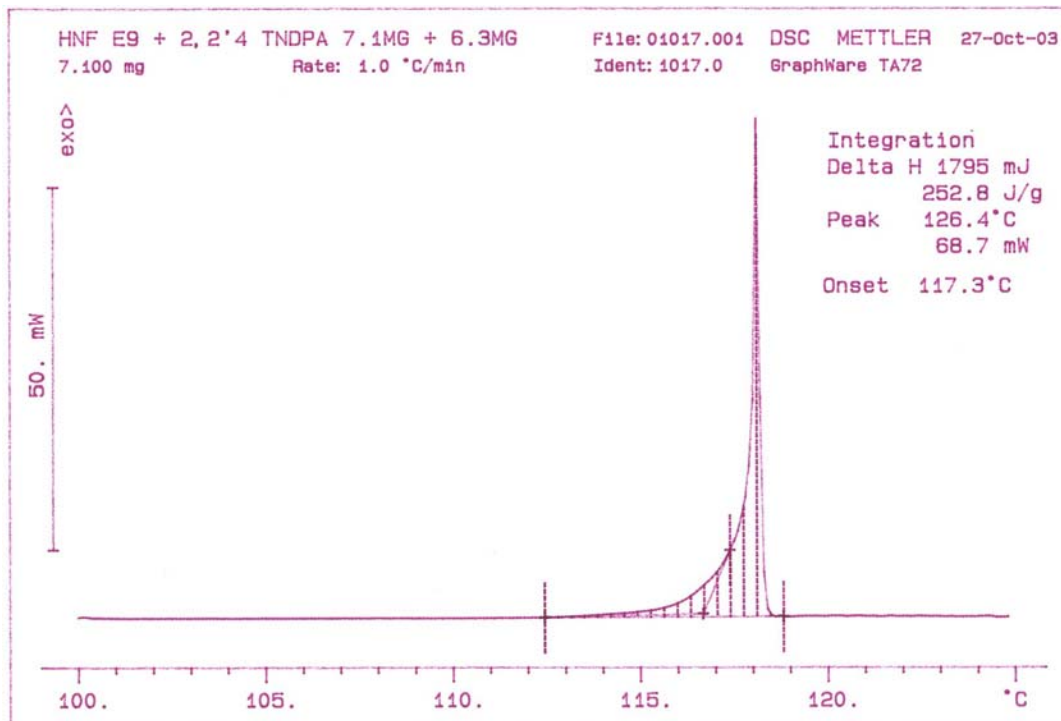
Figure 52 – DSC Trace Ref 1017 – HNF + 2,2',4-TNDPA

2.5.3.1 N-NO-2NDPA / HNF Reaction

The initial trial between HNF and N-NO-2NDPA (Figure 42) indicated a very rapid reaction occurring during the 2 minute settling time at 100°C. As reaction was observed to start prior to completion of the preliminary 100°C settling period, it was taken as being indicative of a large scale chemical incompatibility. Figure 42 shows two exothermic peaks, one at the initial start temperature followed by a second exothermic peak with an onset of 114.4°C, peak temperature 121.7°C. the first peak is attributed to chemical incompatibility between HNF and the stabiliser derivative. The second peak is attributed to unreacted HNF within the sample pan. The possible presence of HNF, even following the large scale decomposition observed was a very interesting observation. It had been expected that any level of chemical breakdown of HNF would rapidly lead to large scale HNF degradation via catalysis of decomposition by the initial degradation products; this does not appear to be the case in this sample. Again, unreacted HNF being present in the sample pan after reaction with N-nitroso samples, indicated that the concentration of the N-NO derivative was the limiting reagent in the reaction. The results also strengthen the results from Section 3.3 that indicate that HNF gas / solid autocatalysis is not as significant within HNF degradation as first proposed. A preliminary trial to assess the overall sample thermal response (Figure 46) was undertaken under a different thermal profile but similar sample masses to Trial 1002 (Figure 42). Table 6 shows the test data.

The results from Figure 42 again highlight two reactions occurring beyond the 90°C achieved at 2K/min which were not seen in the slower 1K/min rate; however, there is a significantly reduced "HNF" peak at 120°C. This suggests that the preliminary reaction has a more marked effect on HNF degradation if allowed to process at a slower rate. By starting analysis at 25°C it was proposed to allow the reaction to occur and achieve steady state whereas at 1K/min trials starting at 100°C, the reactions are biased towards simultaneous reaction and merging of the two thermal processes. As a consequence, they are seen as one thermal change in the DSC trace.

To further investigate the effect of N-NO-2NDPA on HNF a third series of trials were undertaken. Table 7 and Figure 53-57 show the sample traces associated with the trial

File Ref	Mass HNF (mg)	Moles HNF (x 10^{-5})	Mass N-NO-2NDPA (mg)	Moles N-NO-2NDPA (x 10^{-5})	Molar Ratio HNF :NO	Peak 1 Onset	Peak 1 Peak Temp	Peak 1 Enthalpy (J/g)	Peak 2 Onset	Peak 2 Peak Temp	Peak 2 Enthalpy (J/g)	Peak 3 Onset	Peak 3 Peak Temp	Peak 3 Enthalpy (J/g)
1005 (Control)	7.50	4.098	0	0	0	0	0	0	0	0	0	117.9	127.5	770.0
1006*	7.1	3.880	7.1	2.92	1.33	92	97.0	371.4	N/D	107.6	235	N/D	N/D	N/D
1010	1.0	0.546	7.0	2.881	0.19	102.4	103.5	14.0	104.6	107.0	25.2	N/D	N/D	N/D
1011	2.0	1.093	7.1	2.92	0.37	103.9	107.7	209.4	109.1	109.9	26.1	N/D	N/D	N/D
1012	3.0	1.640	7.1	2.92	0.56	97.7	104.9	947.7	N/D	N/D	N/D	112.6	121.0	516.3
1013	4.0	2.186	6.9	2.84	0.77	102.7	107.8	597.2	N/D	N/D	N/D	114.8	117.3	118.8
1014	5.0	2.732	6.6	2.716	1.01	105.1	111.0	633.7	N/D	N/D	N/D	114.7	120.1	472.6
1002	6.9	3.770	7.3	3.004	1.25	103.5	108.8	618.2	N/D	N/D	N/D	114.4	121.7	1078.8

* 25 – 130°C at 2K/Min. All Other Samples Heated at 1 K/Min – No Initial Settling Time (All others samples 100-130°C 1K/Min). Peak 1 and 2 are attributed to direct reaction of HNF with the nitroso moiety of NO-2NDPA. Peak 3 is attributed to unreacted HNF within the sample pan.

Table 7 : DSC Analysis of HNF : N-NO-2NDPA Mixtures.
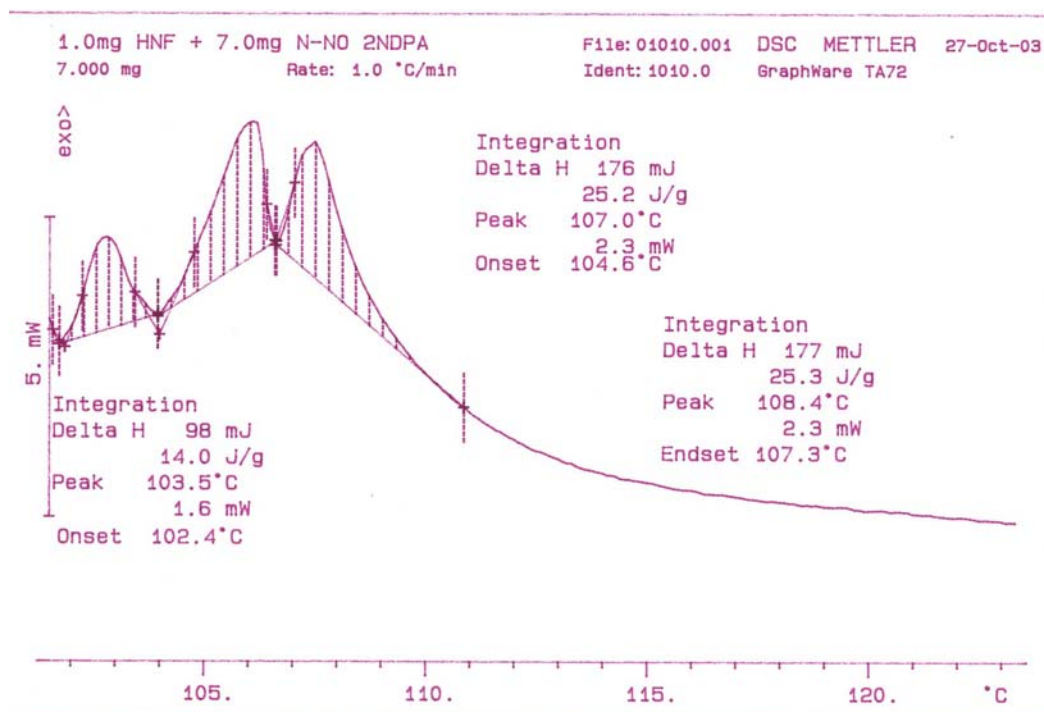
Figure 53 – DSC Trace Ref 1010 – 1.0mg HNF + 7.0mg N-NO-2NDPA
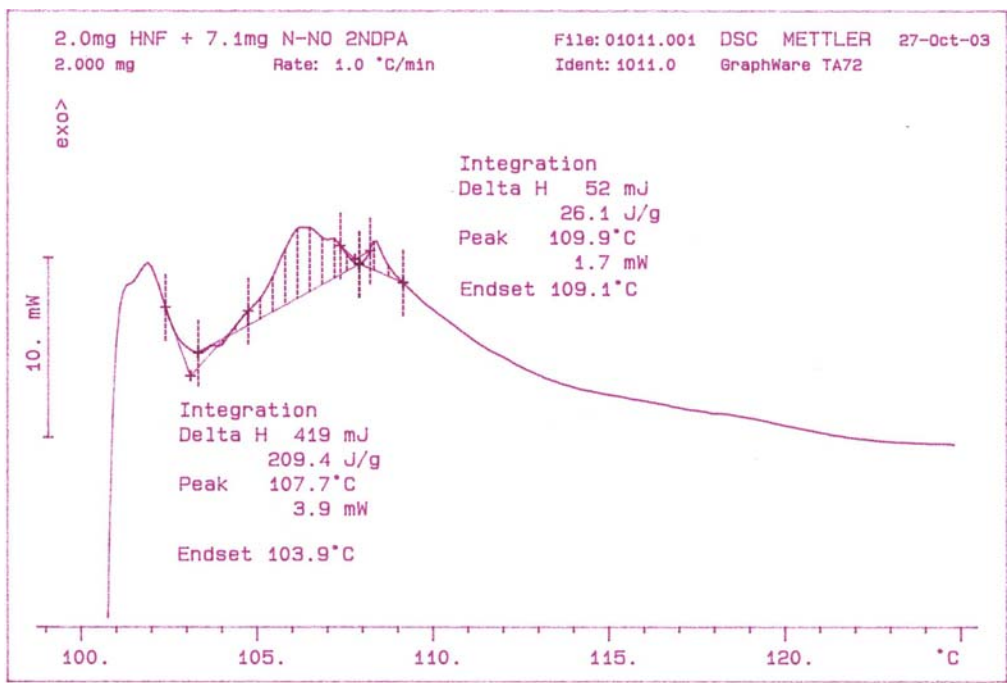
Figure 54 – DSC Trace Ref 1011 – 2.0mg HNF + 7.1mg N-NO-2NDPA
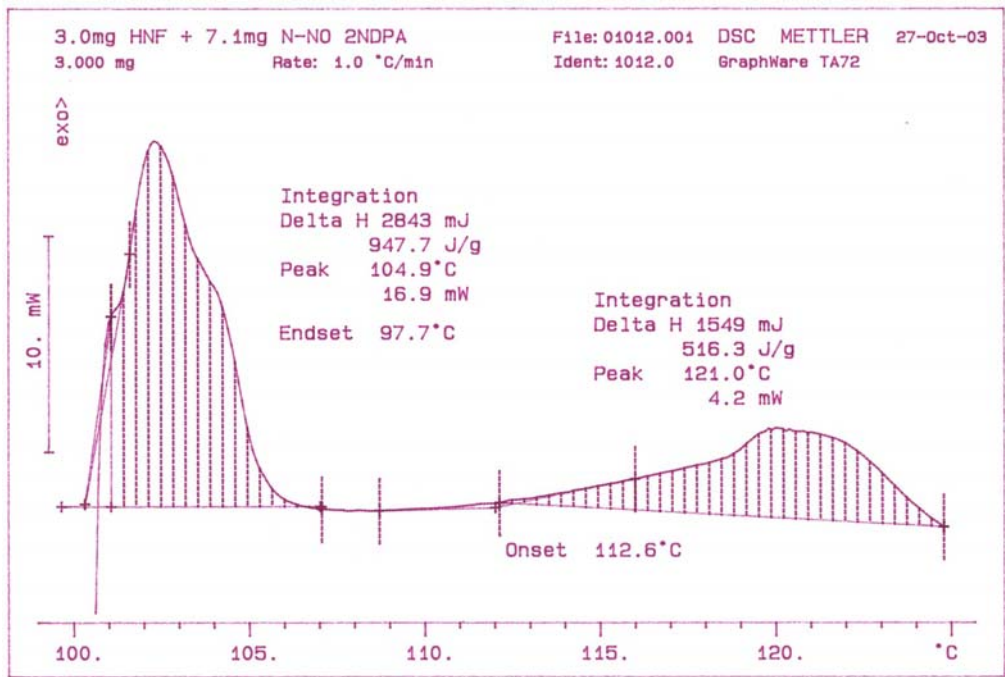
Figure 55 – DSC Trace Ref 1012 – 3.0mg HNF + 7.1mg N-NO-2NDPA
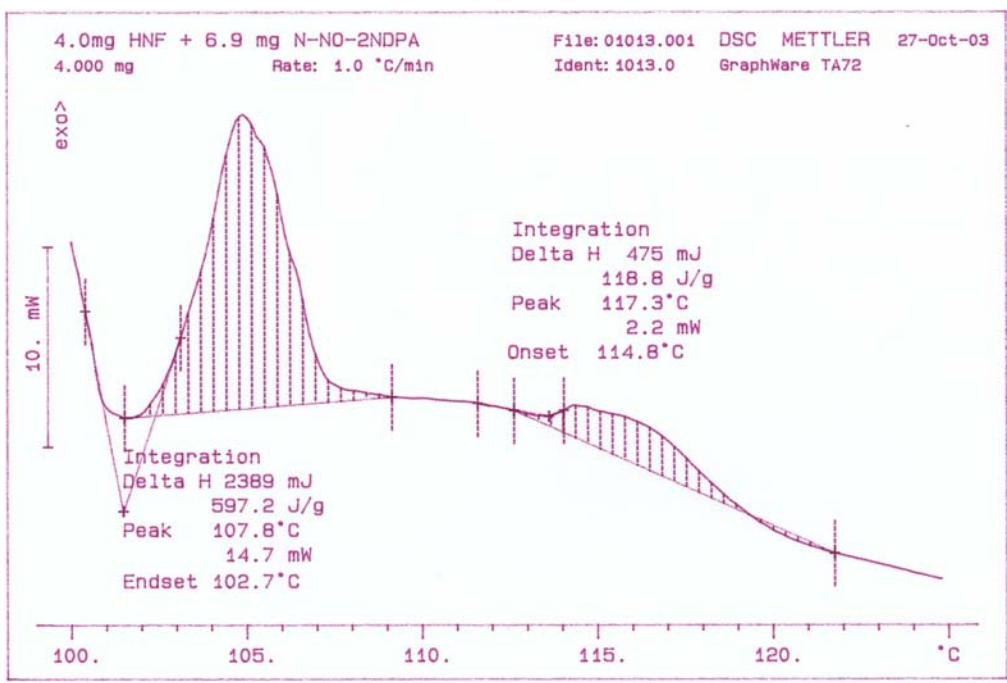
Figure 56 – DSC Trace Ref 1013 – 4.0mg HNF + 6.9 mg N-NO-2NDPA
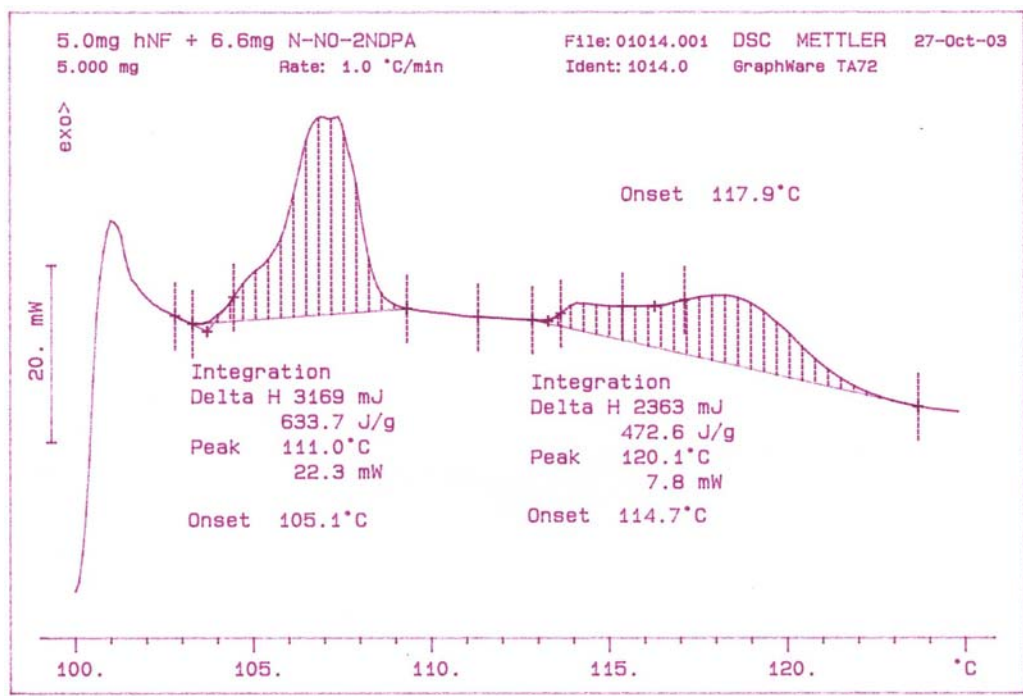
Figure 57 – DSC Trace Ref 1010 – 5.0mg HNF + 6.6 mg N-NO-2NDPA

The analysis gives an indication of stoichometry associated with the reaction course. The results suggest that testing with a molar ratio of between 0.37 and 0.56 N-NO-2NDPA :HNF, no HNF remains unreacted. Beyond this value, some HNF remains within the sample pan for further decomposition at ~ 120°C. Although further work would be required to ascertain the exact stoichometry, the data suggests that reaction falls in the ratio range of 2:1 to 7:4 N-NO-2NDPA :HNF. This agrees well with the reaction quoted by Schmidt [103] between hydrazine and nitroso compounds where he proposes two alternative reaction courses (as shown in Figure 58).
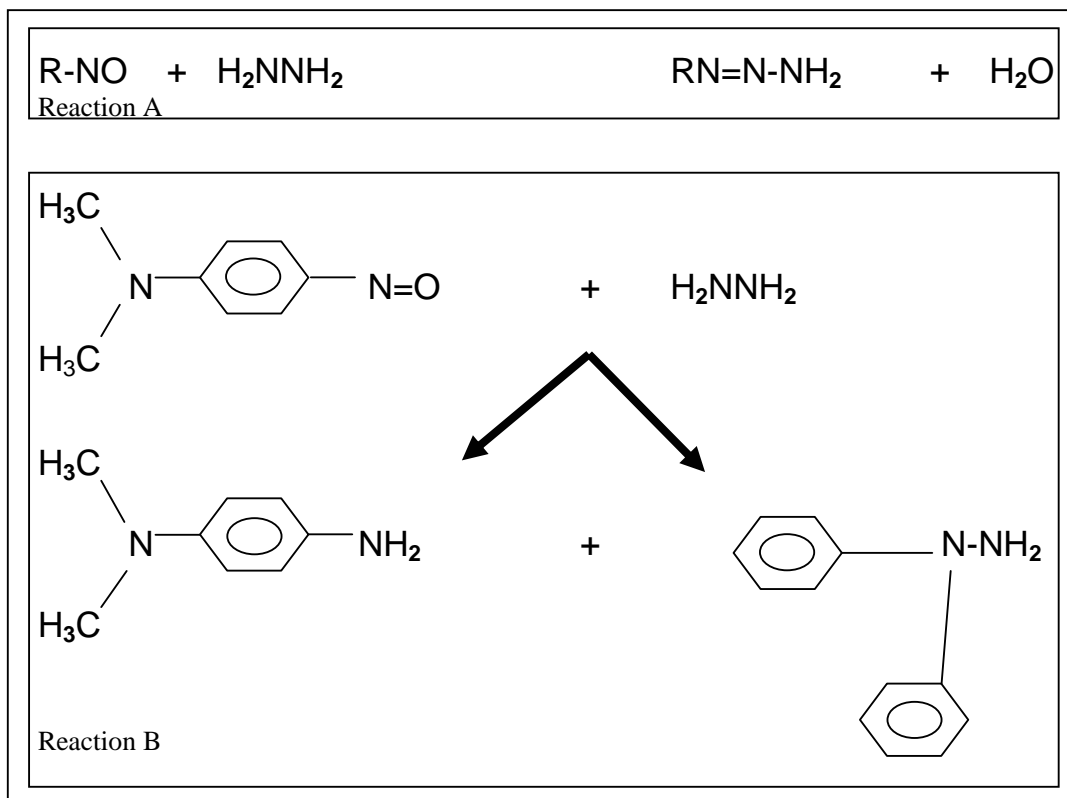
Figure 58 – Reaction of N-NO Compounds with Hydrazine [103]

The experimental stoichometry assessment suggests that a reaction similar to reaction B in Figure 58 is more likely to be observed than the 1:1 stoichiometry of the first reaction listed.

Comparison of the HNF decomposition peak data in Tables 6 and 7 shows that the HNF decomposes during the HNF : N-NO-2NDPA stoichiometry studies at a very slightly lower temperature. This might reflect that :-

1) Any HNF present is undergoing some catalytically induced degradation with other HNF degradation products within the sample pan

2) Any HNF present is no longer pure following thermal ageing and so the decomposition of a derivative is being observed

3) There is formation of higher nitrated derivatives of 2NDPA, that in turn show reaction with HNF to sharpen / accelerate the eventual decomposition

4) An experimental effect (eg improved heat flow characteristics due to a change of state of products)

It is proposed that all of the above have some contribution to the reduction in HNF peak temperature in the trials although options 1 and 2 are proposed to have the lowest contributions. If autocatalytic breakdown was occurring to accelerate degradation, reaction of the gaseous species with HNF would be expected to occur at a near constant rate. This rate would serve to merge the various exothermic peaks observed in the N-NO-2NDPA / HNF thermal process. The peak separation between the end of peak 2 and the start of peak 3 in some traces suggests that no reaction is occurring during this stage of the storage period. The time gap for this separation is typically in the order of 5 minutes which at a temperature in excess of 100°C , would be expected to sufficient for interaction to occur. Not to show a reaction during this period suggests that any gaseous species in the pan have no direct effect on the HNF present. The gaseous species may serve to accelerate HNF decomposition once HNF reaches its thermal limit but this thermal limit is apparently not catalysed by other species. If the sample was cooled during the 5 minute gap between peak 2 and peak 3, it is proposed that no further decomposition would occur, however long the gaseous species were in contact with the remaining HNF crystals.

The formation of a derivative between the HNF and the Nitroso groups present must be a possibility. However, the ability of any derivative to survive high temperature storage is thought unlikely. There is a general acceptance that derivatives of hydrazine are thermally unstable [41] [93] [103] and so, in the harsh environment of the sample pan, derivatives would not be predicted to survive. It is also likely that any derivative formed would act as an impurity on the HNF surface, and likely act as a centre for instability as predicted from early studies that showed purity level was crucial to HNF stability. [1] [2] [13] [14] [15] If this was occurring the products would destabilise any remaining HNF; this is not observed in the test results.

Option 3 seems a likely route to explain the changes in peak temperature. Oxidation of the nitroso group must be a likely reaction course during trials to form a dinitrated NDPA derivative. Although the data is incomplete, Table 6 suggests that the 2,2' dinitrated derivative of 2NDPA does appear to show mild chemical incompatibility with HNF. As this

is likely to be a product of N-Nitroso oxidation, it must be a potential route to mild incompatibility occurring during storage.

Option 4 reflects the observation that many of the reaction products formed during the reaction appear as liquids post storage. A liquid phase within the sample pan would lead to more efficient heat flow from the DSC heating element to the sample, thus leading to a shift to lower observed temperatures, even without chemical incompatibility. This is thought to be the most likely explanation of the lowering of HNF peak temperature measured. However, it is not possible to determine whether this improved thermal coupling has occurred during these trials.

2.5.4 - Conclusions

N-NO-2NDPA has been identified as the principal source of incompatibility between HNF and 2NDPA derivatives. Rapid and large scale degradation of HNF is observed a ~ 90°C due to the presence of the N-nitroso moiety. Reaction appears to occur in a stoichometric ratio of between 2:1 and 7:4 N-NO-2NDPA :HNF and is likely to be linked to oxidation of the nitroso group.

N-NO-pNMA also shows a large degree of chemical incompatibility with HNF but does not appear as reactive as the 2NDPA analogue. This may relate to the greater degree of charge delocalisation present in the 2NDPA structure allowing more easy reaction (oxidation) of the Nitroso group in that derivative compared to the pNMA analogue.

Mild chemical incompatibility may be present between both 2NDPA and 2,2'-DNDPA with HNF although this is a comparatively mild effect and the results may be test specific. Further trials would be required to investigate the significance (if any) of interaction of the derivatives with HNF.

2.6 Ageing of Potential Hydrazine Scavengers with HNF

2.6.1 Introduction

A series of potential hydrazine scavenger materials had been sourced from chemical suppliers to investigate whether they would be beneficial against HNF (and also HNF based propellant) degradation at elevated temperature. GASTEC trials (detailed in Section 2.3) had indicated that hydrazine was being liberated from crystalline HNF at 60°C and removal of the reactive species was seen as being beneficial. Preliminary testing to assess the degree of chemical compatibility of the scavengers with HNF was carried out to identify viable candidate

materials. Following this selection process, a more detailed GC-MS based study was carried out.

2.6.2 Experimental

For the preliminary chemical compatibility studies, 1g of HNF was added to 1g of each scavenger and sealed into a 10ml glass vials with a septum cap fitted. Test samples were then stored at 80°C for 4 days. Following storage, samples were assessed for any visible signs of degradation (colour change, foaming etc) with the most promising candidates being taken forward for trial by GC-MS. The GC-MS Head Space Analysis was carried out using a GC-MS MD800 benchtop quadrupole mass spectrometer (Thermo Finnigan) with HS 2000 headspace analyser. Data analysis / capture was via an Xcalibur data control system and comparison of standards against an NIST spectral library. The column utilised was a PLOT fused silica, CP-PoraPLOT Q (Varian), of 25m length, 0.25mm internal diameter and an 8µm film thickness. Oven temperature was set to 150°C with a carrier gas of helium operating at a flowrate of 2.2ml/min. The injector split flowrate was 110ml/.min with a splitting ratio of ratio 50. The MS Source was via Electron Impact (EI) ionisation at 200°C, with fragment detection being over a full scan in the mass range 12-245 at 4.1 scan sec^{-1}. The detector sensitivity was set to 185v, emission 350µA.

2.6.3 Results and Discussion

2.6.3.1 Preliminary Testing

The compatibility of HNF with each of the potential hydrazine scavengers given in Table 2 was assessed by visible inspection in sealed conditions after elevated temperature storage. Results from these trials are shown in Table 8

1g of HNF +	Observation	Result after 4 days at 80 deg.c
Sodium sulphide	Reacted instantaneously and violently on contact, rapidly liberating gas	Highly incompatible
Sodium Thiosulphite	HNF crystals turned orange / brown. Other crystals turned yellow and become aggregated	Incompatible and Unusable
Anhydrous Sodium Sulphite	**All sample turned yellow and aggregated into a single mass**	**Possibly usable**
Ammonium carbonate	24 hours. Sample decomposed to a yellow film on the wall of the vial and dark orange on base. No evidence of HNF remaining	Incompatible and Unusable
Sodium Thiocyanate	All sample formed brown / red friable solid with slight aggregation	Incompatible and unusable
Ammonium Peroxydisulphate	**Surface remained white but lower surfaces all became yellowed. Sample aggregated but became free flowing with very light pressure**	**Possibly usable**
Quinol	Quinol crystals turned grey. HNF crystals become dark brown.	Incompatible and unusable
Di-n-butylamine	24 Hours : Viscous liquid layer (possibly gelled) in base of vial, bubbling slightly. No HNF present. 96 Hours : Glass in vial discoloured with all sample evaporated / decomposed. No evidence of HNF or dibutylamine present	Incompatible and unusable

Table 8 : Compatibility Results For Potential Stabilisers of HNF (Items in **bold** suggest that they have a potential use within propellant development trials)

From these trials, anhydrous sodium sulphite and ammonium peroxydisulphate were selected as the candidate materials for further assessment in propellant formulation studies.

2.6.3.2 Headspace GC-MS Analysis of HNF Samples

A series of HNF based samples were stored at 70°C for up to 80 hours. At regular intervals, individual samples were removed from heating and the gaseous composition above the sample determined by headspace GC-MS.   Identification of the analyte species was undertaken by correlation of the retention time and assessment of the individual mass spectrum. Table 9 shows the samples chosen for assessment

Analyte	Second Material	Mass Ratio
HNF	------	1
HNF	PolyNIMMO	1:1
HNF	Ammonium Peroxydisulphate	1:1
HNF	Sodium Sulphite	1:1

Table 9 : Test Samples for GC-MS Headspace Analysis

Figures 59 to 68 show the evolution of various species during the analysis. The HNF control sample (Figure 59) shows that the dominant species lost during the storage period is the previously identified contaminant, isopropyl alcohol (propan-2-ol).   The release of this material from the control sample appears to progress in a near linear fashion. However, the low frequency of sampling does give some degree of subjectivity as to the "between point" data and the start of loss of IPA from the crystal surfaces. In addition to release of IPA, N_2O is also evolved and the concentrations of nitrogen and oxygen are seen to increase. These results agree well with those detailed by Pearce [92] and Bellerby [104] although no significant increase in carbon dioxide concentration is observed during these trials, presumably due to the comparatively short storage period assessed.
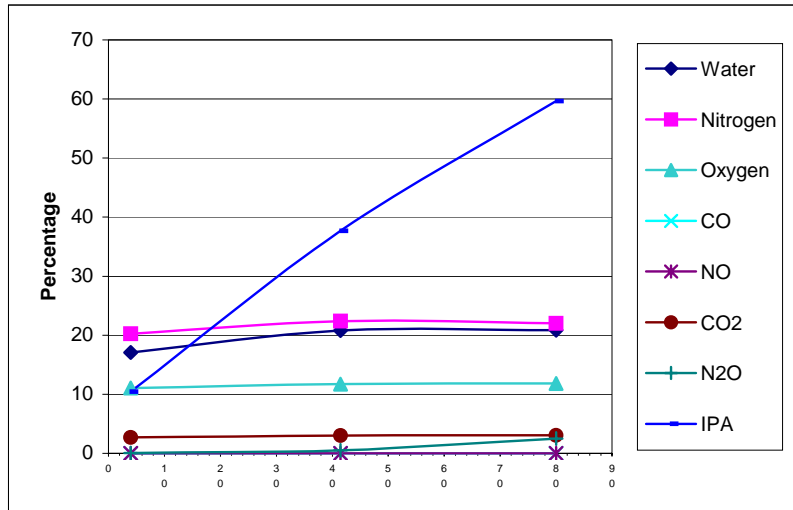
Figure 59 – Evolution of Gaseous Products From HNF Control Sample During Storage at 70°C

Comparison of the HNF control (Figure 59) with those from the test samples (Figures 60-63) indicate significant differences between them. The evolution of IPA is observed to follow a Gaussian (or distorted Gaussian) profile on the three mixed sample traces compared to the linear evolution of the control. Even taking into account the low frequency of testing for the HNF control data, it still suggests that the IPA is being removed from the test samples by reaction during storage. All of the mixed sample formulations show an induction period before the loss of IPA is initiated.
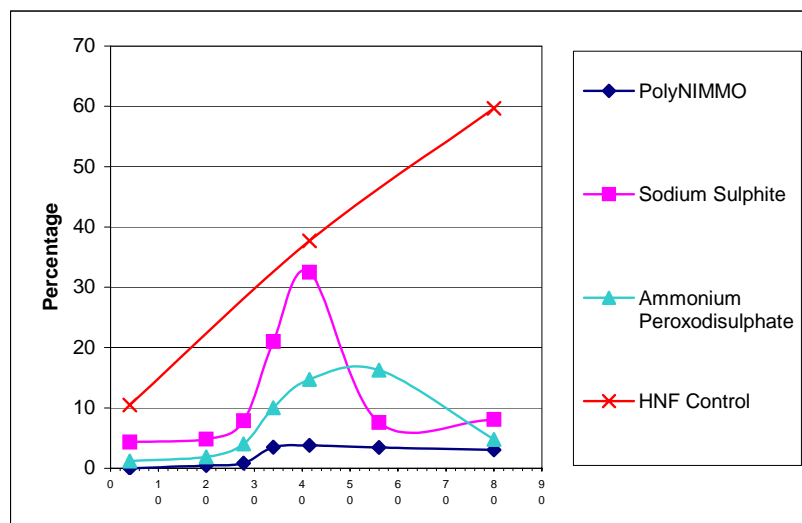
Figure 60 – Evolution of IPA From Samples During Storage at 70°C

This induction period prior to the first detection of IPA is proposed to be due to rate of migration of the solvent to the crystal surface; Figure 60 shows that this induction period is similar for all test samples. The loss of a peak maxima for IPA in the mixed samples coincides with more rapid evolution of other gaseous species from the sample (Figures 61 to 63). This is most evident in the sodium sulphite sample (Figure 63) where little liberation of gaseous species occurs in the sample until the concentration of IPA has fallen to a minimum.
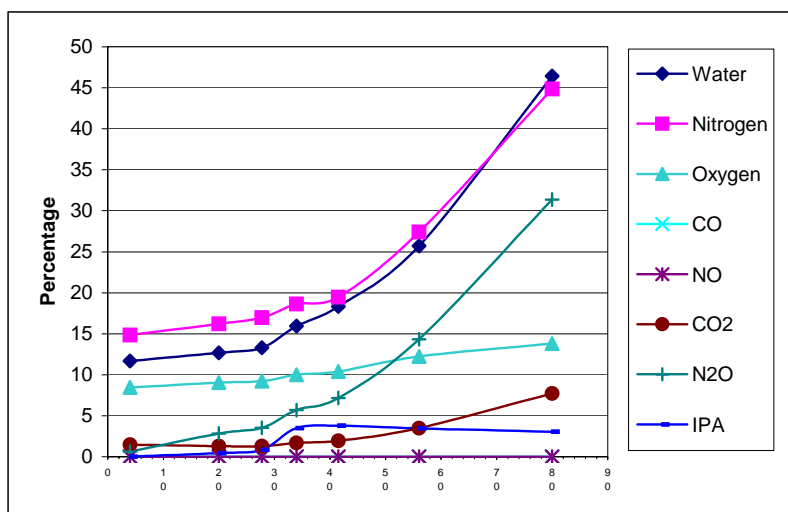
Figure 61 – Evolution of Gaseous Products From polyNIMMO / HNF Sample During Storage at 70°C
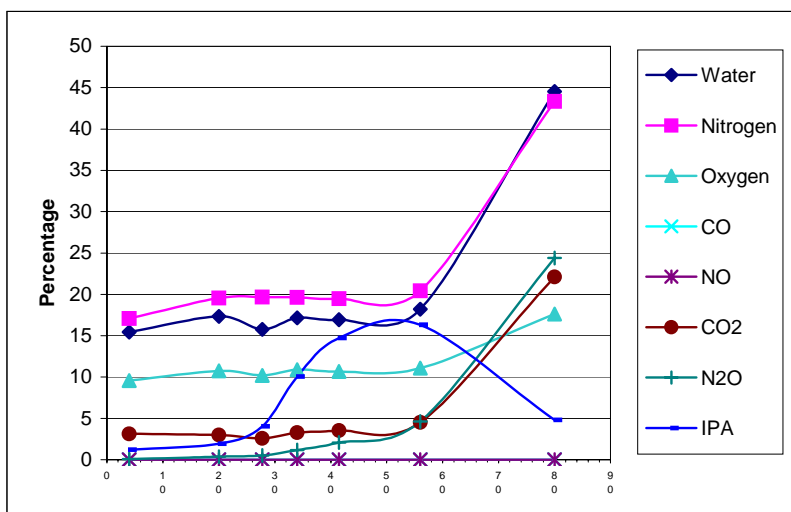
Figure 62 – Evolution of Gaseous Products From Ammonium Peroxodisulphate / HNF Sample During Storage at 70°C
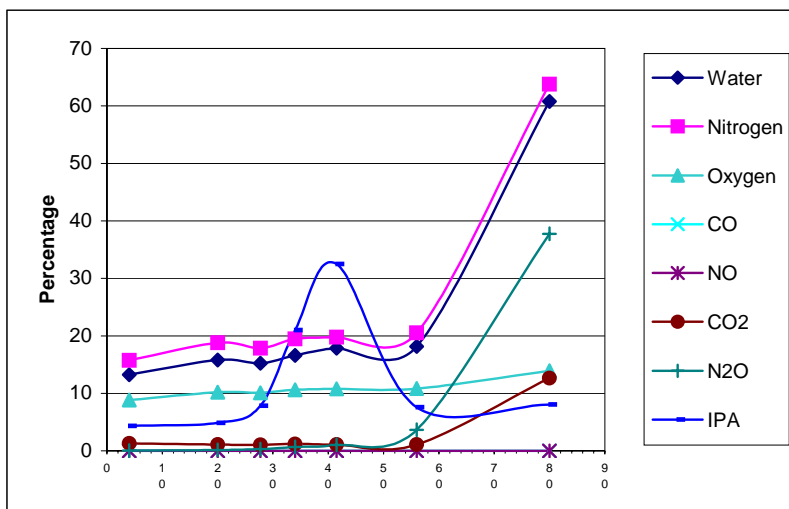
Figure 63 – Evolution of Gaseous Products From Sodium Sulphite / HNF Sample During Storage at 70°C

The lack of apparent reaction between HNF and IPA in the control sample suggests that no direct interaction occurs between the species. This indicates that the formation of alternative gaseous species in the test samples comes from a secondary incompatibility. In the presence of secondary materials, IPA appears to enhance the stability of the overall sample until it is depleted. This agrees with the functional group studies shown in Section 1.5.2.4 for the action of alcohols on HNF reaction / stabilisation. It must also be noted that the control sample (Figure 59) shows only mild chemical breakdown during storage
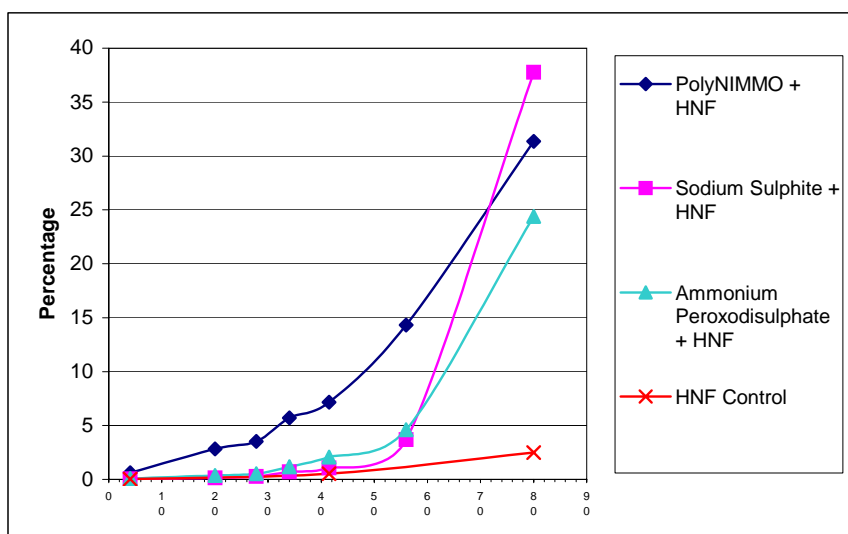
Figure 64 – Evolution of N_2O From Samples During Storage at 70°C
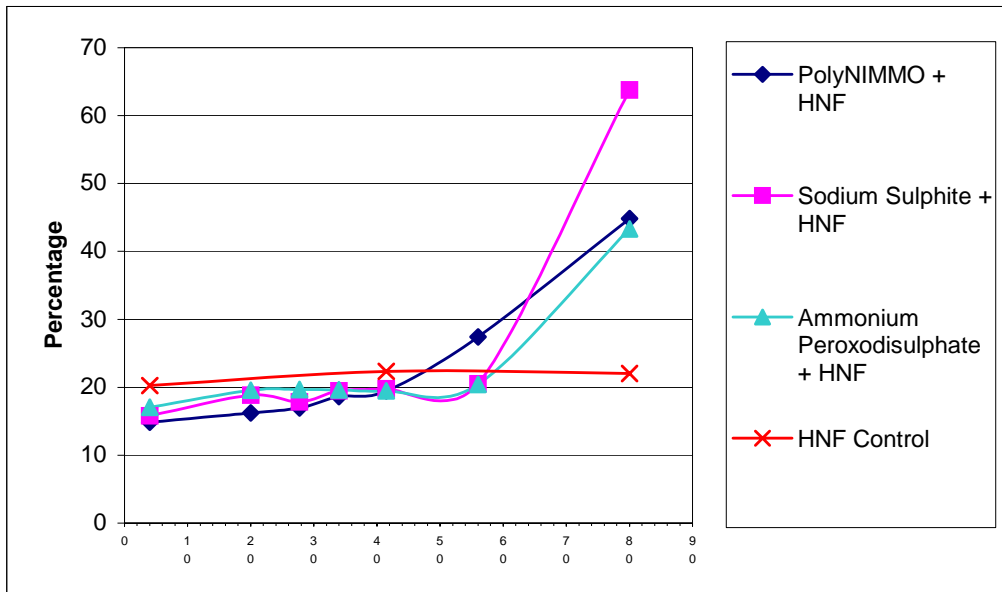
Figure 65 – Evolution of Nitrogen from Test Samples During Storage at 70°C
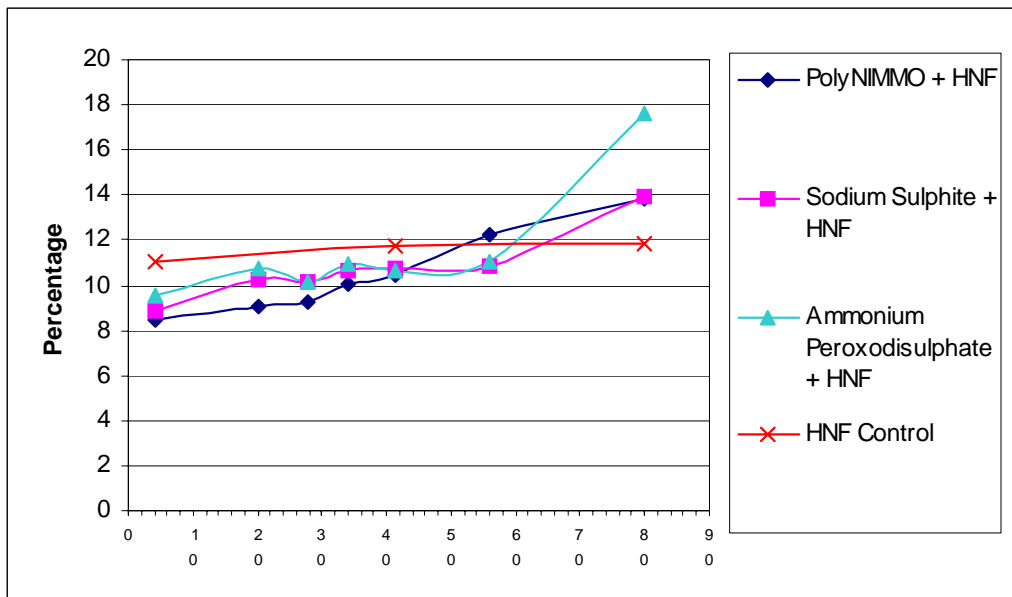
Figure 66 – Evolution of Oxygen From Test Samples During Storage at 70°C
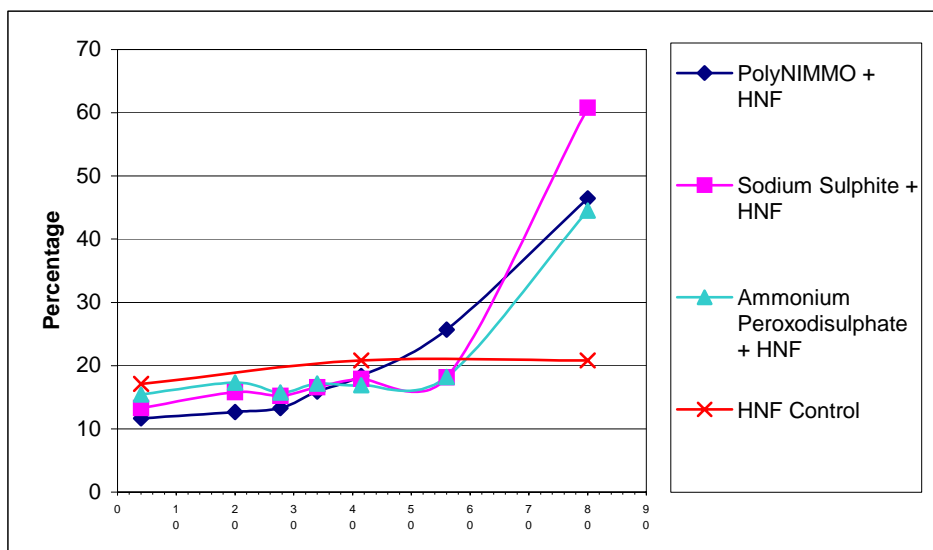
Figure 67 – Evolution of Water From Samples During Storage at 70°C
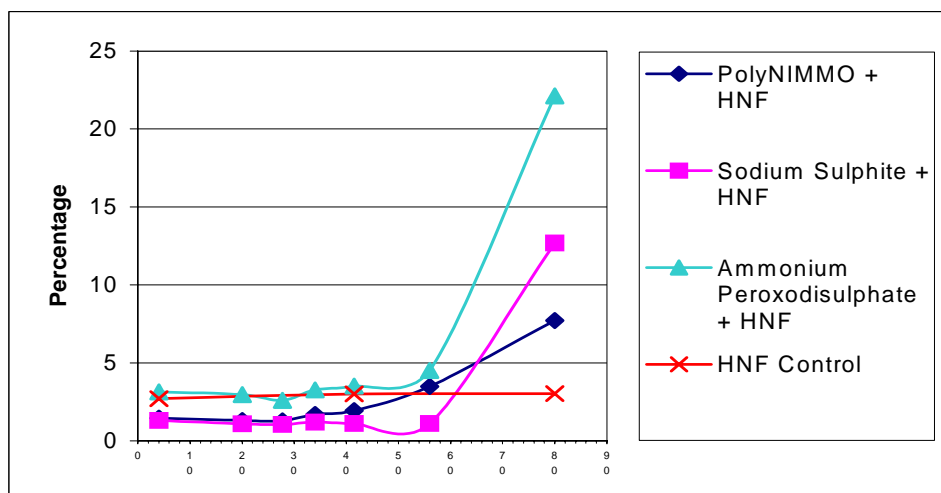
Figure 68 – Evolution of Carbon Dioxide From Samples During Storage at 70°C

This indicates that, although the hydrazine scavengers may aid stability of HNF compared to polyNIMMO, they ultimately show chemical incompatibility by accelerating the chemical decomposition of HNF. Of the materials tested, sodium sulphite was the most incompatible at the end of storage even though inhibiting liberation of other gaseous species for the longest storage period. The long contact time between the scavengers and HNF suggest that this is not a primary chemical compatibility but driven by a secondary reaction product or exhaustion of a reagent.

Bellerby et al [104] detail the overall reaction for HNF degradation as

3 x HNF → 2 x Ammonium Nitroformate + 3 x Nitrogen (I) Oxide + Water + Ammonium Formate

(Reaction R17)

and that the driving force in this reaction is the formation of nitrous acid. GASTEC studies (Section 3.2) although limited in scope suggested a possible reaction scheme of

HNF → Hydrazine → Amine Intermediate → Hydrazoic Acid + Ammonia + Nitrogen
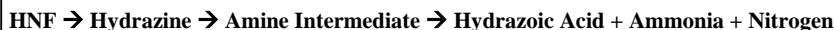
(Reaction R18)

The GC-MS data indicates that within the polyNIMMO sample, evolution of N_2O is occurring from the start of heating, regardless of the concentration of IPA (Figure 64). This suggests the reaction of Bellerby et al [104] to liberate N_2O is occurring independently of the IPA present. In the presence of Sodium Sulphite and Ammonium Peroxodisulphate, Figure 64 suggests liberation of N_2O is retarded (most markedly in the Sodium Sulphite samples). This suggests that the reaction of Bellerby et al is being modified in the presence of these scavengers. Therefore the presence of IPA does not inhibit the reaction scheme of Bellerby but the combination of IPA + either of the solid hydrazine scavengers is the dominant effect affecting gas evolution. This does not liberate any additional gaseous products during storage and so suggests that reaction is not via the hydrazine liberation suggested from GASTEC trials. However, the increased nitrogen content observed in Figure 65 and the increase in water content as shown in Figure 67 may be related to hydrazine reaction possibly via oxidation as shown in reactions R10 or R11. Schmidt [103] states that the decomposition of hydrazinium diperchlorate is "accelerated by the addition of perchloric acid" and implies that the long induction period prior to rapid decomposition observed during ageing of hydrazinium diperchlorate is attributed to the time taken for the first formation of perchloric acid by transfer of a bridging hydrogen to the perchlorate ion. Verneker and Sharma [129] details that for the diperchlorate, the rate determining step is the diffusion of perchlorate ions or hydrazinium ions to preferential sites within the crystal where a proton transfer can occur. They also suggest that interstitial cavities can increase reactivity. The loss of IPA from the crystal matrix may accentuate decomposition of the HNF present in a similar way. However, this seems unlikely as a similar level of decomposition would be observed in the HNF control. This points to a reaction between IPA and the hydrazine scavengers as the primary additional reaction occurring in the test samples.

The reaction between IPA and the scavengers is hypothesised to occur via a combination of related, concurrent reactions. In all samples, it is proposed that reaction is initiated by the loss of hydrazine from the solid (as detected during GASTEC colorimetric trials in Section 2.4.2). It is proposed that hydrazine is not detected during these GC-MS due to the test conditions and possible on column degradation / reaction of the species). In the absence of an oxidising

species (other than HNF) this initiates the reaction detailed by Bellerby [104] liberating N_2O. In the presence of an oxidising species (eg sodium sulphite or ammonium peroxodisulphate), the hydrazine liberated is proposed to be oxidised to nitrogen via diimide formation ie

Hydrazine + Oxidiser → HN=NH (+2H$^+$ + 2e$^-$)

HN=NH + Atmospheric Oxygen → N_2 + 2H$_2$O [118]
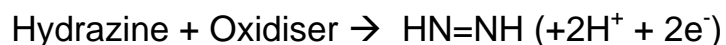
(Reaction   R19)

This removes the active hydrazine species from the reaction vessel but contributes to the increase in concentration of nitrogen and water as indicated in Figures 64 and 67.

Simultaneously with the oxidation of hydrazine, IPA migrates to the surface of the HNF crystals and starts to be lost from the surface after the induction period of ~ 28 hours. In polyNIMMO, it is proposed that the IPA liberated is held within the polymer matrix and does not undergo further reaction. This is the explanation for the low level of IPA detected and the near constant concentration observed in the polyNIMMO / HNF sample beyond its maximum value (Figure 60). As storage continues, the concentration of IPA increases as the migration to the crystal surface continues. In the presence of a strong oxiser other than HNF, it becomes oxidised to propanone ie

Propan-2-ol   + oxidiser   → Propanone [118]

(Reaction R20)

The rate of oxidation of propan-2-ol would then be related to the oxidising strength of the scavenger. From Figure 60, the lower oxidising power * of sodium sulphite allows a sharp concentration peak to form (~ 33% at peak maximum) where the higher oxidising power of ammonium peroxodisulphate leads to a more rapid reaction (and reduction of peak maximum to ~ 15%). Functional group analysis (Section 1.4.2.4) has indicated the higher level of chemical incompatibility between ketones and HNF compared to alcohols. The lack of reaction between IPA and HNF (ie a strong oxiser) is likely related to the relative insensitivity of hydrazine towards reaction with alcohols [103] [118] .

* The oxidising power of the sulphite and peroxodisulphate ions has been inferred from the electrochemical potential for reaction of the ions as given by Lide [130]

The reduction in IPA concentration detected in the sodium sulphite and ammonium peroxodisulphate samples compared to the HNF control also indicates that direct reaction is occurring to remove the product.

Trials of excess propanone addition to EVAP grade HNF by the author has been shown to evolve rapid but low level effervescence [110] . This high rate of reaction between HNF and propanone is proposed to be the explanation why no propanone is detected in the GC-MS headspace analysis. This propanone / HNF reaction is also the possible source of the CO_2 observed (Figure 68).

From Figures 65-68, the rate of evolution of all other species except CO_2 detected within the sample vials differ markedly between the sodium sulphite and ammonium peroxodisulphate samples. Generally, analytes are liberated more rapidly from sodium sulphite samples once reaction starts. It can be observed that the rate of liberation of CO_2 from each test sample is more closely matched for the two samples (ie the gradient for liberation are similar for the two samples in Figure 68) and so may relate more closely to the initial concentration of IPA.

Once IPA to propanone conversion is initiated, it is proposed to promote the formation of N_2O and water. However, the rapid evolution and exponential form of the evolution of the gaseous products observed in Figures 60-63 is proposed to be due to an additional reaction occurring to promote hydrogen transfer across the bridging hydrogen of the hydrazinium / nitroformate bond. This reaction is proposed to be via direct reaction of the carbonyl group an the hydrazinium ion. This hypothesis was discussed in more detail in Section (Figure 11) but an intermediate species is shown in Reaction R21 is proposed, leading to the formation of a hydrazone, thus inducing hydrogen transfer to the nitroformate ion.
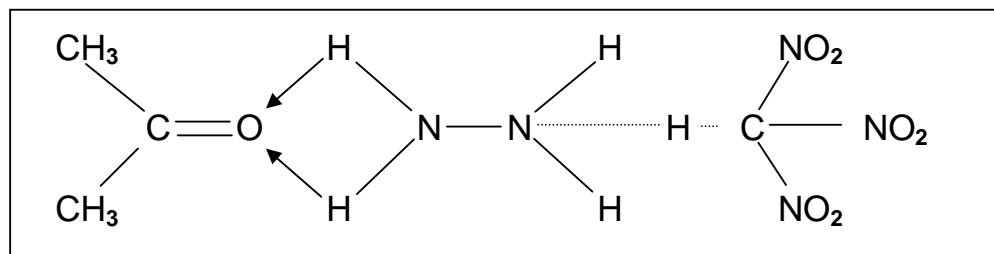
(Reaction R21)

Reaction R22 shows the proposed products of the rearrangement of the intermediate in reaction R21 to form final products.

$$(CH_3)_2 C = N - NH_2 \quad + \quad HC(NO_2)_3 \quad + \quad H_2O$$

Nitroform
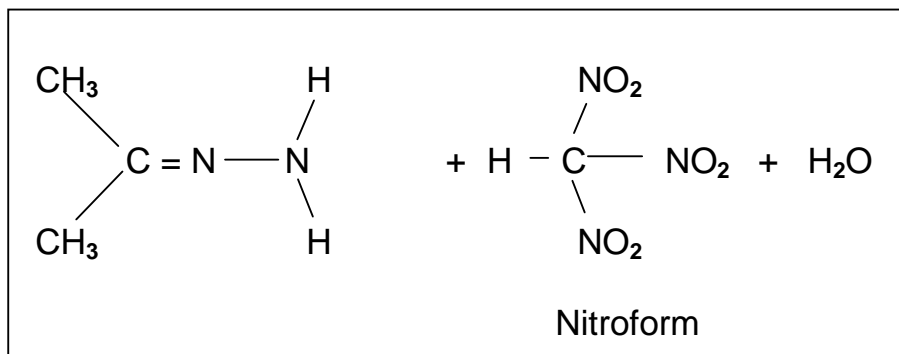
(Reaction R22)

The incompatibility of HNF with NO-2NDPA (Section 2.4.4.3) has already highlighted the "hydrazine-like" qualities of HNF. It does not seem unreasonable that hydrazone formation may also occur with propanone. Further study would be required to investigate this reaction further but it does provide a method to explain the observed data

2.6.4 Conclusions

Liberation of gaseous species from HNF in combination with secondary materials has been investigated. In addition to the reaction course detailed by Bellerby et al [104] , reaction appears to be intimately linked to the evolution and eventual decay of the contaminant Iso-propyl alcohol and also the low level evolution of hydrazine during thermal decomposition of HNF.

2.7 Conclusions from Analysis of HNF

Data analysis gives a number of conclusions and hypotheses from HNF analysis and accelerated ageing. The principal contaminant detected in the HNF sample was the residual processing solvent, isopropyl alcohol (propan-2-ol).During GC-MS studies, it was proposed that this solvent (via its oxidation to propanone) was a possible route to higher levels of gassification in the HNF present. Anhydrous Sodium Sulphate and Ammonium Peroxodisulphate may act as oxidisers to remove the contaminant IPA. The concentration of IPA appears to be linked to the timing of an increase in rate of degradation of HNF. In addition to this decomposition mechanism, trials suggest that the reaction course suggested by Bellerby et al [104] to liberate Ammonium Nitroformate is concurrent with any secondary IPA / HNF reaction. However, Colorimetric Analysis of gaseous products has highlighted some gaseous reaction products that were not detected by GC-MS – most notably hydrazine. The reaction course suggested by the colorimetric analysis is

```
┌─────────────────────────────────────────────────────────────────────────┐
│                                                                           │
│  HNF ────▶ Hydrazine ────▶ Amine Intermediate ────▶ Ammonia + Nitrogen + Hydrazoic Acid │
│                                                                           │
└─────────────────────────────────────────────────────────────────────────┘
```
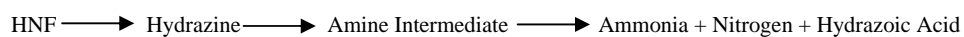
With a transient reaction stoichometry of :-

```
┌─────────────────────────────────────────────────────────────────────────┐
│                                                                           │
│  HNF ────▶ 1 [H+] + 1 Hydrazine + 2 Ammonia + 1 Amine Intermediate        │
│                                                                           │
└─────────────────────────────────────────────────────────────────────────┘
```
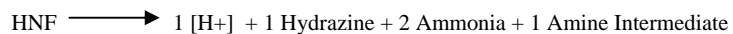
The hydrazoic acid liberated within this reaction is then proposed to react further, possibly with atmospheric oxygen to form water, nitrogen or nitrogen oxides; the products formed are dependent on a range of possible reaction course [127]

Although some researchers have suggested that the thermal degradation of HNF is an autocatalytic process, DSC studies suggest that gaseous products from HNF degradation do not catalyse the solid decomposition reaction but do affect the mechanism of decomposition once thermal decomposition is encountered. This may suggest that any catalysis that might be observed occurs within a condensed phase but this is not evident from the test results. Finally, DSC Analysis of HNF + Nitrated Derivatives of 2NDPA / pNMA indicate that N-NO-2NDPA + HNF has been shown to be highly chemically incompatible. N-NO-pNMA exhibits marked chemical incompatibility with HNF but to a lesser extent than N-NO-2NDPA. 2NDPA and 2,2'-DNDPA may exhibit mild incompatibility but all higher nitrated derivatives assessed exhibited no marked incompatibility

The overall reaction course for ageing of HNF is hypothesised to follow the reaction course shown in Figure 69.
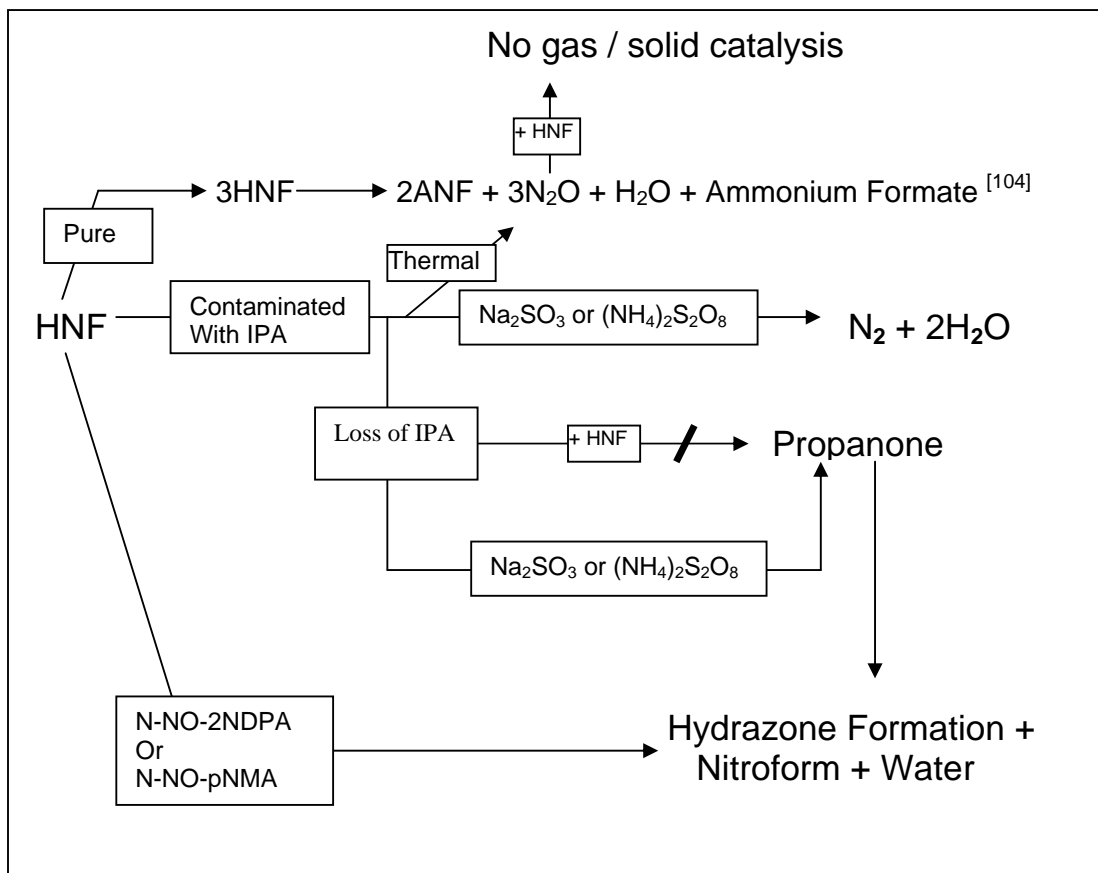
Figure 69 - Overall Hypothesis for thermal Degradation of HNF.

3.Investigations of HNF-Based Propellants

3.1 Introduction

The overall commercial aim of this study into HNF centred on the development of a HNF based propellant for use within a tactical missile system. To achieve this, a study to extend the understanding of the ageing behaviour of HNF within a series of polyNIMMO based propellants was undertaken. Elevated temperature storage of a series of polyNIMMO / HNF propellants incorporating the various denitration stabilisers and hydrazine scavengers was undertaken. Propellant samples were stored at a range of elevated temperatures (80°C, 60°C and 40°C) and sampled at regular intervals. The analyses carried out to assess the changes occurring within the propellant matrices were :-

1) Visual assessment to assess changes in test samples during storage

2) Mass loss to assess gassification or volatilisation effects

3) Aqueous extraction of HNF and HNF derivatives to assess loss of soluble species

4) THF extraction of polymer residues to assess breakdown of the polymer binder

5) HPLC analysis of stabiliser residues to assess the extent of their degradation within the propellants

In combination, these datasets were to allow wider consideration of aspects of the progression of propellant breakdown (ie HNF, stabiliser and polymer breakdown) to give a wider view of the degradation scheme. By interpretation of the observations and conclusions from each individual analytical method, it was hoped to build up a detailed picture of overall propellant ageing character.

Two different stabiliser types were envisaged for use within the propellant formulations ;these were :-

a) denitration stabilisers * for protection of the polyNIMMO backbone, and

b) hydrazine scavengers active against HNF degradation products

* The term "denitration stabiliser" is applied to those stabilisers that react against NOx and HNOx species liberated from the degradation of energetic materials containing the nitrate ester (-O-NO$_2$), nitramine (-N-NO$_2$) or nitro (-C-NO$_2$) moieties. A range of these stabilisers is shown in Figure 5.

Both Bunyan [51] and Manelis [62] have shown that 2NDPA is a suitable stabiliser for control of polyNIMMO degradation; this was selected as a suitable denitration stabiliser for the HNF / polyNIMMO system. In combination with 2NDPA, pNMA was chosen for investigation due to its widespread use in double base propellant technology as a co-stabiliser with 2NDPA. Although concerns about the chemical incompatibility of 2NDPA and HNF [113] were considered, it was decided that the residues formed from the incompatibility reaction (in combination with the denitration reactions) would help elucidate a wider range of possible reactions occurring during storage. Section 2.5 had highlighted the high level of chemical incompatibility between N-Nitroso-2NDPA and HNF and the formation of this derivative could be one source of the apparent chemical incompatibility of 2NDPA with HNF within propellant systems.

Section 2.6 had identified Sodium Sulphite and Ammonium Peroxodisulphate for possible use as hydrazine scavengers with HNF. These hydrazine scavengers were investigated as potential co-stabilisers with pNMA and 2NDPA in the propellant formulation. If a series of sequential or simultaneous reactions were occurring in the propellant formulation (eg denitration from the polyNIMMO polymer backbone and hydrazine formation from chemical degradation of HNF), then a mixed stabiliser / scavenger system was thought to be a possible route towards improved propellant stability.

3.2 Experimental

3.2.1 Propellant Preparation

Samples were manufactured from dihydroxy polyNIMMO and EVAP grade HNF. Preparation of each formulation was undertaken by initially drying all materials (with the exception of the isocyanate) to a water content of < 0.2%. DBTDL in hexane to act as cure catalyst was then added to the required quantity of polyNIMMO. The hexane was removed under vacuum and the DBTDL distributed throughout the polyNIMMO sample at a concentration of 200ppm. The trifunctional isocyanate Desmodur N100 is added to provide an NCO : OH equivalence of 1.2. The use of excess isocyanate was undertaken to allow for potential precure reactions between HNF and the isocyanate moiety. This base polymer matrix was then thoroughly mixed and degassed under vacuum. Addition of HNF at a 65% level was then undertaken and the sample mixed until smooth and free from material clumping. Subsamples of the propellant precure were taken (nominally 20g) and the desired level of stabiliser / scavenger added to the subsample. The resulting paste was lightly compressed to form a 5-10mm thick slice and cured at ambient (25°C) temperature. After 24 hours storage, the samples had all cured to a firm rubber. This method is a "plus addition" method of propellant production meaning that a base formulation is used throughout the trials

and the stabiliser added to the subsample. This results in changes in the overall ingredient percentage of any individual ingredient (eg plus addition of 10% of an ingredient reduces the relative percentages of all components by a ratio of 100/110) but the plus addition method provides a common basis for sample comparison. For each series of trials, subsamples (typically 0.5 or 1g) were placed into dry, 10ml glass vials which were then sealed with a septum.

3.2.2 Propellant Formulations

The formulations were designed to assess the effectiveness of denitration stabilisers and hydrazine scavengers at varying storage temperatures and overall percentages. The hydrazine scavengers identified in Section 2.6 were investigated both in isolation and in combination with denitration stabilisers to assess any stabiliser synergy. A series of propellant formulations were prepared for analysis to incorporate the various stabiliser systems proposed. The compositions are shown in Table 10.

	HNF	polyNIMMO	Stabiliser	Isocyanate (N100)	NCO/OH Ratio	DBTDL
STO1	65	28.92	None	6.08	1.2	200ppm
STO2	65	28.92	+ 1% (of Total) 2NDPA	6.08	1.2	200ppm
STO3	65	28.92	+ 8% (of Total) 2NDPA	6.08	1.2	200ppm
STO4	65	28.92	+ 16% (of Total) 2NDPA	6.08	1.2	200ppm
STO5	65	28.92	+ 1% (of Total) pNMA	6.08	1.2	200ppm
STO6	65	28.92	+ 8% (of Total) pNMA	6.08	1.2	200ppm
STO7	65	28.92	+ 16% (of Total) pNMA	6.08	1.2	200ppm
STO8	65	28.92	+ 0.5% pNMA + 0.5% 2NDPA	6.08	1.2	200ppm
STO9	65	28.92	+ 4% pNMA + 4% 2NDPA	6.08	1.2	200ppm
STO10	65	28.92	+8% pNMA + 8% 2NDPA	6.08	1.2	200ppm
STO11	65	28.92	+ 2% pNMA + 1% 2NDPA	6.08	1.2	200ppm
STO12	65	28.92	+ 2% 2NDPA + 1% pNMA	6.08	1.2	200ppm
STO13	65	28.92	+ 1% (of Total) 2NDPA + 1% Total Anhydrous Na_2SO_3	6.08	1.2	200ppm
STO14	65	28.92	+ 1% (of Total) 2NDPA + 1% Total Anhydrous $(NH_4)_2S_2O_8$	6.08	1.2	200ppm
STO15	65	28.92	+ 1% (of Total) pNMA + 1% Total Anhydrous Na_2SO_3	6.08	1.2	200ppm
STO16	65	28.92	+ 1% (of Total) pNMA + 1% Total Anhydrous $(NH_4)_2S_2O_8$	6.08	1.2	200ppm
STO17	65	28.92	+ 1% Anhydrous Na_2SO_3	6.08	1.2	200ppm
STO18	65	28.92	+1% Anhydrous $(NH_4)_2S_2O_8$	6.08	1.2	200ppm

Table 10 – Propellant Formulations

3.2.3 Propellant Storage

Propellant sampling was designed to assess the formulation over a period that encompassed both low levels and high levels of degradation whilst supplying details of the period of transition between the two. The sampling times for each formulation are given in Table 11.

Temperature	For single stabiliser, pNMA based formulations STO5, STO6, STO7, STO15, STO16, STO17, STO18				
80	2 Hr	6 Hr	12 Hr	24 Hr	48 Hr
60	7 Hr	24 Hr	44 Hr	88 Hr	176 Hr
40	28 Hr	85 Hr	170 Hr	341 Hr	682 Hr
	For single stabiliser, 2NDPA based formulations STO2, STO3, STO4, STO13, STO14				
80	12 Hr	24 Hr	28 Hr	35 Hr	48 Hr
60	16 Hr	48 Hr	80 Hr	100 Hr	130 Hr
40	24 Hr	130 Hr	250 Hr	390 Hr	700 Hr
	For mixed stabiliser, pNMA / 2NDPA based formulations ST8, ST9, STO10, STO11, STO12				
80	2 Hr	6 Hr	12 Hr	35 Hr	48 Hr
60	7 Hr	24 Hr	48 Hr	80 Hr	100 Hr
40	24 Hr	85 Hr	130 Hr	180 Hr	370 Hr

Table 11 : Sampling Regime for Propellant Samples

The times chosen were based on predictions for previous HNF propellant testing [110] . Generally, the storage times at each temperature for each individual formulation were planned to achieve similar degrees of reaction for each test sample at the end of the maximum storage period. This was achieved using the estimation that, for a given chemical process with a constant reaction rate, the reaction rate will be approximately doubled for every 10°C increase in storage temperature. The intermediate sampling times were varied slightly to overlap times of predicted importance for the degradation (predicted from previous storage data [110]) or to fit into convenient work patterns.

3.3 Results and Discussion

3.3.1 Visual Inspection

Samples were stored in a fan assisted oven at 80°C, 60°C or 40°C for the time periods detailed in Table 10 with samples being removed for assessment at various intervals It was observed that at 80°C storage, a number of samples ignited or partially ignited during storage. In the later stages of storage, samples generally showed some degree of softening, eventually forming viscous liquids after long term storage. This extent of reaction was less commonly observed at lower temperatures. Post storage, the analysis regime outlined in Section 3.1 was applied.

3.3.2 Mass Loss

After each storage period, a test vial was removed from storage. The septum cap was removed and the sample allowed to stand for 10 minutes to allow the removal of any gaseous products that had not reacted with other species within the vial. The sample was then reweighed to assess the mass loss that had occurred during storage.

Assessment of the mass loss from samples during storage was planned to give an understanding of sample gassification or volatilisation during storage. The level of volatilisation / gassification and the effect of stabiliser combinations on this level was taken as an indication of stabiliser efficiency. Assessment of stabiliser efficiency over a range of storage temperatures then indicates whether mass loss and stabiliser efficiency is temperature dependent. Figures 70 to 78 show the mass loss graphs for the three propellant classes (ie pNMA, 2NDPA or mixed stabiliser systems) stored at 80°C, 60°C and 40°C.
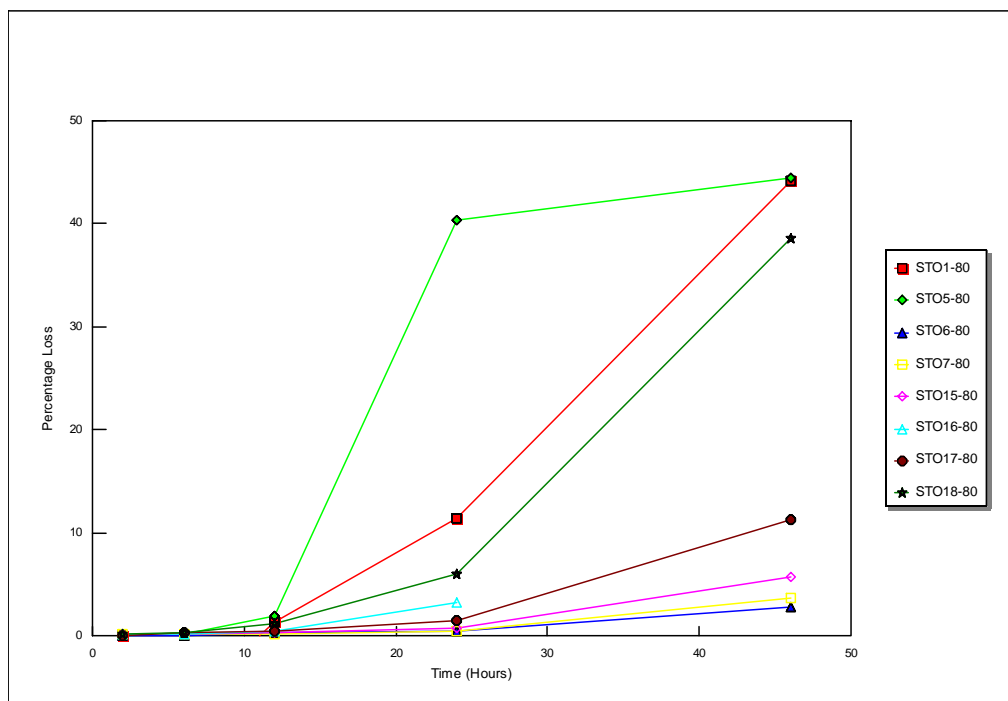
Figure 70 : Mass Loss of pNMA and Hydrazine Scavenger Stabilised Propellants at 80°C

Figures showing the 80°C data (Figure 70, 71 and 72) generally indicate an induction period for decomposition followed by higher rate mass loss. This is generally also observed at 60°C (Figure 73. 74 and 75) and 40°C (Figure 76. 77 and 78) . This mass loss profile suggests that propellant degradation is a two-stage process. During the induction period, an initiating reaction is occurring without promoting any mass loss via large-scale propagation to the bulk sample.
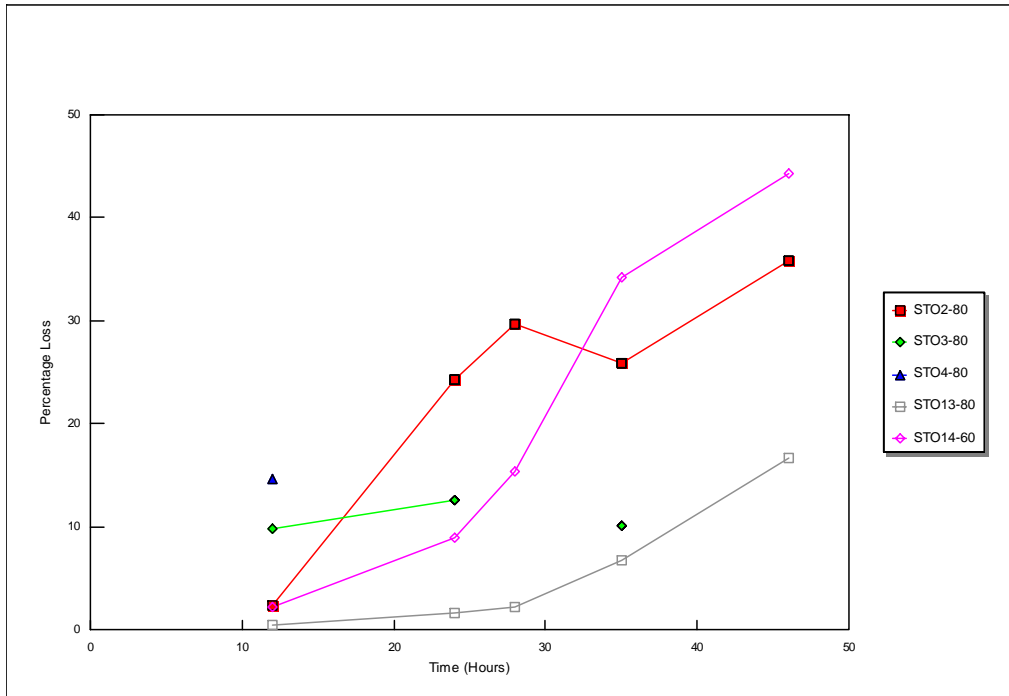
Figure 71 : Mass Loss of 2NDPA Stabilised Propellants at 80°C
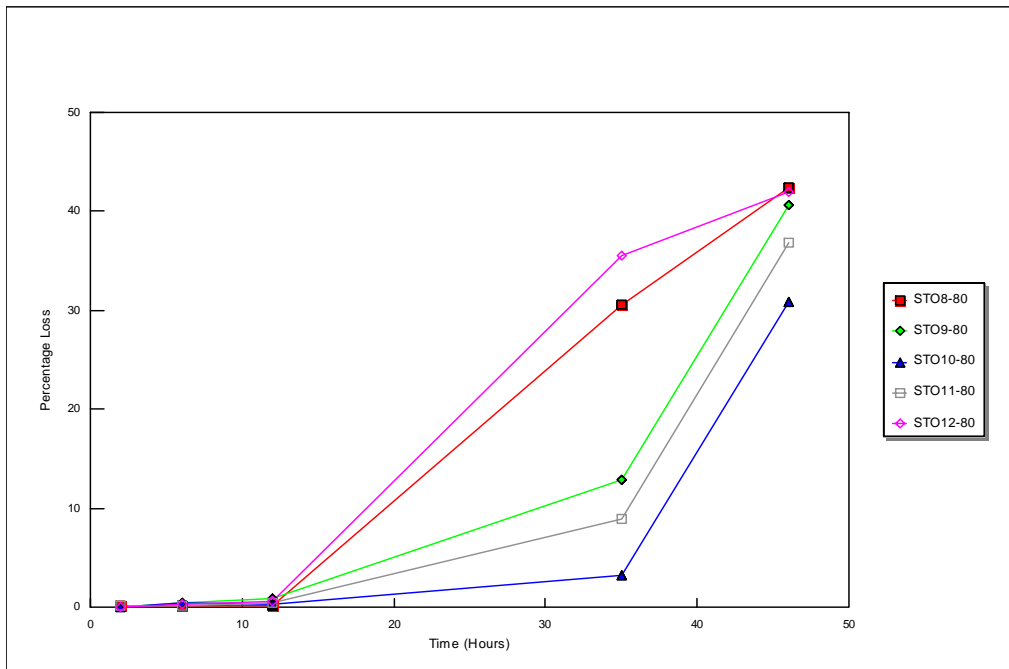
Figure 72 : Mass Loss of pNMA / 2NDPA Stabilised Propellants at 80°C

However, once a critical level of one (or more) products of the initiating reaction has been achieved, more rapid (and possibly autocatalytic) breakdown is observed In addition to the general induction / propagation mass loss profile, a number of formulations show reduced mass loss compared to the control sample STO1 The reduction in mass loss suggests some degree of improved stability is present in the stabilised samples compared to the control. This in turn suggests control of the reaction driving degradation, most likely via control of a product liberated from the initiating reaction.
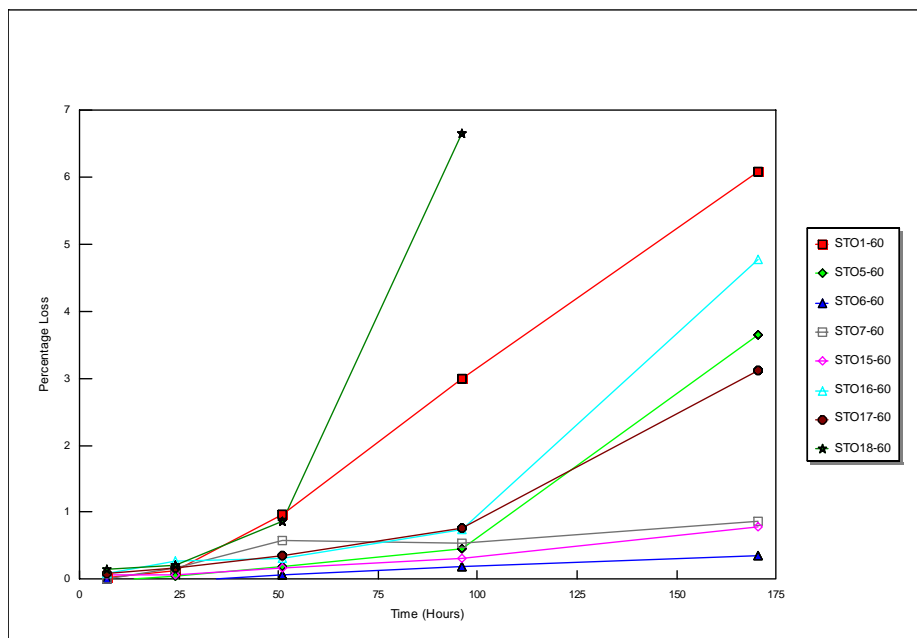
Figure 73 : Mass Loss of pNMA and Hydrazine Scavenger Stabilised Propellants at 60°C
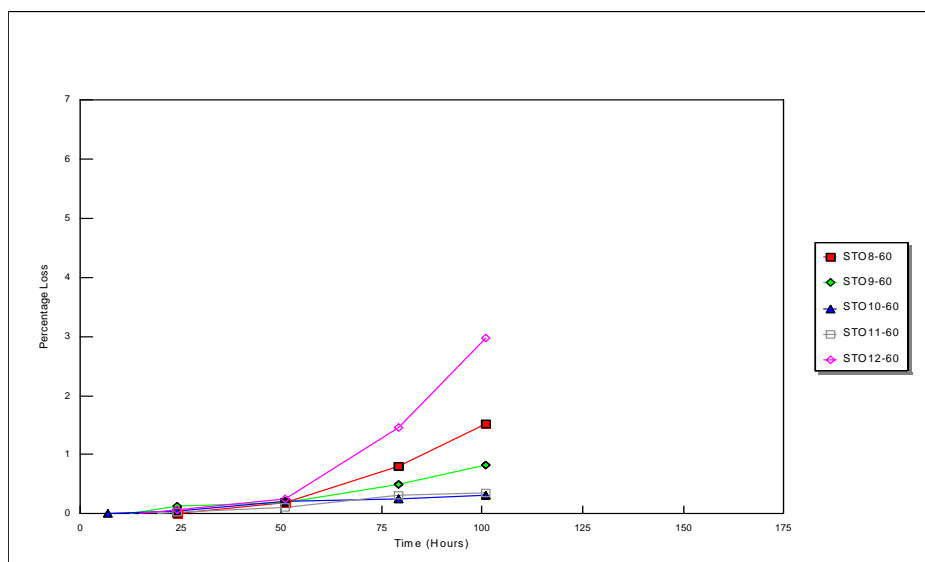
Figure 74 : Mass Loss of pNMA / 2NDPA stabilised Propellants at 60°C
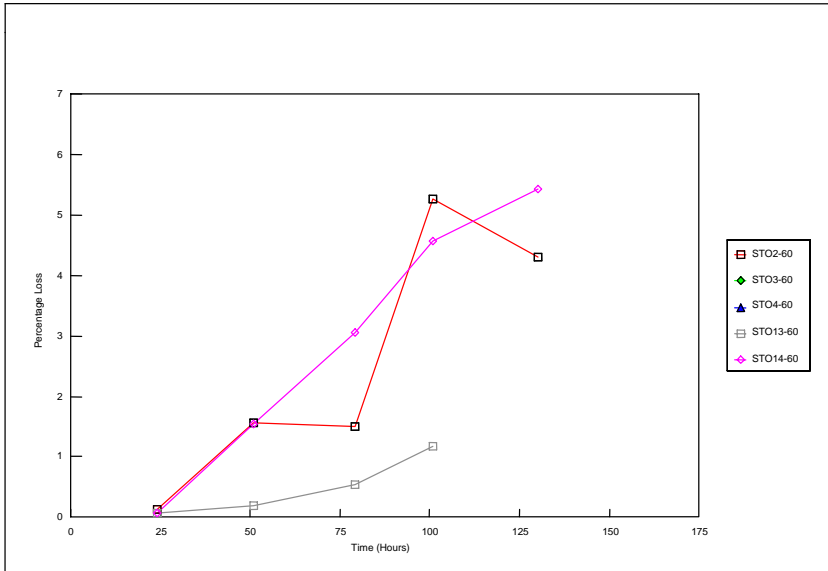
Figure 75 : Mass Loss of 2NDPA stabilised Propellants at 60°C
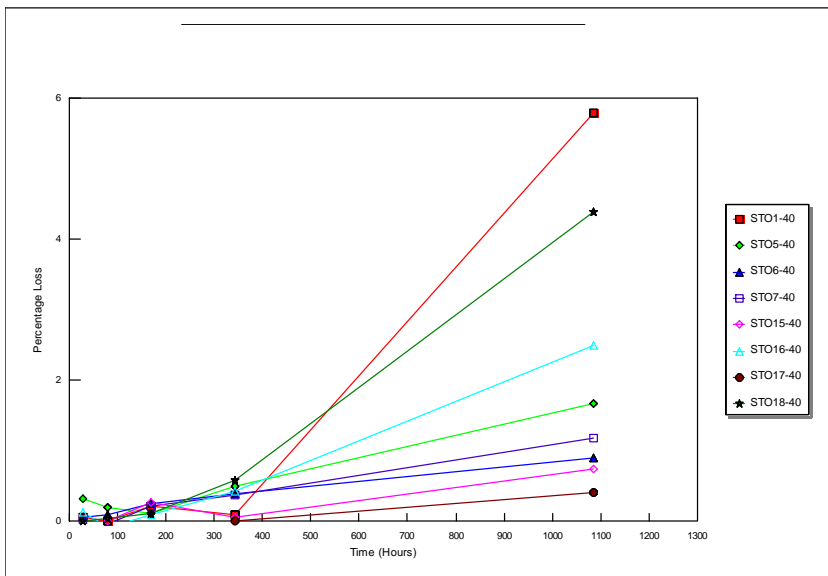
Figure 76 : Mass Loss of pNMA and Hydrazine Scavenger Stabilised Propellants at 40°C
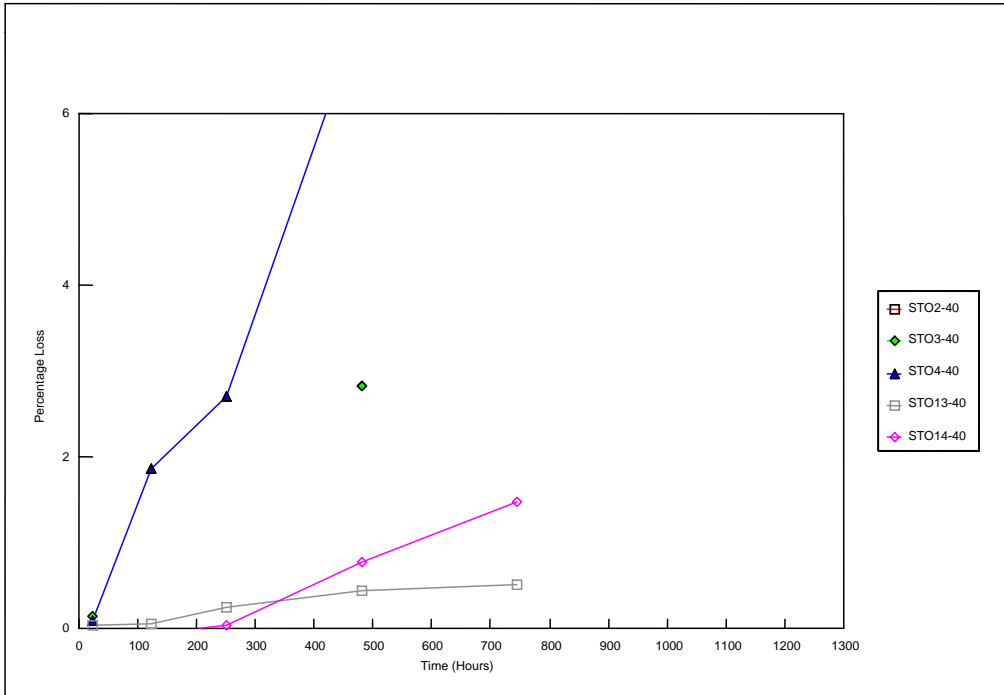
Figure 77 : Mass Loss of 2NDPA stabilised Propellants at 40°C
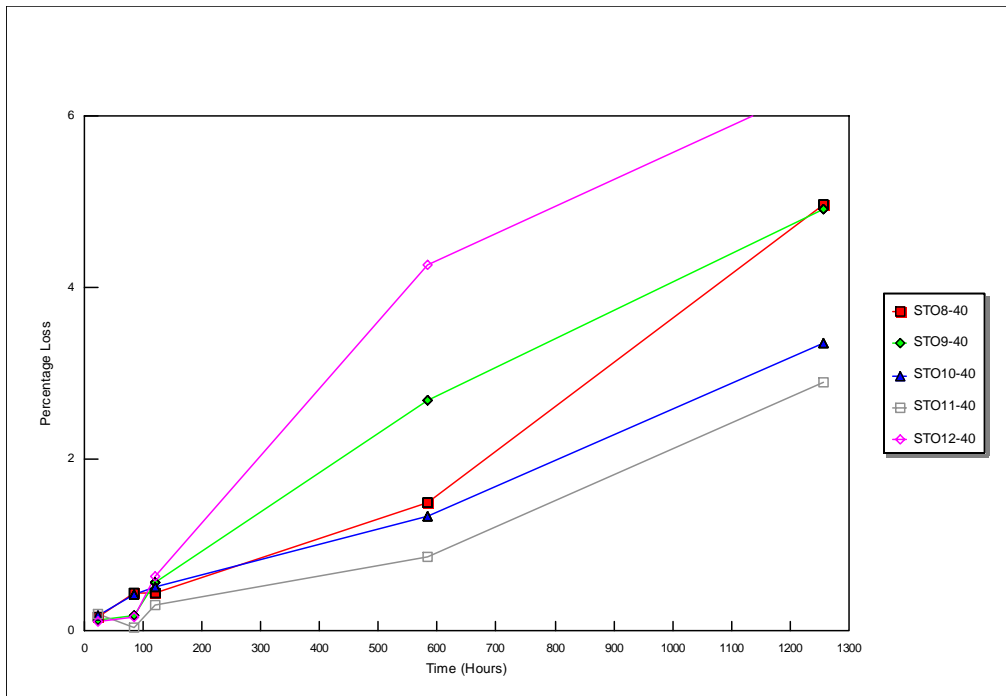
Figure78 : Mass Loss of pNMA / 2NDPA stabilised Propellants at 40°C

Figures 70 to 78 show the mass loss determined at each temperature for each test sample. These are summarised in Table 12 in terms of overall mass loss.

80°C	60°C	40°C
Lowest Mass Loss		
STO6	STO6	STO17
STO7	STO10	STO15
STO15	STO11	STO6
STO17	STO15	STO7
STO13	STO7	STO5
STO10	STO9	STO13
STO16	STO17	STO14
STO11	STO5	STO16
STO2	STO16	STO11
STO18	STO13	STO10
STO9	STO8	STO18
STO8	STO12	STO9
STO12	STO1	STO8
STO1	STO2	STO12
STO5	STO14	STO1
STO14	STO18	STO3
STO3	STO3 (Not Assessed at 60)	STO4
STO4	STO4 (Not Assessed at 60)	STO2 (Not Assessed at 40)
Highest Mass Loss		

Table 12 - Comparison of Mass Loss Data at Each Test Temperature

The arrows in Table 12 connect the relative position of each individual sample at each temperature. It can be observed that for the majority of samples, the position of test samples across the temperature range varies with storage temperature. Changes in position across Table 12 suggest a possible change in the reaction mechanism of degradation at different temperatures. Correlation of the actual mass loss at each temperature has also to be taken into account and is detailed in the text

It is proposed that at each temperature, the dominant decomposition mechanism occurring within the propellant matrix determines the position of the sample in Table 12. For example, in formulation STO5 (Figures 70, 73 and 76) the 1% pNMA present is predicted to function primarily as a stabiliser that reacts with NOx species formed within the test matrix. In Table 12, this stabiliser function appears to become progressively more effective as the temperature is decreased (ie it has a position higher up the table at 60°C and 40°C degrees compared to 80°C.). This suggests that liberation of NOx is lessened with reduced temperature and the stabiliser is "active" within the propellant formulation for longer during storage. The observation also suggests that the formation of NOx is an important part of the ageing mechanism. Other stabiliser systems appear to be more effective at 80°C and 40°C than at

60°C (e.g. in samples STO17, STO13 and STO18) whilst others show little change (e.g. the stabilisers present in formulations STO1, STO6, STO8, STO12, STO15, and STO16).

By relating the position of samples in Table 12 to the absolute mass loss achieved, an assessment of stabiliser efficiency and temperature effect can be inferred. As previously detailed, the storage time periods at each temperature were selected to give an approximately equal level of reaction at the end of storage. The mass loss from the unstabilised control sample (STO1) provides a measure of any underlying propellant degradation mechanism rate without any modification by stabiliser species. If a reaction mechanism leading to mass loss is present, this should be highlighted in the control sample data. If the level of mass loss when compared against the control sample STO1 is accentuated by the addition of a secondary material, the secondary material can be inferred to be detrimental to the stability of the propellant system. Conversely, if the level of mass loss is reduced relative to the control sample then the secondary material can be inferred to be advantageous to the stability of the propellant system.

STO1 Control Sample :- The position of the sample in Table 12 is fairly consistent at all temperatures. Figure 79 indicates that the level of mass loss observed at each temperature is very similar at 60 and 40°C suggesting a similar reaction course for the mass loss reaction that has also progressed to a similar degree in both samples. At 80°C, a significantly higher mass loss is observed, suggesting that a different mechanism is present at this temperature.
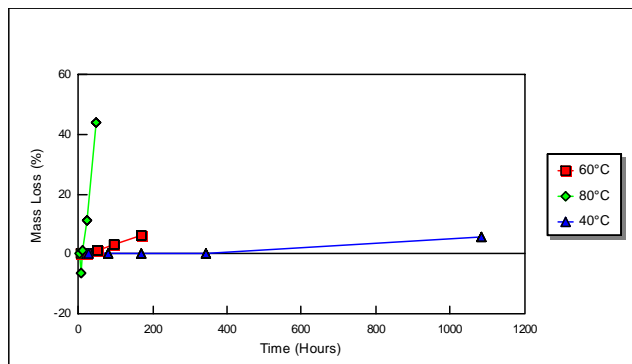
Figure 79 : Mass Loss Data for Sample STO1

As sample STO1 is the control sample for these trials, it must be concluded that all test samples will show this suspected change in reaction mechanism at 80°C unless the stabiliser affects the reaction course. The relative efficiency of each of the stabilisers at 80°C compared to STO1 reflects their application against this high temperature initiation / propagation reaction.

STO2, STO3, STO4 : A high rate of decomposition is observed within all 2NDPA loaded samples; this is seen in Figures 80 and 81. The detrimental reaction of 2NDPA and HNF which has been identified (via N-NO-2NDPA formation as detailed in Section 2.4.4) and is proposed to be the source of the significant mass loss observed. This suggests that reactions to support nitrosation are occurring within the propellant matrix. . Within the figures, insufficient sample was available of STO2 and STO4 for trials at 40°C and 60°C respectively to be completed
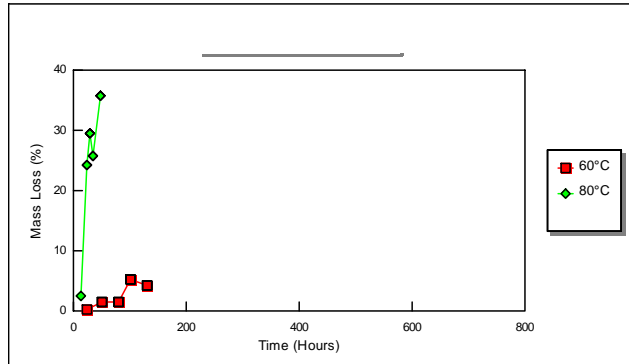
Figure 80 : Mass Loss Data for Sample STO2
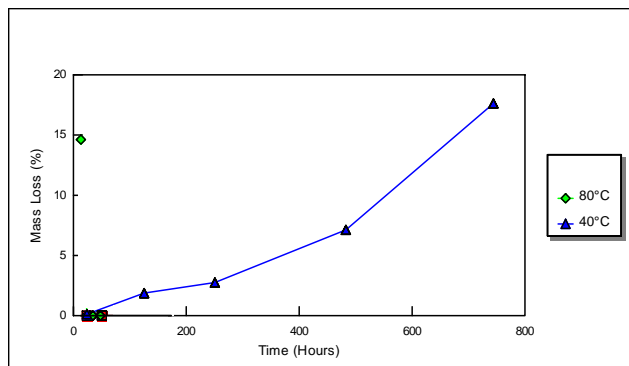
Figure 81 : Mass Loss Data for Sample STO4

STO5 : The relative effectiveness of the stabiliser in STO5 compared to STO1 improves with reduced temperature (ie appears at higher positions at 60°C and 40°C in Table 12 than at 80°C; this is also shown in Figure 82). This change in efficiency reflects the efficiency of the pNMA present within the system. Table 12 shows that samples with high pNMA contents (e.g. STO6 and STO7) show good performance in reducing mass loss at high temperatures. This suggests that the removal of NOx species aids sample longevity. Within sample STO5 (with comparatively low pNMA levels) it is hypothesised that the denitration of the base

matrix at 80°C liberates NOx species at concentrations in excess of the maximum activity of the stabiliser present. Under these conditions, the stabiliser rapidly becomes fully nitrated and so loses its ability to reduce reaction propagation towards large scale sample degradation. The excess NOx species are then free to propagate the degradation reaction further, possibly via direct reaction with HNF. At lower temperatures, the level of denitration is reduced and so the activity of the stabiliser against NOx is maintained for longer. The improved relative efficiency with reducing temperature also suggests that denitration of the base matrix is significantly reduced at lower temperatures.
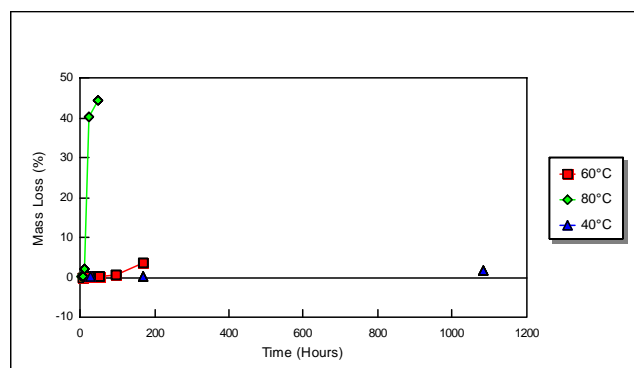
Figure 82 : Mass Loss Data for Sample STO5

STO6 / STO7 : Table 12 suggests that high levels of pNMA provide good stabilising effect, significantly reducing mass loss especially at high temperature. The mass loss at 80°C in STO6 (Figure 83) and in STO7 (Figure 84) is significantly less than within the control sample (STO1). This lower mass loss suggests that the initiating reaction for propellant degradation is driven predominantly by "free" NOx species within the matrix. However, if this was the sole reaction within the test sample during ageing at 80°C , it would be expected that there would be minimal mass loss until the stabiliser was fully depleted. Although it is possible (but unlikely) that the stabiliser would have been fully depleted during storage at 80°C, the mass loss seen at 60°C cannot be associated solely with NOx production (as this would certainly all be taken up by the stabiliser). This slow degradation shown within the samples indicates that there is a degree of competition between reactions of NOx with the stabiliser and that of NOx with other species within the matrix (e.g. HNF) or that a second, non-associated reaction is occurring (possibly thermal degradation of HNF). The similarity of mass loss data for sample STO6 at 40°C and 60°C suggests that the same reaction is occurring in the sample at both storage temperatures. This implies that any additional reactions involving NOx or HNOx species leading to autocatalysis are fully controlled by the addition of the stabiliser.
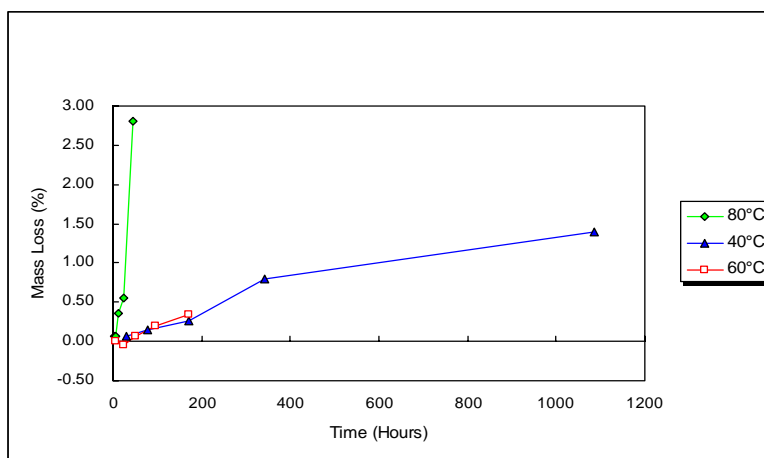
Figure 83 : Mass Loss Data for Sample STO6

Although providing very good stabilising effects at high temperatures, as storage temperatures decrease. The relative effectiveness of the stabiliser also decreases. This tallies with the previous suggestion that NOx liberation is not the dominant degradation mechanism at low temperature. The near coincidence of STO6 and STO7 with STO5 (1% pNMA) at 40°C appears to confirm the suggestions that the control of NOx species becomes less significant at lower temperatures but also that control of NOx species is critical to aiding sample longevity at higher temperatures. At 60°C, the sample with the highest level of pNMA (STO7, 16%) shows inferior stability with temperature compared to STO6 (8%). This reduced performance may suggest that the HNF / N-NO-pNMA reaction product identified as reactive against HNF in Section 2.4.4   may also be leading to a destabilising effect when excess pNMA is present.
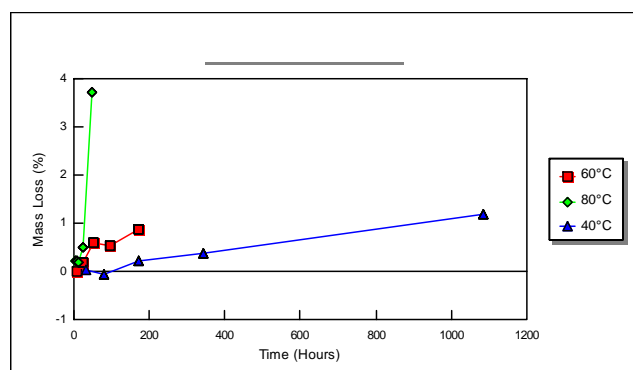
Figure 84 : Mass Loss Data for Sample STO7

STO8 / STO9 / STO10 : From Figure 85-87, at all temperatures, as the overall stabiliser content increases, the mass loss decreases (ie STO10 always exhibits lower mass loss than STO9 that is always superior to STO8). The graphs of STO2-4 indicate that the presence of 2NDPA has a detrimental effect on propellant mass loss but this is not seen within samples STO8-10. The improvement can most likely be attributed to the increasing pNMA content. Sequential reaction of pNMA and then 2NDPA, with each species trapping NOx species, is the predicted order of reaction from other sources [78] [82] . This strengthens the hypothesis that NOx liberation is the driving reaction for propellant failure and so the pNMA trapping would be expected to minimise propellant degradation. The sequential nature of pNMA followed by 2NDPA nitration also appears to mitigate against the formation of N-NO-2NDPA (ie if N-NO-2NDPA was forming at any part of the ageing process, a higher level of direct reaction of N-NO-2NDPA and HNF would be expected leading to higher levels of propellant degradation).

Although not as marked as in purely 2NDPA based systems, there is evidence that an HNF / 2NDPA reaction is occurring. If 2NDPA were playing no part at all in the propellant decomposition until pNMA activity was minimal, it would be expected that the mass loss of mixed stabiliser systems would align closely with those of purely pNMA stabilised analogues. The test results show that this is not the case. Comparison of STO10 (8% pNMA + 8% 2NDPA) and STO6 (8% pNMA) show that the stabiliser effectiveness only begins to align at 60°C. This suggests that at 80°C, 2NDPA may play a minor role in degradation even before pNMA is depleted. However, if this were the same reaction seen in STO2-4, it would be expected that the mixed stabiliser samples would not survive storage.

It is proposed that there is a direct reaction between HNF and 2NDPA but that this does not occur to a significant degree. At 80°C, it does lead to some mass loss but at a comparatively low level and possibly without significant destabilisation of the overall propellant system. Once nitrated derivatives of 2NDPA are formed however, they appear to lead in driving the degradation of HNF and the propellant base matrix. In addition to explaining the lack of 2NDPA / HNF reaction before full pNMA depletion has occurred , this hypothesis also explains why the continued, long term activity of 2NDPA in reacting with NOx species does not serve to safeguard the test sample longevity in the same way as pNMA / NOx reactions appear to do. Put another way, if the driving reaction for degradation in the formulations was NOx liberation, the removal of NOx species by 2NDPA would be expected to be beneficial (unless there was a second species present that had greater affinity for the NOx products). However, significant propellant degradation is actually observed.

It is observed that as temperature decreases, STO8 shows little or no change in relative stabiliser efficiency compared to STO1. However, both STO9 and STO10 show significantly reduced mass loss at 60°C compared to 80°C followed by a significantly higher relative loss at 40°C . This again suggests that there may be a different reaction mechanism operating at each of the different temperatures.

Accelerated ageing of the propellant samples is proposed to result in a series of complex equilibrium reactions. The relative dominance of each reaction is temperature dependent (ie different mechanisms dominate at different temperatures) and also time dependent (ie the reactions change in priority with the duration of the test, dependent on reagent growth / decay etc). The following processes are thought to be the most important:

1)   NOx liberation from polyNIMMO via HNF / polyNIMMO reaction
2)   Reaction of pNMA with NOx species
3)   2NDPA/ HNF direct reaction
4)   NOx / secondary reagent (HNF ?) reaction
5)   HNF degradation
6)   Inhibition of the 2NDPA / HNF and HNF degradation reactions by pNMA (or nitrated pNMA derivatives)
7)   Reaction of 2NDPA with NOx species
8)   Reaction of HNF with nitrated derivatives of 2NDPA
9)   Reaction of N-NO-2NDPA with HNF

It can be considered that direct loss of NOx species from the nitroformate ion in HNF with polyNIMMO could be occurring within the formulations during storage. However, this is thought unlikely as this reaction would progress at the same rate within each test sample and be dependent on the HNF / polyNIMMO ratio. Further trials would be required to locate any possible loss of NOx species from HNF (these are given in stabiliser depletion trials detailed later).

At 80 and 60°C, the dominant reactions are initially proposed to be (in order of importance) 1,2,,6 and 3. It is proposed that these reactions are dominant until pNMA activity is reduced to a minimum. Once this pNMA activity is at a minimum, reactions 9,4,3,5,7,8 are proposed to be dominant leading to a more rapid mass loss.   An illustration of this is seen in the comparison of mass loss in samples STO10 and STO6 at 80°C . Although both samples contain 8% pNMA, the addition of 2NDPA (in sample STO10) is detrimental to the mass loss

at 80°C but not at 60°C. This could be explained by the pNMA activity having fallen to a minimum at 80°C during the ageing process (ie reaction 2 has reached its limit and no further reaction is possible. The dynamic equilibrium formed between the various reactions is then modified with other reaction mechanisms becoming dominant. At 60°C it is proposed that the same reaction course is followed as at 80°Cbut at a lower rate of polyNIMMO denitration (ie reaction 1 is observed). In STO10 with a higher stabiliser content it is proposed that a pNMA activity minimum is not achieved at 60°C or 40°C and so all NOx products from reaction 1 are trapped by reaction 2 and are not available for reactions 4 or 8 to occur. At 60°C this appears to increase the effect of the inhibiting reaction 6 and minimise that of reaction 4. However, at 40°C this does not occur as the mass loss is seen to increase compared to 60°C. This could be explained by reduced denitration of polyNIMMO at this lower temperature. A lower rate of denitration and associated reaction results from either termination or minimisation of reactions 1,2, and 6 is proposed to leave reactions 3 and 5 to dominate. Both of these reactions are detrimental to propellant longevity and so are proposed to lead to propellant degradation at this lower temperature.
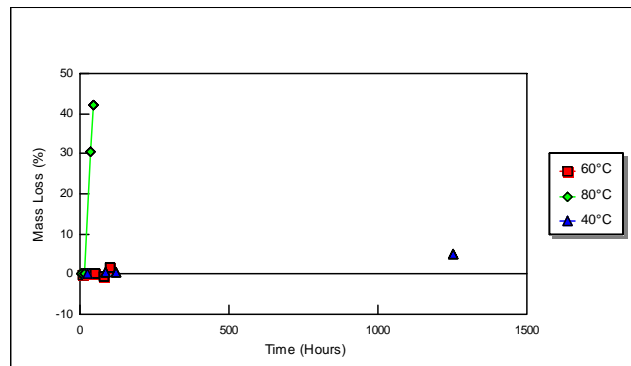
Figure 85 : Mass Loss Data for Sample STO8
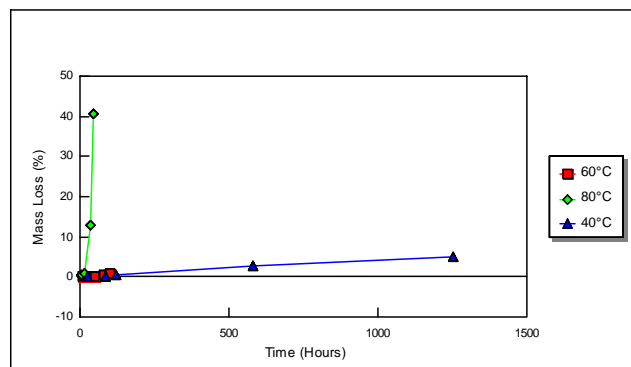
Figure 86 : Mass Loss Data for Sample STO9
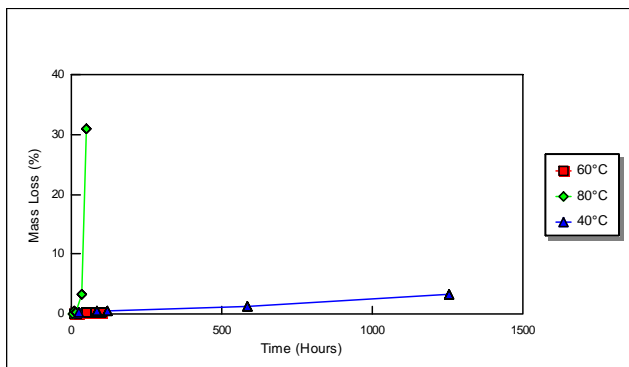
Figure 87 : Mass Loss Data for Sample STO10

STO11 and STO12 : STO12 (2% 2NDPA and 1% pNMA, Figure 88) showed virtually no change in position in Table 12 at all temperatures whereas STO11 (2% pNMA, 1% 2NDPA Figure 94) shows significant changes between mass loss at different temperatures. This suggests that the effect of the 2NDPA : pNMA ratio is important in determining the position of any equilibrium formed between different degradation reactions within the propellant system. This is not surprising considering the significance of nitrated 2NDPA derivatives on HNF stability and the predicted sequential nature of pNMA / 2NDPA nitration. Where 2NDPA is dominant, the mass loss exhibited is very much more pronounced than when pNMA dominates, due to the depletion of pNMA within the reaction vessel. The results for this sample mirror those of the previous discussions.
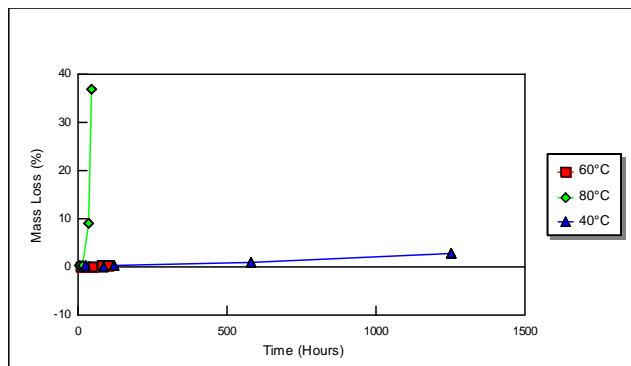
Figure 88 : Mass Loss Data for Sample STO11
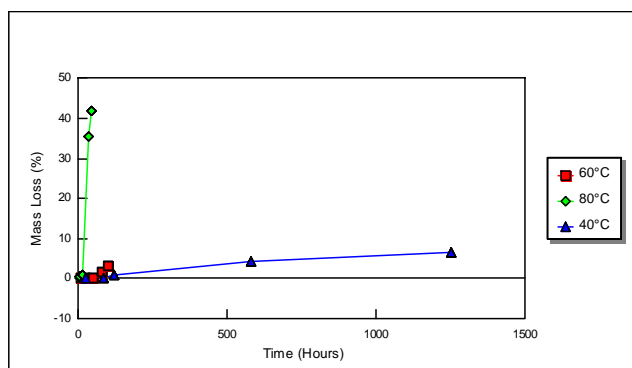
Figure 89 : Mass Loss Data for Sample STO12

STO13, STO14, STO15, STO16, STO17, STO18 : Figures 90 to 95 show the test results for this series of samples. Section 2.4.5.3 highlighted the potential reaction between IPA and the hydrazine scavengers incorporated in the formulation. The additional action of the potential hydrazine scavengers were to either remove water from the reaction vessel or to y remove hydrazine. Either of these reactions was expected to be beneficial to sample longevity but separation of the contributions of each reaction was not possible during this data review.

In STO14 (2NDPA + $(NH_4)_2S_2O_8$), there is little relative difference in effectiveness between the reaction at 80°C and 60°C but there is a significant improvement at 40°C; this is shown in Figure 91. This is proposed to be due to the initial formation of nitrated 2NDPA derivatives at higher storage temperatures that are not in evidence at such high concentrations at 40°C. Comparing this against the pNMA analogue (STO16) in Figure 93 shows that there is virtually no change in relative effectiveness across the temperature range with good results shown at all temperatures and STO14 and STO16 nearly coinciding at 40°C.

Nitration of the pNMA component of STO16 would be expected to be complete at 80°C (as evidenced from the ageing of STO5) but the addition of $(NH_4)_2S_2O_8$ significantly improves the ageing character of the material (See Figure 93). The near coincidence of samples at 40°C confirms the previous proposal that denitration is not the dominant driving mechanism for propellant decomposition at this temperature. If HNF / polyNIMMO catalysed denitration or polyNIMMO denitration were the driving force for breakdown of polyNIMMO / HNF propellants, the very low level of pNMA present in STO16 would not be sufficient to reduce mass loss as significantly as it does in this sample. It is therefore proposed that the presence of the pNMA / $(NH_4)_2S_2O_8$ pair serves to inhibit the rate at which further propellant breakdown occurs after the initial loss of NOx species. This may be by stopping liberation during reaction of an autocatalytic species or by inhibiting the initial loss of NOx from the base matrix. This suggests that liberation of hydrazine or water (ie the perceived action of the

scavenger present) are critical to the growth and propagation of the degradation reaction following initial denitration to liberate NOx species.

The inhibitory mechanism seen in STO16 does not appear to be observed in the 2NDPA / $(NH_4)_2S_2O_8$ analogue (STO14) due to the increased reaction between HNF and nitrated derivatives of 2NDPA (as previously detailed). Even at low level nitration of the 2NDPA present, this is proposed to lead to rapid and widespread HNF degradation.

The situation is not quite so clear for Na_2SO_3 analogues STO13 (Na_2SO_3 + 2NDPA shown in Figure 90) and STO15 (Na_2SO_3 + pNMA Figure 92). At 80°C, both stabiliser systems perform well, even where 2NDPA is present. STO15 shows less change in position across the temperature range in Table 12 whereas STO13 appears to show decreased efficiency at 60°C. Comparing Figure 94 STO17 (1% Na_2SO_3) against Figure 95 STO18 (1% $(NH_4)_2S_2O_8$) shows that the stabilisation system of STO18 is significantly less effective at 60°C than at 80°C or 40°C but at all temperatures is it significantly less effective than that in STO17. From that observation, it is proposed that Na_2SO_3 reacts via a second unidentified reaction that may be similar to that seen within $(NH_4)_2S_2O_8$. However, Na_2SO_3 appears to be the more effective in reducing the mass loss from the propellant system.

Overall it is proposed that the reaction of the scavengers with either hydrazine or water serves to minimise propagation and growth of the propellant degradation mechanism. When combined with pNMA, this significantly slows mass loss.
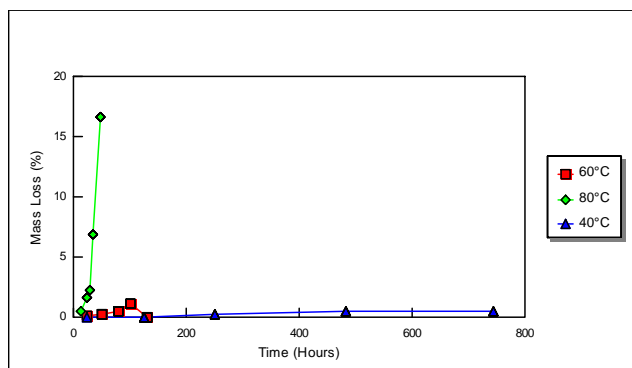
Figure 90 : Mass Loss Data for Sample STO13

When comparing the absolute mass losses observed with these samples, it can be seen that both STO14 and STO18 fail to significantly reduce mass loss at 80°C compared to the control. This can be explained in terms of denitration of the polyNIMMO chain. In STO14, the primary nitration of 2NDPA, caused by loss of NOx from polyNIMMO, accelerates HNF

degradation, as previously proposed via the N-NO-2NDPA / HNF reaction. In STO18, the data suggests that the stabiliser has no effect on the reaction mechanism observed in the control STO1. Of the other samples, STO15 and STO16 (both containing pNMA) reduce the mass loss presumably by trapping NOx species. STO17 shows an interesting result indicating that anhydrous Na_2SO_3 alone is sufficient to reduce mass loss compared to the control. It is proposed that the mass loss that is observed in STO17 at 80°C is directly attributed to an unidentified HNF/NOx reaction but without the progression of this reaction into the second autocatalytic phase (e.g. via liberation of water or hydrazine). This appears to confirm that the HNF / NOx reaction is a critical reaction within unstabilised systems . This suggests that a two (or more) component stabiliser system will be required to stabilise the basic HNF / polyNIMMO propellant system.
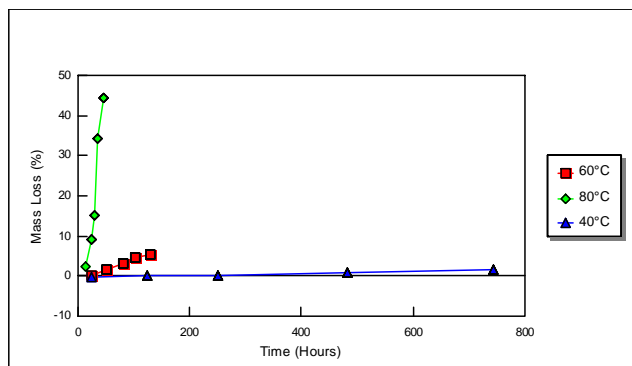
Figure 91 : Mass Loss Data for Sample STO14
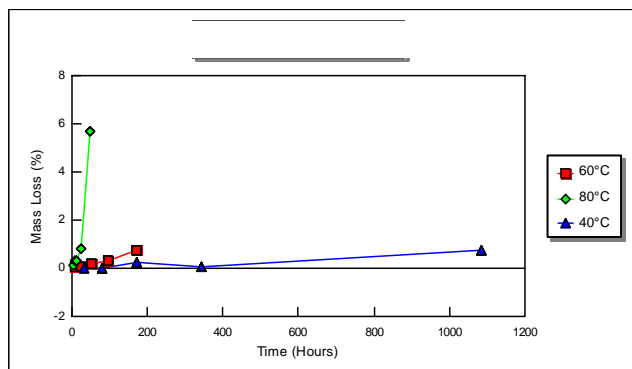
Figure 92 : Mass Loss Data for Sample STO15
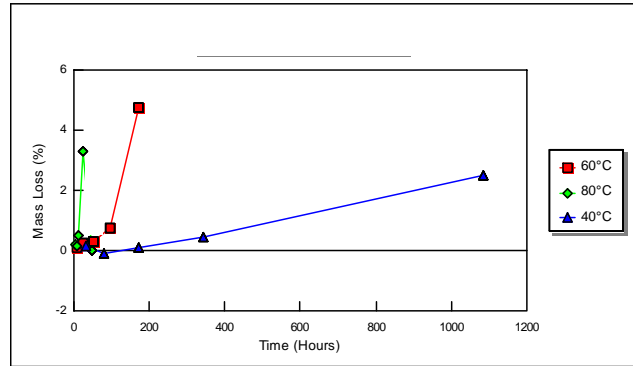
Figure 93 : Mass Loss Data for Sample STO16
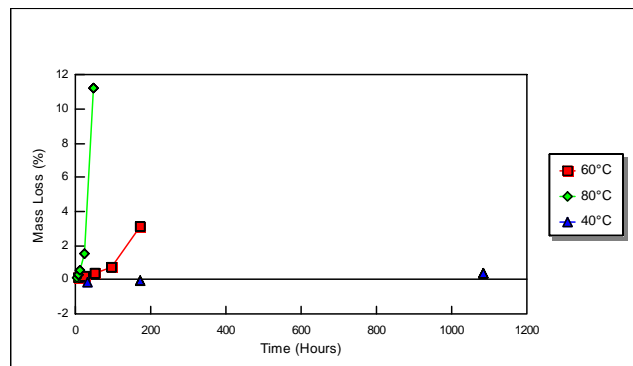
Figure 94 : Mass Loss Data for Sample STO17
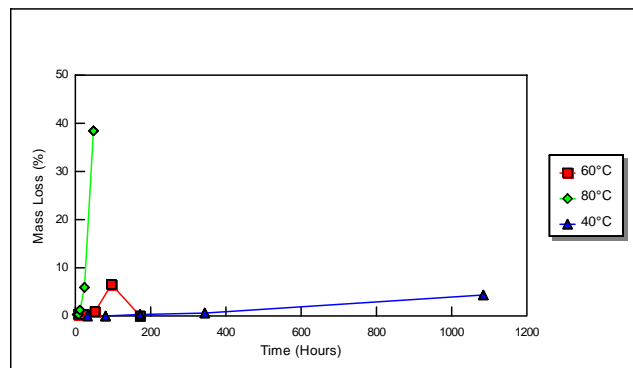
Figure 95 : Mass Loss Data for Sample STO18

3.3.2.1 Conclusions From Mass Loss Studies

It is proposed that a complex, dynamic equilibrium is present between various reactions within the degradation scheme for HNF / polyNIMMO propellants. The primary degradation system appears to be liberation of NOx followed by hydrazine (or possibly water) formation. n addition to this, a competition between reactions of an HNF / NOx reaction and a NOx /

stabiliser reaction appear critical to degradation propagation with the relative dominance of these competing reactions determining the overall rate of propellant degradation.

The reaction course is proposed to change significantly between 80°C and lower temperatures, driven primarily by the reduction in loss of NOx species from within the test matrix. The previous reaction identified between HNF and NO-2NDPA or NO-pNMA is proposed be more significant as the storage temperature decreases. Once formed, the nitrosoated derivatives are proposed to react directly with HNF, leading to widespread decomposition.

A detailed overview of the inter-relatedness of the mass loss data at all three test temperatures indicates:-

1)   At different temperatures, different propellant reactions drive the overall degradation schemes (as opposed to the same reaction being observed at differing rates). At higher temperatures, denitration is the dominant driving reaction. As temperature decreases, hydrazine (or water) liberation appears to be the driving force for propellant degradation

2)   Removal of NOx and HNOx species is important to achieve propellant longevity at elevated temperatures. However, this effect is less marked at lower storage temperatures.

3)   At lower temperatures, the lower level of denitration observed within the propellants lead to the likely formation of nitrosated species (especially NO-2NDPA) that show high levels of direct reactivity with HNF.

4)   The direct reaction of NOx and HNOx with HNF is likely to be the mechanism for sustained propellant degradation following the induction / initiating phase of reaction

5)   The potential for competition between HNF and denitration stabilisers for reaction with NOx species is an important aspect of propellant reactivity.

6)   Secondary hydrazine formation following reaction between HNF and NOx is a possible additional important degradation mechanism that requires chemical control.

7)   2NDPA is not directly detrimental to propellant longevity but the formation of Nitroso-2NDPA causes significant degradation when in contact with HNF.

8)   There may be an added mechanism for improved polyNIMMO stability associated with the reaction of Sodium Sulphite with the polymer.

From mass loss assessment data, the overall reaction course during storage is proposed to be a complex reaction equilibrium that is temperature dependent. Figure 96 summarises the

proposed dominant reaction course at each storage temperature and describes the changes in reaction inferred from the data review.

polyNIMMO Based, HNF Loaded Propellant	80°C	Denitration of polyNIMMO reaction is dominant driver for degradation. Further reaction leads to competition between denitration stabilisers and HNF for reaction with NOx and HNOx species Low levels of N-NO products formed Lowest relative contribution from thermal decomposition of HNF Formation of reactive secondary products (e.g. hydrazine / water) occurs mainly from HNF / HNOx/ NOx reaction. These products drive secondary degradation reactions
	60°C	Little or no denitration of polyNIMMO and direct NOx reaction with HNF is marginal Higher levels of N-NO products formed resulting in direct reaction with HNF Highest relative contribution of thermal decomposition of HNF Formation of reactive secondary products (e.g. hydrazine / water) occurs mainly from HNF / N-NO reactions and HNF thermal degradation. These products drive secondary degradation reactions
	40°C	Denitration of polyNIMMO and subsequent direct reaction with HNF is reduced Higher levels of N-NO products formed resulting in direct reaction with HNF Contribution from thermal decomposition of HNF becomes important Formation of reactive secondary products (e.g. hydrazine / water) occurs mainly from HNF / N-NO reaction. These products drive secondary degradation reactions

Figure 96 - Overall Reaction Summary from Mass Loss Studies

3.3.3 Aqueous Extraction

3.3.3.1 Introduction

The principal water soluble component in each of the propellant systems prior to storage was HNF. By determination of the levels of aqueous extraction, assessment of the changes in HNF content with elevated temperature storage could be inferred. Although this is a convenient approximation, it is appreciated that other water soluble species may be encountered during the analysis. Section 1.4.2 detailed various thermal reaction mechanisms [104] [108] to produce ammonium nitroformate (ANF), acids or other water soluble residues. In addition to these, ion exchange between HNF and hydrazine scavengers (e.g. formation of Hydrazinium Peroxodisulphate $(N_2H_5)_2S_2O_8$ from HNF and Ammonium Peroxodisulphate) is also possible to envisage. Although these products complicate the interpretation of the aqueous extraction data, the data provides additional supporting data for an overall interpretation of reaction course.

After each storage period, 0.2g of each test sample was accurately weighed into a glass sample vial. The sample was washed with a number of aliquots of deionised water until the washings displayed no yellow discoloration. The samples were then dried over P_2O_5 until constant weight was achieved.

3.3.3.2 Storage at 80°C

Figures 97 to 99 show the aqueous extraction data for the 3 classes of propellant stored at 80°C. The graphs show the change in mass of a test sample as a percentage of the original mass after treatment with water and subsequent drying. It can seen from the graphs that a number of the formulations show higher values of extraction compared to the control sample (STO1). This implies better retention of HNF in stabilised samples. As observed for the mass loss data, there appears to be an induction / initiation reaction at the start of storage where little change in aqueous extraction with time occurs. It is observed that there is some variation in the initial values of aqueous extraction between samples. This variation is proposed to reflect that some stabilisers / scavengers show some degree of solubility during the trial, thus co-extracting with any HNF present. It also reflects the "plus addition" effect of sample preparation. This "plus addition" method of preparation as detailed in Section 3.2 undertook to produce a stock of material containing HNF, polyNIMMO and isocyanate and then adding stabiliser to a series of subsamples. Where high levels of stabiliser were added (e.g. 16% pNMA) this has an obvious effect on the overall percentage of solids in the formulation. For example, in the case of 16% pNMA addition to a 65% HNF loaded system the final HNF concentration over the whole formulation drops to ~ 56%.This is proposed to be the most

likely source of the variation in initial extraction values. Because of these effects, the changes observed within the test data with ageing has been assessed.
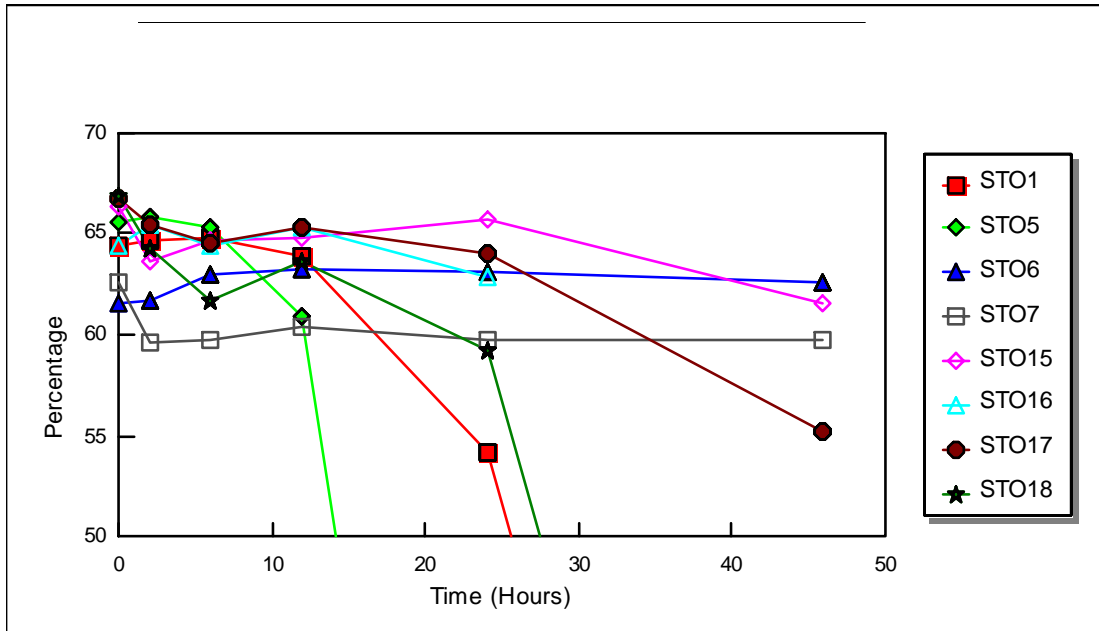
Figure 97 : Aqueous Extraction From Propellants at 80°C – pNMA, Hydrazine Scavenger and Control
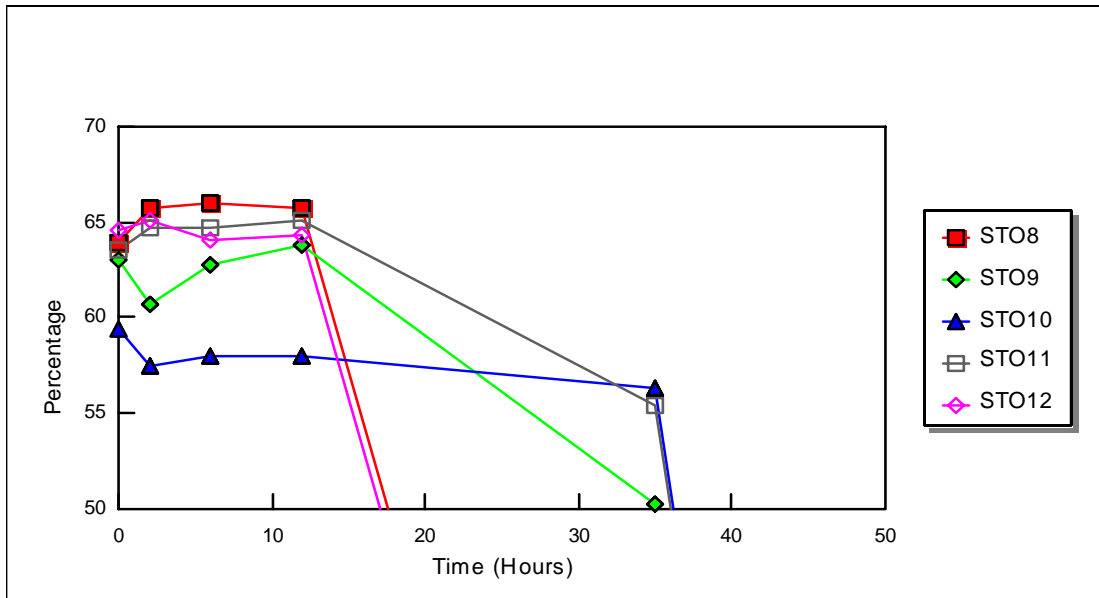
Figure 98: Aqueous Extraction from Propellants at 80°C – Mixed Stabiliser Type
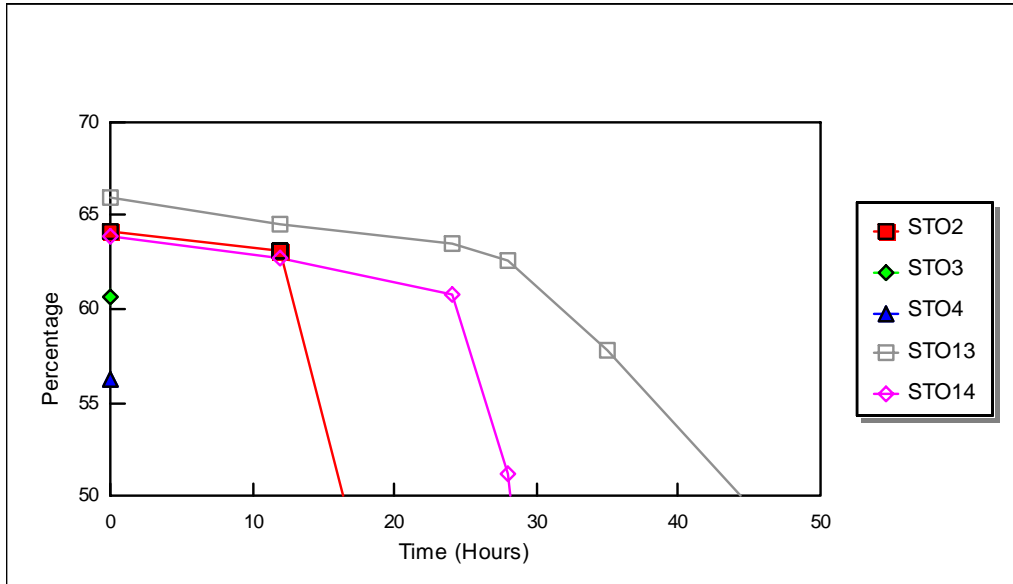
Figure 99 : Aqueous Extraction from Propellants at 80°C – 2NDPA Stabiliser Type

Table 13 ranks the aqueous extraction data achieved at 80°C and relates it to stabiliser type. Where more than one formulation is present in any category, the order of entry relates from "best" to "worst" compliance with the category.

Assessment Criteria	Formulations That Comply
Formulation sustains near constant (< 5% decrease) in aqueous extraction throughout ageing period	STO6 = STO7 > <u>STO15</u>
Sample survives to > 40 hours with aqueous fraction > 50%	**STO17**
Aqueous fraction retained at > 50% for between 30 and 40 hrs	*STO10 = STO11 =* **STO13** > *STO9*
Aqueous fraction retained at > 50% for between 20 and 30 hrs	<u>STO16</u> > **STO18** > STO1 > **STO14**
Aqueous fraction retained at > 50% for between 10 and 20 hrs	*STO12 = STO8 =* **STO2** > STO5
Aqueous fraction retained at > 50% for < 10 hours	**STO3** = **STO4**

STO1 is the control (unstabilised) sample
Items in **bold** are 2NDPA based
Items in *italics* are mixed pNMA / 2NDPA stabiliser systems

Items <u>underlined</u> contain hydrazine stabilisers.
Items in normal text are pNMA based.
Items in font **STOXX** format are single hydrazine stabilised systems without pNMA or 2NDPA

Table 13 : Assessment of aqueous extraction values from propellant samples at 80°**C**

Using the criteria given in Table 13, the data suggests that at 80°C:-

1) Formulations with high levels of pNMA (STO6 and STO7) show the greatest retained aqueous extraction with time. This suggests that the HNF present is retained within the samples and confirms the beneficial nature of pNMA on propellant stability suggested during mass loss studies. The perceived action of pNMA is to remove NOx species from the initial propellant degradation. Therefore this aqueous extraction data appears to confirm that the reaction of NOx species (and its removal by pNMA) plays an important role in HNF propellant degradation.

2) Addition of anhydrous sodium sulphite to the propellant formulations leads to higher aqueous extraction. This is most obvious in sample STO13 (2NDPA + Na_2SO_3) when compared against STO2 (2NDPA) as an analogous formulation without the additive. Part of this improvement is associated with the proposed HNF / N-NO-2NDPA reaction scheme detailed in Section 2.4.4.

3) Without the addition of a second stabiliser / scavenger material, 2NDPA formulations always exhibit inferior performance in terms of lower aqueous extraction compared to an unstabilised sample. Samples STO3 and STO4 (containing high levels of 2NDPA) both ignited before the first storage assessment period at 80°C (12 hours). This highlights the detrimental effect of 2NDPA on HNF propellant longevity.

4) Addition of anhydrous sodium sulphite in isolation (STO17) is superior to the majority of alternative stabilised systems. This again suggests that liberation of hydrazine or water (and subsequent control by the scavenger) may play an important role in propellant degradation. However, it is not conclusive as to which product (if either) is present.

5) Addition of anhydrous sodium sulphite facilitates a significant reduction in the overall required additive level to still achieve high aqueous fraction ie retain HNF. For example, the level of aqueous extraction achieved for STO15 (1% pNMA + 1% Na_2SO_3 at an overall additive level of 2% produces an aqueous extraction value very similar to formulations STO6 (8% pNMA) and STO7 (16% pNMA)). The reaction of NOx species with HNF has been identified as an important reaction mechanism in polyNIMMO / HNF propellant degradation. The comparatively low level of pNMA in sample STO15 suggests that he Sodium Sulphite present either influences (retards) NOx production from any HNF / polyNIMMO reaction or reduces secondary degradation reactions (e.g. control of hydrazine and reduction of direct reaction of hydrazine and HNF).

6) Little difference between STO6 (8% pNMA) and STO7 (16% pNMA) is observed during the ageing period suggesting that the activity of pNMA has not been fully depleted during the storage period (ie the stabiliser is still available to undergo further reaction with HNOx or NOx species at the end of the ageing period). Extended ageing of these formulations would be beneficial to determine the relative benefit of pNMA content.

7) In mixed pNMA / 2NDPA systems where the concentration of pNMA = 2NDPA (ie STO8, STO9 and STO10), the higher the overall stabiliser content, the better the retention of aqueous fraction. This is suggested to be solely a reflection of pNMA content. In mixed pNMA / 2NDPA systems where the concentration of pNMA is dissimilar to 2NDPA (STO11 and STO12), the systems with higher 2NDPA content (STO12) show inferior properties to those of the formulation with the higher pNMA content (STO11).

8) In isolation, the action of anhydrous ammonium peroxodisulphate is inferior to that of anhydrous sodium sulphite but still shows some small degree of improvement compared to the control sample (ie produces a higher aqueous extraction value over time).

3.3.3.3 Storage at 60°C and 40°C

Figures 100 to 102 show the aqueous extraction data for propellant storage at 60°C with Figures 107 to 109 showing 40°C storage results. For both sets of test data, samples STO3 and STO4 were removed from storage prior to ageing due to the large incompatibility observed during 80°C trials. At 40°C there was insufficient sample of STO2 to conduct testing.
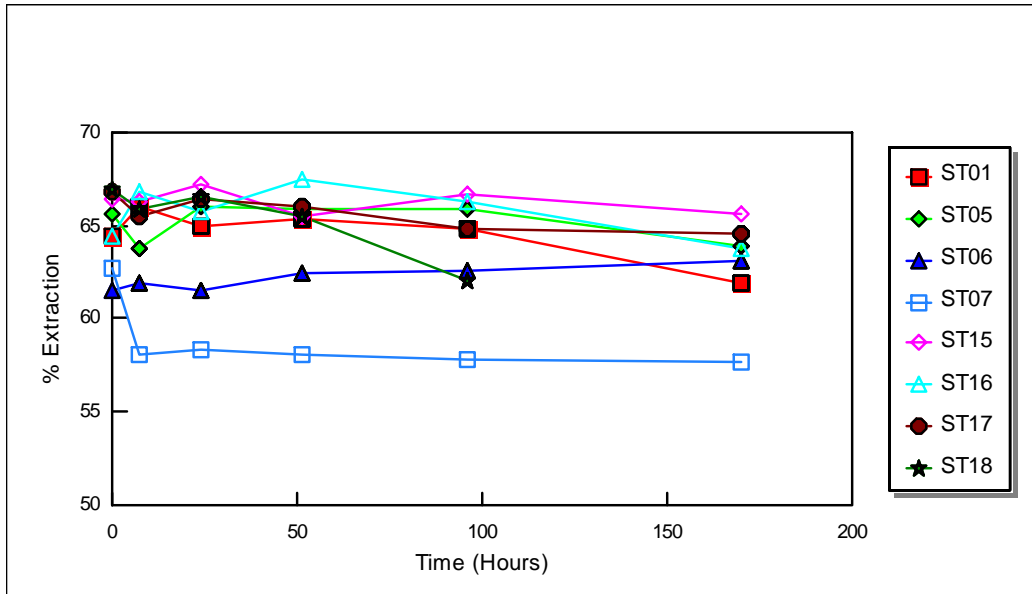
Figure 100 : Aqueous Extraction from Propellants at 60°C – pNMA, Hydrazine Scavenger and Control Sample Type
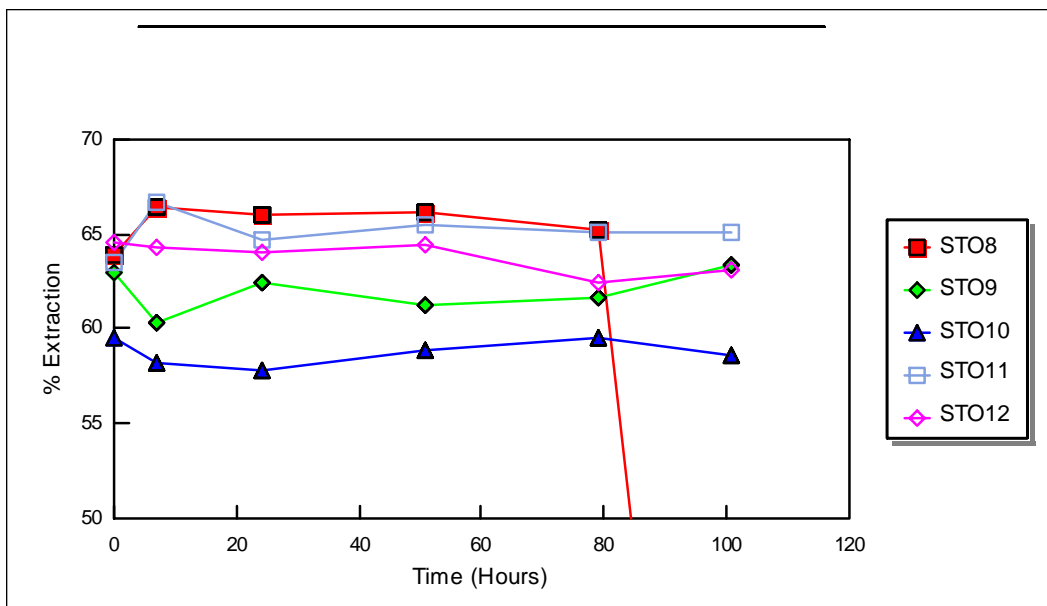
Figure 101 : Aqueous Extraction from Propellants at 60°C - Mixed Stabiliser Type
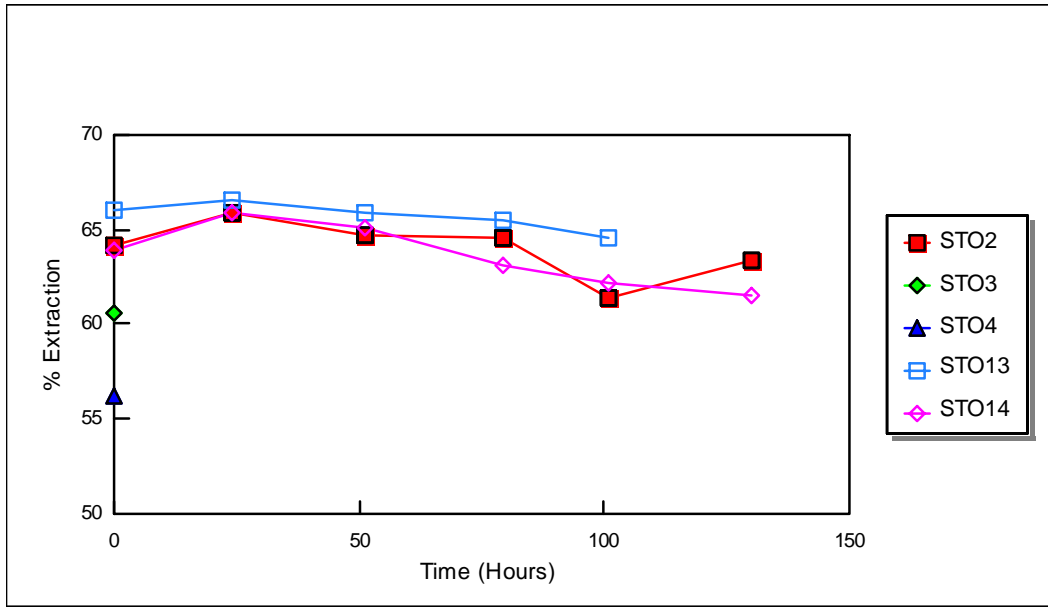
Figure 102 : Aqueous Extraction from Propellants at 60°C – 2NDPA Stabiliser Type
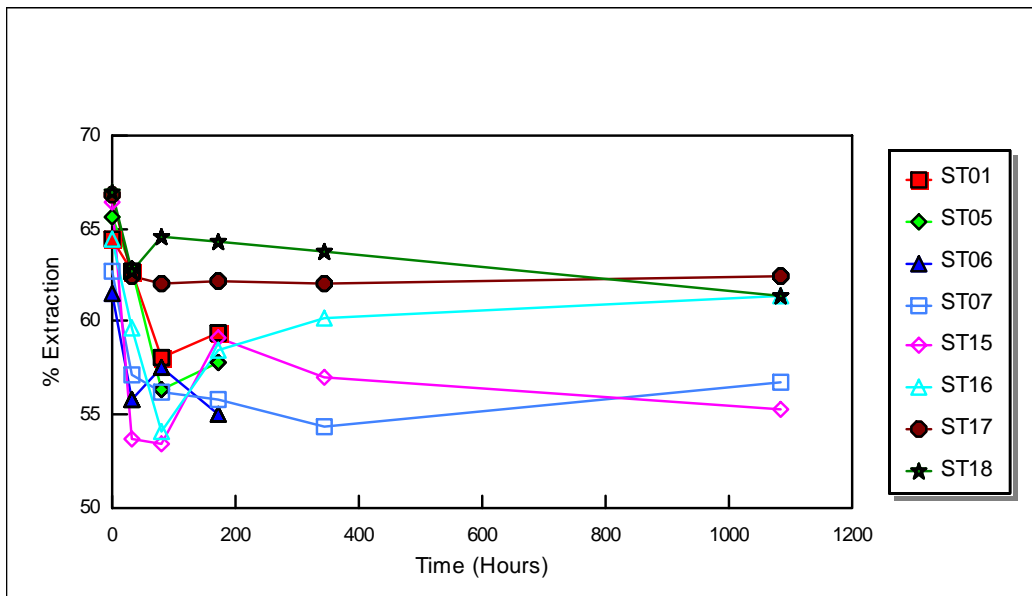
Figure 103 : Aqueous Extraction from Propellants at 40°C – pNMA, Hydrazine Scavenger and Control Stabiliser Type
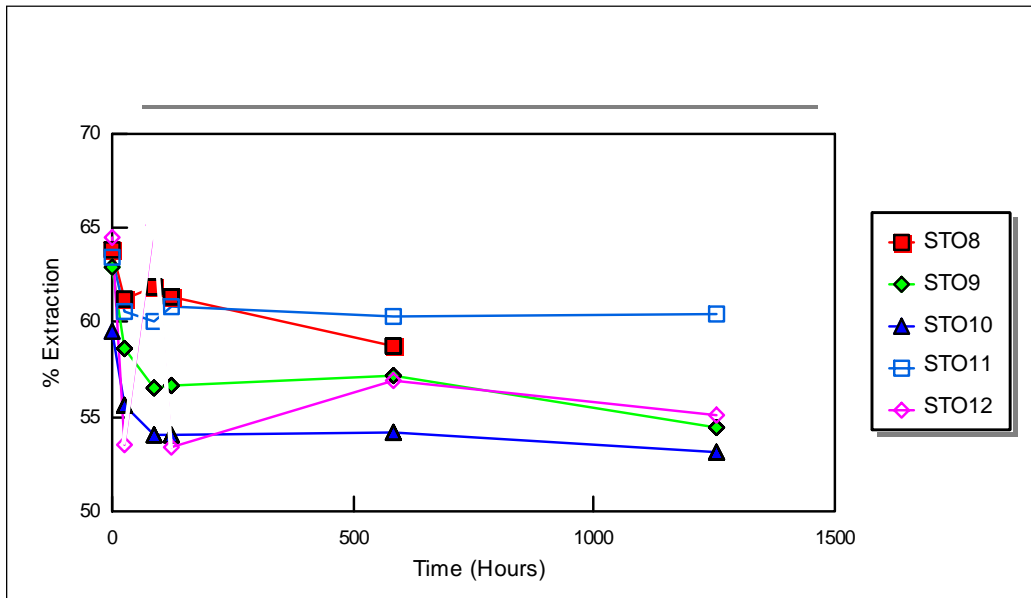
Figure 104: Aqueous Extraction from Propellants at 40°C - Mixed Stabiliser Type
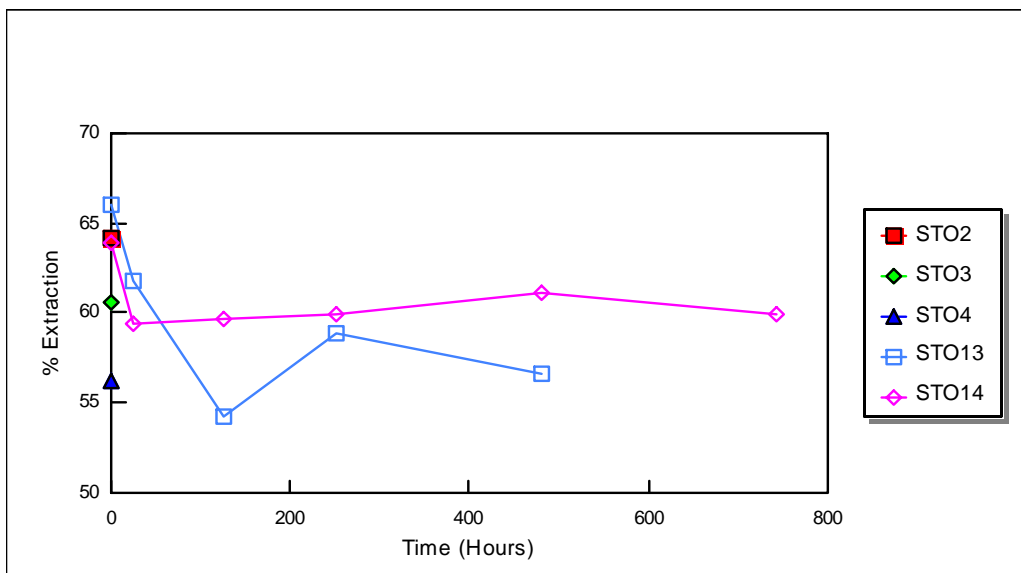
Figure 105 : Aqueous Extraction from Propellants at 40°C– 2NDPA Stabiliser Type

It can be seen that the reduction in aqueous fraction over the storage period is minor for the majority of samples at both 60°C and 40°C, typically showing < 5% change. As previously discussed, the storage times were selected to provide similar degrees of reaction in all samples. The lack of significant reaction at 60 and 40°C appears to support the previous proposal given in Section 3.5.2 that a change in reaction mechanism is observed at 80°C rather than acceleration / retardation of a single reaction mechanism. Mass loss data analysis suggested a reaction at 80°C dominated by denitration of polyNIMMO with the resulting NOx and HNOx species reacting further with HNF.

3.3.3.4 Comparison of Aqueous Test data at 80, 60 and 40°C

Figures 106 to 121 show the aqueous extraction data for each individual test sample at each test temperature within the first 200 hours storage. It is evident that in most cases the 40°C storage trials have resulted in lower extraction fractions than the 60°C trials. This suggests that HNF loss has progressed further at the lower temperature. This result appears counter intuitive but does align with the previous proposal of a complex mixture of competing schemes as given in Section 3.5.2.2

More detailed review of the figures is given below.
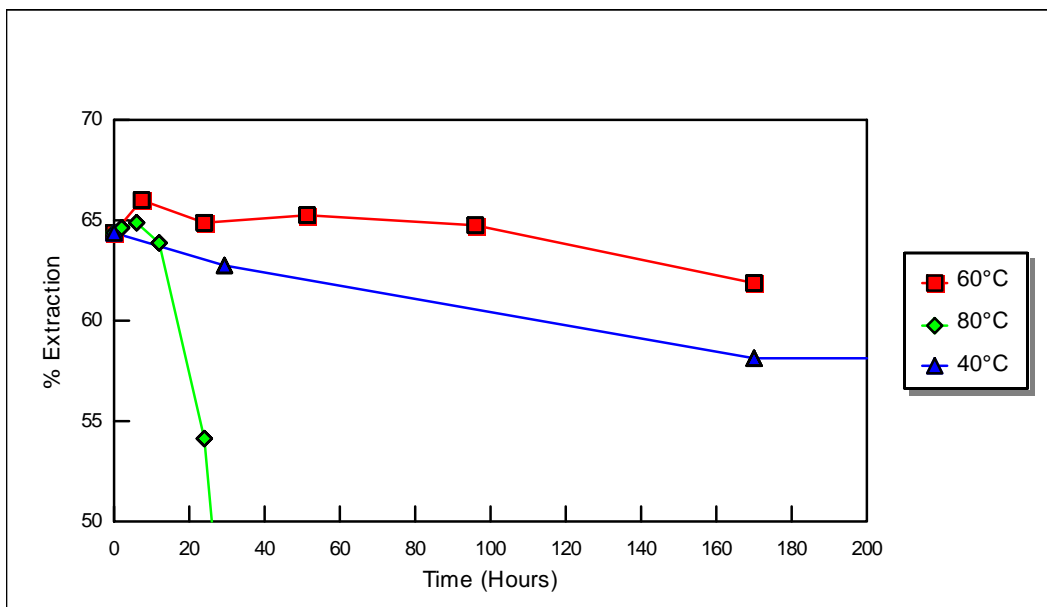
Figure 106 : Aqueous Extraction Data from Propellant STO1

STO1 (Unstabilised) – Figure 106 shows a rapid decrease in aqueous extraction value after 18 hours of storage is observed at 80°C indicating extensive HNF loss. . At 60°C, there is very little change in aqueous extraction up to 98 hours storage. Beyond this point, the rate of change appears similar to that observed at 40°C (ie the data lines run near parallel). The overall decrease in aqueous extract at 60°C is comparatively low and lower than that seen at 40°C. Interestingly, aqueous extract decrease at 40°C appears to occur at a near constant rate up to 168 hours storage. The apparent lack of reaction at 60°C for the first 98 hours compared to the steady decrease at 40°C would suggest that the liberation of a volatile species might be one part of an explanation of the apparently anomalous behaviour. The similarity of aqueous extraction rate at higher storage periods of 40°C and 60°C storage may suggest that a similar reaction is occurring in both environments. If this is the case, the apparent delay in the initiation the reaction at 60°C may suggest that the loss of a volatile species is the driving reaction present, possibly IPA. In the 40°C test sample, it is proposed that any volatile liberated will be retained for a longer period and reacts to degrade the propellant due to contact between the volatile and the remaining propellant. In the 60°C sample, the contact time is reduced and so degradation progresses at a much lower rate. However, once a critical degree of degradation has occurred, the reaction may progress independent of the rate of volatile generation.
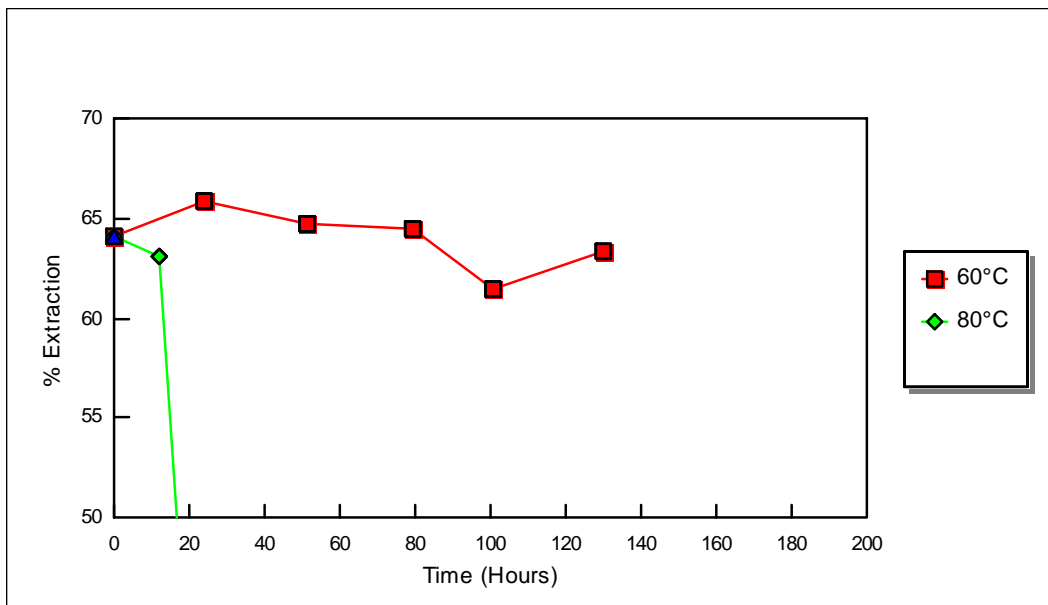
Figure 107 : Aqueous Extraction Data from Propellant STO2

Aqueous extraction data for **STO2** (1% 2NDPA) is given in Figure 107. At 60°C the aqueous fraction for this sample is retained at a high level throughout the ageing period. This confirms the proposal that no significant direct reaction between 2NDPA and HNF occurs at this temperature and that a different reaction course is followed at 80°C (where rapid decrease in aqueous extract value is observed). The retention of aqueous fraction also implies that no significant N-NO-2NDPA / HNF reaction has occurred during storage at 60°C.
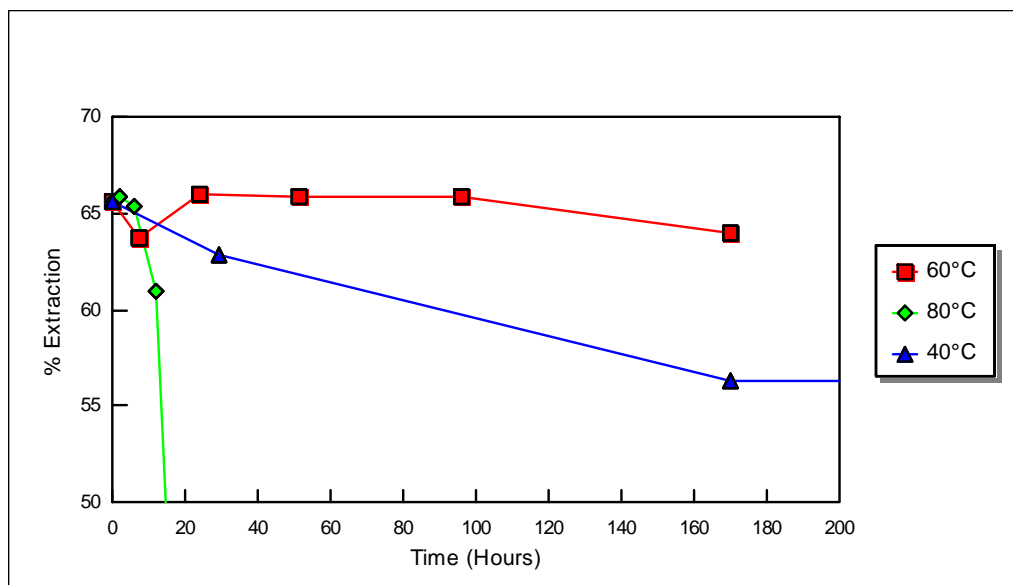
Figure 108 : Aqueous Extraction Data from Propellant STO5

STO5 (1% pNMA) – This sample emphasises the increase in reduction in aqueous fraction between 40°C and 60°C is shown in Figure 108. Again at 60°C, very little reduction in aqueous extract is observed but at 40°C a more marked reduction is seen. Comparison of the extraction values at 80°C for the control sample (STO1) against this sample suggests that the aqueous extraction decrease more rapidly in this sample than in the control. This may suggest that the action of the pNMA / HNF reaction (likely through the Nitroso derivative) is of greater significance than previously proposed.
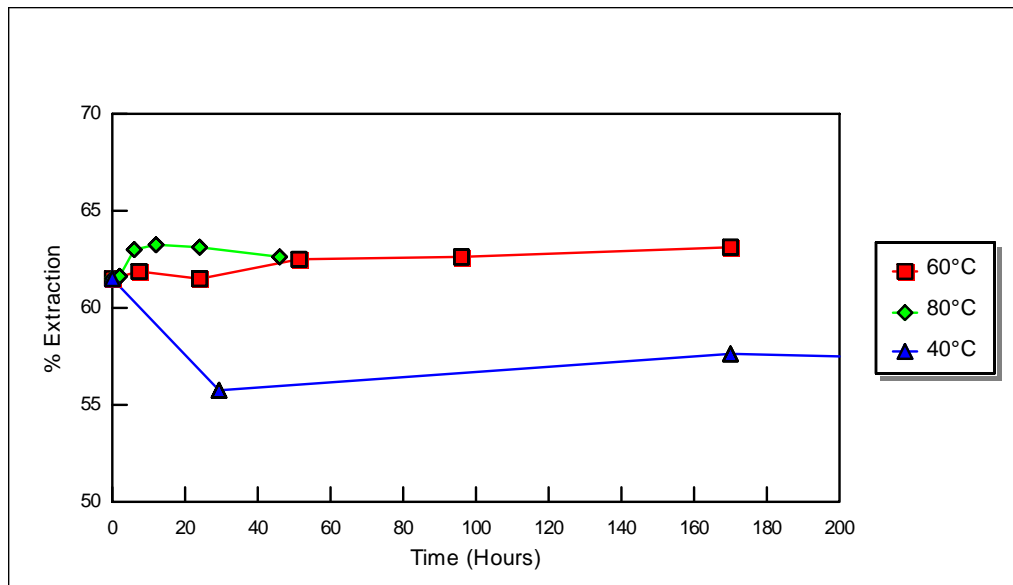
Figure 109 : Aqueous Extraction Data from Propellant STO6

STO6 (8% pNMA) – Previous analyses of sample mass loss has suggested that the presence of high levels of pNMA reduces mass loss from the test sample. Figure 109 indicates that the stabiliser present has maintained both the 80°C and 60°C aqueous extraction values at similar levels. Comparing this against sample STO5 (1% pNMA) it implies that at 80°C, in STO6 the added pNMA maintains propellant integrity for an increased period (and never achieves a state of autocatalytic breakdown). This appears to confirm the proposal that liberation of NOx species is the primary route by which propellant breakdown is catalysed. The lack of significant change over the ageing period suggests that there is little or no secondary reactions which are occurring in this period to degrade the sample. It also implies that only once NOx concentration has reached a critical value does HNF degradation start to occur. The initial reduction in aqueous extraction value seen at 40°C is not observed in sample STO5 or the control STO1 and this may suggest that a direct reaction occurs between the excess stabiliser and this is the cause of reduction in aqueous fraction.
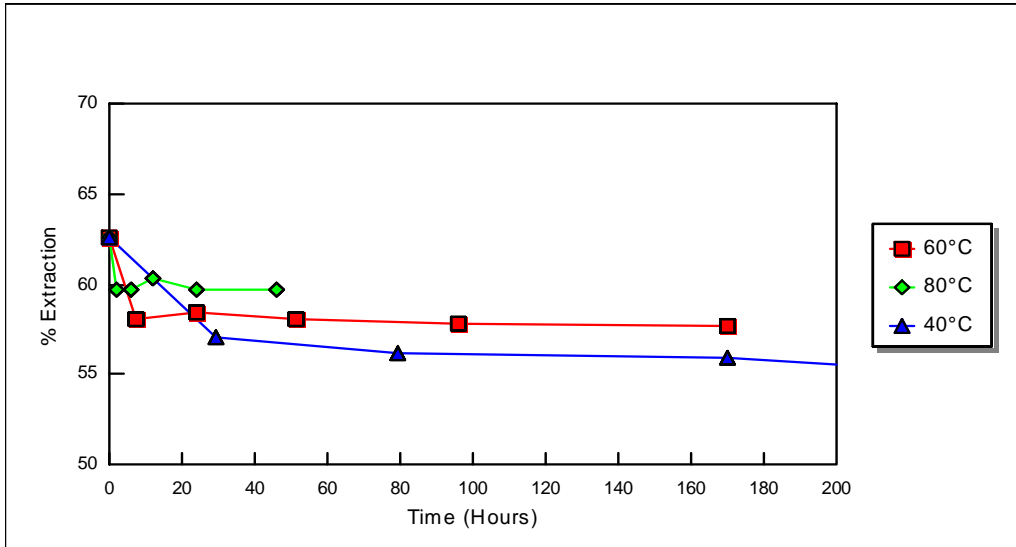
Figure 110 : Aqueous Extraction Data from Propellant STO7

STO7 (**16% pNMA**) – A similar situation occurs within this test sample as within STO6 (Figure 109) where the 80°C and 60°C samples showing similar reductions in aqueous fraction with time. However, in formulation STO7 (Figure 110), the 40°C sample also shows a similar profile. This suggests that the additional pNMA present plays a role in reducing HNF loss; this is contrary to the proposal suggested by the results from STO6. The most likely explanation for this behaviour is that there is a critical value of pNMA required to stabilise HNF degradation at each temperature. Within the complex degradation equilibrium detailed in Section 3.2, at higher concentrations of pNMA at 40°C, this serves to minimise any alternative reaction course.
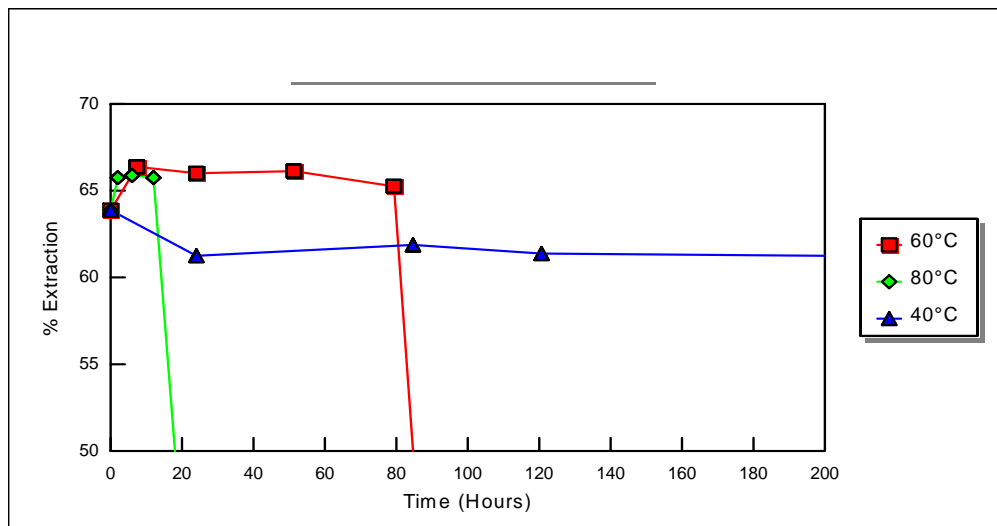
Figure 111 :Aqueous Extraction Data from Propellant STO8

STO8 (0.5% pNMA + 0.5% 2NDPA) – Comparison of the Figures for STO5 (1% pNMA) (Figure 108) and STO8 (0.5% pNMA + 0.5% 2NDPA) (Figure 111) suggest that the reduction in aqueous fraction at 80°C is more rapid in the STO5 sample. This was unexpected as it was predicted that the stabiliser function of the pNMA would be rapidly depleted in STO8, allowing nitrosoated derivatives of 2NDPA and pNMA to be formed (and subsequently these nitrosoated derivatives drive reaction forward with HNF). It is possible that mixed denitration stabilisers systems have other unidentified reaction mechanisms present within them; possibly inter-molecular nitration as suggested by Sammour et al [84] However, a more likely explanation is that the rate of denitration from polyNIMMO at 80°C is higher than at all other test temperatures; this may drive the stabiliser reaction towards nitration rather than nitrosoation. This minimises the formation of N-NO-2NDPA and N-NO-pNMA in preference to formation of ring nitrated 2NDPA derivatives and 2,4-dinitro-pNMA. The higher number of reaction sites in 2NDPA would then reduce any HNF / NOx reaction activity. This appears to strengthen the hypothesis that the rate of denitration within the propellants, the probability of formation of N-NO species and the direct reaction of either NOx or N-NO derivatives with HNF are critical to overall sample longevity.
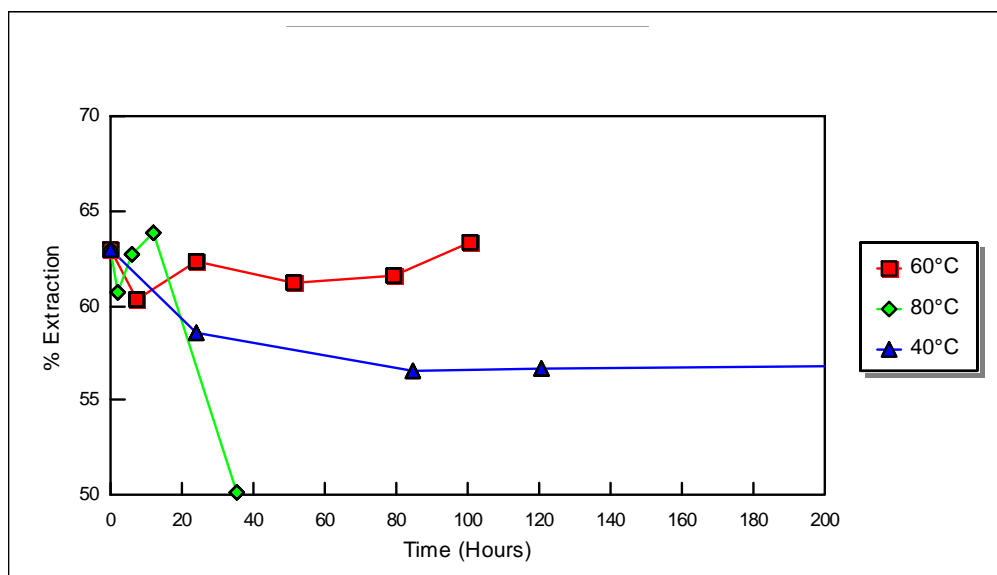
Figure 112 : Aqueous Extraction Data from Propellant STO9

STO9 (4% pNMA + 4% 2NDPA) – Figure 112 shows the data observed. It is not dissimilar to that shown in STO8 although aqueous extraction values are retained for longer periods within this test sample. An interesting effect at 80°C is the initial decrease and then increase in soluble fraction during the first 4 data points. This is attributed to experimental error as

during this period comparison against STO8 and STO10 shows that this increase is not observed within these analogous samples.
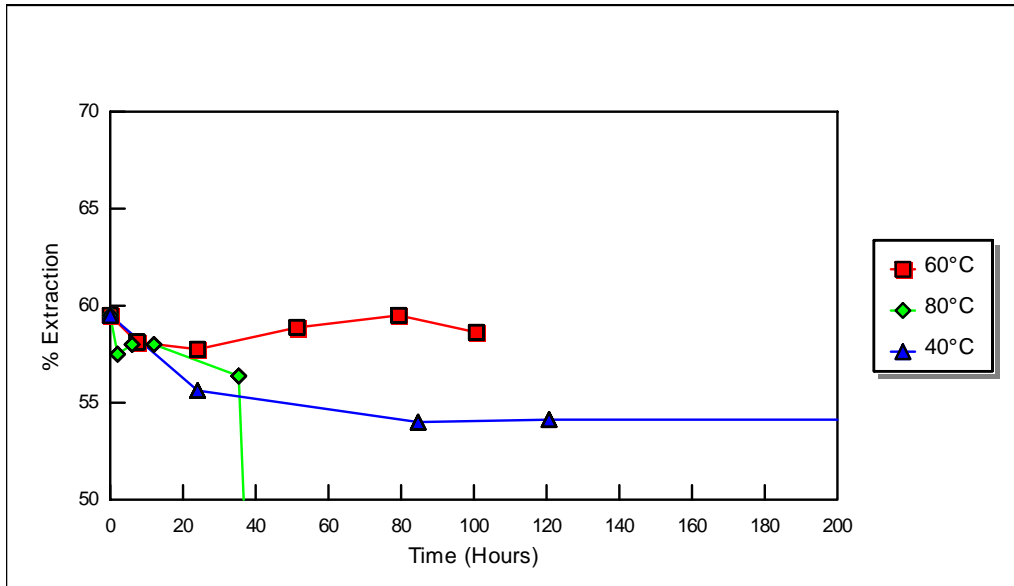
Figure 113 : Aqueous Extraction Data from Propellant STO10

STO10 (8% pNMA + 8% 2NDPA) – Figure 113. Again, similar data is achieved as in STO8 and STO9 although aqueous extraction values are maintained for slightly longer with this sample due to the higher overall stabiliser level. This implies that control of NOx species directly affects loss of HNF from the formulation.
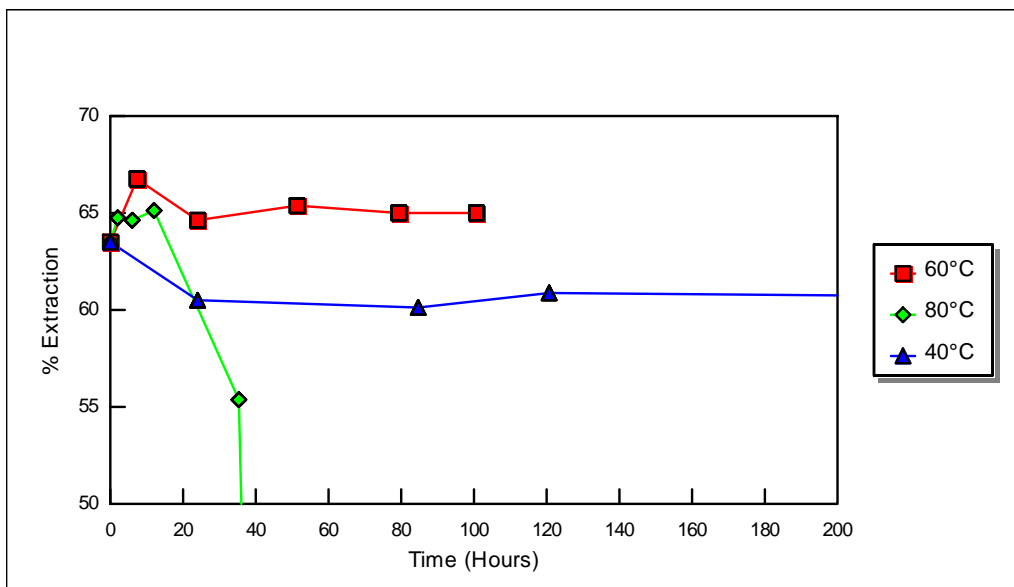
Figure 114 : Aqueous Extraction Data from Propellant STO11
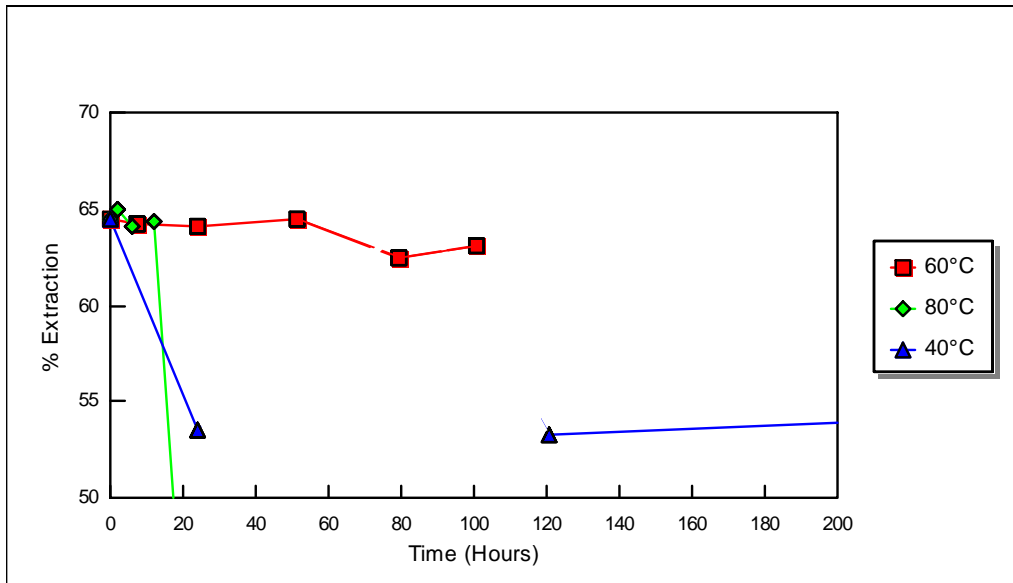
Figure 115 : Aqueous Extraction Data from Propellant STO12

STO11 (2% pNMA + 1% 2NDPA) / STO12 (2% 2NDPA + 1% pNMA) – Figures 114 and 115 show the data for these test samples. Inverting the pNMA : 2NDPA ratio for these samples shows little effect on aqueous extraction values. The sample with the higher 2NDPA content (STO12) shows a more rapid reduction in aqueous extraction at 80°C but at 60°C and 40°C the samples behave in very similar ways. This again implies that the reaction course at 40°C and 60°C is similar with a change in reaction course at 80°C. If the degradation reaction is determined primarily by release of NOx species and subsequent reaction with HNF, then this suggests that at both 60 and 40°C, the concentration of NOx never exceeds a value sufficient to saturate the pNMA stabiliser present.
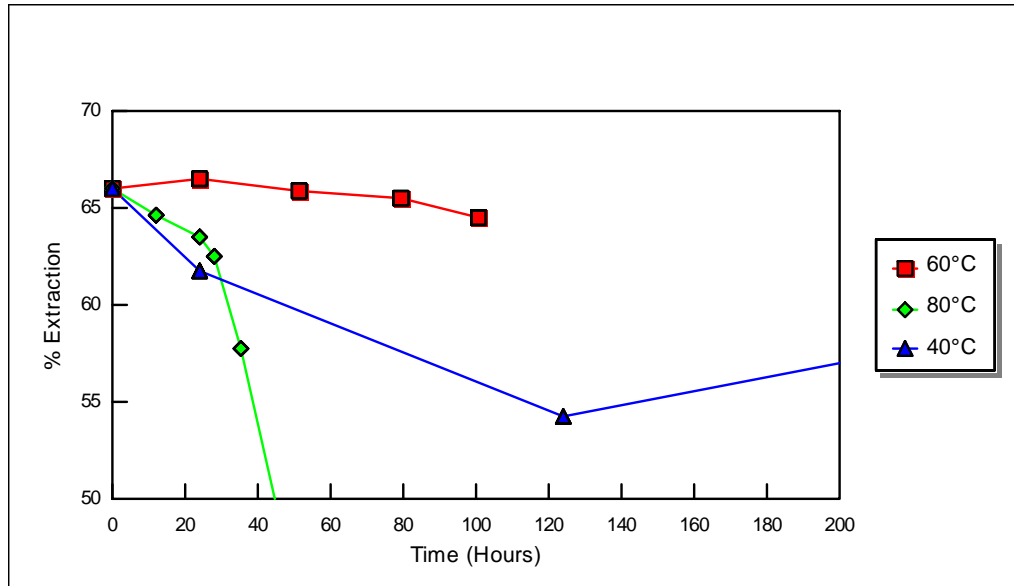
Figure 116 : Aqueous Extraction Data from Propellant STO13
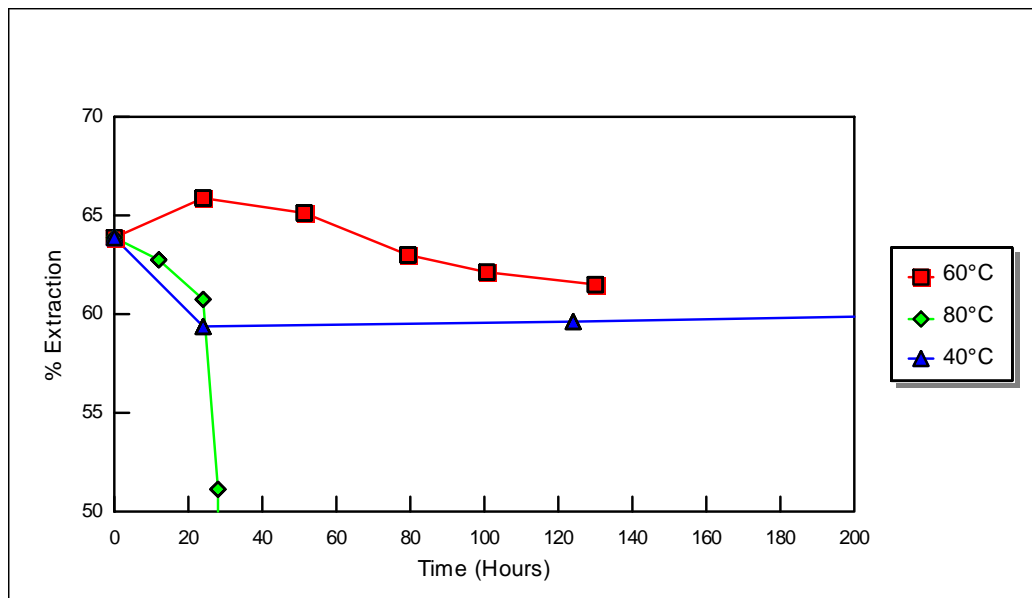
Figure 117 : Aqueous Extraction Data from Propellant STO14

STO13 (1% 2NDPA + 1% Na$_2$SO$_3$) / STO14 (1% 2NDPA + 1% (NH$_4$)$_2$S$_2$O$_8$) – The test sample data are shown in Figures 116 and 117. The addition of the hydrazine scavengers has significantly reduced the rate of reduction in aqueous fraction at 80°C. Comparison to a single 2NDPA stabilised system (formulation STO2 (Figure 107)) shows this reduction in aqueous fraction. This would suggest that within a pure 2NDPA based system, that it is not solely the proposed reaction of HNF with N-NO-2NDPA that is the driving force. These results suggest

that it is necessary to control a secondary reaction also. As the presence of the salts appear to control this reaction to some degree, this secondary reaction is most likely the formation of hydrazine or water or control of a decomposition product from an HNF / NO-2NDPA reactions. The reduction of the mass loss suggests that the additional reaction liberates at least one other volatile species but that this volatile does not lead to further propellant degradation. This further suggests that the secondary reaction produced from the initial HNF / nitrated 2NDPA degradation is the reaction that requires careful control in these propellant systems.

STO15 (1% pNMA + 1% Na$_2$SO$_3$) / STO16 (1% pNMA + 1% (NH$_4$)$_2$S$_2$O$_8$) - Both of these test samples shown in Figures 118 and 119 shows good levels of aqueous extraction at 80°C and 60°C. Following the previous arguments, this suggests that the formation of nitrated derivatives of pNMA has no detrimental effect on the stability of the remaining propellant. At 60°C STO16 may show slightly inferior properties than STO15. At 40°C, both samples show a rapid reduction in aqueous fraction suggesting that a change in mechanism is occurring at this temperature compared to 80°C and 60°C.
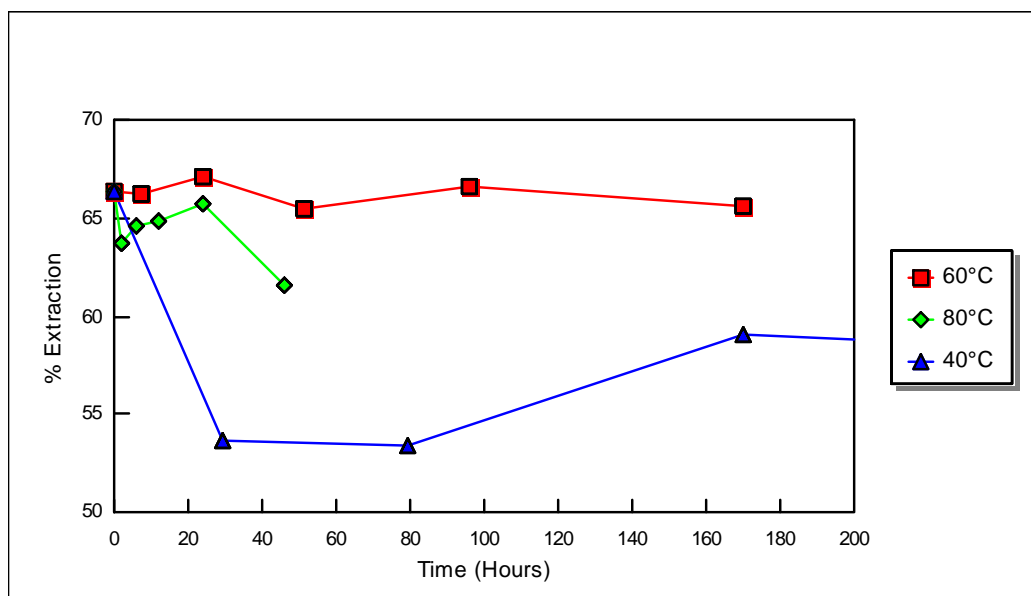
Figure 118 : Aqueous Extraction Data from Propellant STO15
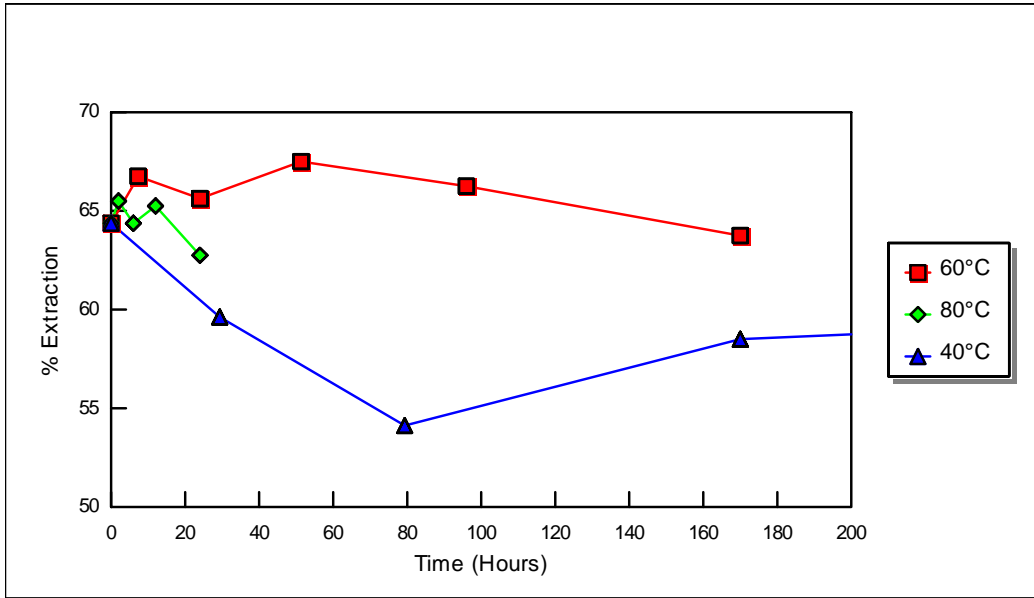
Figure 119 : Aqueous Extraction Data from Propellant STO16
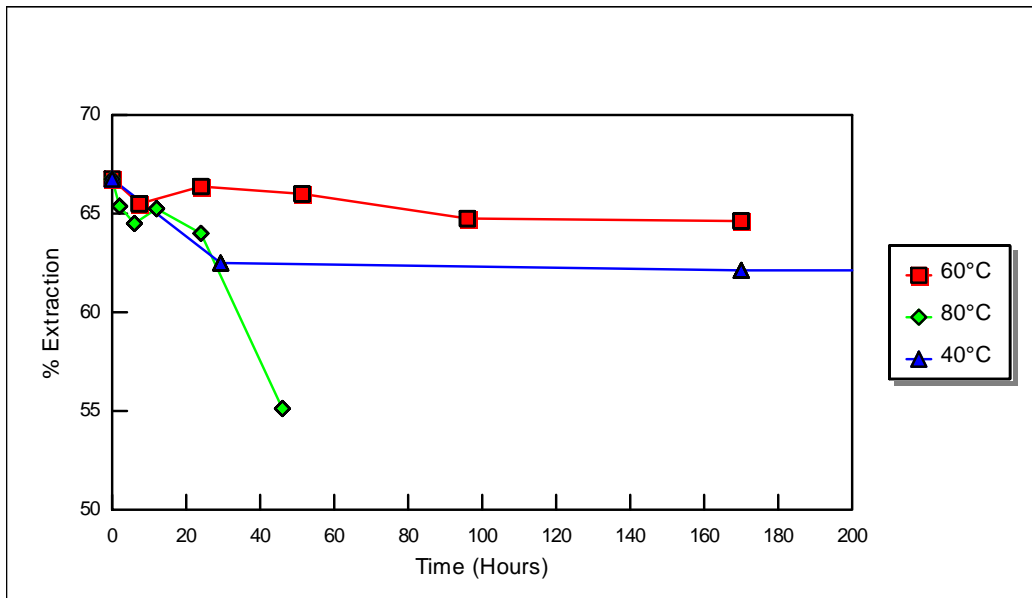
Figure 120 : Aqueous Extraction Data from Propellant STO17
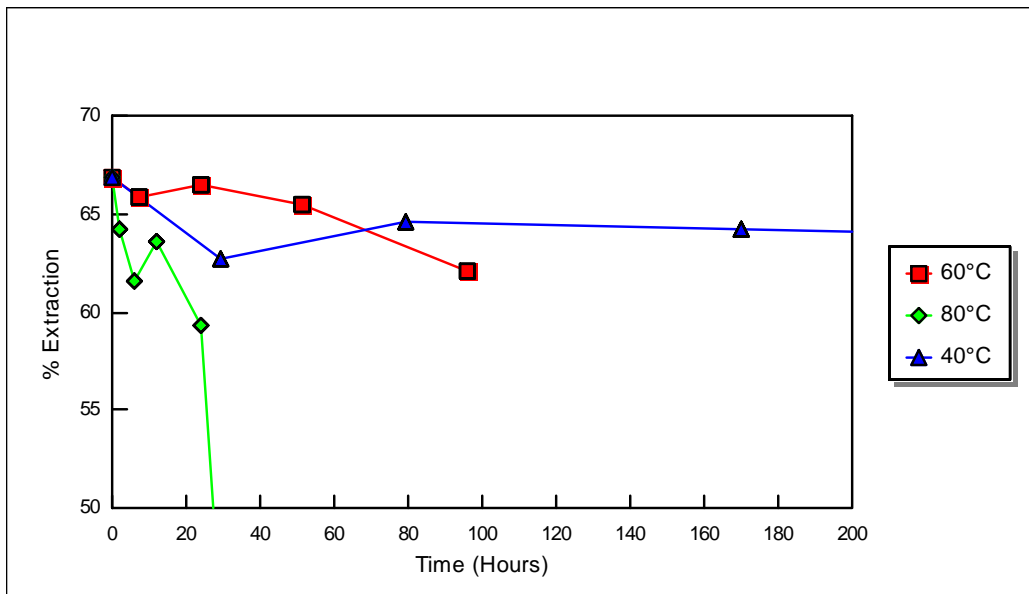
Figure 121 : Aqueous Extraction Data from Propellant STO18

STO17 (1% Na$_2$SO$_3$) / STO18 (1% (NH$_4$)$_2$S$_2$O$_8$) – From Figures 120 and 121, in isolation, neither hydrazine scavenger functions as effectively as when in combination with denitration stabilisers; compare the data from Figures 120 and 121 with Figures 116-119. . Figure 97 shows that at 80°C, formulation STO17 shows increase aqueous extract compared to the control sample (STO1) suggesting reaction of HNF. STO17 is also superior in performance to formulation STO18. However, neither isolated scavenger system performs as well as when encountered in combination with pNMA (Figure 118 and 119). This emphasises that a dual scavenger / denitration stabiliser component system is required to provide the highest level of improved propellant stabilisation. At 60°C, formulation STO18 shows a slow decline in aqueous fraction that suggests that there is a direct reaction between the stabiliser and other ingredients within the test matrix (as this is not seen significantly in the control sample STO1). The data at 40°C for both samples shows that the aqueous extraction value is maintained at high levels throughout the ageing period. This may suggest that the change of mechanism for degradation at 40°C is based upon liberation of either hydrazine or water (i.e. the products against which the hydrazine scavengers are proposed to have an effect).

3.3.3.5 Conclusions from Aqueous Extraction Measurements

Much of the aqueous extraction data supports and refines the conclusions from the mass loss data study (Section 3.5.2). The conclusions specific to the aqueous extraction study are :-

1) pNMA control of NOx and HNOx species is the critical reaction path at elevated temperature (80°C and 60°C) to minimise loss of HNF and aid sample longevity (in terms of retention of HNF).

2) An unidentified but dominant degradation reaction occurs in the samples at 40°C. This reaction can be controlled by the presence of either hydrazine scavenger (Sodium Sulphite or Ammonium Peroxodisulphate).

3) The action of the hydrazine scavengers appear to reduce the reaction initiated between N-NO-2NDPA and HNF at all temperatures. This may be via reaction with the products produced from that reaction or possibly via oxidation of Nitroso derivatives to Nitro derivatives at lower temperature.

4) Addition of hydrazine scavengers in combination with denitration stabilisers appears the most effective at maintaining high solids within the sample compositions.

Figure 122-124 build on the reaction description proposed in Figure 96 and incorporates the conclusions from the aqueous extraction data to give an indication of the proposed function of each of the stabiliser / scavenger species.

Figure 122

polyNIMMO Based, HNF Loaded Propellant

80°C

NOx / HNOx Produced. Possibly inhibited by scavengers

Unstabilised

+ HNF ⟶ Degraded HNF + PN

2NDPA / pNMA

pNMA reaction with NOx / HNOx controls loss of HNF

XS NOx *HNOx*

Hydrazine + Water + Other Degradation products

Unstabilised

Nitrated Derivatives of 2NDPA / pNMA

$NaSO_3 / (NH4)_2S_2O_8$

Conversion of Chemically Active Products (e.g. Hydrazine) to Less Reactive Products

Activity of Stabilisers Falls to Minimum

Activity of Scavengers Falls to Minimum

Figure 122 – Dominant polyNIMMO / HNF Propellant Degradation Reaction at 80°C

Figure 123

polyNIMMO Based, HNF Loaded Propellant

60°C

NOx / HNOx Produced

Unstabilised

+ HNF ⟶ Degraded HNF + PN

2NDPA / pNMA

pNMA reaction with NOx / HNOx controls loss of HNF

Unstabilised

Hydrazine + Water + Other Degradation products

Unstabilised

$NaSO_3 / (NH4)_2S_2O_8$

Nitrosoated Derivatives of 2NDPA / pNMA

$NaSO_3 / (NH4)_2S_2O_8$

Conversion of Chemically Active Products (e.g. Hydrazine) to Less Reactive Products

Protection of HNF – Possibly Via Oxidation of N-Nitroso Species to N or C Nitro Compounds

Activity of Scavengers Falls to Minimum

Figure 123 – Dominant polyNIMMO / HNF Propellant Degradation Reaction at 60°C

139
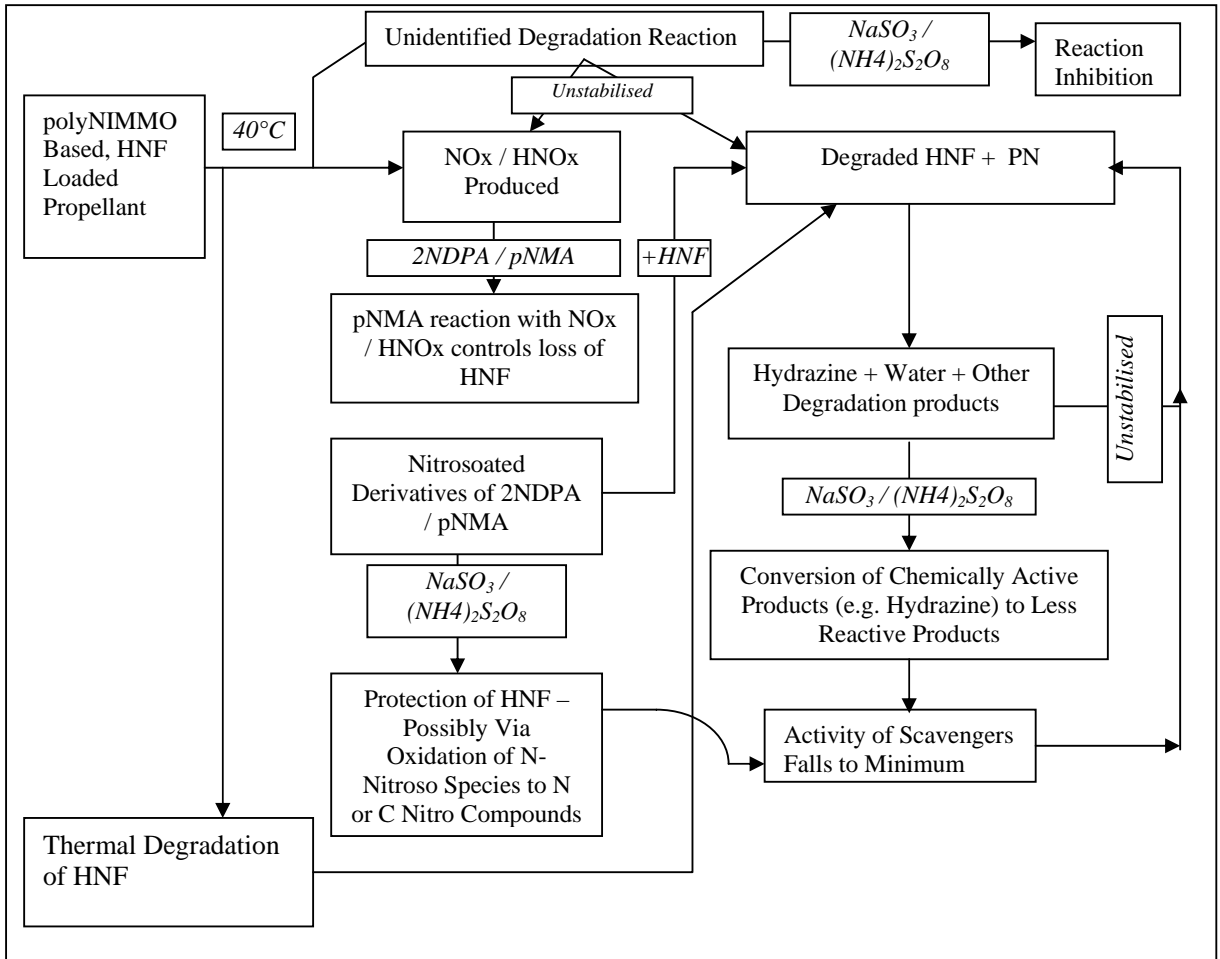
Figure 124 – Dominant polyNIMMO / HNF Propellant Degradation Reaction at 40°C

3.3.4 THF Extraction

3.3.4.1 Introduction

Bunyan et al [51] and Manelis [62] detail analysis of polyNIMMO in both the precured and post cured state to assess polymer degradation / decomposition. The present study of HNF / polyNIMMO propellants undertakes quantitative measurement of the THF insoluble fraction of post storage residues to assess whether there has been appreciable polymer breakdown during storage. Data received from the manufacturer (Nobel Enterprises) gave solubilities of PolyNIMMO in THF of near 0% for a fully cured isocyanate based block polymer and near 100% for the uncured polymer [117]. Although residues from decomposition would not be identical to the uncured polymer, an increase in solubility with decreasing chain length was also predicted by the manufacturer [117]. Assessment of the growth of THF soluble residues gave an indication of degree of degradation of the isocyanate cured polymer backbone. An increase in insoluble residue can be attributed to a range of reaction courses such as :-

- increasing PolyNIMMO chain length (eg by completion of incomplete cure or extension of polymer framework due to additional crosslinking reactions)
- loss of soluble materials from matrix during storage (eg via volatilisation, gassification, etc)
- change in solubility of materials present (eg chemical reaction to reduce electronegativity, increase in ionic character etc)

An increase in THF soluble residue levels can primarily be attributed to :-

i)   decreasing PolyNIMMO chain length due to cleavage of the polymer backbone
ii)   changes in solubility of species in the matrix (eg changes in solubility of 2NDPA derivatives due to degree of derivative nitration)

For analysis, 0.03g of the residue from aqueous extraction trials was taken and placed into a 10ml sealed vial with 10ml THF. The vial was allowed to stand for 48 hours to extract any soluble polymeric fractions. The THF was discarded, the residue dried and then reweighed to assess the THF soluble fraction. All THF extraction trials were undertaken on samples that had previously undergone aqueous extraction in order to minimise possible effects from HNF solubility within the solvent or any undesirable reactions (eg oxidation) of THF by HNF.

3.3.4.2 Results and Discussion of THF Extraction Data
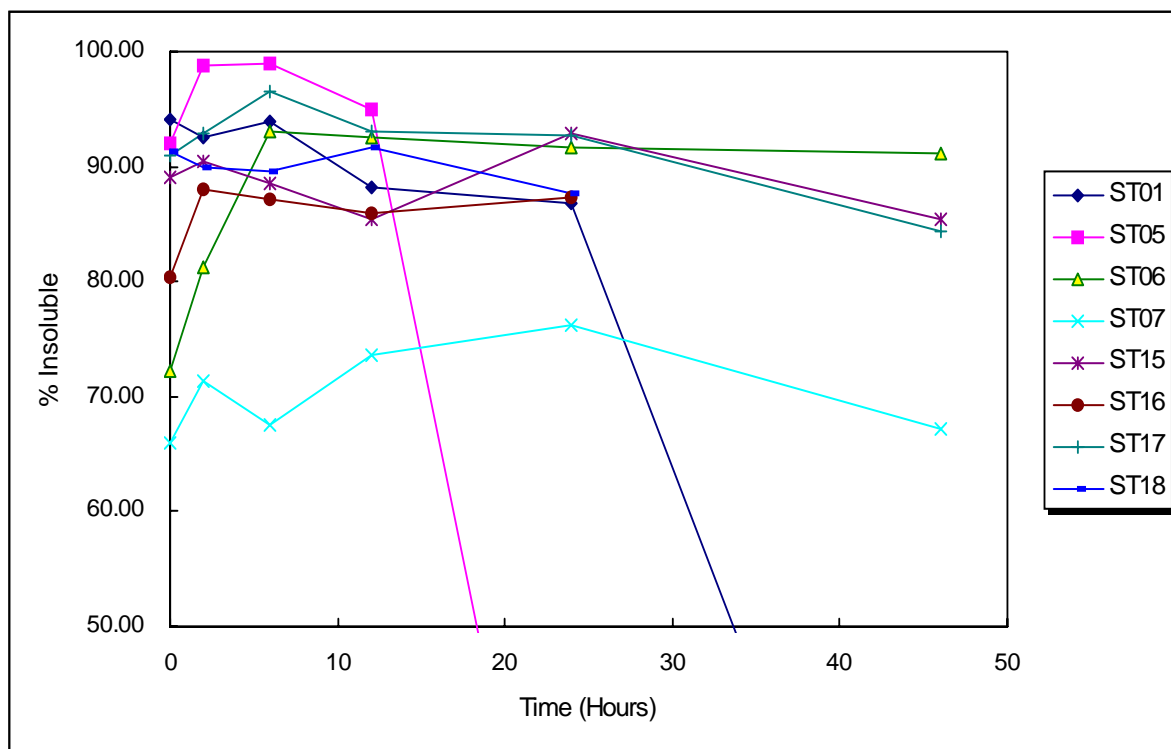
Figure 125 : THF Extract from pNMA, Hydrazine Scavengers and Control Sample Formulations at 80°C
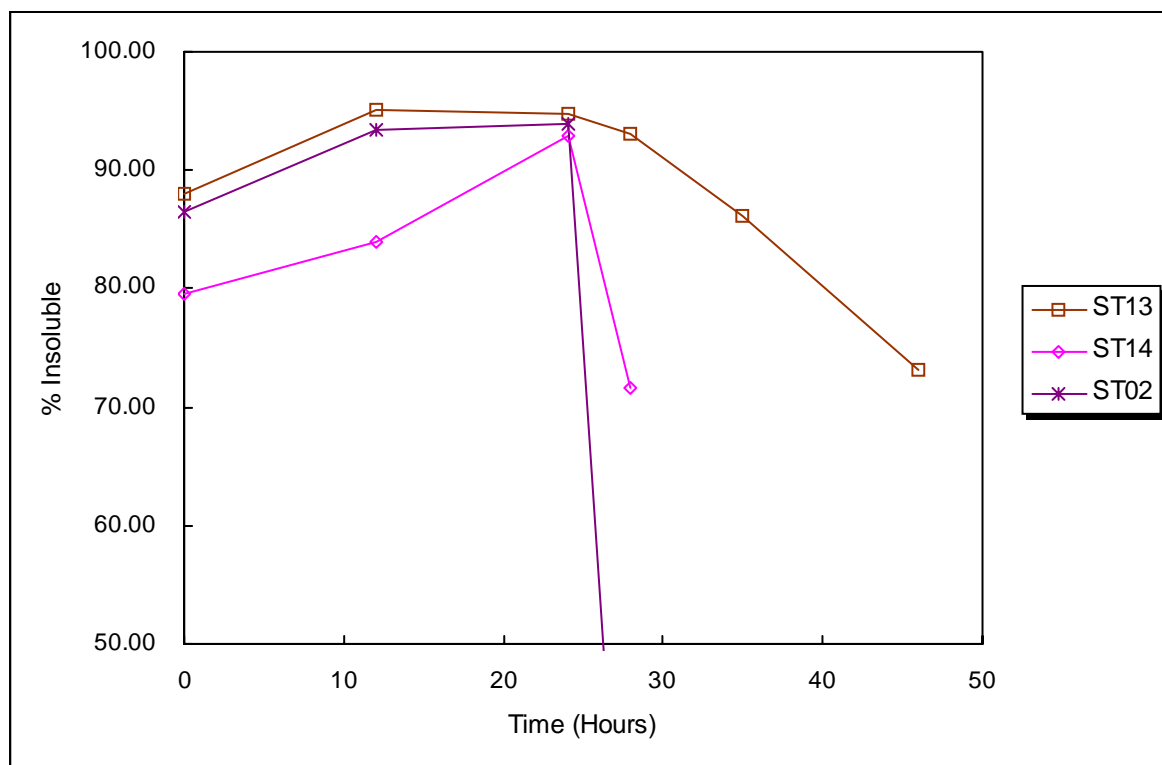
Figure 126 : THF Extract from 2NDPA Based Formulations at 80°C
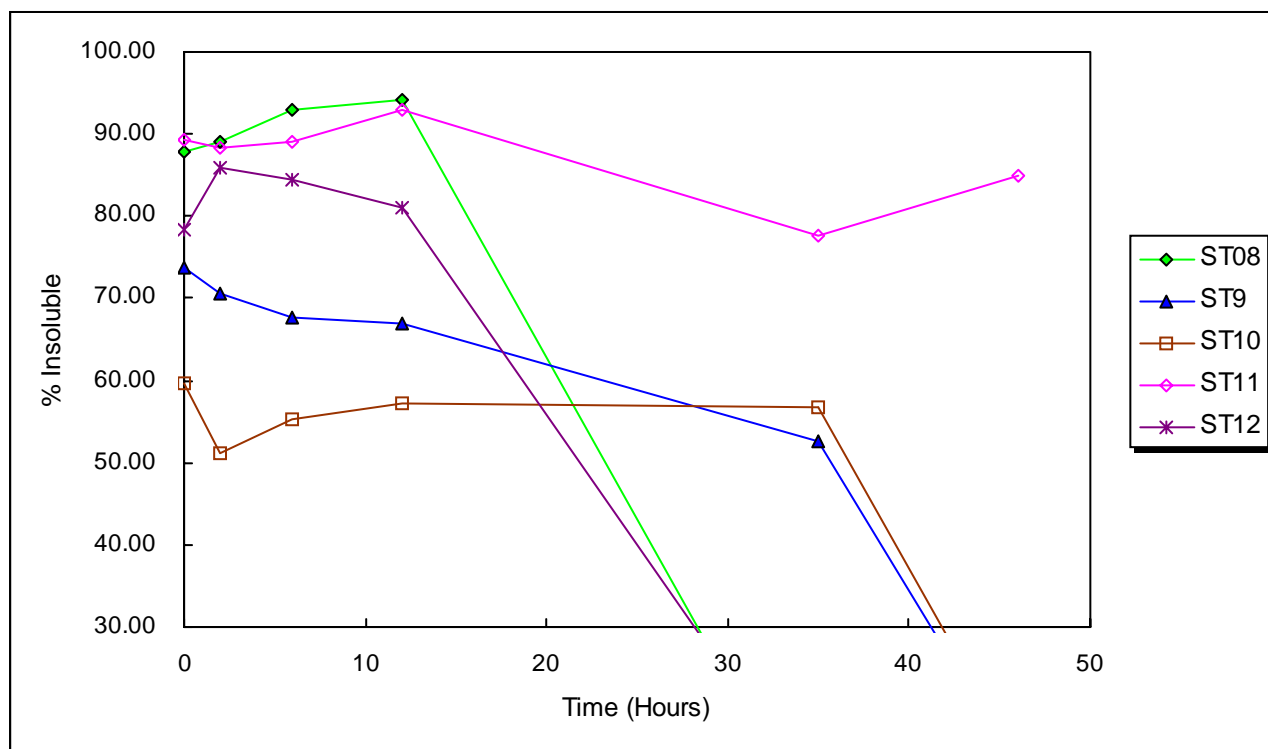
Figure 127 : THF Extract from Mixed Stabiliser Formulations at 80°C

Figures 125 to 127 show THF extraction data for each propellant type at 80°C. It is observed that the majority of samples show little or no significant variation in insoluble fraction with time.. Those samples that do show changes in soluble fractions generally contain 2NDPA in the formulation suggesting that a 2NDPA (or N-NO-2NDPA) / HNF reaction or products of that reaction is affecting the polymer backbone. This general lack of change in insoluble fraction for the majority of samples is an unexpected result as it had been presumed that propellant degradation at elevated temperature proceeded (at least in part) via polymeric breakdown into smaller molecular fragments. This polymeric breakdown was thought to be the explanation of softening of the samples followed by liquefaction observed visibly during storage.

At 60°C (Figures 129 to 131) and 40°C (Figures 132 to 134) very low levels of change are observed in the polymer extraction graphs. This again suggests that little or no degradation to the polymeric backbone has occurred during the extended ageing periods.
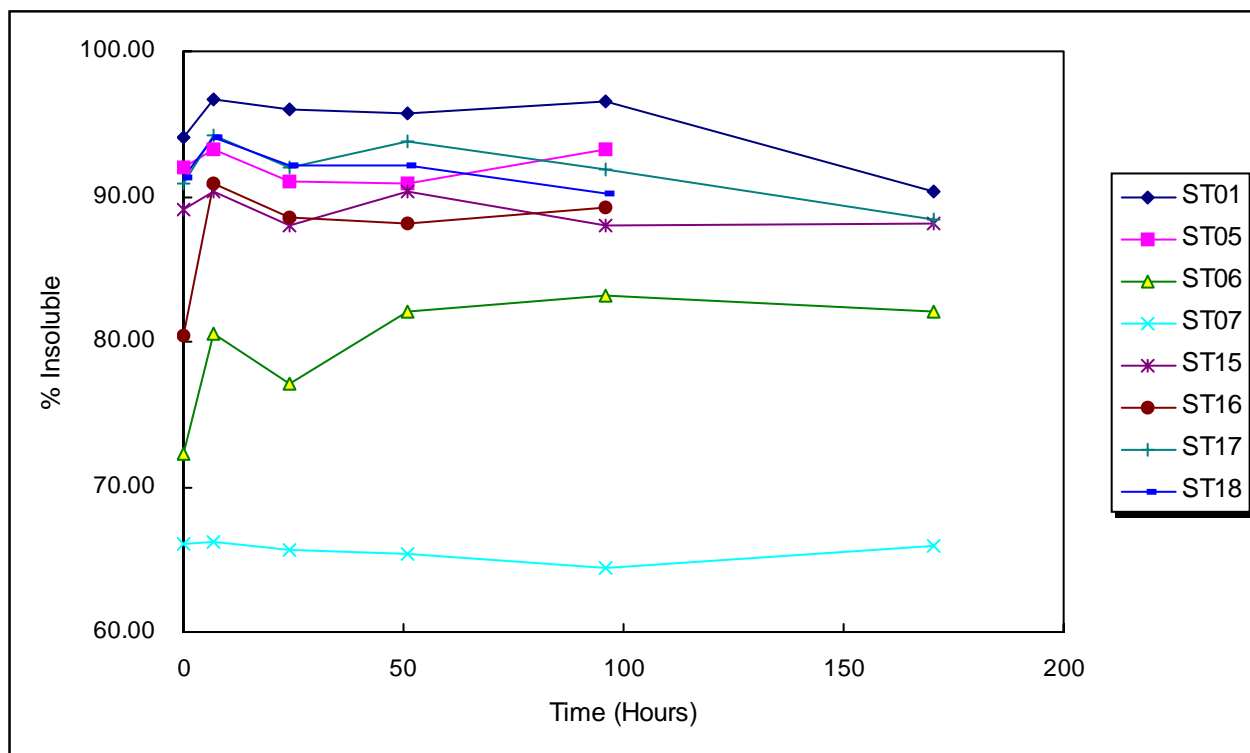
Figure 128 : THF Extract from pNMA, Hydrazine Scavengers and Control Formulations at 60°C
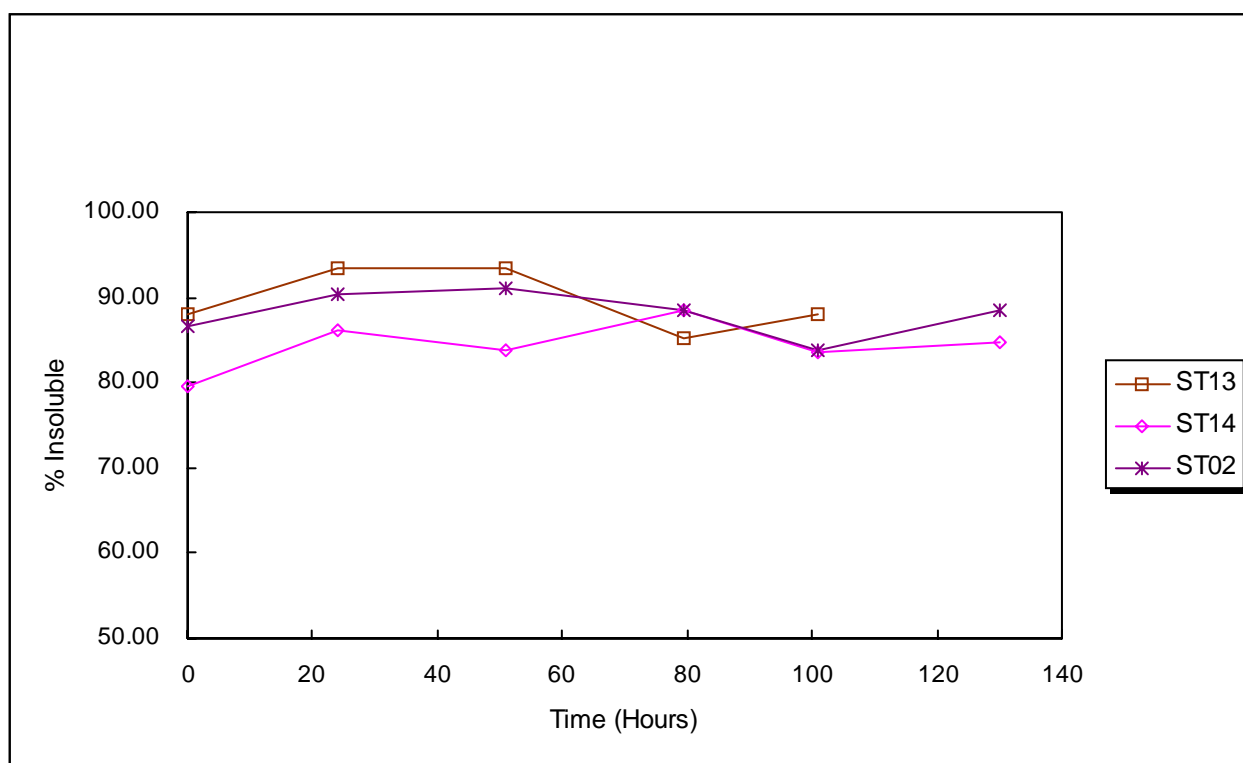
Figure 129 – THF Extract from 2NDPA Stabilised Samples at 60°C
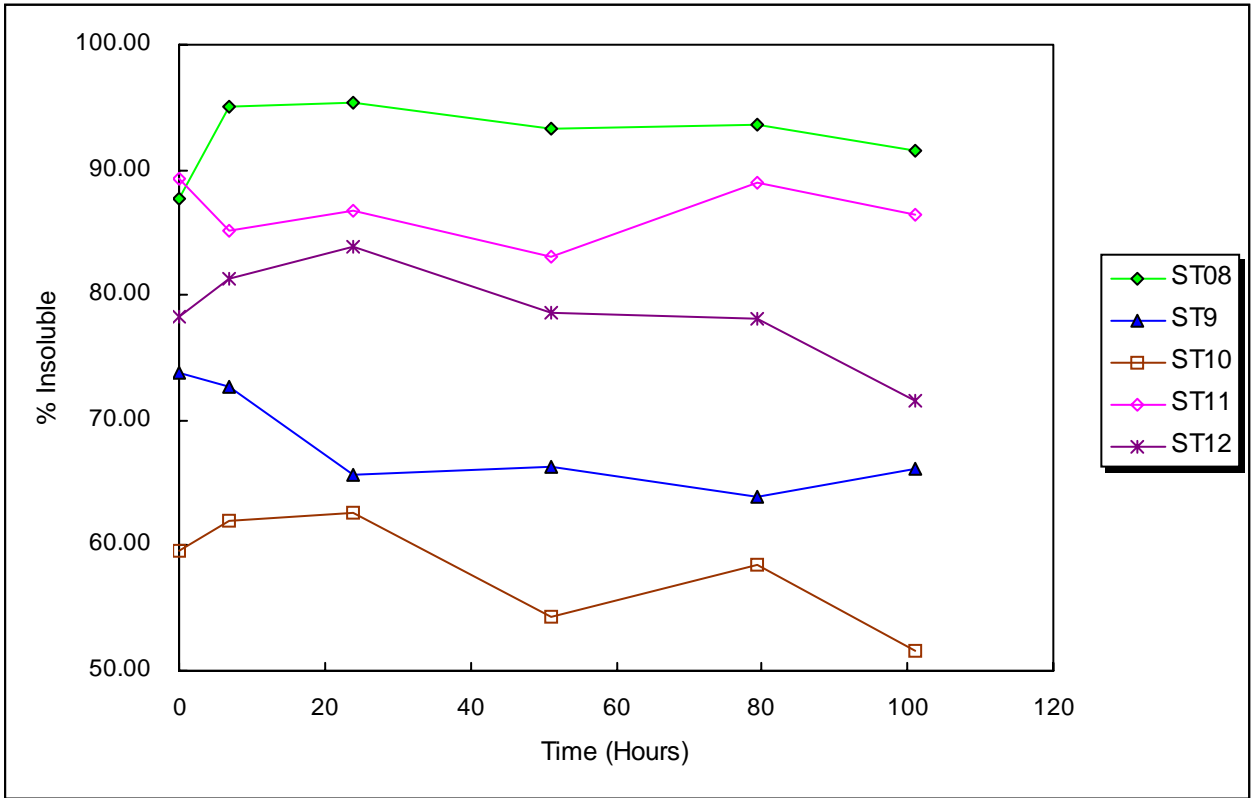
Figure 130 – THF Extract from Mixed Stabilised Samples at 60°C
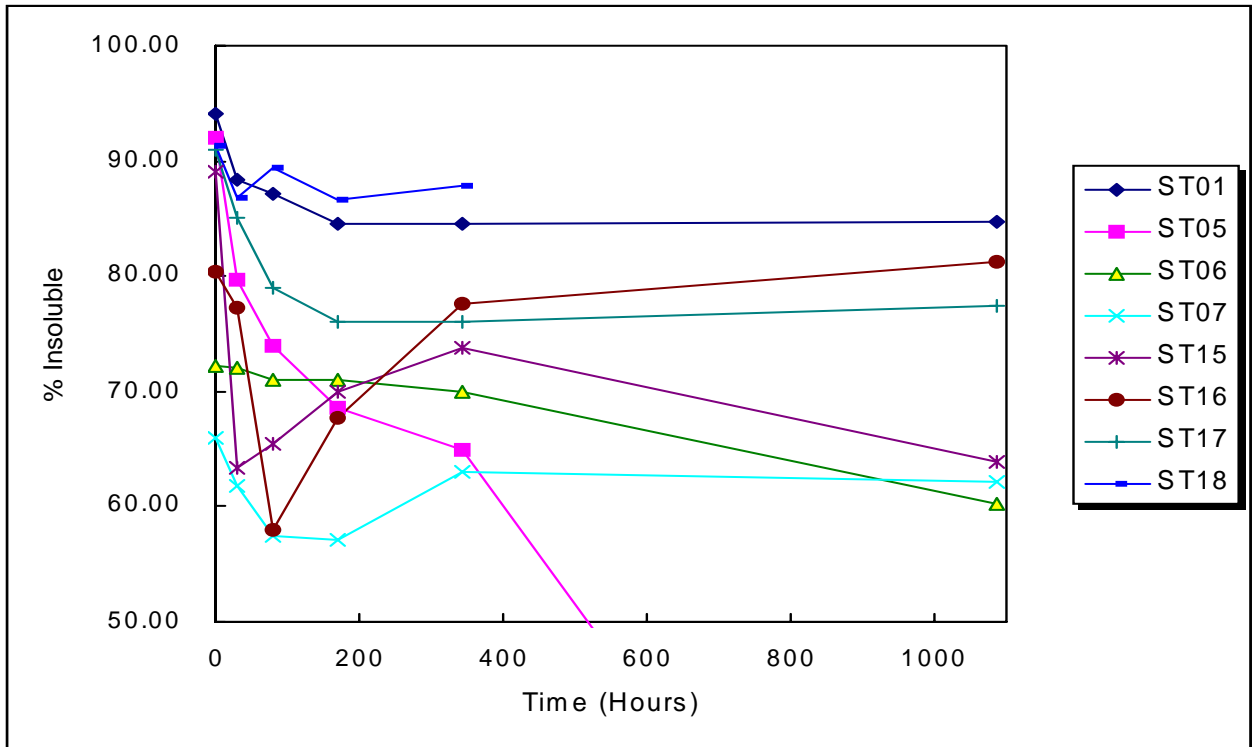
Figure 131 – THF Extract from pNMA. Hydrazine Scavengers and Control Formulations at 40°C
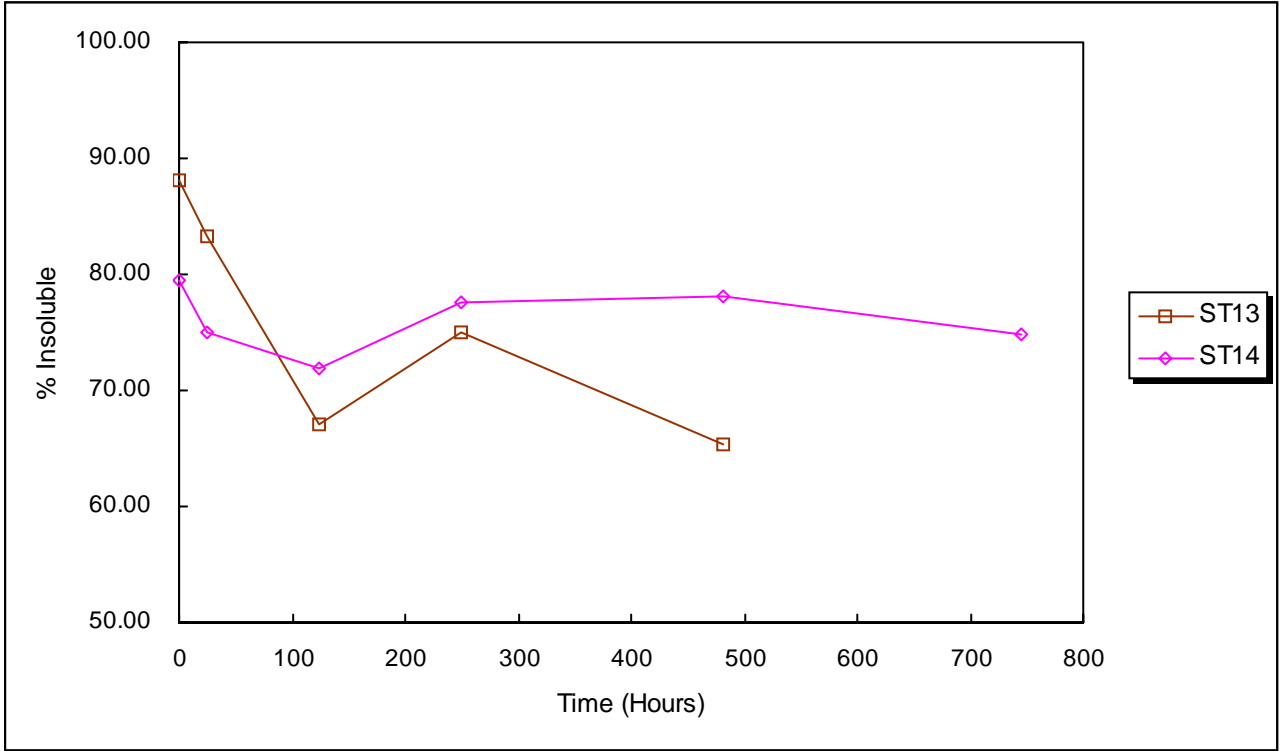
Figure 132 – THF Extract from 2NDPA Stabilised Samples at 40°C
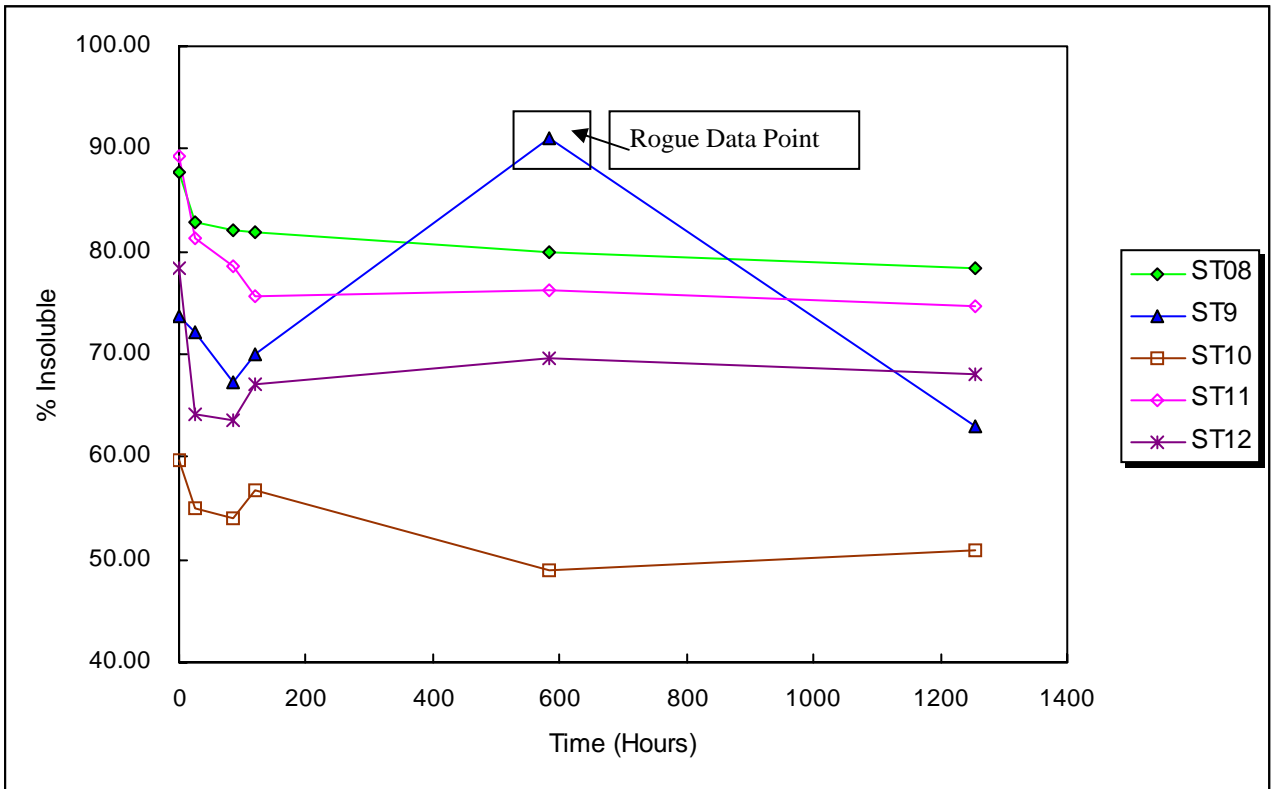
Figure 133 – THF Extract from Mixed Stabilised Samples at 40°C

The low level of extract for many samples, even at 80°C suggest that the degradation reaction of the polymer in HNF / PolyNIMMO propellant systems proceeds primarily via degradation of the HNF present, almost independent of direct reaction of HNF with the polymer. This is most evident with sample STO7 at 80°C (Figure 125). For this sample, the THF extract is similar throughout the whole ageing period (48 hours). If direct reaction of HNF with polyNIMMO was occurring (eg via the oxetane or polyurethane links on the polymer backbone) then the THF extracts would be similar to the control sample (STO1); Figure 125 shows that this is not the case. This suggests that degradation of the polymer backbone is a via a secondary reaction (eg between polyNIMMO and an HNF degradation product) rather than a primary reaction with HNF. Also, if the rate of polymer breakdown was dependent on direct polyNIMMO / HNF reaction, the rate of change of THF extract would be expected to be constant; again this is not observed. The rapid change in THF extract after 24hours storage at 80°C for STO1 suggests a change in reaction mechanism at this point after an initial induction period. The absence of rapid change in other test samples suggests that this change in reaction mechanism is controlled via the addition of denitration stabilisers or hydrazine scavengers. Only in the later stages of degradation does polymer breakdown intensify (presumably via interaction of HNF degradation products and unreacted polymer), ultimately leading to liquefaction. This apparent change in mechanism is reinforced by the graphs from the 60°C and 40°C storage samples that show very little change in THF extraction value during storage.

Figures 135 to 150 show the THF soluble fraction from the various formulations at different storage temperatures. It can be observed from the figures that there are some general differences in extraction profile between storage temperatures. The various extraction profiles are shown in Figure 134.
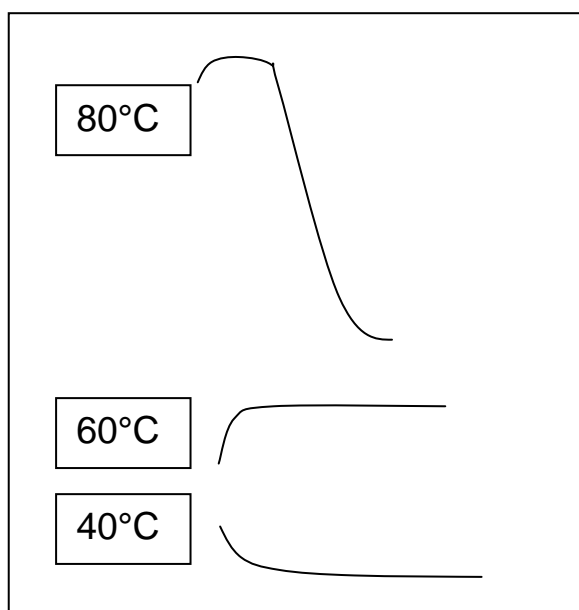
Figure 134 – Schematic Peak Profiles Observed in THF Extraction Data Plots

The peak profiles at 60°C and 40°C shown in Figure 134 would suggest that any reaction occurring has achieved a steady state within the system. This would further support the suggestion that direct polyNIMMO / HNF reaction is not a dominant reaction within the ageing process – direct reaction would be expected to be a continuous process, continuing until exhaustion of one of the reagents. These peak profiles suggest that a self-limiting reaction is occurring. For the 80°C and 60°C data, the slight increase in insoluble fraction before achieving steady state is likely due to further reaction of uncured polymer ingredients (eg uncured polyNIMMO or uncured isocyanate). This further reaction may relate to extension of polymer curing, direct HNF reaction with uncured products or possibly reaction of the isocyanate present with water. As the polymer base matrix was the same in all test formulations, the change in insoluble fraction between samples at any temperature would be expected to be similar. Variation in this increased insolubility may help to elucidate the source of this additional reaction.

Figure 135 show the THF insoluble fraction for the control sample at all three storage temperatures. It can be observed that, although there is some variation between the data sets, 80°C is the temperature at which large-scale depletion of the polymer chain occurs. However, even at this temperature, there appears to be an initial induction period where polymer breakdown is low. This agrees well with the previous observations in mass loss and aqueous extraction studies.
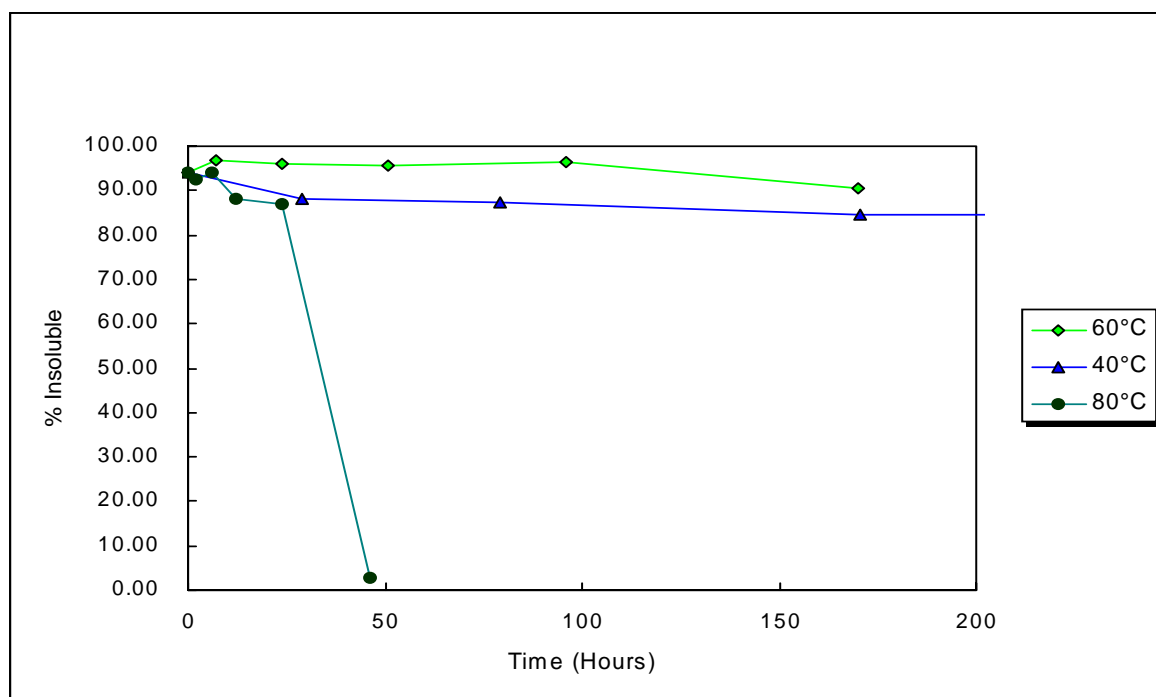
Figure 135 – Variation in THF Insoluble Fraction With Storage Temperature for Sample STO1
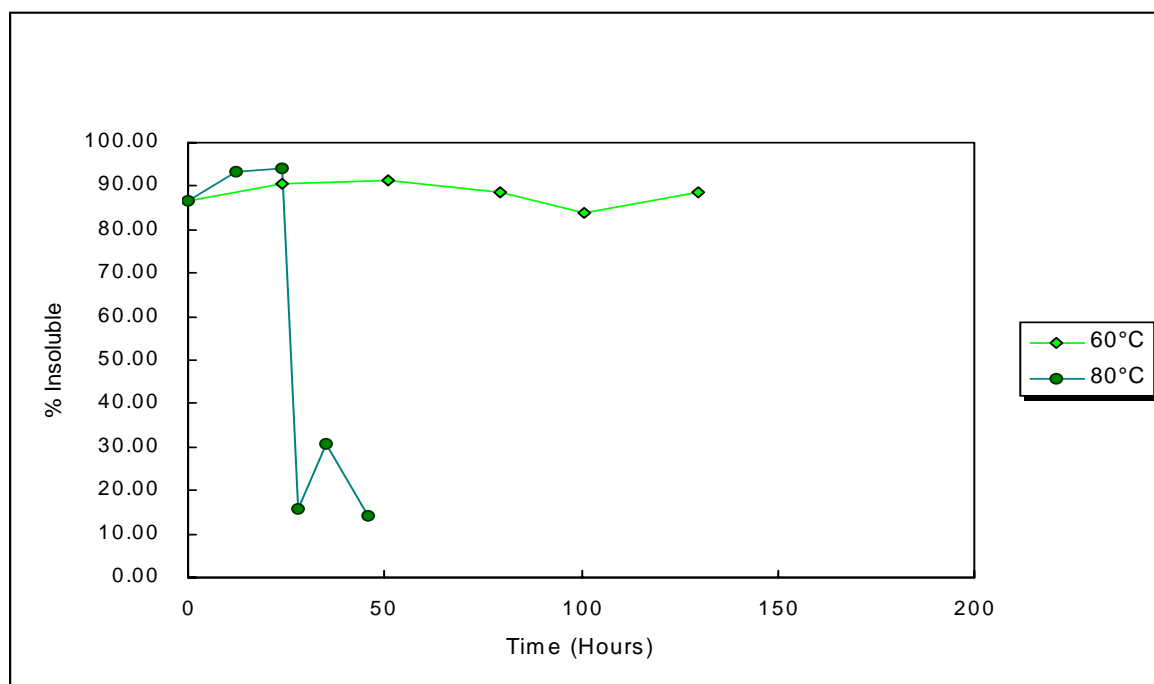
Figure 136 – Variation in THF Insoluble Fraction With Storage Temperature for Sample STO2

Within Figure 136 (and comparison against Figure 135) it indicates that there is a reduction in the induction period compared to the control sample at 80°C. This suggests that the action of 2NDPA within the propellant formulation accentuates polymer breakdown. However, at 60°C, very little polymer breakdown occurs. This again suggests that it is not direct reaction of 2NDPA and HNF that is detrimental to the polymer backbone. This implies that reaction is between either a derivative of 2NDPA with HNF or reaction of an HNF degradation product with 2NDPA that drives polymer breakdown.

Sample STO5 (Figure 137) shows an initial large increase in THF insoluble residue. This is also seen in Figure 138 and 139. The presence of pNMA appears to lead to development of this peak in all formulations that it is incorporated (see Figures 137, 138, 139, 140, 141, 142 and 148 for details).
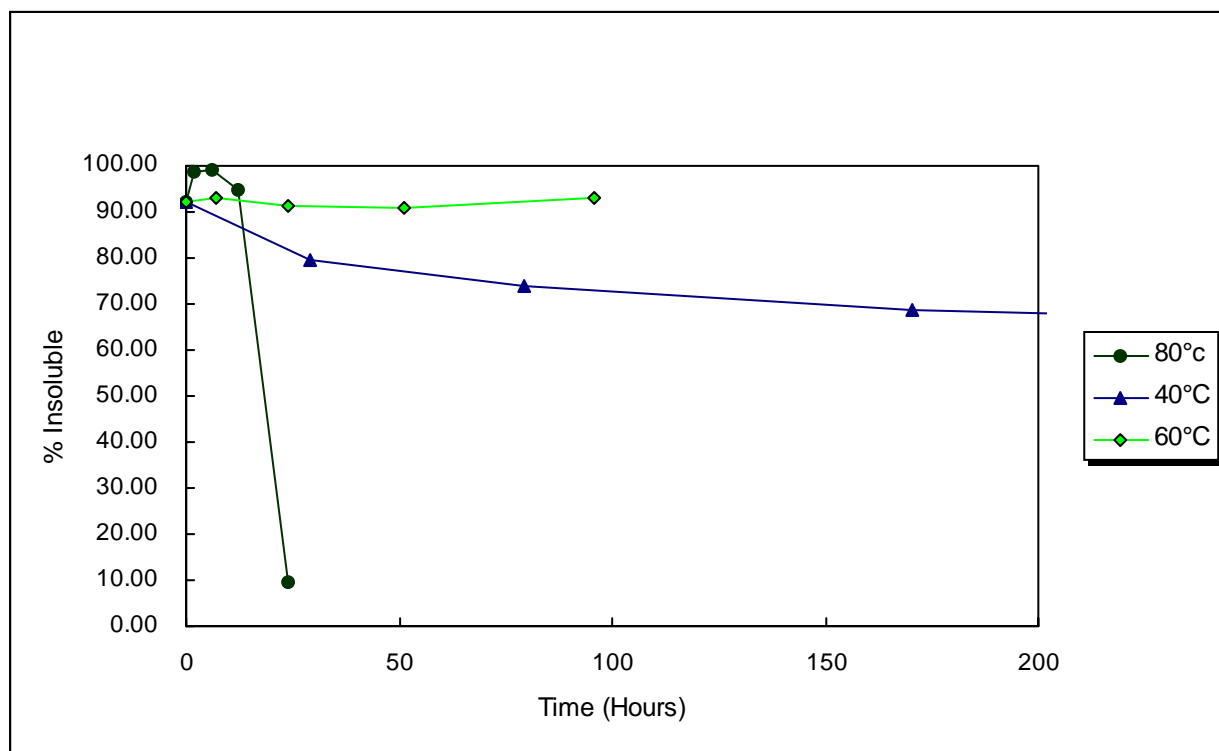
Figure 137 – Variation in THF Insoluble Fraction With Storage Temperature for Sample STO5

Comparison of the temperature dependence of STO6 (8% pNMA) (Figure 138) shows a large degree of separation between datasets, with the formulation eventually achieving steady state within all storage conditions. This achievement of steady state at all temperatures is rare within the test data, with STO16 (1% pNMA + 1% Ammonium Peroxodisulphate, Figure 148) being the only other sample to show this trend. Extended ageing of both of these formulations beyond the storage period observed would have been of benefit to assess whether the equilibrium position remained constant. The separation of these datasets might be indicative of a preliminary polymerism step being present and possibly being inhibited by the basicity of the stabiliser present. This inhibition of reaction might explain why the initial THF extraction data for formulation STO5 ie ~72% whereas in the control sample it is > 90%. During extended storage at 80 and 60°C, the curing reaction can initially continue to finish the cure cycle. The lack of step on the 40°C data suggests that this is too low a temperature to thermally catalyse this curing reaction. The steady state following this initial increase in insoluble residues reaction is a reflection of the stabiliser efficiency. Comparison of STO7 (16% pNMA) would maybe be expected to show a similar plateau character. However, as detailed in the mass loss assessment data, formulation STO7 appears to show reduced stabilising efficiency compared to the STO6 sample and this is seen again in Figure 139, especially at the 80°C storage temperature.
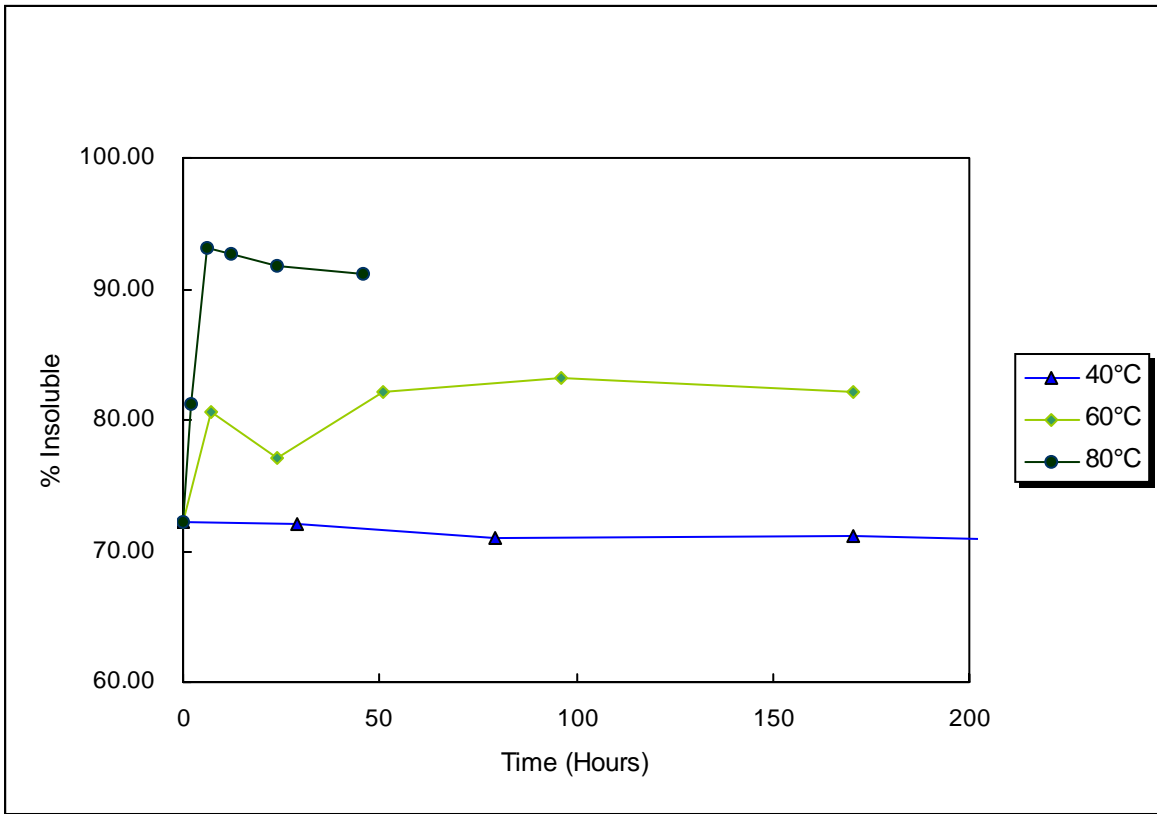
Figure 138 – Variation in THF Insoluble Fraction With Storage Temperature for Sample STO6
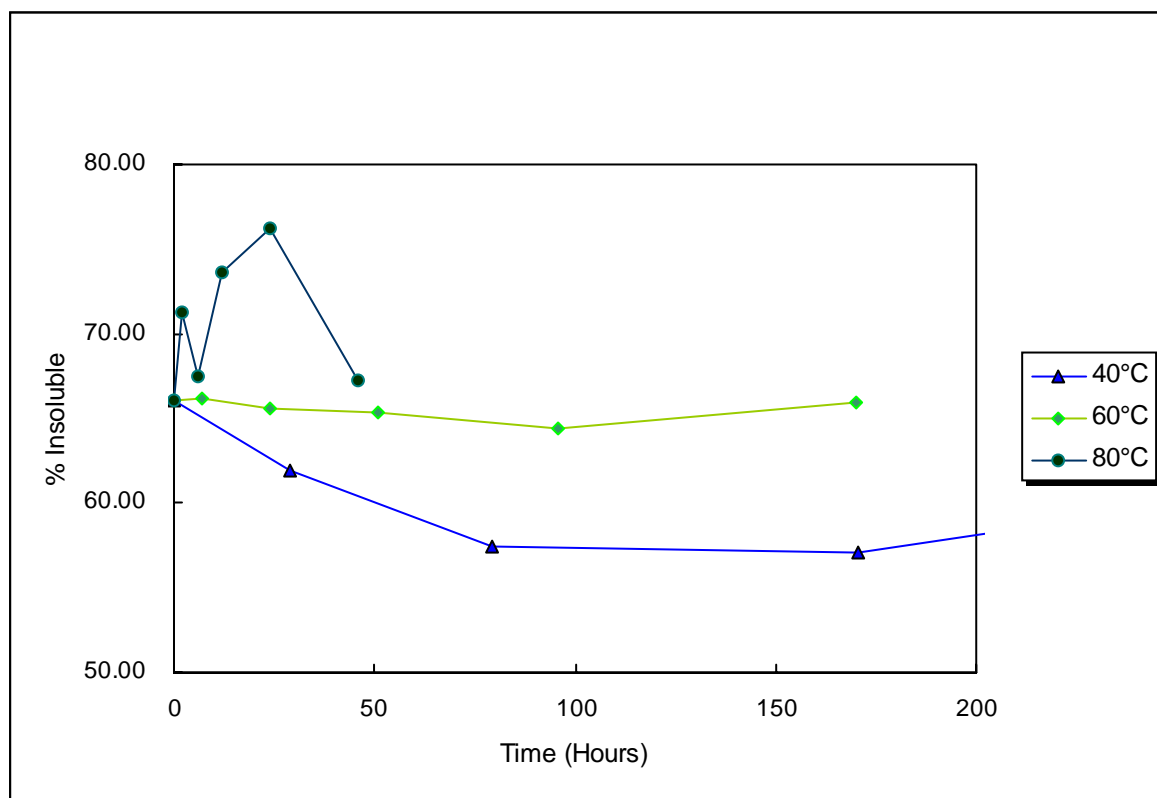
Figure 139 – Variation in THF Insoluble Fraction With Storage Temperature for Sample STO7

Figures 140 –142 show the effect of increased stabiliser content in a pNMA : 2NDPA ratio of 1:1. The figures show that, during storage at 80°C, increasing the overall stabiliser level increases the length of the induction plateau at the start of storage prior to polymer degradation. However, once polymer degradation starts, the additional stabiliser present does not significantly affect the rate of polymer breakdown. This implies either the exhaustion of one (or both) of the stabiliser species or liberation / generation of a chemically active species at the end of the induction period (possibly linked to stabiliser exhaustion) which results in rapid reaction with the polyNIMMO polymer backbone.
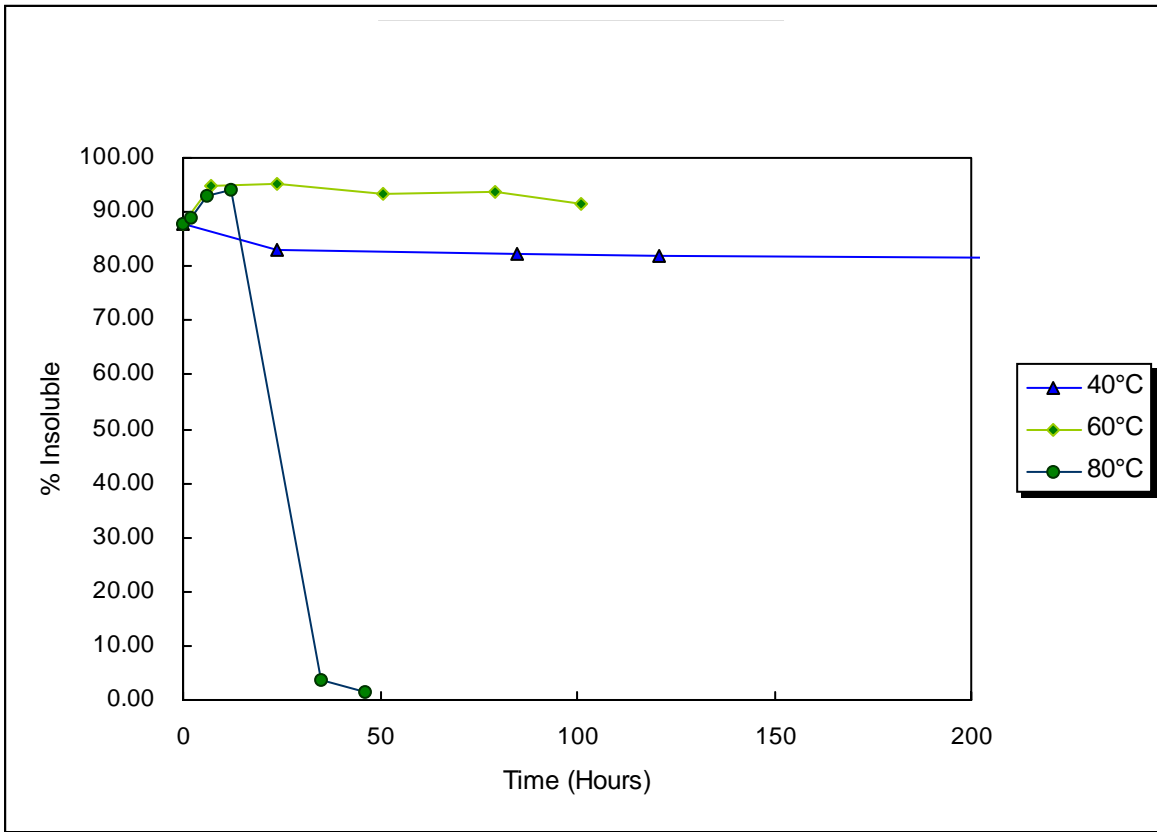
Figure 140 – Variation in THF Insoluble Fraction With Storage Temperature for Sample STO8
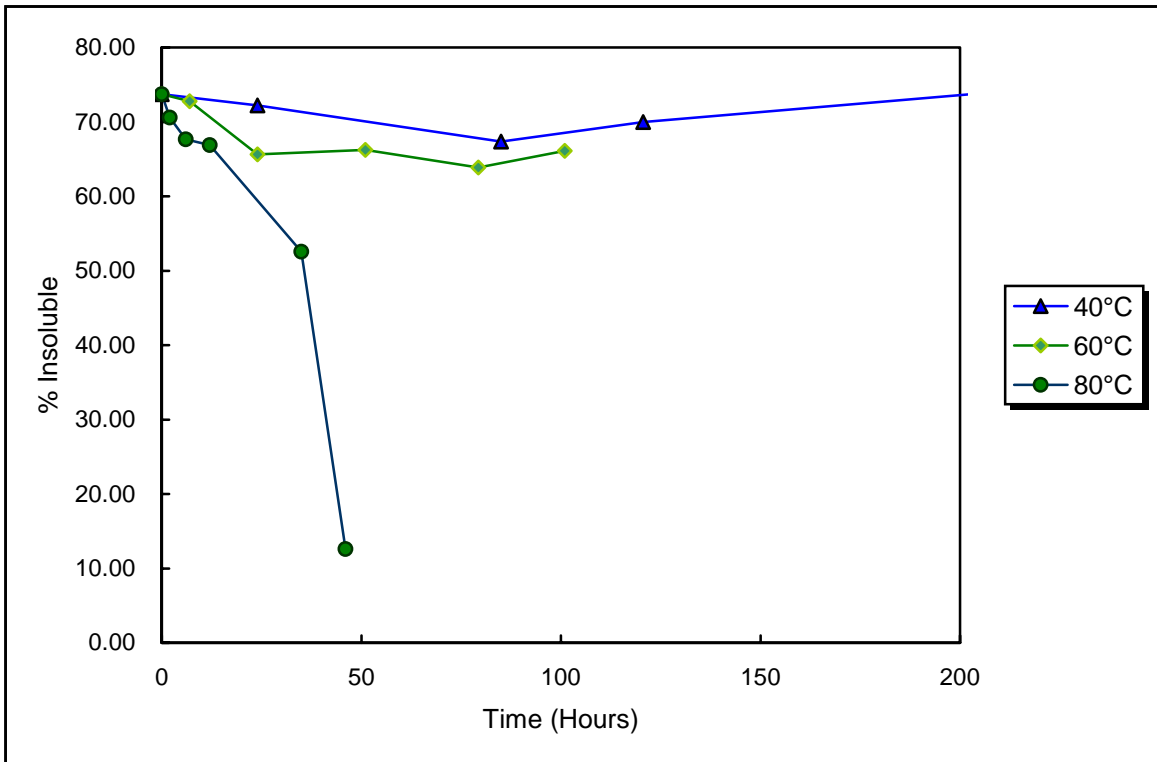
Figure 141 – Variation in THF Insoluble Fraction With Storage Temperature for Sample STO9
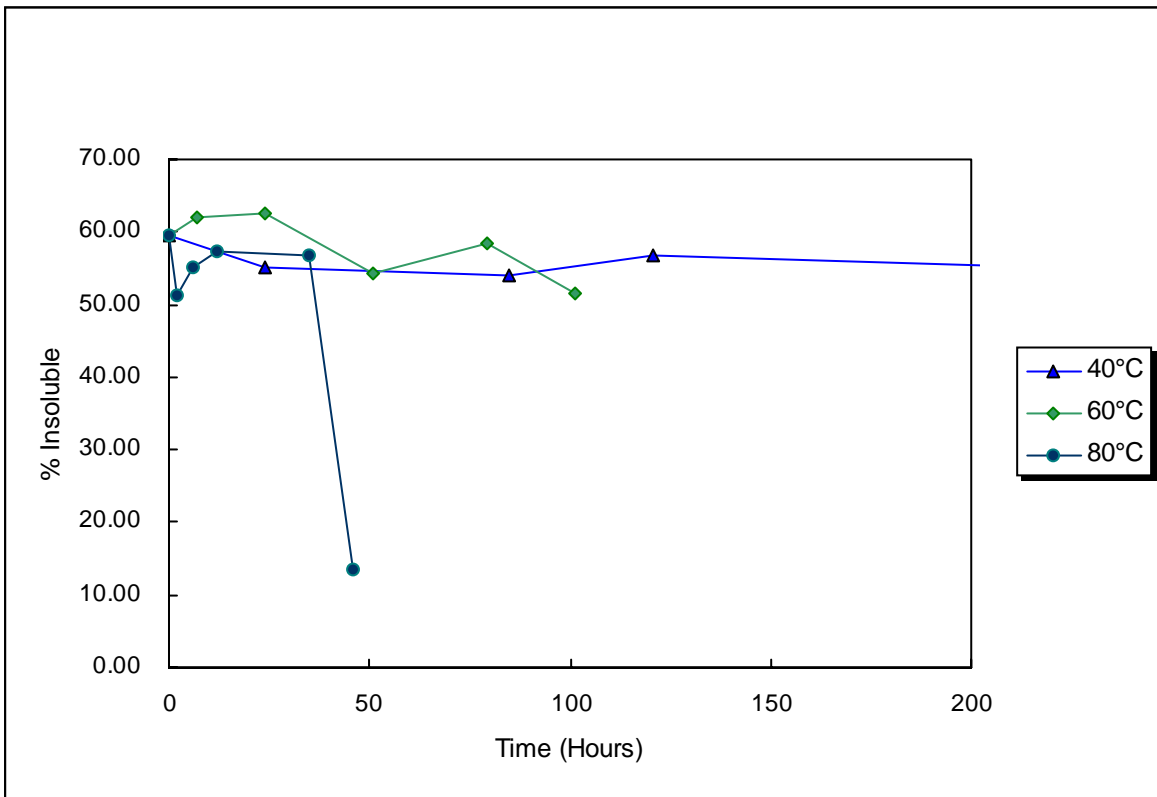
Figure 142 – Variation in THF Insoluble Fraction With Storage Temperature for Sample STO10

Comparison of 143 and 144 shows that sample STO11 (2% pNMA : 1% 2NDPA) is significantly superior to the STO12 analogue (2% 2NDPA : 1% pNMA) at 80°C. This again emphasises the need for control of the NOx species but also that 2NDPA is detrimental to sample longevity.
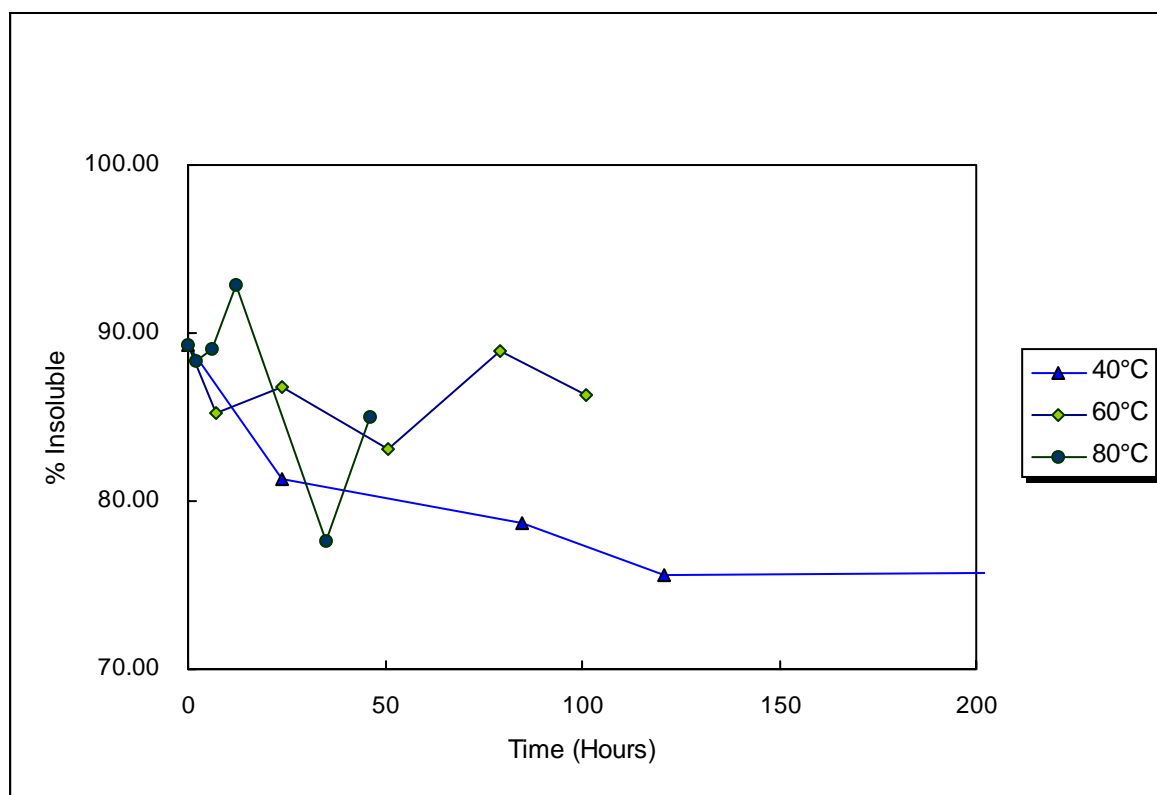
Figure 143 – Variation in THF Insoluble Fraction With Storage Temperature for Sample STO11
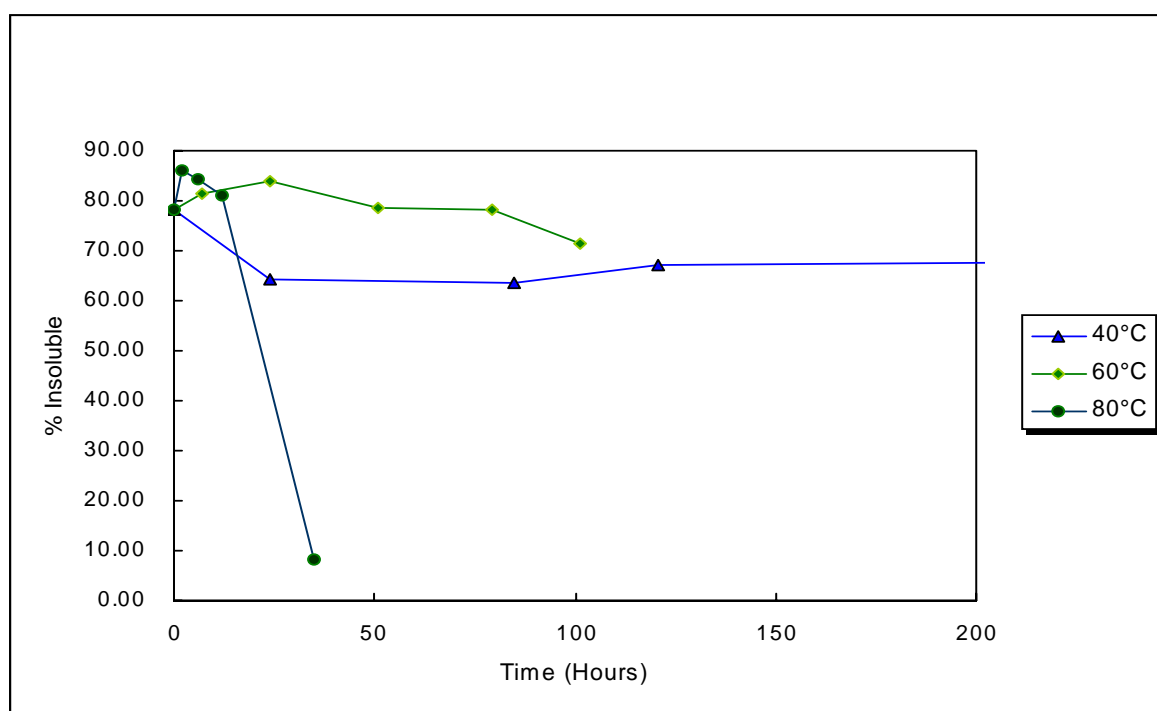
Figure 144 – Variation in THF Insoluble Fraction With Storage Temperature for Sample STO12

Finally, Figures 145 – 150 show the samples containing hydrazine scavengers sodium sulphite or ammonium peroxodisulphate. All these samples show a decrease in insoluble residues at 40°C although this is least marked in ammonium peroxodisulphate containing samples and is comparatively minor in STO14 (1% 2NDPA + 1% Ammonium Peroxodisulphate).The reduction in insoluble residue is more marked in samples where hydrazine scavengers are present alongside denitration stabilisers than when hydrazine scavengers are encountered singly. This would suggest that there might be an additional reaction present between these materials and the polymeric backbone at lower temperatures.
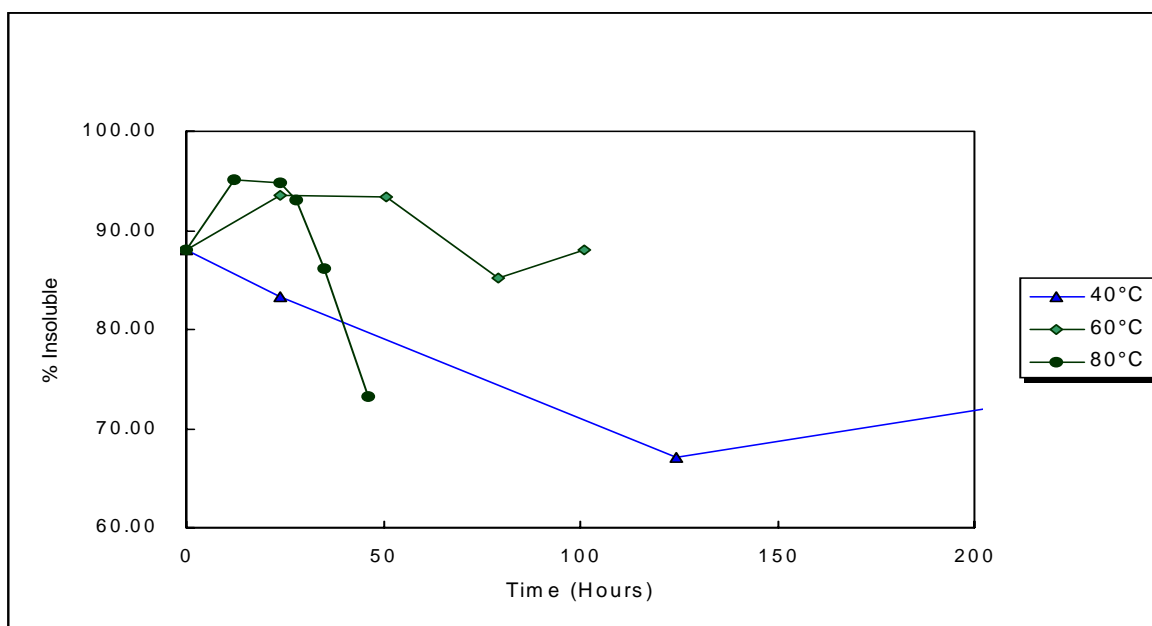
Figure 145 – Variation in THF Insoluble Fraction With Storage Temperature for Sample STO13
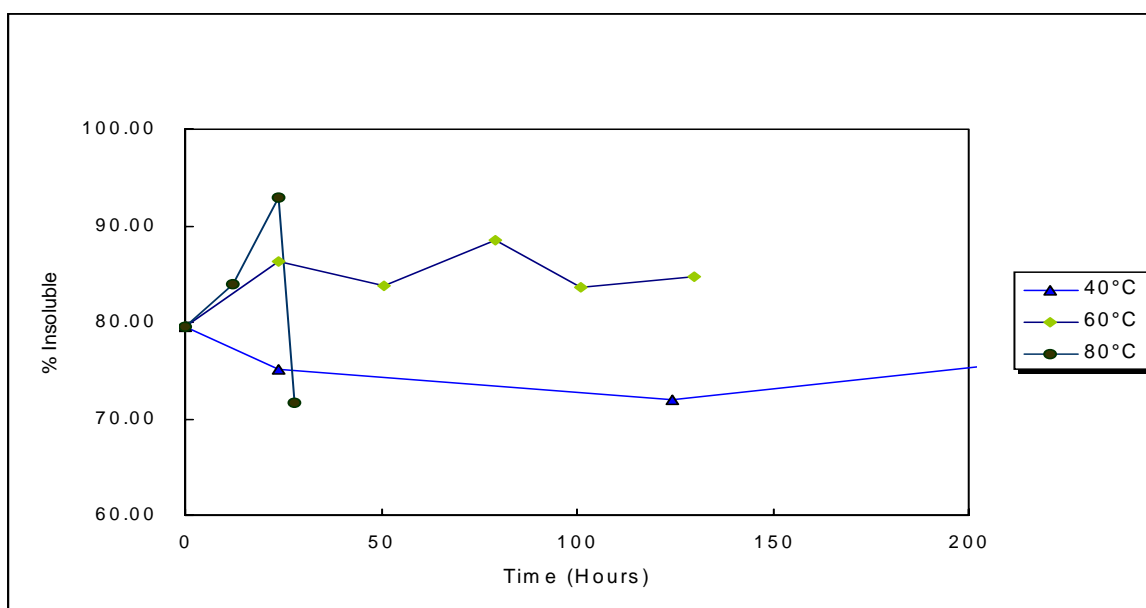
Figure 146 – Variation in THF Insoluble Fraction With Storage Temperature for Sample STO14
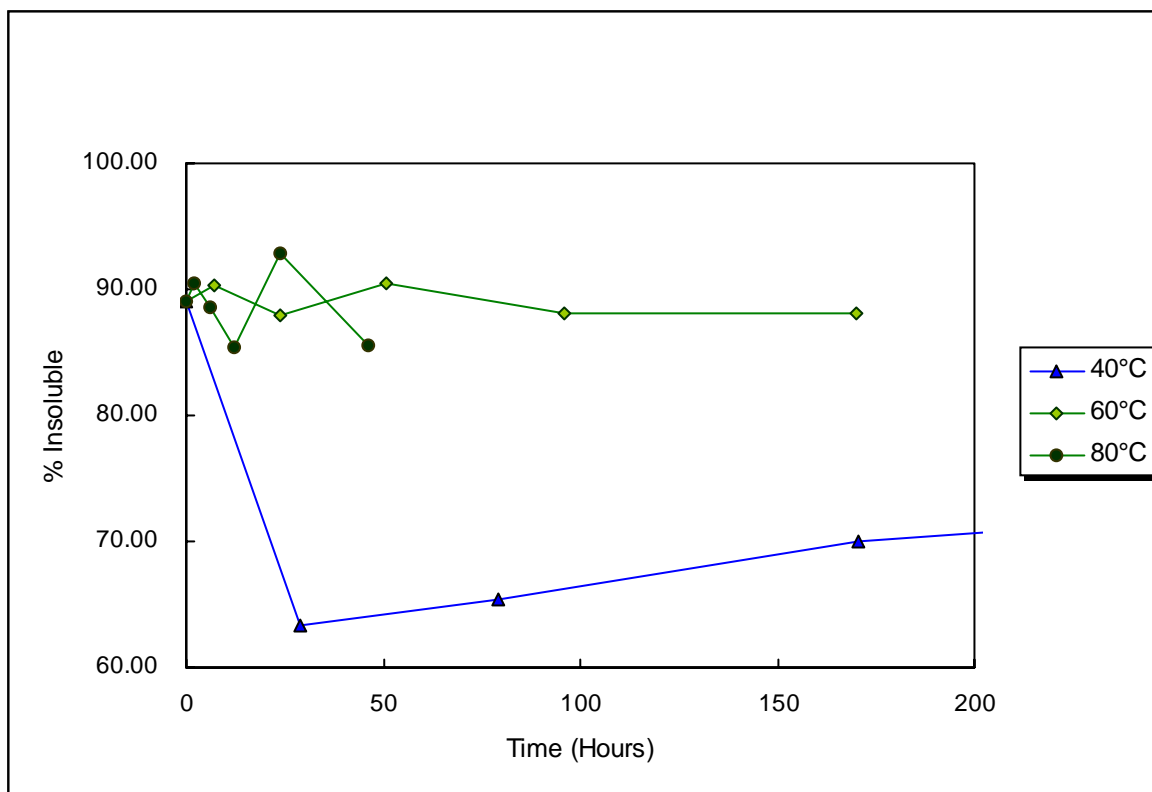
Figure 147 – Variation in THF Insoluble Fraction With Storage Temperature for Sample STO15
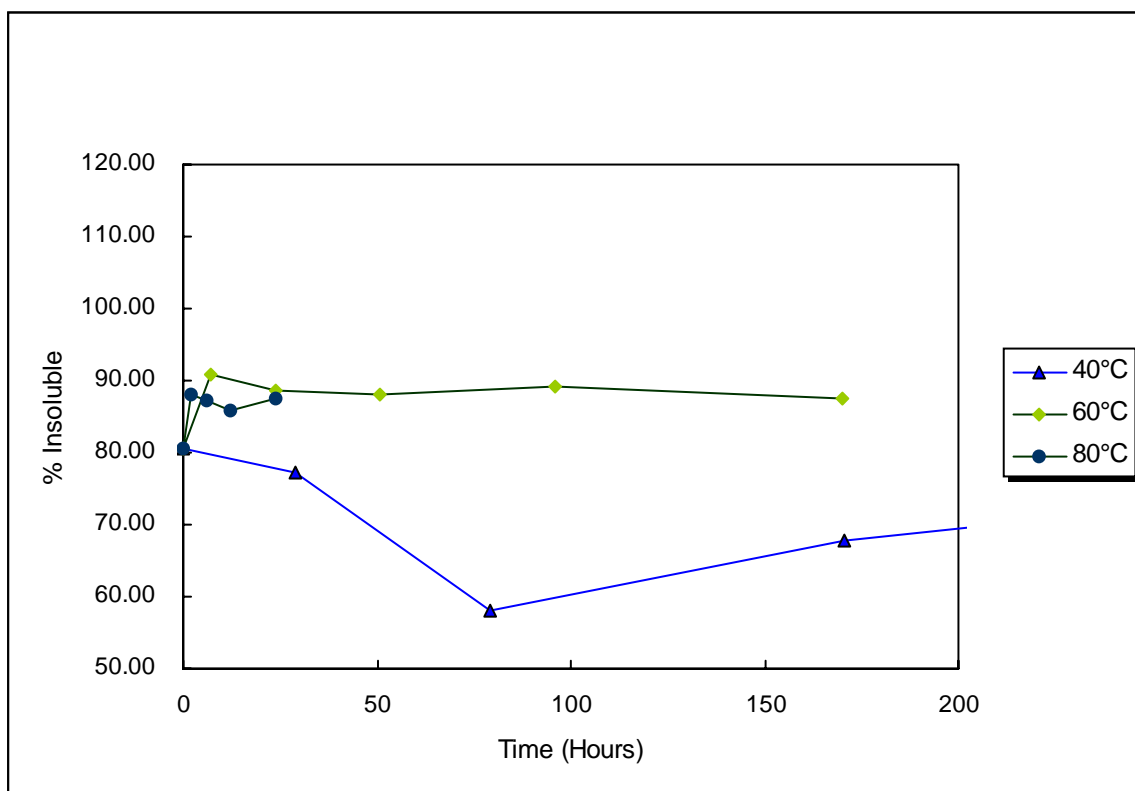
Figure 148 – Variation in THF Insoluble Fraction With Storage Temperature for Sample STO16
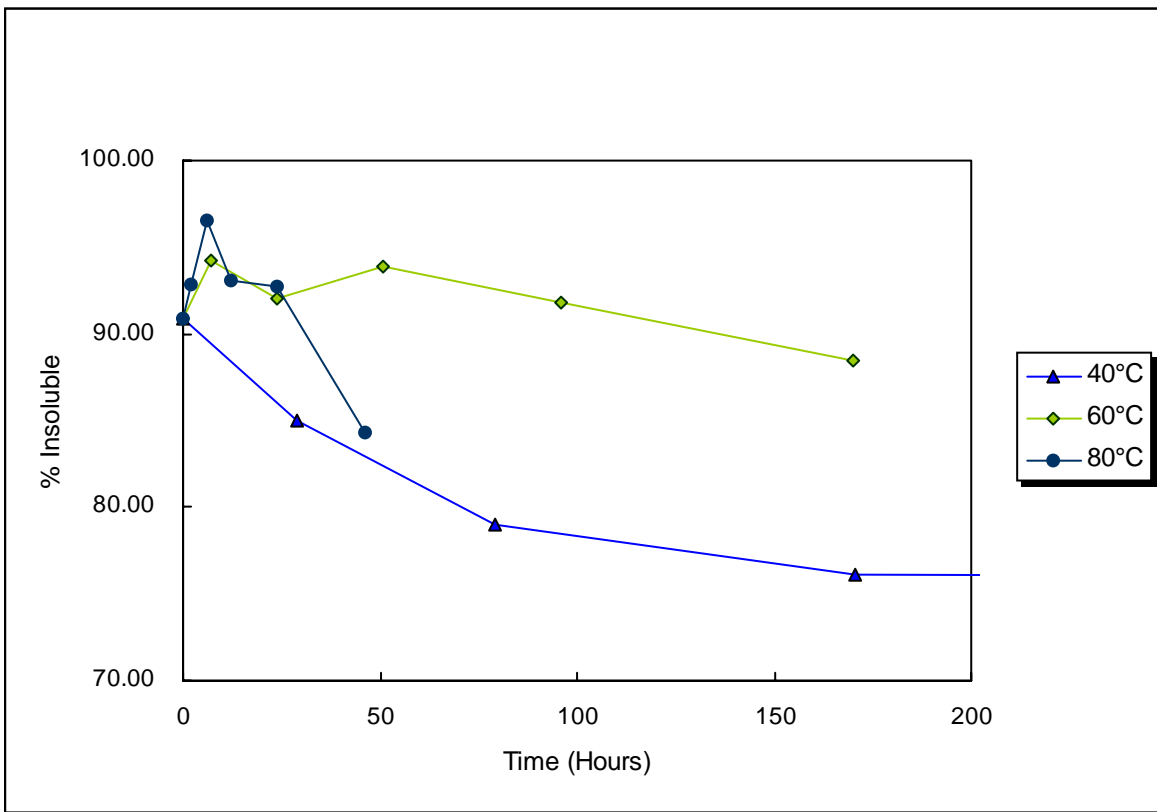
Figure 149 – Variation in THF Insoluble Fraction With Storage Temperature for Sample STO17
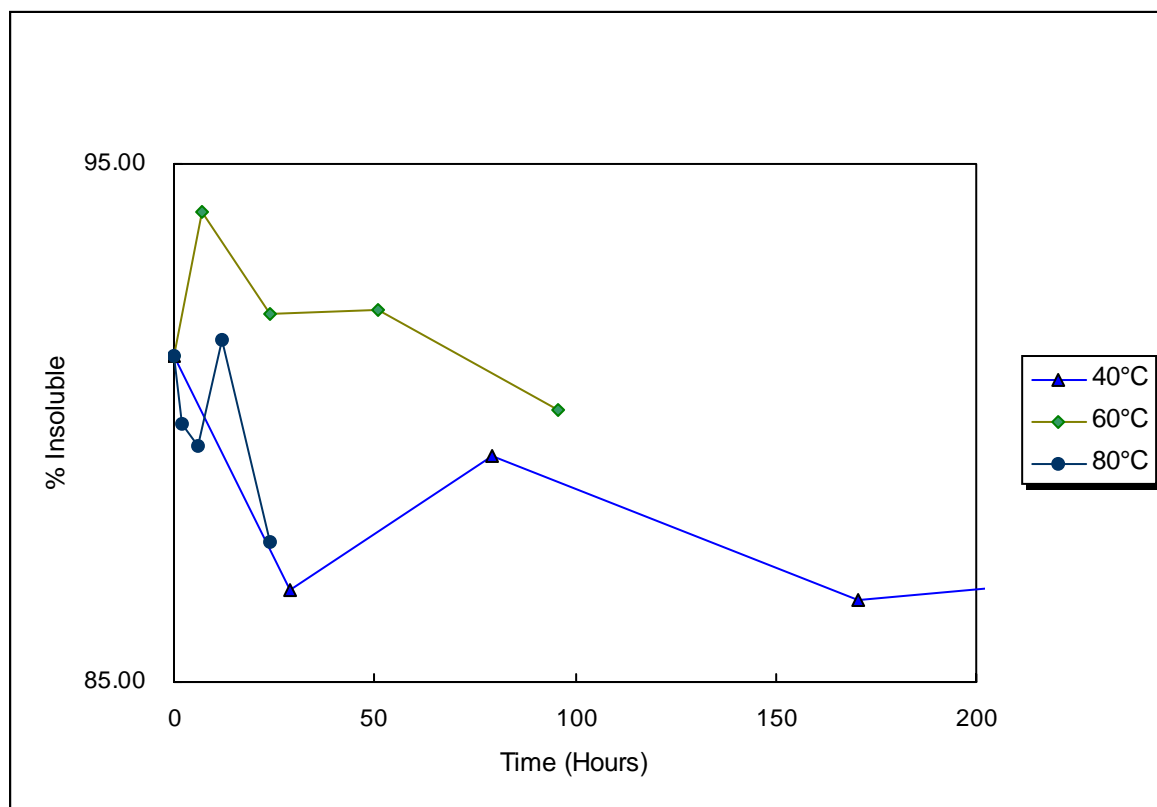
Figure 150 – Variation in THF Insoluble Fraction With Storage Temperature for Sample STO18

From Figures 135-150, the samples that can be seen to show a significant degree of reaction at some point within the ageing period are :-

At 80°C

STO1   (Start of Reaction 24 Hours) - Control Sample – Figure 135

STO5   (Start of Reaction 12 Hours) - 1% pNMA – Figure 137

STO8   (Start of Reaction 12 Hours) - 0.5% pNMA + 0.5% 2NDPA – Figure 140

STO9   (Start of Reaction 30 Hours) - 4% pNMA + 4% 2NDPA – Figure 141

STO10 (Start of Reaction 35 Hours) - 8% pNMA + 8% 2NDPA – Figure 142

STO12 (Start of Reaction 12 Hours) - 2% 2NDPA + 1% pNMA – Figure 143

At 60°C

STO10 (Start of Reaction 24 Hours) - 8% pNMA + 8% 2NDPA (Figure 142)

At 40°C

STO5   (Start of Reaction 12 Hours) - 1% pNMA, gave a marked reaction (Figure 137).

In addition, those samples that showed increased polymer deterioration at 40°C compared to 60°C were

STO1 – Control Sample (Figure 135)

STO5 – 1% pNMA (Figure 137)

STO8 – 0.5% pNMA + 0.5% 2NDPA (Figure 140)

STO12 – 2% 2NDPA + 1% pNMA (Figure 144)

STO13 – 1% 2NDPA + 1% Sodium Sulphite (Figure 145)

STO15 – 1% pNMA + 1% Sodium Sulphite (Figure 147)

STO16 – 1% pNMA + 1% Ammonium Peroxodisulphate (Figure 148)

STO17 – 1% Sodium Sulphite (Figure 149)

STO18 – 1% Ammonium Peroxodisulphate (Figure 150)

With the exception of STO5 and the control sample STO1, all of the samples that exhibit a significant reaction at either 80,60 or 40°C contain 2NDPA. This again suggests that direct reaction between HNF and PolyNIMMO is not the principle contributor to polymer breakdown (ie if direct reaction was occurring, it would be expected to be observed in all test samples to a similar degree, regardless of stabiliser system). Studies in Section 2.5 have shown that the formation of N-NO-2NDPA and its subsequent reaction with HNF is one driving force for propellant degradation. A second driving force has been suggested as the reaction (and reaction products) of HNF with HNOx and NOx species. The removal of NOx species (eg by the addition of pNMA) has been shown to be an important controlling mechanism to retard further propellant degradation. The reaction also suggests that NOx and HNOx species are being liberated during the degradation at a comparatively high rate. Section 1.2.2 detailed possible chain scission reactions in polyNIMMO via loss of NOx species. The work of Bunyan et al [51] also detail that this is a comparatively slow process (ie that polyNIMMO is an explosive with a comparatively high thermal stability, even at high temperature).

3.3.4.3 Conclusions from THF Extraction Studies

The results from these THF solubility trials appears to suggest that polymer breakdown is low within the propellants tested until late within the ageing period. This would suggest that autocatalytic chain scission via the release of NOx from the nitrate ester is not occurring before this induction period has been completed. This implies that the loss of NOx, if centred on the denitration of the nitrate ester moiety, is not leading to appreciable chain scission..

4 Correlation of THF Fraction, Mass Loss and Aqueous Extraction Data

4.1 Discussion of 80°C Data

Before undertaking a review of the stabiliser depletion data, a more detailed correlation of mass loss data, aqueous extraction data and THF extraction data is thought beneficial. The individual analyses of each data set given in Section 3.3 have resulted in a number of reactions identified or proposed as being present within the degradation scheme of polyNIMMO / HNF propellants. Data correlation is hoped to focus more closely on the overall propellant degradation scheme.

One of the dominant reactions is the control of degradation shown by control of free NOx species; this reaction shows that free NOx species are being liberated and also that they promote further reactions within the propellant matrix. There are a number of methods by which this liberation of NOx could be occurring; these are :-

1) Loss of NOx species from polyNIMMO leading to chain scission
2) Loss of NOx species from HNF
3) Loss of NOx species from polyNIMMO not leading to chain scission

No significant chain scission (Option 1) has been detected during this THF extraction data and so this is not thought to be a viable explanation for the low level of scission but apparently high levels of NOx liberated.

The direct loss of NOx species from HNF (Option 2) appears an unlikely reaction course as loss of NOx would be expected to lead to wide spread decomposition of the HNF molecule. However, Bellerby et al [104] have indicated that nitrous acid plays an important role in the decomposition chemistry of HNF (as detailed in Reaction R4) via various intermolecular reactions. As such, both options 2 and 3 above could explain NOx liberation.

By comparison, the majority of formulations that show increased polymer breakdown at 40°C compared to 60°C contain the hydrazine scavengers. This implies that there is an additional reaction occurring between the polymer and these additives.

By cross-reference of aqueous extraction, mass loss and THF extraction data, a more detailed assessment of the contribution of each reaction course and the interrelatedness of the reactions can be made. Table 14 shows the three sets of data at each test temperature.

Sample Ref		80°C				60°C				40°C		
		Δ Mass Loss % *	Δ Aq Extract % *	Δ THF Extract % *		Δ Mass Loss % *	Δ Aq Extract % *	Δ THF Extract % *		Δ Mass Loss % *	Δ Aq Extract % *	Δ THF Extract % *
STO1	Control	44.2	64.7	5.85		6.09	4.19	6.4		5.78	3.39	3.65
STO2	+1% 2NDPA	35.79	30.98	79.17		4.31	2.48	1.84		Not tested		
STO3	+8% 2NDPA	Did Not Survive Storage				Not Tested				Not Tested		
STO4	+16% 2NDPA	Did Not Survive Storage				Not tested				17.6	Not Tested	
STO5	+1% pNMA	44.49	65.1	90.23		3.65	0.2	-0.07		1.67	5.07	78.38
STO6	+8% pNMA	2.81	-1.0	-10.03		0.35	-1.25	-1.5		1.4	0.78	20.89
STO7	+16% pNMA	3.71	-0.08	4.05		0.87	0.45	0.31		1.18	0.40	-0.20
STO8	+ 0.5% pNMA + 0.5% 2NDPA	42.37	65.8	91.57		1.53	1.11	3.82		4.97	2.5	4.5
STO9	+4% pNMA +4% 2NDPA	40.58	60.67	57.99		0.83	-2.98	6.66		4.92	4.16	9.18
STO10	+8% pNMA +8% 2NDPA	30.89	57.47	37.68		0.32	-0.45	10.24		3.36	2.54	4.15
STO11	+2% pNMA +1% 2NDPA	13.40	64.76	86.0		0.35	1.67	-1.17		2.90	0.06	6.5
STO12	+2% 2NDPA +1% pNMA	42.0	65.05	84.95		2.97	1.21	9.7		6.38	-1.53	-3.76
STO13	+1% 2NDPA +1% Na_2SO_3	16.64	15.84	21.91		1.17	1.98	5.48		0.51	5.17	17.97
STO14	+1% 2NDPA +1% $(NH_4)_2S_2O_8$	44.32	62.73	86.0		5.43	61.57	86		1.48	-0.5	0.22
STO15	+1% pNMA + 1% Na_2SO_3	5.72	2.16	4.98		0.78	0.6	2.24		0.75	-1.58	-0.5
STO16	+1% pNMA + 1% $(NH_4)_2S_2O_8$	6.02	2.68	0.67		4.77	2.99	3.28		2.50	-1.68	-4.05
STO17	+1% Na_2SO_3	10.02	9.36	12.14		3.12	0.88	5.79		0.40	-0.02	7.66
STO18	+1% $(NH_4)_2S_2O_8$	38.57	64.2	76.17		6.64	3.78	3.84		4.39	1.3	1.09

* = Data value at final measured data point.

Table 14 - Comparison of Mass Loss, Aqueous Extraction and THF Extraction Data

From previous sections, Δ Mass% has been taken as indicative of formation of gaseous products from HNF, polyNIMMO or both. Aqueous extraction has been taken as indicative of residual HNF in the formulation. THF fraction has been taken as indicative of low chain polyNIMMO residues being formed. However, the data in Table 14 for the control sample (STO1) at 80°C indicates that the aqueous extraction assumption of reaction does not align with the mass loss data. The change in aqueous extraction value (64.7%) between the start and end of the ageing period suggests that all the HNF in the formulation (65%) has been lost. This is in comparison to an associated mass loss of only 44.2% over the same storage period. This implies that at least part of the initial HNF has not been converted into gaseous products; if all HNF had gassified, then the mass loss would be close to the starting value of 65%.

The most likely explanation of this observation is that some degree of water insoluble residue has been formed within the formulation from HNF degradation. Figure 151A-B show details of ageing HNF in isolation at 80°C. Figure 151A shows water soluble residues and mass loss for the sample. It can be seen that, over the storage period of 100 hours, there are no water insoluble residues produced

based on retention of solids on a No:4 sintered glass filter plate) even though a mass loss is observed. Associated with the ageing, Figure 151B shows the change in pH within the sample over the ageing period achieved from a 10% solution of the solid residue in water.

A

B
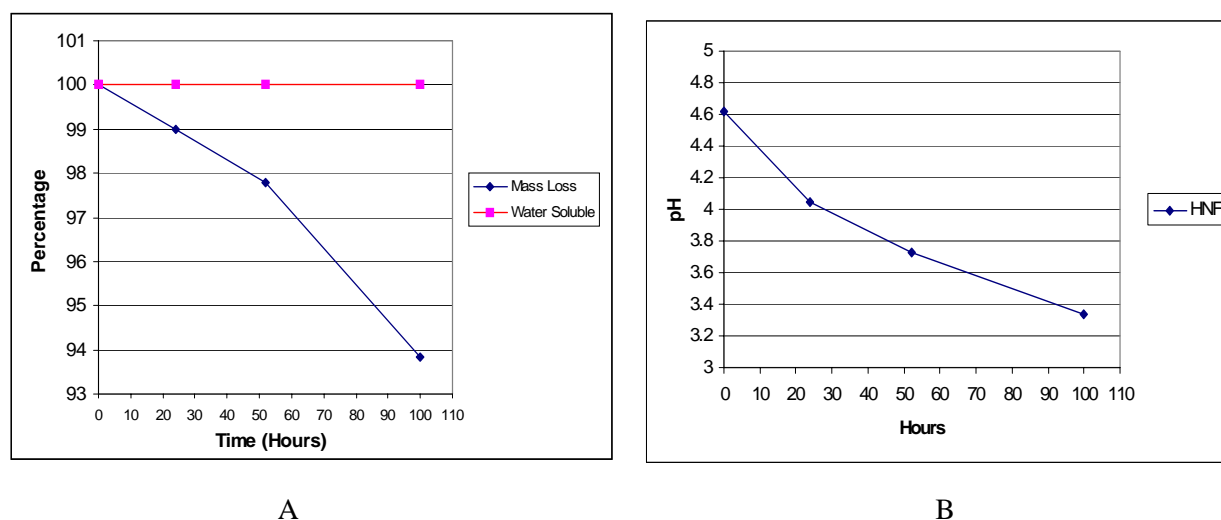
Figure 151A – Mass Loss and Water Insoluble Residues During Ageing of HNF at 80°C

Figure 151B – pH Variation of Residues During Ageing of HNF at 80°C

Although Figure 151A shows that there is a mass loss during storage, the water soluble residues associated with this mass loss are 100%. This indicates that any water insoluble residue being retained during ageing of polyNIMMO / HNF propellant formulations must form from reaction between polyNIMMO and HNF or polyNIMMO and HNF degradation products. It also indicates that the mass loss from thermal degradation of HNF is comparatively small. The higher levels of mass loss from propellant samples must therefore be due to polyNIMMO / HNF interaction. Data for STO1 in Table 14 shows a comparatively low change in THF soluble fraction (5.85%) over the ageing period at 80°C. This suggests that the formation of any insoluble residue between HNF and polyNIMMO does not lead to appreciable polymer breakdown, even with the release of NOx species.

Merrow and Dolah [131] describe the reaction of nitrate esters with hydrazine as detailed in reactions R23 and R24.

$$RONO_2 + N_2H_4 \longrightarrow RO^- + H_2N-^+NH_2-NO_2$$

$$H_2N-NH_2-NO_2 \longrightarrow ROH + H_2N-NHNO_2$$
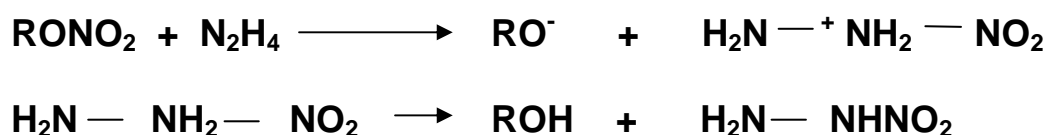
(Reaction R23)

This reaction product is then proposed to react further to lose nitrous acid via

$$H_2N - NHNO_2 + N_2H_4 \longrightarrow H_2NNHNHNH_2 + HNO_2$$
Tetrazene

$$HN = NH + N_2H_5^+ \, NO_2^-$$
Diimine
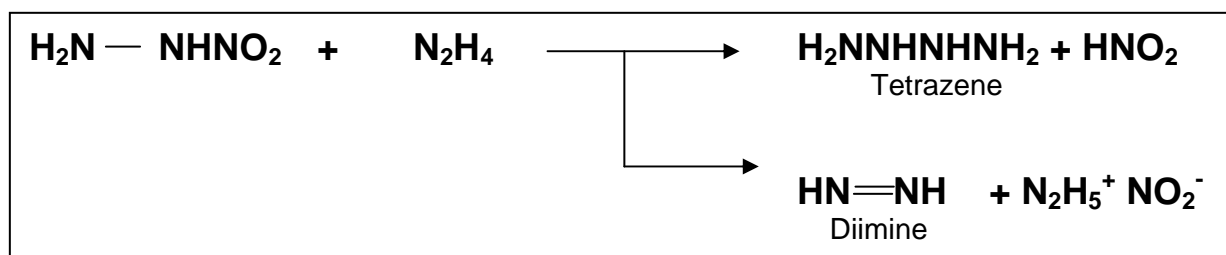
(Reaction R24)

The decreasing value of pH with storage given in Figure 151B may reflect this liberation of nitrous acid. The diimine formed can then react further to form hydrazoic acid and ammonia as detailed in Section 2.4.5.3.1 . A similar reaction course could be hypothesised for the reaction of nitrate ester with HNF as given in Figure 152 . However, the charged state of the hydrazinium ion makes the formation of this product appear unlikely. The hypothetical reaction of HNF with the nitrate ester moiety can be rationalised in terms of bond order by elimination of HNO_2 from the final molecular structure. However, this leaves the overall reaction unbalanced for electrical charge (and would therefore be expected to lead to wider HNF degradation).

$$R-O-NO_2 \; + \quad H_2N-NH_2 \cdots H^+ \quad {}^-C(NO_2)_2 - NO_2$$

$$R-O^- \; + \quad H_2N(NO_2)-NH_2 \cdots H^+ \quad {}^-C(NO_2)_2 - NO_2$$
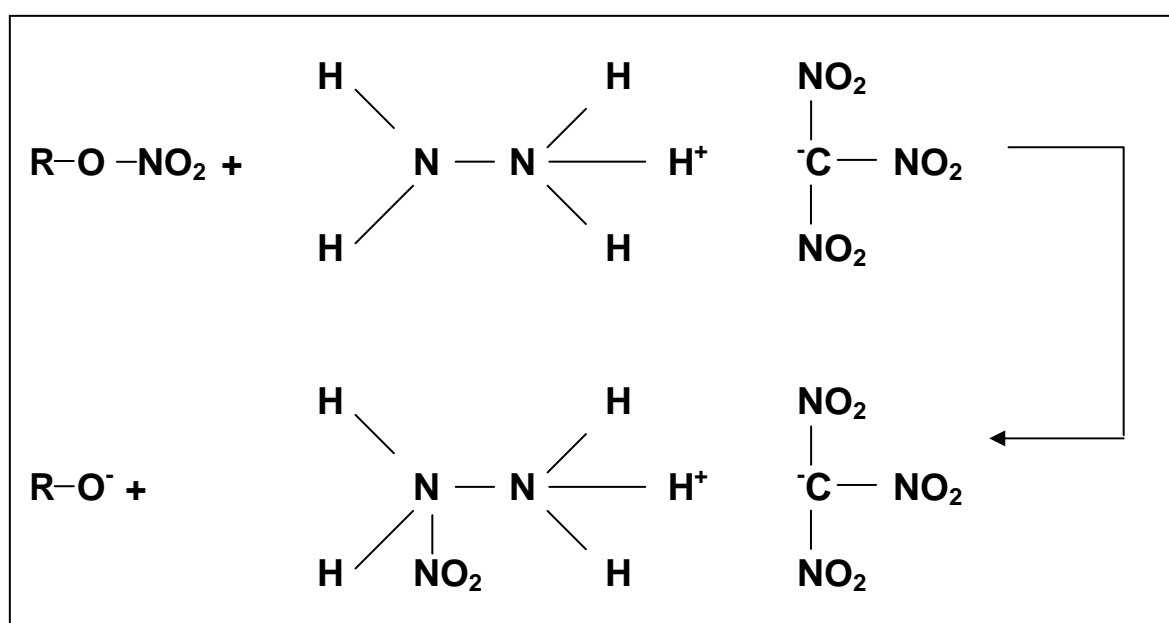
Figure 152 - Hypothetical Reaction of HNF with the Nitrate Ester Moiety at 80°C

However, previous data assessment have indicated that the control of NOx species is important to sample longevity (the data in Table 14 reinforces this). For example compare the data given for formulation STO7 (16% pNMA) against that of the unstabilised control sample STO1). The ability of pNMA to increase sample longevity suggests that NOx and HNOx species are being liberated during the ageing period. Section 1.4.2 4 discussed the effect of functional groups on HNF and proposed that

distortion of the electron cloud of the terminal –NH$_2$ group of the hydrazinium ion may be playing a part in explaining the data observed (as given in Figure 11). Building on the reaction course suggested above in Figure 152 and incorporating the proposal from functional group analysis, it is proposed that the loss of NO$_2$ may be facilitated by formation of a bridging molecule as given in Figure 153.

The NO$_2$ formed is then free to react further with either HNF or denitration stabiliser molecules. This hypothetical reaction provides a route by which the nitrate ester side chain can "trap" aqueous soluble products to form insoluble products whilst still leading to loss of NOx species but reduced overall mass loss.
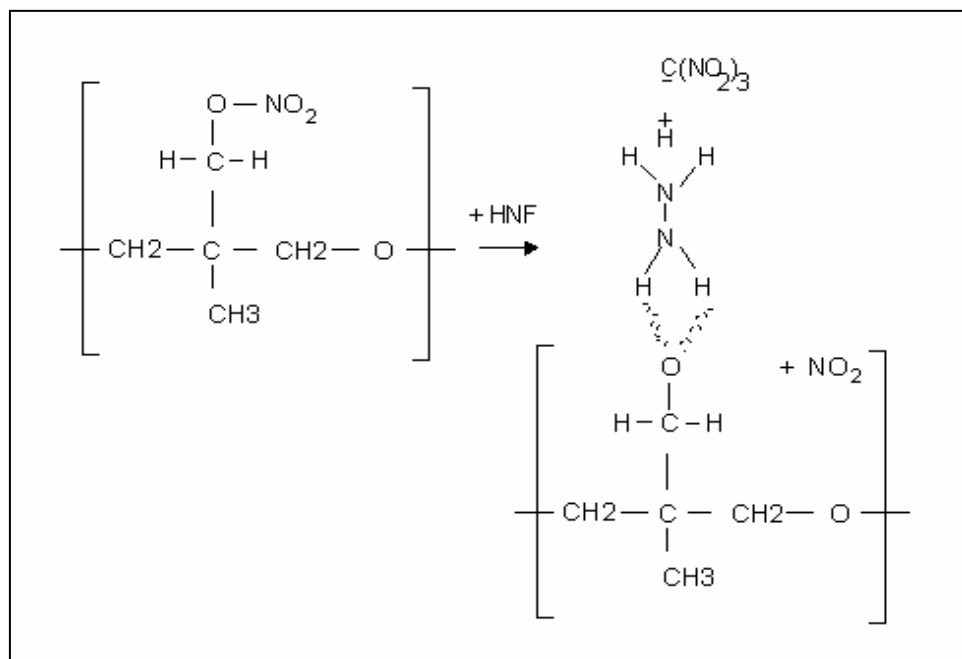
Figure 153 - Hypothetical Interaction of HNF with polyNIMMO to Release NO$_2$

Although this loss of NO$_2$ from the polyNIMMO structure via an HNF bridging molecule initially appears unlikely, it does help to explain the mass, aqueous extraction and THF data observed. The reaction is similar to that proposed by Oyumi et al [132] who suggested a similar reaction between the strong oxidiser Ammonium Perchlorate (AP) and polyNIMMO (as shown in Figure 154). Oyumi proposed that this reaction progressed via hydrogen bonding between the ammonium perchlorate crystal surface and polyNIMMO to facilitate the initial loss of the nitro group followed by the eventual loss of formaldehyde.
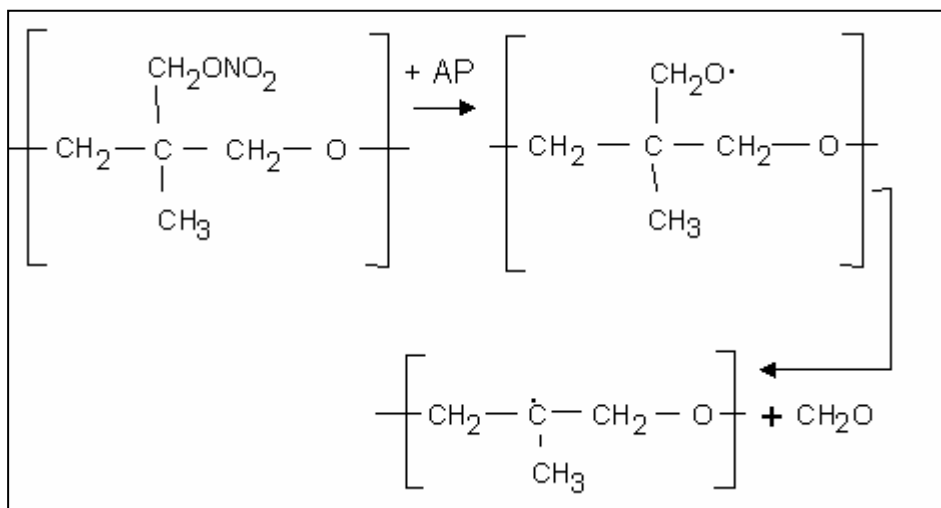
Figure 154 : Reaction of PolyNIMMO with Ammonium Perchlorate [132]

Within the analogous HNF / polyNIMMO reaction it is proposed that the second part of the Oyumi et al proposal does not occur due to the HNF molecule aiding the stability of the complex formed. Section 1.4.2 drew attention to the fact that hydrogen bonding is strong within the HNF molecular structure. In addition, Schmidt [103] details that "one of the pronounced features in hydrazine and derivatives is the presence of hydrogen and lone pair electrons on the same molecule. Hydrogen bonding contributes significantly to the material properties". It does not seem unreasonable to assume that some degree of hydrogen bonding or charge delocalisation will be encountered within the polyNIMMO / HNF propellant system. Cleavage of the $O-NO_2$ bond may allow delocalisation of the charge on the oxygen atom and HNF molecule reaction pair, extending this charge over the larger polymer structure. This delocalisation of charge would be expected to aid stabilisation of HNF in the complex.

Table 14 has shown the differences between the mass loss and aqueous extraction data for the control sample STO1 at 80°C and the formation of an HNF / polyNIMMO complex may provide an explanation for this apparent discrepancy seen between the datasets. Aqueous solubility measurement compared to mass loss data for the control sample STO1 at 80°C indicates a 20.5% difference between the two data sets. It is hypothesised that mass loss preferentially leads to loss of the nitroformate moiety of the HNF bridging structure (Figure 155 Reaction A) whereas aqueous extraction leads to full solvation of both hydrazinium and nitroformate ions (Figure 155 Reaction B). The retention of the hydrazine structure on the polyNIMMO backbone provides an explanation of the apparent reduced mass loss in STO1. Even if a bridging molecular structure is not formed directly, storage of HNF in Section 2.4.4 showed the detection of hydrazine in the decomposition gases. This would potentially allow reaction of free hydrazine with polyNIMMO to liberate NOx via a similar

reaction to that shown in Figure 155, Reaction A. Following this rationale, it is possible to consider reaction of hydrazine or HNF at other position on the polymer backbone (eg at the polyurethane linkages) by analogous reactions .
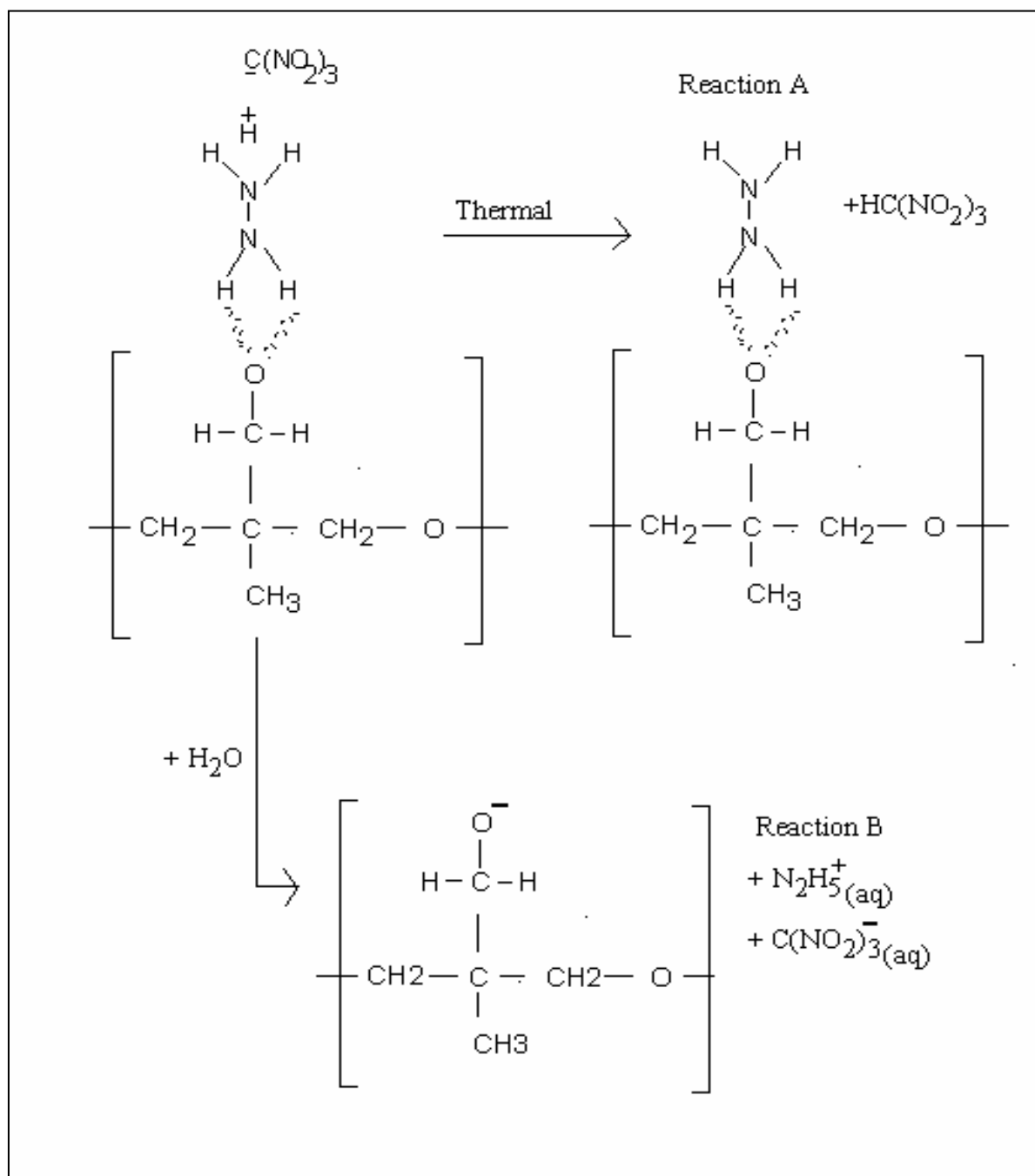
Figure 155 - Hypothetical Reaction of HNF with polyNIMMO and Effect of Elevated Temperature Storage or Aqueous Extraction on Intermediate Formed.

The structure proposed for the reaction product of HNF and polyNIMMO leads to retention of hydrazine (RMM 32). Out of a total RMM for HNF of 183, this equates to a 17% retention in mass

which is very close to the 20.5% (64.7% - 44.2%) difference observed between the mass loss and aqueous extraction test data for STO1. The significantly reduced levels of mass loss and aqueous extraction observed at lower storage temperatures (ie 60 and 40°C) for the control samples suggests that this bridging mechanism is reduced at these lower temperatures.

Continuing with the review of 80°C data in Table 14, comparison of the data for sample STO11 (2% pNMA + 1% 2NDPA) and STO12 (2% 2NDPA + 1% pNMA) indicates that Δ THF fraction and Δ Aqueous fractions observed are very similar for each of the two samples. This suggests a similar reaction course has occurred in both test samples leading to widespread polymer breakdown and loss of HNF. However, the mass loss data from STO11 is significantly lower than that of STO12 suggesting that within this test sample, the loss of Aqueous fraction during ageing has not been via gassification but via formation of water insoluble products. Results from formulation STO2 (1% 2NDPA) and comparison against the data from the control sample (STO1) indicates that the consequence of addition of 2NDPA to the HNF / polyNIMMO formulation is a marked increase in Δ THF fraction (ie polymer breakdown), a reduction in Δ aqueous extraction and a slight reduction in mass loss. This implies that the changes in mass loss data for STO11 and STO12 are likely due to the consequences of reaction of N-NO-2NDPA with HNF but with reaction being retarded by the higher pNMA content of STO11 (due to sequential reaction). This retardation is observed again by comparison of the various data for formulations STO8 (0.5% pNMA + 0.5% 2NDPA) , STO9 (4% pNMA + 4% 2NDPA) and STO10 (8% pNMA + 8% 2NDPA). Results from these samples indicate that increasing the overall stabiliser level leads to reduction in all Δmass loss / Δaqueous extraction and Δ THF extraction values. This variation in level of propellant degradation for each sample can be viewed as being different position in the same reaction (ie if the storage period at 80°C had been extended, all formulations would have eventually progressed to the same degree of reaction along the same reaction path). The data also reflects a modification to the reaction course encountered in the control sample (as suggested in Figure 153). The difference in Δ THF fraction between STO1 and STO8 at 80°C indicates that the presence of low level pNMA and 2NDPA leads to an increase in polymer breakdown compared to the control. If reaction progression is assumed to terminate once all HNF is lost from the formulation, then the loss of all aqueous fraction (65.8% Δ Aq fraction) in sample STO8 indicates that the reaction has progressed to completion. Using HNF loss as an indicator of reaction progression (with HNF loss reflected in the Δ Aqueous extraction data), the Δ Aqueous extraction data for formulations STO11 and STO12 both suggest that reaction has also reached completion in these samples; this is also the case for sample STO5 (1% pNMA). [For samples STO9 and STO10, reaction at 80°C has not progressed to completion as evidenced by the reduced Δ aqueous extraction data]. The lowest level of reaction at 80°C is seen in formulation STO6 where it exhibits an improved performance compared to the control STO1. Within formulation STO6, an increase in Δ

THF is observed (ie a negative figure is shown) suggesting some degree of residual cure is occurring in the sample. This residual cure may have been present in all test samples but was not observed significantly due to rapid direct reaction of uncured material with HNF or may have been specific to STO6 possibly occurring via inhibition of cure due to the high stabiliser content included. The results are inconclusive as to the source of this residual curing material.

Sequential reaction of pNMA followed by 2NDPA progressing via nitrosated derivatives with eventual conversion to nitro derivatives has been well documented [76-90]. The low level of reaction in formulation STO6 at 80°C indicates that control of NOx species (by pNMA reaction) minimises loss of HNF from the propellant formulation and also protects the polymer present. This implies that in HNF / polyNIMMO formulations, NOx (and its subsequent control) plays an important role in continued reaction within the formulation. However, it also indicates that the direct reaction of HNF and polyNIMMO to release NOx species (Figure 153) cannot be the initiating reaction for propellant degradation. The level of polyNIMMO and HNF in all the test formulations is equivalent in all samples; any direct HNF / polyNIMMO driven decomposition would progress to the same degree of conversion in all samples over the same storage period. The control / minimisation of propellant decomposition by the addition of excess pNMA shows that a secondary reaction process is occurring. A revised hypothesis for explanation of the test data at 80°C is that the reaction in Figure 153 is part of the initiating process for propellant degradation but that this reaction occurs in all samples at 80°C at a comparatively low level to encourage loss of NOx species. The consequences and level of this denitration reaction is then further modified (ie accelerated, retarded or inhibited) by other propellant ingredients. As such, other reactions must be present which eventually lead to propellant degradation. From Table 14, in sample STO6, a mass loss of 2.81% is observed with apparently little or no propellant degradation (in terms of Δ THF or Δ Aqueous extract). This mass loss is proposed to be from pure thermal decomposition of HNF. Figure 68 details the loss of various gaseous products from HNF / polyNIMMO during elevated temperature storage , principally N_2O Nitrogen and water. Section 2.4.2 also details gaseous products detected by GASTEC analysis – principally hydrazine, ammonia and an acid species. The 2.81% mass loss observed in sample STO6 at 80°C is proposed to be due to representative of nitrogen and N_2O loss from the sample, formed either from hydrazoic acid formation or direct reaction of liberated hydrazine with a strong oxidiser (as shown in Reactions R15 or R19). Section 2.4.3 also indicated that these various species for HNF degradation did not exhibit autocatalytic behaviour with HNF. Therefore, accentuated reaction in the propellant formulations must be due to interaction between either HNF or HNF degradation products with other propellant ingredients or propellant degradation species. As pNMA has been shown to reduce reaction and the predicted action of pNMA is to remove NOx and HNOx species, one of the interactions that carry forward propellant degradation must involve the interaction of NOx or HNOx species with HNF.

Sammour et al [76] details the reactions that control NOx species liberated from nitrate ester degradation (and subsequent reaction of these species with denitration stabilisers). These reactions are summarised in Reaction 25.

$$—O—NO_2 \longrightarrow {}^-OH + NO_2 \xrightarrow{H_2O} HNO_2 \rightleftharpoons N_2O_3 + H_2O$$

H From Water

$${}^-OH + NO_2 \updownarrow N_2O_4 \xrightarrow{H_2O} NO+ + NO_3^-$$

$$N_2O_3 + H_2O \updownarrow^{H_2O} NO^+ + NO_2^-$$
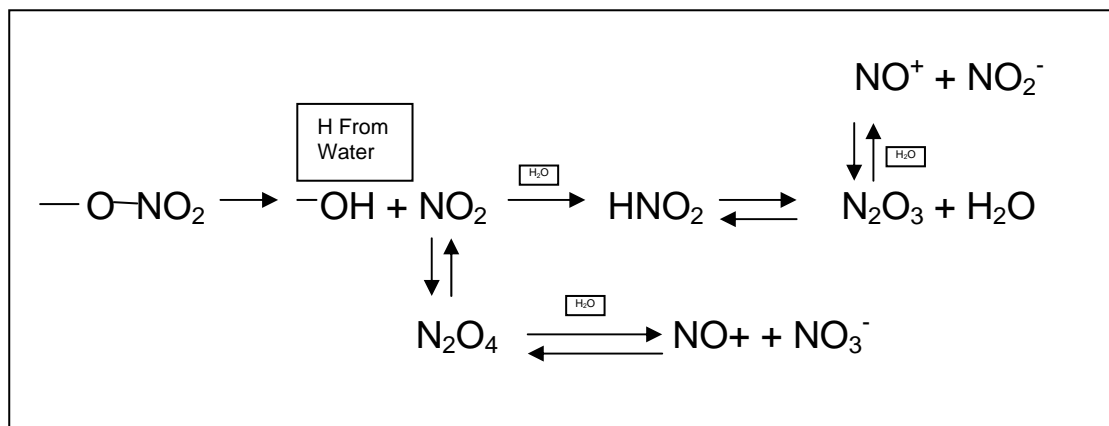
(Reaction R25)

It can be seen that water plays an important role in all of these reactions. HNF solvation effects have also been shown to affect propellant stability in other studies [110]. It is possible to envisage that the water liberated from the thermal degradation of HNF directly destabilises the nitrate ester moiety of polyNIMMO to destabilise the overall system. This destabilising effect of water has been observed in double base propellant formulations where nitrocellulose and nitroglycerine (both containing the nitrate ester group) are present. However, in the case of polyNIMMO, the uncured polymer has a slight desiccating effect if left exposed to air (exhibiting mild opacity when "wet"). When trialled in this "wet" state, no marked destabilising effect has been observed due to the water present compared to dry samples [110]. This implies that direct water / polyNIMMO reaction is unlikely to be a destabilising reaction in isolation within the propellant formulations at 80°C.

Koroban [108] does however detail the reaction of the hydrazinium ion with nitrous acid (Figure 9, reaction (d)) and this reaction forms the basis for the revised reaction mechanism for ANF formation given by Bellerby et al [104]. Taking this slightly further, Doherty et al [134] have shown that in aqueous based, hydrazine / nitrous acid reactions where the ratio of hydrazine to acid is low, the mechanism follows the reaction course shown in Reaction 26.

$$HNO_2 \ + \ N_2H_5^+ \ \longrightarrow \ NH_2NHNO \ + \ H_2O \ + \ H^+$$

$$NH_2NHNOH$$

$$\boxed{+ \ NO^+} \longrightarrow H^+ + HN_3 + HNO_2$$

(Reaction R26)

This reaction leads to the regeneration of nitrous acid. This would have obvious implications on propellant longevity if this series of reactions were occurring in polyNIMMO / HNF propellant formulations.

In addition to the reactions of hydrazinium ion with nitrous acid, the formation of water from HNF during ageing also has obvious implications on ionic dissociation in any HNF present. Any low level concentration of water in the formulation will aid and encourage ion dissociation potentially affecting the overall active pH of the formulation. Figure 151B details the pH changes observed during accelerated rate ageing of HNF with residues showing increasing acidity with crystal ageing. Any change in pH would be expected to further destabilise HNF present.

Starting from the reaction hypothesis for reaction at 80°C detailed in Figure 153 and the proposals for reaction course developed in Figure 96 and Figure 122-124, a modified hypothesis can be developed. This modified hypothesis is given in Figure 156. The various reactions present within the scheme given in Figure 156 helps explain the effect of the various stabilisers on the propellant degradation. It has previously been highlighted that if direct HNF / polyNIMMO reaction was occurring, the level of denitration observed in all samples would be determined solely by the ratio of concentrations of HNF : polyNIMMO. As these levels are the same in all propellant formulations, the higher levels of reaction observed in some samples compared to others indicates that this is not the primary driving reaction for propellant degradation. Within the revised hypothesis in Figure 156, reaction is driven (and initiated) by the thermal decomposition of HNF and (specifically) by the liberation of water or hydrazine. However, once initiation has occurred, it is proposed that the continued degradation is via the reaction of NO+ with HNF to form a "nitrosated" intermediate structure and the eventual regeneration of nitrous acid. This regeneration of acid is proposed to lead to autocatalytic breakdown of the formulation. The hypothesis given in Figure 156 for propellant breakdown at 80°C suggests that the liberation of products from the thermal degradation of HNF is critical to the reaction course (especially hydrazine, water and nitrous acid). Sodium sulphite within these formulations is

introduced as an anhydrous salt and so would be expected to have an effect on overall water content in the propellant during ageing as well as having a degree of oxidising power. In comparison, ammonium peroxodisulphate (although potentially reacting with water), has its primary character of being the stronger oxidising agent. Both are present to remove hydrazine. Because of these differing functions, comparison of the effectiveness of the hydrazine scavengers in isolation within the HNF / polyNIMMO formulations should aid extension of the hypothesis. The 80°C data in Table 14 for formulations STO17 (1% Na_2SO_3) and STO18 (1% $(NH_4)_2S_2O_8$) indicate that in isolation the two scavengers achieve significantly different effects. The data indicates that in formulation STO18, the reaction has reached completion (based on the loss of HNF indicated by the Δ Aqueous extract data) whereas STO17 shows a lower level of overall reaction. This starts to aid interpretation of the mechanism by which these scavengers function within the formulation. Although the relative desiccating efficiency and reactivity against hydrazine of the scavengers is unclear, it can be observed that when the scavengers are combined with denitration stabilisers in formulations STO13-16 there is a similar marked effect. In STO15 and STO16 containing pNMA, the overall level of degradation in the formulations is lower than in the control sample STO1. The main difference in the datasets is the larger degree of polymer breakdown in sample STO15 (4.98%) compared to STO16 (0.67%). This implies that the incorporation of Ammonium Peroxodisulphate is more effective than Sodium Sulphite in controlling polymer degradation. However, when in the presence of 2NDPA (formulations STO13 and STO14) and also in the absence of any denitration stabilisers (STO17 and STO18), the situation is reversed with the sulphite being superior. This confirms that the action of the scavengers must be wider than acting as a simple trap for free water molecules

HNF $\longrightarrow$ N$_2$H$_4$ + H$_2$O + N$_2$ + N$_2$O + ANF + HNO$_2$

+ HNF

Support for Ionic
Dissociation /
Solvation

+ PN

+ PN

+ H$_2$O

HC(NO$_2$)$_3$ + H—N—H + NO$_2$ $\longrightarrow$ HNO$_2$ $\rightleftarrows$ N$_2$O$_3$ + H$_2$O

N$_2$O$_4$
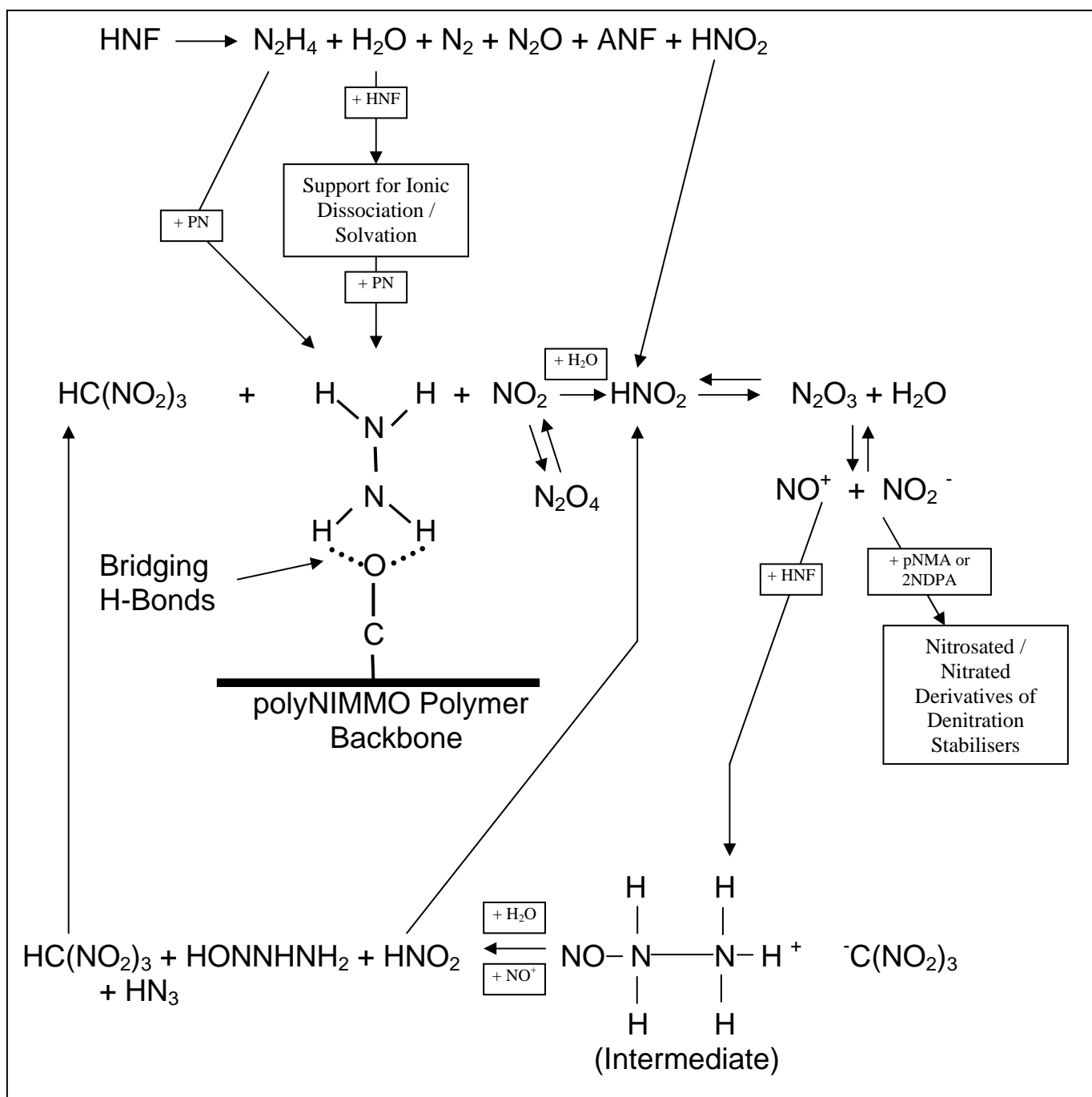
NO$^+$ + NO$_2$$^-$

Bridging
H-Bonds

H ···· O ···· H

C

polyNIMMO Polymer
Backbone

+ HNF

+ pNMA or
2NDPA

Nitrosated /
Nitrated
Derivatives of
Denitration
Stabilisers

H   H

+ H$_2$O

HC(NO$_2$)$_3$ + HONNHNH$_2$ + HNO$_2$ $\longleftarrow$ NO—N——N—H $^+$ $^-$C(NO$_2$)$_3$
+ HN$_3$

+ NO$^+$

H   H

(Intermediate)

Figure 156 - Hypothetical Reaction Course for HNF / polyNIMMO Propellant Degradation at 80°C

It is proposed that the hydrazine scavenger molecules have a multiple role in the propellant formulations. Firstly as desiccant removing water liberated from the thermal decomposition of HNF; secondly as oxidiser to oxidise Nitroso derivatives of denitration stabilisers to nitro analogues; and thirdly to remove free hydrazine from the matrix. Figure 157 shows the extended hypothesis.

HNF $\xrightarrow{\text{A}}$ $N_2H_4 + H_2O + N_2 + N_2O + ANF + HNO_2$

I2 $+ (NH_4)_2S_2O_8$ → ANF

I1

+ PN

B

+ Na_2SO_3 or $(NH_4)_2S_2O_8$

C

B1 Release of Water

Trapping / Removal of Water

+ HNF

B2

PolyNIMMO Polymer Backbone Breakdown

A1

Hydration Limit of Scavengers Achieved

B4

I3

+ HNF

+ Na$_2$SO$_3$ or $(NH_4)_2S_2O_8$

C1

Reaction Limit of Scavengers Achieved

I

Support for Ionic Dissociation / Solvation

B3

Hydrazone Formation + Nitroform + Water

+ PN

D

+ PN

+ H_2O E1 E2

$HC(NO_2)_3$ + H—N—H + NO_2 → HNO_2 ⇌ $N_2O_3 + H_2O$

F E3

N$_2$O$_4$

NO$^+$ + NO$_2$$^-$

J

H—N—H

G O

Bridging H-Bonds

C

polyNIMMO Polymer Backbone

+ HNF   + pNMA   + 2NDPA

E5   E6

E4

N-NO-pNMA   N-NO-2NDPA

E7 + HNF   E8 + HNF

E9   E10

E11 + Na$_2$SO$_3$ or $(NH_4)_2S_2O_8$ E12

Di-nitro-methyl aniline

C-Nitro Derivatives of 2NDPA

I

H1

H

$HC(NO_2)_3$ + HONNHNH$_2$ + HNO$_2$ + HN$_3$

+ H_2O

+ NO$^+$

NO—N—N—H $^+$ $^-$C(NO$_2$)$_3$

H   H

H   H

(Intermediate)

X = Reference Point for Discussion in Text

Figure 157 – Extension of Reaction Course for HNF / polyNIMMO Propellant Degradation at 80°C

From this hypothesis, the relative position of the desiccating nature of the scavengers, their reactivity against hydrazine and their oxidising power determines the propagation of reaction; this is via the balance of the relative strengths of reactions B1/B2/B3 (control of water), C1 and D (reaction of hydrazine with scavengers or polyNIMMO) and E9/E10 (oxidation) in Figure 157 for the scavengers. From the data in Table 14, the data for formulation STO18 compared against STO17 suggests that sodium sulphite has a greater effectiveness in trapping water or reaction with hydrazine via reactions B1/B2 or C1 than ammonium peroxodisulphate, thus limiting reaction at points B1/B2 and C1. The effect on position B1/B2 for sodium sulphite would not be surprising as the additive is an anhydrous salt. However, GC-MS analysis of HNF in the presence of the scavengers (Section 2.4.5) indicated in Figure 74 that the evolution of water is rapid in the later stages of storage of test samples of HNF / hydrazine scavengers at 70°C. This evolution appears to coincide with the depletion of closely IPA within the sample. Within the samples containing the hydrazine scavengers, it does not appear that any water liberated is particularly closely bound to the scavenger salts. This implies that, although control of water liberation (reaction B) might be important within the overall propellant reaction course (eg in facilitating reactions after position E1), the principle reaction of the scavengers is via reactions C1 (direct reaction against hydrazine) and E9/E10 (oxidation). This suggests that all reactions containing sodium sulphite will be controlled more strongly at points C1 than ammonium peroxodisulphate based formulations. Comparison of formulations containing either of the scavengers in combination with 2NDPA (ie formulations STO13 / STO14) indicates that the ammonium peroxodisulphate analogue (STO14) has a Δ Aq Extraction of 62.73%. This suggests loss of nearly all HNF from the formulation during the ageing period. By contrast, STO13 (containing sodium sulphite) has lost only 15.8%. The analogous pNMA formulations STO15 and STO16 suggests that the degree of reaction is similar for both samples (based on HNF content) although polymer breakdown is accentuated in the Sodium Sulphite analogue (4.98% Δ THF fraction in STO15, 0.67% Δ THF fraction in STO16). This implies that the large-scale differences in the 2NDPA analogue data arises from the 2NDPA present. The hypothesis in Figure 157 reaction E10 suggests oxidation of N-NO derivatives of denitration stabilisers to nitrated derivatives. However, if this oxidation was occurring, the higher oxidising power of the peroxodisulphate would be expected to show greater effectiveness in removal of N-NO species compared to sodium sulphite. This in turn would reduce reactions E7 and E8 of N-NO species with HNF and thus protect the overall propellant longevity. Rapid reaction of HNF / N-NO-2NDPA (ie E8) has been demonstrated (Section 2.4.4) and has been shown to be detrimental to HNF longevity. However, the results from formulation STO14 indicate that the peroxodisulphate is ineffective in reducing propellant breakdown. This is in contrast to the sodium sulphite analogue (formulation STO13) which shows some improvement in sample longevity compared to the control sample STO1. This would require an inversion of the actual oxidising power of the additives if oxidation strength was the driving force for reaction. The

conclusion from this analysis is that reaction E9 of N-NO-2NDPA with ammonium peroxodisulphate is not occurring and rapid progression of reaction of N-NO/2NDPA with HNF is dominant. This in turn implies that the oxidising power of the scavengers does not contribute to the reaction course in 2NDPA formulations (ie reactions E10 and E12 do not occur but E8 is dominant). The superiority of sodium sulphite in these formulations is proposed to arise solely from its contribution in controlling reaction branch C1 (and possibly a minor effect from control of B1/B2). The similarity of results for pNMA scavenger formulations (STO15 / STO16) is proposed to reflect the lower level of reactivity proven for N-NO-pNMA with HNF compared to that of HNF / N-NO-2NDPA (see Section 2.4.4) and also competition for NOx species between reactions E4, E5 and E6. During propellant degradation, it is proposed that reaction progresses to position E3 and NO^+ and NO_2^- is available for direct reaction with either pNMA, 2NDPA or HNF (dependent on the stabiliser system present). pNMA has been shown to be more active than 2NDPA as stabiliser in double base propellants [82]-[89] and reacts preferentially with HNOx and NOx species when encountered in combination with 2NDPA. For the polyNIMMO / HNF formulations, it is proposed that if pNMA is present (either in isolation or in combination with 2NDPA) it preferentially reacts with NO^+ to form N-NO-pNMA (reaction E5). This reaction dominates until the activity of the pNMA falls to an undetermined level. Once this level is achieved, if 2NDPA is present, it then starts to react with the liberated NO+ to form N-NO-2NDPA. (reaction E6). For either of these N-Nitroso derivatives, direct reaction with HNF (reactions E7 or E8) and subsequent formation of a hydrazone (reaction J) is the most detrimental to propellant longevity. Section 2.4.4.2 showed a significantly different rate of reaction between either of the two nitroso compounds with HNF, the reaction rate of reaction E8 >> rate of reaction of E7. Because of this significantly different rate of reaction, the benefits of reactions E11 and E12 to remove the nitroso species and increase propellant longevity would be significantly different. On formation of N-NO-2NDPA, as reaction E10 is proposed to not occur, reaction E8 with HNF will occur almost instantaneously; this is not the case with the analogous pNMA reaction E7. This allows the degradation reaction to be retarded (or stopped) on the formation of N-Nitroso-pNMA. Further reaction will then depend on competition between reactions E (NOx + HNF) and E5 (NOx + pNMA) and not on reaction E7 (N-NO-pNMA + HNF). Overall, this implies that the difference in oxidising power for the two scavengers is not as beneficial to propellant longevity as their desiccating powers and relative reactivities against hydrazine.

The formation of ANF via ion transfer with ammonium peroxodisulphate (reaction I2) is a possibility and this reaction might explain the difference in mass loss at 80°C between the control sample and STO18 (44.2% and 38.5% respectively). The explanation of why, in isolation, ammonium peroxodisulphate does not retard polymer degradation (reaction E4) via ANF production at position I2 is that reaction E4 is possibly dependent on liberation of water in reaction A but more likely reflects the activity of ammonium peroxodisulphate at reaction C1 becoming rapidly depleted. This limits the

effectiveness of the reactant on minimising polymer breakdown via reaction I1. The depletion of the activity of denitration stabilisers at positions E5 and E6 is obviously important to the overall competition between reactions E4/E5 and E6 and so should be included on the hypothesis. The assessment of the action of the hydrazine scavengers also suggests that the direct liberation of nitrous acid and release into the propellant matrix (Reaction A1) is not occurring as a dominant reaction at this temperature. If reaction A1 was occurring, the autocatalytic sequence initiated by reactions following on from E1 would not be significantly modified by either scavenger material if oxidising power is not a contributing factor. Comparison of propellant degradation at 80°C in Table 14 indicates that there are significant differences between the data for the control STO1 and formulations STO17 and STO18. This implies that, although reaction A1 may be occurring, it is not the driving force for propellant breakdown. Review of the 80°C data for mixed pNMA / 2NDPA formulations (STO8 to STO10) indicate that the simple interpretation of sequential nitrosation of pNMA followed by 2NDPA nitrosation does not fully explain the dataset. If in any sample, sequential reaction was occurring. and pNMA activity against NOx had not become fully depleted then, for example, STO10 (8% pNMA / 8% 2NDPA) would show very similar test results to STO6 (8% pNMA). From the 80°C data in Table 14 this is clearly not the case. By any measure, reaction has progressed significantly further in mixed samples compared to the single pNMA stabilised system. It is proposed that this may reflect the conclusions of Bellerby et al [76] who proposed a slow reversible transnitrosation reaction between N-NO-pNMA and 2NDPA. The reaction suggested was :-

$$\boxed{\text{N-NO-pNMA} + \text{2NDPA} \rightleftharpoons \text{pNMA} + \text{N-NO-2NDPA}}$$
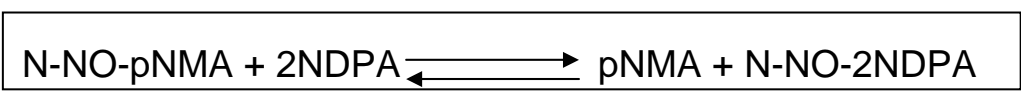
(Reaction R27)

Even if produced at low levels via this reaction, the very high reactivity between HNF and N-NO-2NDPA would be expected to lead to rapid removal of this product (via reaction E8). Via Le Chatalier's principle, this would lead to increased production of N-NO-2NDPA if the system was in equilibrium. This transnitrosation reaction is proposed to be the source of the increased degree of reaction in mixed denitration stabiliser systems compared to single pNMA equivalents. The higher the overall pNMA content, the less pronounced the transnitrosation reaction. This again agrees with Bellerby et al [76] who suggest that transnitrosation occurs more markedly in equilibrium. Higher pNMA content in a formulation leads to preferential NOx reaction with pNMA via reaction E5. Only once a high degree of conversion of pNMA to N-NO-pNMA has occurred would an equilibrium be expected to occur. Thus higher pNMA contents discourage transnitrosation in preference to nitrosation / nitration of pNMA. Including these extra considerations for reaction course, gives the hypothesis for polyNIMMO / HNF propellant decomposition as given in Figure 158.

Figure 158 – Revised Hypothetical Reaction for HNF / polyNIMMO Propellant Degradation at 80°C

The revised hypothesis given in Figure 158 explains the majority of propellant, 80°C storage data. However, for samples STO6 (8% pNMA) and STO7 (16% pNMA), although mass loss and aqueous extraction are similar for the two samples, there is increased Δ THF extraction in the sample with the higher stabiliser content; this was unexpected and not explained by the hypothesis. The data suggests that reaction I1 of the reaction scheme given in Figure 158 has progressed further in the sample with the higher pNMA content. This branch of the hypothesis requires production of reaction products via reactions D and/or E1. However, within each propellant formulation, the levels of these reactions would be expected to be equivalent until the stabiliser activity for reaction against HNOx and NOx is depleted. The increased reaction suggests the possibility of a low level (but significant) reaction between pNMA and HNF. Figures 159A to 159D show DSC analyses of a 1:1 mixture of

pNMA :HNF at both 10k min^{-1} and 1K min^{-1}.Figures 159A and 159B indicate that the onset temperature for HNF decomposition in isolation and in the presence of pNMA are very similar (132.7°C and 133.9°C respectively).   Large scale chemical incompatibility between the two compounds would result in a marked reduction in peak decomposition temperature. This is not observed and so there is no large scale incompatibility present between the components. The thermal profiles do show that the presence of pNMA markedly affects the decomposition mechanism of the HNF present, forming a second large exothermic peak starting reaction at 152°C. This is presumably via oxidation of the pNMA present or via reaction of HNF degradation products with pNMA and a similar trend is observed in Figure 159D at a lower heating rate.
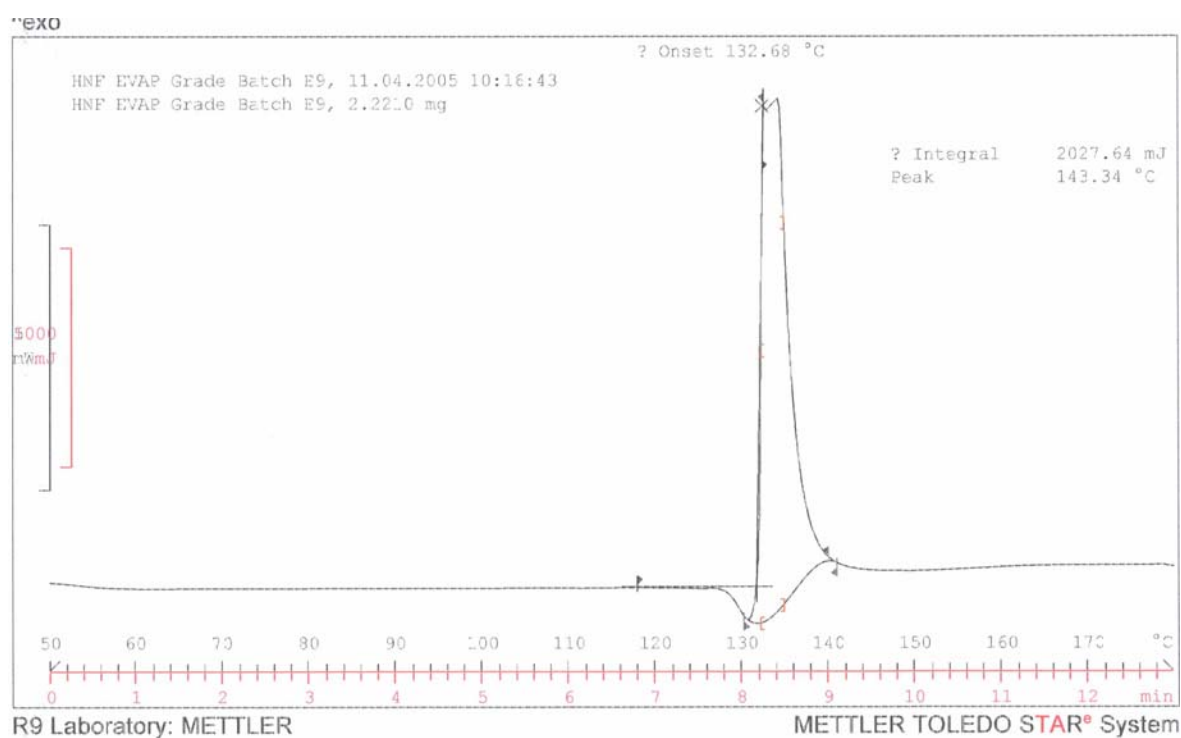
Figure 159A – DSC Analysis of HNF 10K Min^{-1}
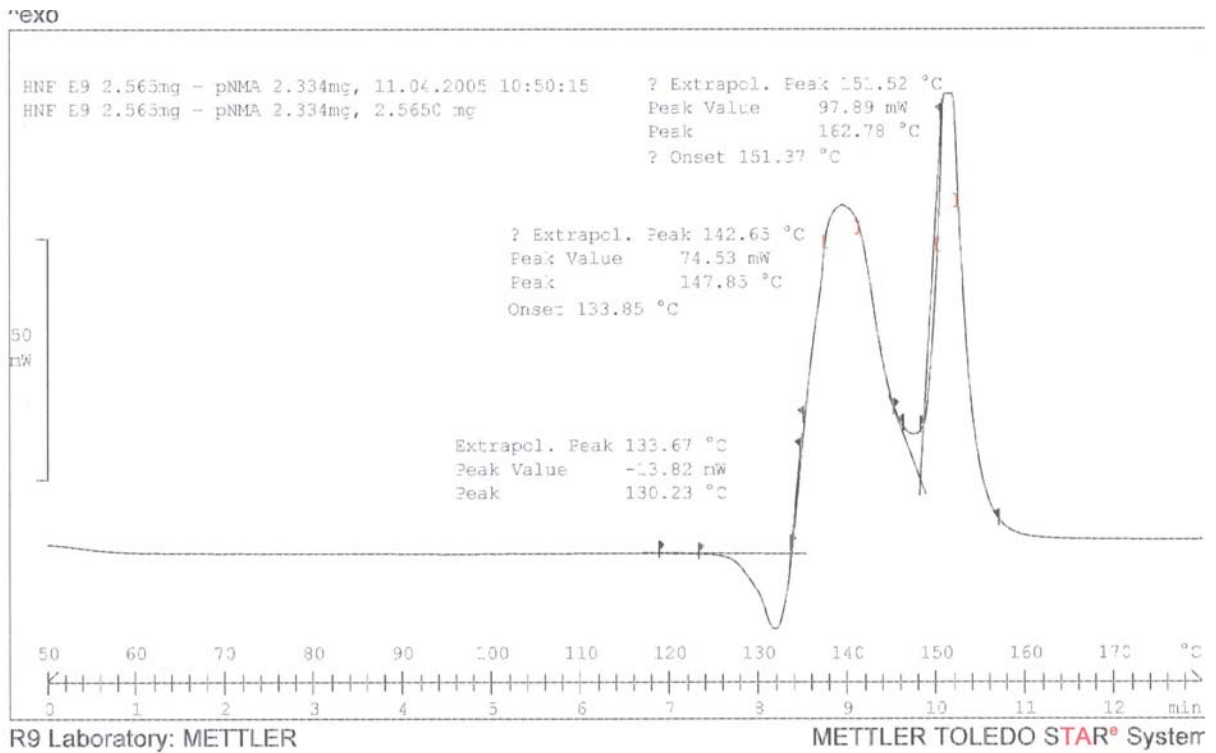
Figure 159B - DSC Analysis of 1:1 HNF :pNMA 10K Min^{-1}
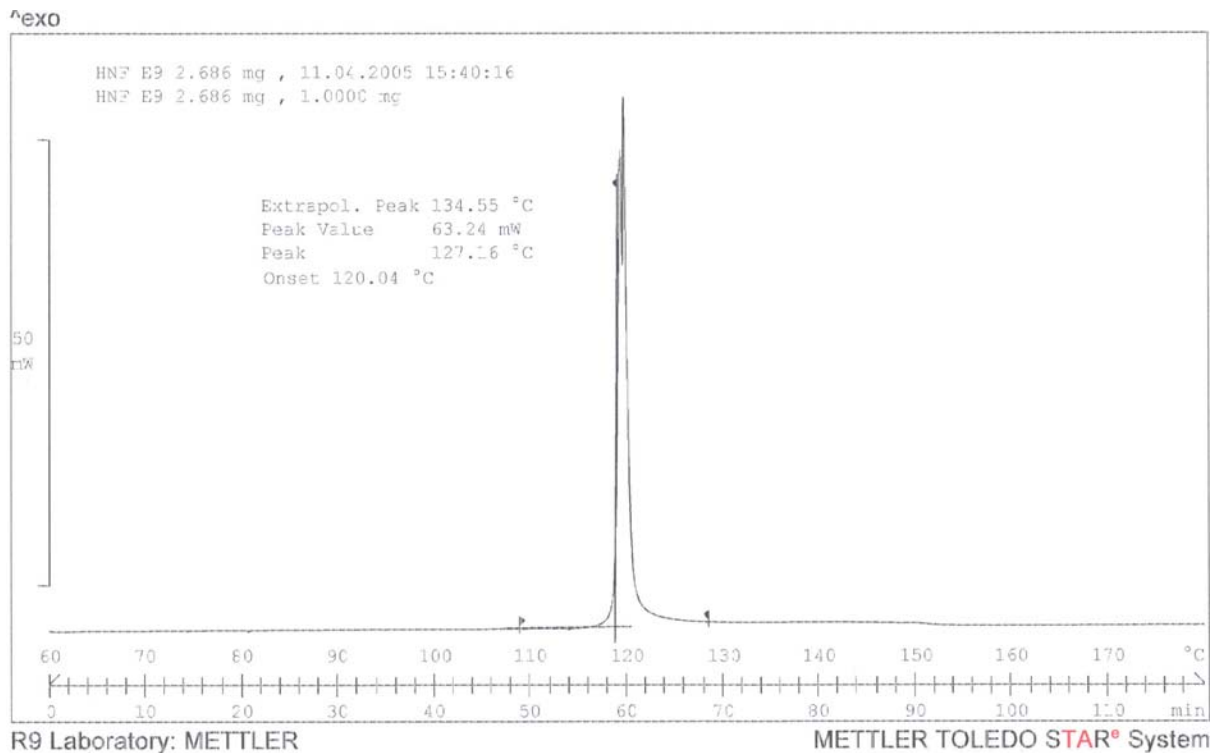
Figure 159C - DSC Analysis of HNF 1K min^{-1}

^exo

ENF E9 2.844mg + pNMA 2.651mg, 11.04.2005 13:09:09
ENF E9 2.844mg + pNMA 2.651mg, 1.0000 mg

Extrapol. Peak 121.83 °C
Peak Value   3.67 mW
Peak   114.15 °C
Onset 117.52 °C

Extrapol. Peak 123.48 °C
Peak Value   21.97 mW
Peak   131.37 °C
Onset 126.38 °C

10 mW

60   70   80   90   100   110   120   130   140   150   160   170   °C
0   10   20   30   40   50   60   70   80   90   100   110   min

R9 Laboratory: METTLER   METTLER TOLEDO STAR^e System
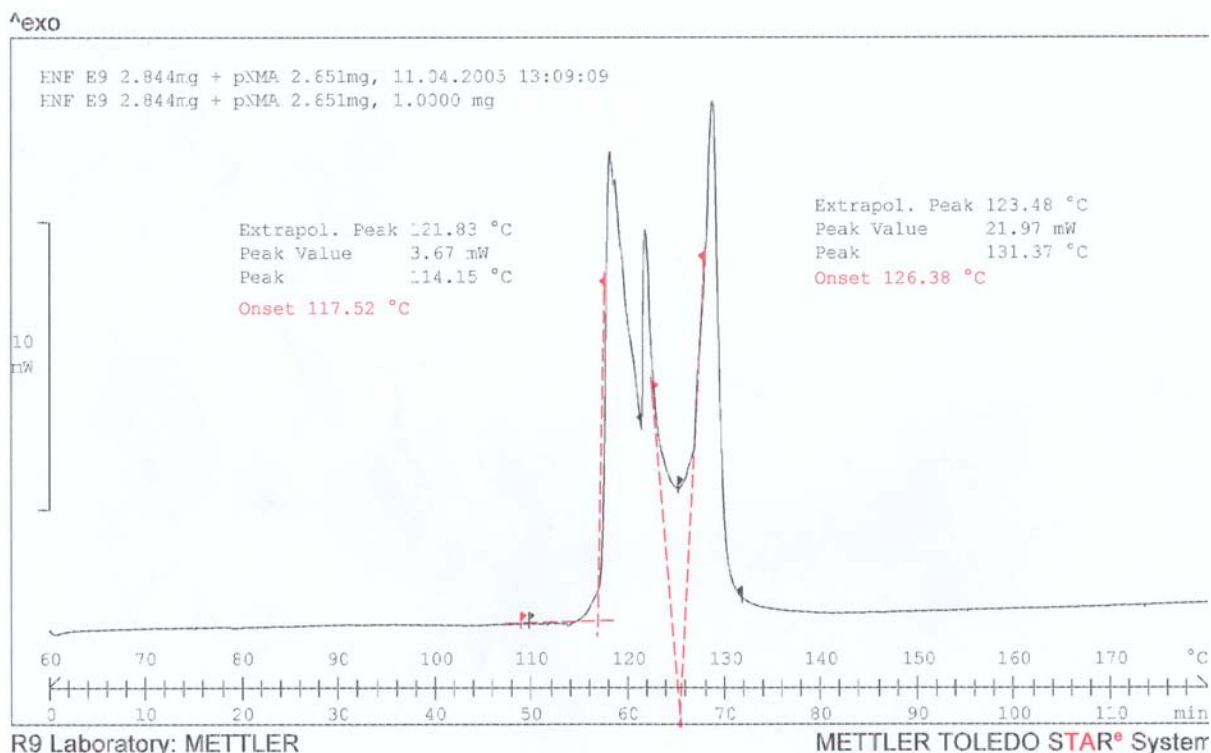
Figure 159D - DSC Analysis 1:1 HNF : pNMA at 1K min^{-1}

Comparison of the data achieved at 1K min^{-1} (Figures 159A and 159B) indicates onset temperatures of 120.0°C for pure HNF and 117.5°C for the pNMA / HNF mixture; this might suggest a low level chemical incompatibility between the species. The presence of the second exothermic peak does highlight that pNMA can play an active role in reaction with degradation products from high rate HNF thermal decomposition. The comparatively short storage time for the HNF within these DSC studies would encourage the HNF decomposition reaction to more closely follow the reaction proposed by Brill [98] for "instantaneous" decomposition ie

$$HNF \longrightarrow 2NO + CO_2 + 2H_2O + 3/2\ N_2 + 1/2H_2$$
(Reaction R28)
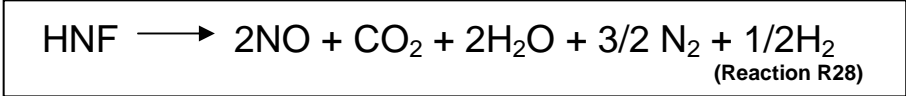
For these reaction products, possibly the reaction of NO with pNMA leads to the second exotherm although prediction of exhaust products during reaction of HNF / pNMA is suggested to liberate predominately CO, H_2 and N_2 [11] which implies preferential oxidation and disruption of the pNMA structure will occur within the sample pan. Further trials would be required to determine the reaction products produced during these DSC trials.

Optimum conditions for the low-level reaction between HNF and pNMA to occur would be to have high contact time between the ingredients and also have pNMA in "excess". The 80°C test conditions for STO7 fulfil one of these requirements (pNMA in excess) and so this may be the explanation for the increased observed level of reaction observed in the 80°C data.

So, the hypothesis given in Figure 158 is proposed to provide a method for understanding the decomposition of polyNIMMO / HNF propellants at 80°C. the relative strength and or competition between the various reactions shown will be discussed in more details in later sections.

4.2 Extended Correlation of THF Fraction, Mass Loss and Aqueous Extraction Data at 60°C

Applying the 80°C hypothesis in Figure 159 to the 60°C data helps to further extend the hypothesis and data interpretation. In the control sample (STO1) at 60°C, the level of polymer breakdown is similar to that observed at 80°C. However, unlike the 80°C data, there is comparatively little Δ Mass loss or Δ Aqueous extraction during the 60°C storage period. The storage periods had been chosen for analysis were estimated to provide an approximately equal level of reaction in all samples at the end of storage. The apparent similarity of Δ THF extraction data for 80°C and 60°C suggests that the driving reaction for the polymer breakdown (Reaction I1) has progressed to the same degree at both temperatures. This implies that polymer breakdown occurs either independent of HNF breakdown or that there is a limiting reagent for reaction of the HNF / polyNIMMO system. The lower values of Δ mass loss or Δ aqueous extraction data at 60°C compared to 80°C suggest that the reactions that are detrimental to HNF retention (ie reactions following on from reaction E1) have not occurred to a significant degree. This implies that reaction I is dominant at 60°C. However, the positive effect of addition of denitration stabilisers eg in formulations STO5 – 7 show that there is at least some benefit from their incorporation (suggesting that at least some reaction via reaction E1 has occurred during storage).

The significant differences between the 80°C storage data for STO1 and 60°C and 40°C data implies a change in reaction course at 80°C compared to reaction at 60°C or 40°C. The Δ THF fraction result at 60°C implies that reaction D may still be occurring to release NO_2 but that reactions after position E1 are highly temperature dependent. It is proposed that this reflects a competition between the release of nitroform, release of NO_2, and HNF/ polyNIMMO interaction as detailed in reaction R29.
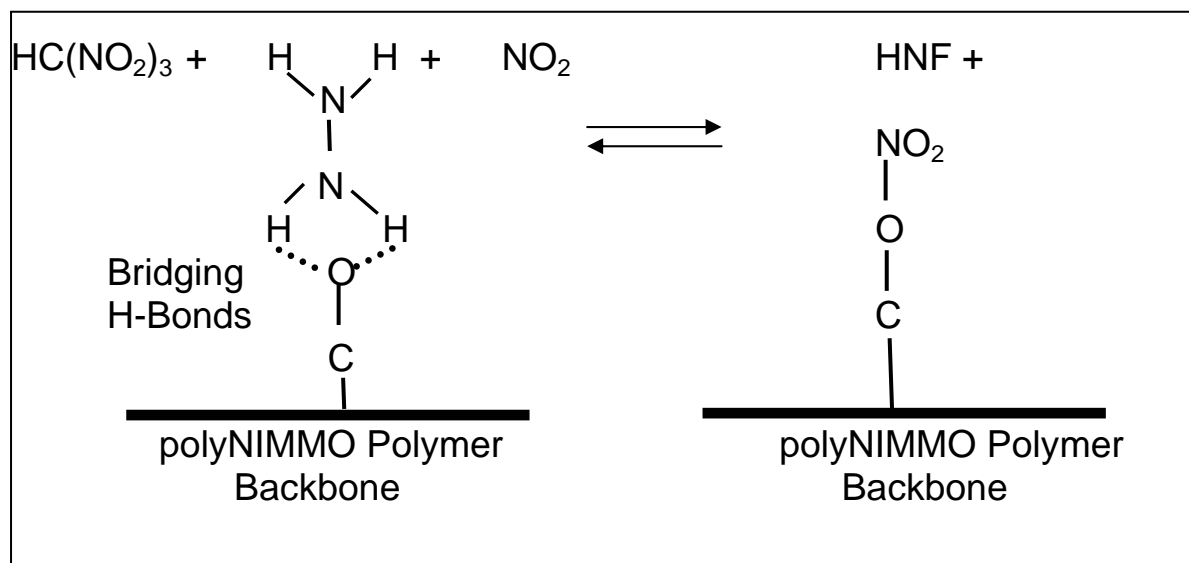
The relative dominance of each reaction would be dependent on the individual reaction kinetics of all reactions occurring within the formulation and the competition between these reactions with changing temperature ie removal of NOx species by denitration stabilisers would move the equilibrium to the left in Reaction R29. The relative position of any competition between reactions would also be affected by liberation or removal of reagents via reactions earlier or later in the reaction scheme (eg rate of reaction A to liberate water / hydrazine as suggested, or reaction E4, E5 or E6 to remove NOx species). Some of these reactions would be interrelated. For example, the lower level of water formation in the primary decomposition of thermal HNF (reaction A) would be expected to influence the removal of NO_2 from polyNIMMO by reduction of the ease by which ionic dissociation may occur. The reduction in water liberated from primary decomposition would also affect the formation of nitrous acid (reaction E1) thus affecting all subsequent reactions in series E of the scheme. This reducing tendency towards nitrous acid formation would in turn lead to a higher dwell time between reagents at position D / G increasing the probability of recombination of reagents into their constituents (ie the right hand side of the equilibrium given above).

As previously suggested, 80°C appears to be a critical temperature for polyNIMMO / HNF propellant storage. Possibly 80°C represents a temperature at which recombination of HNF degradation products is eschewed in favour of dissociation.

From the data in Table 14 and the reactions I1 and I2, the similarity of Δ THF fraction at all three temperatures suggests the likelihood of a reactant being exhausted at all temperatures. Reaction I1 is proposed to be between liberated Nitroform and the polyNIMMO polymer structure. Due to the comparatively low RMM of the repeating unit in the polyNIMMO structure and comparatively high

RMM of the polymer, it would be expected that all moieties within this structure would be at high concentration within the formulation. This high concentration would suggest that exhaustion of these moieties would be unexpected. However, an area that is at a comparatively low concentration in the polymer are the polyurethane linkages formed during the isocyanate cure reaction. Urbanski [137] details a reaction between formaldehyde and Nitroform to give 2,2,2-trinitroethanol is shown in Reaction R30
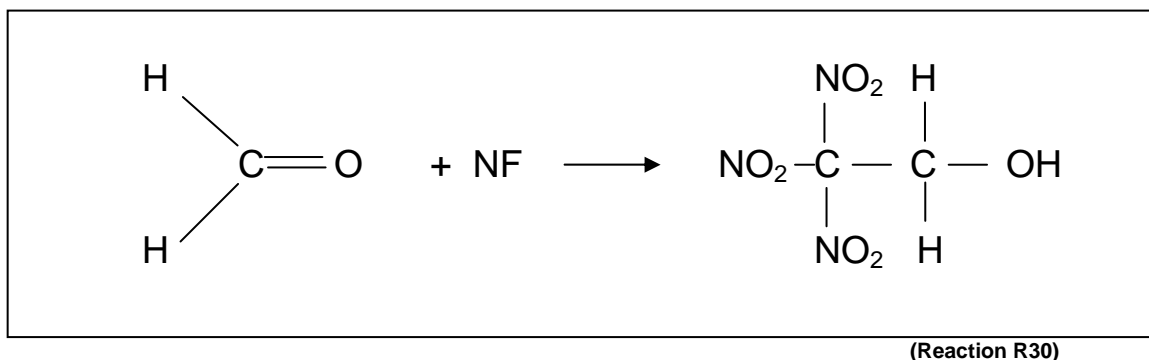
(Reaction R30)

He suggests that the reaction is typical of the reaction of all carbonyl groups with nitroform. The carbonyl group of the polyurethane linkage could therefore be susceptible to an analogous reaction ie

Y and Z = Continuation of the polymer chain structure
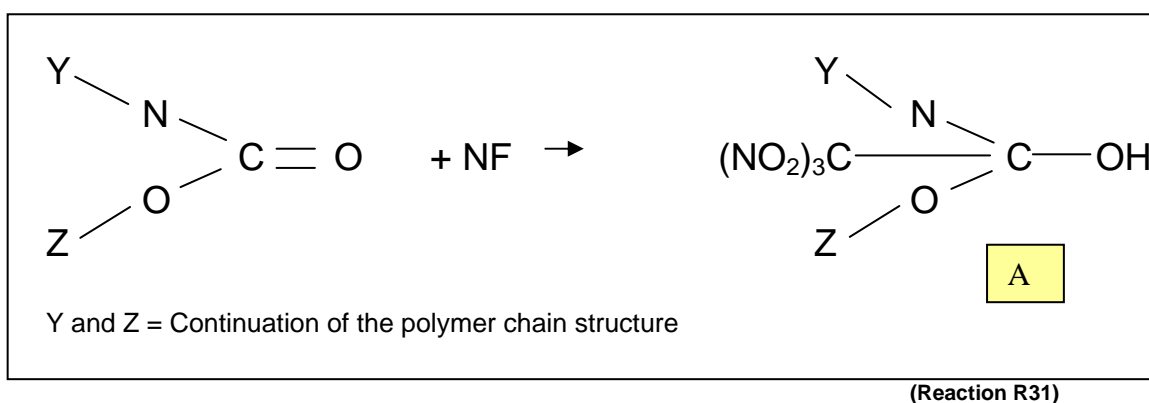
(Reaction R31)

The Δ THF Extraction indicates that polymer breakdown occurs during storage. If this progresses via Nitroform / polyNIMMO reaction, the ungainly structure A in Reaction R31, severely affected by the 3 nitro groups can be envisaged to rearrange to break the polymer chain as given in Reaction R32. Reaction R32 results in trapping the reactive NF molecule whilst also reducing polyNIMMO chain length (effectively increasing the THF solubility of residues). Although this reaction regenerates a carbonyl structure that could show further reaction with NF, the highly nitrated product that would be formed from such a reaction would be expected to have a high degree of steric hindrance and so may not be possible nor stable.
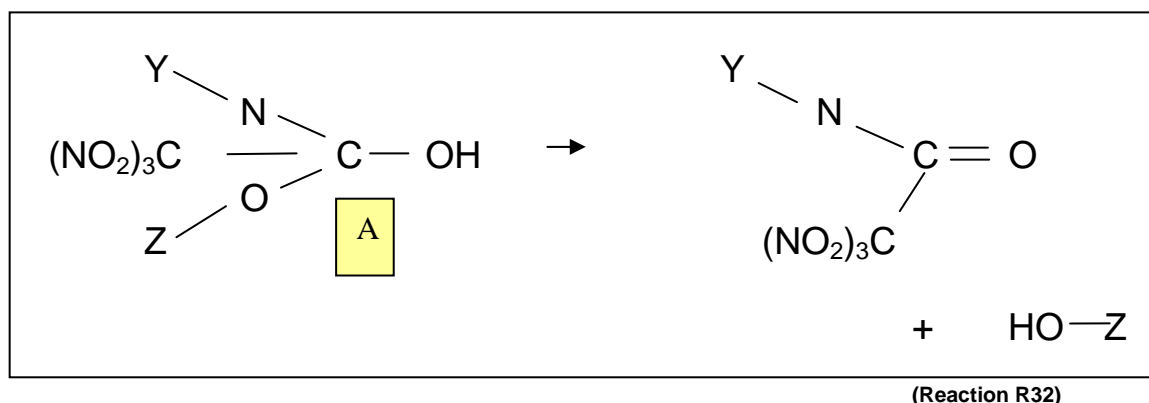
(Reaction R32)

A similar reaction could be envisaged between HNF (or liberated hydrazine) and the carbonyl moiety of the polyurethane linkage as given in Figure 13 to form a hydrazone; this may give an alternative route for removal of hydrazine from the propellant formulation. The possible reaction of the carbonyl of the polyNIMMO with nitroform or hydrazine is envisaged to occur until the polyurethane moiety is exhausted. Once carbonyl exhaustion is achieved, the nitroform is retained within the matrix or lost via evaporation. The detailed action of nitroform reaction would require further study. However, it would be expected to affect the position of the equilibrium between HNF and polyNIMMO (Reaction R27). If this equilibrium is taken as the second driving force for reaction (after the thermal degradation of HNF), excess nitroform will discourage denitration of the nitrate ester moiety (via Le Chatalier's principle). This will lead to a minimisation of all reactions beyond position E1 on Figure 158. When the boiling point of NF is considered (45-47°C at 22mm Hg [130]) this may provide a route by which reaction course modification with temperature could occur. Evaporation of NF from the formulation would result in minimisation of any inhibition of reaction E1 that might occur.

The similarity between Δ THF extraction values at 60°C and 80°C in the control sample suggests that, unstabilised, no other reactions in the base polyNIMMO / HNF formulation lead to polymer breakdown. The 40°C data shows a reduced Δ THF fraction (3.65%) compared to the 60 and 80°C data (6.4% and 5.85% respectively). This reduced Δ THF fraction value at 40°C implies that the reaction has not achieved its final position (ie the polyurethane links have not been exhausted via reaction with nitroform or hydrazine). This 40°C data helps give an indication of the significance of progression of this reaction in relation to further reaction mechanisms in the formulation. From the data given, 3.65% of Δ THF fraction has occurred simultaneously with 3.39% of Δ Aqueous extraction and 5.78% of mass loss. These values are very close to the Δ aqueous fraction and mass loss at 60°C (4.19% and 6.0% respectively). This further implies that polymer breakdown in unstabilised systems is independent of reactions leading to mass loss. Within the hypothesis in Figure 158, this can be seen to be true (ie reactions I1- I6 does not drive reaction A and also reactions I1-I6 serve to minimise reactions after E1 via modification of equilibrium D1). This lack of further

reactions leading to degradation of polymer present indicates polymer degradation is independent of other processes. It also implies that reactions resulting in mass loss and aqueous extraction (eg reaction A and E4) are fully responsible for these changes in properties.

The 20% difference observed at 80°C between the Δ aqueous fraction and mass loss data is not observed at 60 or 40°C. This is suggested to be due to the system not being at equilibrium and likely reflect the differences in equilibrium position for reaction D1 with temperature influenced by the equilibrium given in Reaction R27. It could also infer that reaction A dominates mass loss at 60°C and 40°C but equilibrium D1 (and possibly the loss of nitroform) dominates at 80°C

Reviewing the effect of stabilisation at 60°C indicates that the level of reaction (by any measure) is significantly lower than the reaction observed at 80°C. Also, generally, the stabilised systems reduce degradation compared to the control sample STO1. pNMA loaded formulations STO5, STO6 and STO7 reduce degradation although STO5 (1% pNMA) shows the highest mass loss for the 3 formulations. This implies that all stabiliser activity to remove NOx (reaction E5) has been depleted and branch E15 is being followed in this sample. The result implies that control of branch E4 plays a large part in reducing mass loss. However, the lack of Δ THF fraction for the STO5 formulation implies that the reaction course in Figure 158 must be further modified. If branch E4 was occurring as written, the formation of nitroform would promote reaction I4; this is not being observed in the sample. It implies a method that depletes pNMA (ie reaction E5) but without breakdown of polyNIMMO (reaction D) must be added to the hypothesis.

$+ O_2$ $\overset{A2}{\longrightarrow}$ **$N_2O + H_2O$**
NO_2 / N_2O_4

+ pNMA   L

HNF $\overset{A}{\longrightarrow}$ $N_2H_4 + HN_3 + N_2 + ANF + HNO_2$ I2 $+ (NH_4)_2S_2O_8$

B   I1

+ PN   I3   + PN   I4   ANF

C   Minor

$+ Na_2SO_3$ or $(NH_4)_2S_2O_8$

B1

Release of Water   Trapping / Removal of Water   + HNF   Polyurethane + NF

HO-Z +

B2   Y-N-C=O

+ HNF   Hydration Limit of Scavengers Achieved   B4 $C(NO_2)_3$ Secondary NF Reactions

$+ Na_2SO_3$ or $(NH_4)_2S_2O_8$ I5

C1   Polyurethane Exhausted   I6

Reaction Limit of Scavengers Achieved   B3   Support for Ionic Dissociation / Solvation   Polymer Degradation   Hydrazone Formation + Nitroform + Water

I

+ PN

D   E1   E2   Unexplained Reaction

$HC(NO_2)_3$ +   H   H + NO_2 $\overset{+ H_2O}{\longrightarrow}$ HNO_2 $\rightleftharpoons$ $N_2O_3 + H_2O$ + PN

N   E3   Degraded HNF / pNMA

HNF + PN   D1   F NO^+ + NO_2^- K   J

H   H   G   H

Bridging H-Bonds   O   + HNF   + pNMA   + 2NDPA

C   E5   E6

I   polyNIMMO Polymer Backbone   E4   N-NO-pNMA $\overset{+ 2NDPA}{\underset{Transnitrosation}{\rightleftharpoons}}$ N-NO-2NDPA

+ NOx   E7   + HNF   E8   + HNF

E14   E9   + NOx   E13

E15   E11 $+ Na_2SO_3$ or $(NH_4)_2S_2O_8$ E10   E12

Di-nitro-methyl aniline   C-Nitro Derivatives of 2NDPA

H1   XS NOx / HNOx   E16

H   H   H   + NOx / HNOx

$HC(NO_2)_3 + HONNHNH_2 + HNO_2$ + H_2O NO—N   N—H$^+$ $^-C(NO_2)_3$

$+ HN_3$ + NO^+ Activity of Denitration Stabilisers Fully Depleted

H   H

(Intermediate)

■ = Does not Occur

X = Reference Point for Discussion in Text   X = Modification to Previous Hypothesis

Figure 160 – Addition of 60°C Data to Hypothetical Reaction Course for PN/HNF Propellant

Section 2.8 suggested that the formation of detected N_2O in the overall thermal decomposition of HNF may result from oxidation of hydrazoic acid formed early in the decomposition ie

$$HN_3 \ + \ O_2 \longrightarrow H_2O \ + \ 3/2 \ N_2O$$
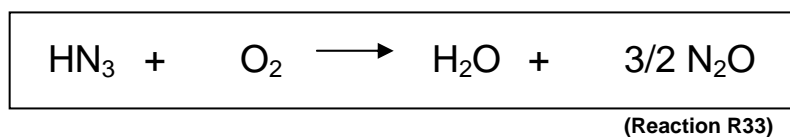
(Reaction R33)

However, the final products of this oxidation is dependent on the HN_3 / O_2 ratio [127] . It is also possible to envisage oxidation via other species (eg NO_2 or HNO_2). However, at higher oxygen : hydrazoic acid ratios, the following reaction products have been proposed

$$HN_3 \ + \ 7/2 \ O_2 \longrightarrow H_2O + 3NO \quad \text{(Reaction a)}$$

$$HN_3 \ + \ 13/2 \ O_2 \longrightarrow H_2O + 3NO_2 \quad \text{(Reaction b)}$$

$$H_2O + 3/2 \ N_2O_4 \quad \text{(Reaction bi)}$$
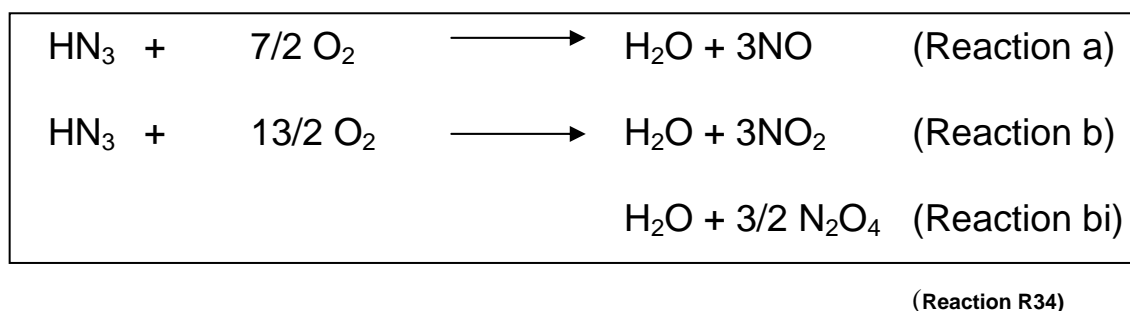
(**Reaction R34)**

At lower levels of thermally driven decomposition (ie lower temperature), the rate of hydrazoic acid liberation from reaction A in Figure 160 would be reduced. The oxygen present in the sample vial starts at the same level for all stored samples. Lower rate evolution of HN_3 would bias reaction towards reactions (a), (b) and (bi) above. Sammour et al [87] has detailed that pNMA is reactive against NO_2 as well as HNO_2. This alternative route towards generation of NOx species provides an alternative route for nitration of the denitration stabilisers. Formation of NO_2 or N_2O_4 at point A on Figure 159 would account for depletion of pNMA without further reaction to lead to polymer breakdown. At lower temperatures, Reaction A could therefore be viewed as being

$$HNF \longrightarrow ANF + HN_3 \xrightarrow{\text{+ XS O2}} H_2O + NO_2 / N_2O_4$$

(Reaction R35)
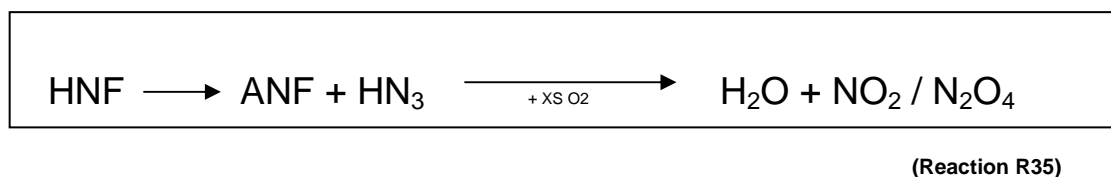
The majority of the remaining 60°C data in Table 14 can now be fitted into the hypothesis given in Figure 27 in a similar manner to the analysis of the 80°C data. At each temperature the significance of each branch of the hypothesis would be expected to vary. This would be especially expected in the rate of reactions A, D, D1, E1, E4, E5, E6 and the reactions leading up to the complete depletion of the denitration stabilisers (reaction E16)

The 60°C results that don't fit so neatly into this revised hypothesis in Figure 160 are the Δ THF fraction values for formulations STO8 –10. At 60°C, increasing the overall stabiliser level leads to an

increase in Δ THF fraction whereas at 80°C the situation is reversed. The result is proposed to reflect the relative ratios of the transnitrosation reaction between pNMA and 2NDPA and HNF / N-Nitroso-2NDPA reaction (reaction E8) after pNMA depletion. At 80°C, the rate of denitration of the polyNIMMO chain is proposed to be high and the NOx / HNOx reactant is in excess with reaction E5 dominant. As temperature decreases, the driving reaction A is reduced and volatilisation of Nitroform is also reduced. This promotes reaction E1 to liberate NO_2 that is rapidly taken up by the dominant reactive species (ie via reactions E4, E5 or E6). The lack of mass loss in the formulation suggests that this dominant reaction stops further degradation of the formulation. This implies that reaction E5 is dominant. As reaction progresses, pNMA activity is depleted, eventually becoming less dominant and other reactions (E4, E6) come into competition. This starts to lead to the degradation of the HNF present via the catalytic links of branch E2 and H1. As the concentration of 2NDPA becomes higher in the overall concentration, the higher the probability of formation of N-Nitroso-2NDPA formation and thus the more rapid lack of pNMA / NOx reaction dominance to remove NOx and minimise reaction E4.

4.3 Extended Correlation of THF Fraction, Mass Loss and Aqueous Extraction Data at 40°C

The 40°C data of Table 14 also generally fits the scheme in Figure 160 but again, a shift in the dominance of some reactions is proposed. The interesting observation of the 40°C data is the overall higher mass loss compared to the 60°C data. However, the mass loss data for the 40°C control sample (STO1) is similar in many cases to the stabilised systems at that temperature. This implies that the action of the stabilisers does not significantly affect the underlying decomposition of the HNF / polyNIMMO matrix (ie reaction A is dominant throughout).

For the 40°C data that has been achieved, the variation in the level of Δ THF fraction for pNMA analogues (STO5-7) is interesting. The higher levels of pNMA lead to a lowering of Δ THF fractions indicating that the polymeric breakdown is being affected by pNMA content. However, the presence of pNMA is detrimental to the propellant reaction leading to polymer breakdown. It does however suggest that a product of pNMA reaction in the formulation leads directly to polymer breakdown. This must centre on the products of reaction J or K. Direct low level reaction of the two reagents has been suggested (Figure 159A-D) but further study would be required to assess the level of reaction occurring after long-term storage at 40°C. It is unclear how this reaction would progress and further work would be required to identify the contribution of this reaction to polymer breakdown.

The differences between STO17 and STO18 suggest that the balance between the minor effect of trapping of water (reaction B1), hydrazine reaction (reaction C1) and oxidation strength (E9 / E10) has changed at this lower storage temperature. At 40°C, the higher oxidising power of the

peroxodisulphate is more important than the ability to trap water or react with hydrazine in the matrix. This is reflected in the formulations where the hydrazine scavengers are present with pNMA (STO15 / STO16) or 2NDPA (STO13 / STO14). Formulations with lower oxidation power (STO13 / STO15) show higher levels of Δ THF (although pNMA formulations are still superior to 2NDPA analogues in reducing overall Δ THF fraction with storage). This implies that the oxidation of the N-NO derivative protects the polymer backbone. This in turn suggests that the higher levels of Δ THF fraction observed in sample STO5-7 at 40°C is due to the reaction products from reaction of HNF with N-NO-pNMA or N-NO-2NDPA reacting with the polymer present (ie reaction products from E7 and E8 with subsequent reaction with polyNIMMO). The products of these reactions are proposed to be nitroform, water and a hydrazone. As discussed previously, the reaction of nitroform and polyNIMMO is proposed to be via the carbonyl group of the polyurethane moiety of the polyurethane bridge in the polymer structure (ie reaction I4) and will be self limiting when the concentration of polyurethane links falls. This suggests nitroform would not lead to an extension of polymeric breakdown. The action of water and hydrazine has also been detailed in the hypothesis (occurring as a driving force at various places in the proposal). This suggests that any additional polymer breakdown must progress via the hydrazone formed or excess hydrazine / water on exhaustion of a reactive species. It is again unclear how this reaction would progress and further work would be required to identify the contribution of this reaction to polymer breakdown.

4.4 Conclusions From Extended Correlation of THF Fraction, Mass Loss and Aqueous Extraction Data

A hypothesis has been developed based on comparison of THF extraction data with mass loss and aqueous extraction data at 80, 60 and 40°C; this scheme is shown in Figure 160. The scheme is proposed to explain the data achieved and suggest various reactions occurring within PN/HNF formulations during storage. At the different storage temperatures it is proposed that different reaction courses dominate the propellant degradation reactions.

The general conclusions of the THF analysis are:-

1) The level of breakdown of the polyNIMMO polymer backbone is comparatively low within the polyNIMMO / HNF propellants during ageing and only become significant at longer ageing periods.

2) PolyNIMMO polymer backbone degradation does not appear to be on the primary path towards propellant breakdown until the later stages of propellant reaction. In these latter stages, rapid liquefaction occurs suggesting attack on the polymeric support by HNF degradation species (eg

hydrazine or nitroform) rather than driven by intermolecular mechanisms (eg via nitrate ester degradation and NOx catalysed bond cleavage).

3) Liberation of hydrazine (major) and / or water (minor) via thermal decomposition of HNF are seen as a driving force in propellant breakdown, as is denitration of polyNIMMO. The control of direct reaction of NOx/HNOx with HNF is also proposed to be a critical step in reducing autocatalytic breakdown of propellant formulations. However, the formation of N-Nitroso compounds (especially N-Nitroso-2NDPA) by reaction of NOx / HNOx species with denitration stabilisers must be minimised as these species react directly and rapidly with HNF. It is proposed that a dual hydrazine scavenger / denitration stabiliser system (1% pNMA / 1% Sodium Sulphite) is the optimum to protect the propellant system at all temperatures.

4.5 Extension of the Hypothesis for PolyNIMMO / HNF Propellant Degradation

The reaction scheme given in Figure 160 has a number of reaction steps. Table 15 lists each reaction step and the evidence available for each step.

Step Ref	Reaction	Evidence of Reaction Occurrence (Literature)	Evidence of Reaction Occurrence (Experimental)
A	Liberation of HNF degradation species	HNF degradation studies by GC-MS by Bellerby et al [104]	Detection of gaseous species during HNF analysis via GC-MS or Colorimetric studies (GASTEC)
A1	Direct liberation reaction of nitrous acid from HNF Degradation	HNF degradation studies by GC-MS by Bellerby et al [104] \n\n Detailed Gas Analysis from HNF Degradation by Koroban [108]	Change in pH infers a non-specified acidic species liberated.
A2	Reaction of Hydrazoic Acid with Oxygen	Reactions identified for hydrazoic acid reaction with oxygen by Hallman [127]	Change in pH infers a non-specified acidic species liberated.
B	Trapping of water by hydrazine scavengers	Sodium sulphite is anhydrous salt. Water liberation detected and shown to be important in HNF degradation by Pearce [92] and Bellerby et al [104] [105]	Differences in efficiency of hydrazine scavengers does not appear to be due to their oxidising power. The anhydrous nature of sodium sulphite gives pointers to an alternative protection mechanism. However, comparison against GC-MS data suggests control of water within the formulation is likely a minor contributor towards propellant degradation
B1	Release of water by sodium sulphite in equilibrium with trapping / removal of water	Dependent on the strength of water / salt bond it is possible that some degree of equilibrium may be set up. However, reaction B2 is expected to be the dominant reaction when water is present	As Reaction B
B2	Hydration limit of scavengers achieved	All desiccants have an efficiency limit (Lide [130]).	The liberation of water within the HNF degradation reaction will inevitably eventually lead to an excess concentration of water.

B3	Support for Ionic dissociation / Solvation	At low levels of water liberation, solvation of an ionic solid will only occur at isolated areas of the crystal structure. Water liberation has been detected and shown to be important in HNF degradation by Pearce [92] and Bellerby et al [104] [105]. Solvated stability of HNF has been shown to be inferior to the solid [128]	Not assessed but inference from data does not appear unreasonable.
B4	Direct reaction of HNF with water.	As Reaction B3	As Reaction B3
C	Direct reaction of hydrazine with polyNIMMO	Inferred from Oyumi [132] and high level of hydrogen bonding in the HNF structure (as inferred from work by Schmidt [103] and crystallographic assessment by Dickens [95])	Studies have detected hydrazine in the decomposition products of HNF (Colorimetric studies - GASTEC). Data analysis indicates loss of NOx species with little or no degradation of HNF or polyNIMMO. Also, data indicates differences in mass loss / aqueous extraction of ~ 20% which this structure serves to explain. **Further study required.**
C1	Direct reaction of hydrazine scavengers with Hydrazine	Audrieth suggests that the presence of these species is beneficial to aqueous hydrazine stability.	The presence of the scavengers influences sample longevity in a number of formulations.
D	Direct reaction of HNF with polyNIMMO	As Reaction C	As Reaction C
D1	Equilibrium between HNF and polyNIMMO reformation and loss of NO_2 from the polyNIMMO structure	No literature to support this reaction	Reaction is inferred from differences in test data at different temperatures.
E1	Formation of nitrous acid from NO_2 + H_2O	Sammour et al [76] detail the cycle of reactions associated with NOx and HNOx liberation.	The action of denitration stabilisers in the data suggests that they are beneficial in protecting propellant longevity. This infers that they are undertaking their perceived action (ie removal of NOx and HNOx species) and thus NOx / HNOx are inferred to be being liberated.
E2	Formation of Nitrogen (III) Oxide and water	Sammour et al [76] detail the cycle of reactions associated with NOx and HNOx liberation.	Is part of accepted cycle of mechanism for nitration / nitrosation of denitration stabilisers pNMA / 2NDPA / Diphenylamine [72]-[90]
E3	Formation of NO+ and NO2- ions	As Reaction E2	As Reaction E2
E4	Direct reaction of NO^+ or NO_2^- with HNF	Hydrazine is used as a scavenger for low levels of NOx and HNOx species in a number of reactions. The "hydrazine like" qualities of HNF would suggest reaction is possible. Doherty et al [134] detail a reaction scheme for hydrazine with nitrous acid to liberate various species. This reaction has been modified to predict the products shown.	If NOx / HNOx species are not removed from the reaction vessel (eg by denitration stabilisers), HNF degradation is observed to be more rapid. This is taken as evidence for direct reaction of HNF with HNOx / NOx species.

E5	Formation of N-NO-pNMA	Generally accepted route for reaction of pNMA with HNOx and NOx species during degradation of double base propellants. Bellerby et al [83] detail the relevant reactions.	As Reaction E1
E6	Formation of N-NO-2NDPA	As Reaction E5	As Reaction E1
E7	Reaction of N-NO-pNMA and HNF	Reactions of Nitroso compounds and hydrazine are given by Schmidt [103]	DSC analysis of the nitroso compound and HNF indicates direct reaction
E8	Reaction of N-NO-2NDPA and HNF	As Reaction E7	As Reaction E7 (but N-NO-2NDPa is more reactive with HNF than the N-NO-pNMA analogue)
E9	Oxidation of N-Nitroso-pNMA groups by hydrazine stabilisers	Suggested to not occur within the propellant matrix	Discounted
E10	Oxidation of N-Nitroso-2NDPA groups by hydrazine stabilisers	As Reaction E9	As Reaction R9
E11	As Reaction E9	As Reaction E9	As Reaction E9
E12	As Reaction E10	As Reaction E9	As Reaction E9
E13	Formation of C-nitrated derivatives of 2NDPA via reaction of further NOx species	The accepted pathway for reaction of 2NDPA with HNOx and NOx species is via N-Nitrosation followed by rearrangement to C-nitrated derivatives [72] – [90]	It is unclear if higher nitrated derivatives of 2NDPA are formed or whether the high reactivity of N-Nitroso-2NDPA with HNF removes all species at this point. **Further study is required**
E14	Formation of C-nitrated derivatives of pNMA via reaction of further NOx species	The accepted pathway for reaction of pNMA with HNOx and NOx species is via N-Nitrosation. Bellerby et al suggest that C-nitration via the Fisher-Hepp rearrangement does not occur due to steric hindrance [83]	It is unclear if higher nitrated derivatives of pNMA are formed or whether the nitration reaction stops at the generation of N-Nitroso-pNMA. **Further study is required**
E15	Reaction of excess NOx / HNOx species with HNF after full depletion of denitration stabilisers	As Reaction E4	As Reaction E4
E16	Reaction of C-nitrated nitrated derivatives of 2NDPA with NOx	Various authors [72]-[90] have shown sequential nitration of diphenylamine or 2NDPA	It is unclear if higher nitrated derivatives of 2NDPA are formed or whether the high reactivity of N-Nitroso-2NDPA with HNF removes all species at this point. **Further study is required**
F	Equilibrium of NO_2 with N_2O_4	Sammour et al [76] detail the cycle of reactions associated with NOx and HNOx liberation. Dimerisation of NO_2 is an accepted reaction within this cycle.	Dimerisation of NO_2 is an accepted reaction within this cycle but direct detection of NO_2 / N_2O_4 in the propellant has not been attempted.
G	Formation of bridging hydrogen bonds between HNF or hydrazine with polyNIMMO.	As Reaction C	As Reaction C

H	Rearrangement of proposed reaction product of HNF / HNO_2 to liberate further HNO_2	As Reaction E4	As Reaction E4. The reaction to liberate nitrous acid does help explain the apparent autocatalytic nature of propellant / HNF breakdown in the test data but no assessment of the formation of the proposed reaction products have been carried out. **Further study is required.**
H1	Autocatalytic regeneration / reaction of Nitrous acid	As Reaction E4	As Reaction E4. The reaction to liberate nitrous acid does help explain the apparent autocatalytic nature of propellant / HNF breakdown in the test data
I	Liberation of nitroform	The liberation of hydrazine in various assessments of HNF ageing [98] [108] would imply that the counter ion (nitroform) would be formed.	No direct detection of nitroform has been carried out on propellant ageing. However, gas analysis studies of HNF [98] [104] [105] have generally failed to detect nitroform. This has been proposed to be due to on-column reaction or reaction with other degradation species.
I1	Reaction of Nitroform with polyNIMMO	Urbanski [135] details a series of reactions of nitroform including substitution across a carbonyl structure	Reaction of polyNIMMO with HNF or HNF degradation products to lead to chain cleavage appears limited by concentration of one reagent. This reagent is proposed to be the polyurethane linkages on the polyNIMMO polymer backbone.
I2	Reaction of nitroform with Ammonium peroxodisulphate to form Ammonium Nitroformate	ANF is formed during HNF degradation [104] [108]. It does not seem unlikely that any free nitroform will react with the hydrazine scavenger ammonium peroxodisulphate to form this product.	The formation of ANF explains a difference between mass loss and aqueous extraction data for the two hydrazine scavengers studies (sodium sulphite and ammonium peroxodisulphate). Separation of ANF formed via thermal degradation of HNF from that of nitroform reaction with ammonium peroxodisulphate would not be easily possible. No further study to be undertaken.
I3	Liberation of hydrazone, nitroform and water from reaction of N-Nitroso compounds and HNF	Reactions of Nitroso compounds and hydrazine are given by Schmidt [103] and suggest formation of hydrazone as a product. The others species listed are suggested to balance equation for HNF.	Detection of the hydrazone has not been undertaken. **Further work required**.
I4	Cleavage of the polymer chain by reaction of nitroform with the polyurethane linkage.	As Reaction I1	As Reaction I1
I5	Exhaustion of Polyurethane reactant	As Reaction I1	As Reaction I1
I6	Secondary nitroform reactions	Koroban [108] details a possible reaction between nitroform and HNF but it is unclear if this reaction has been detected or not.	No study has been undertaken to assess the further reaction of nitroform within the matrix.

J	Formation of hydrazone, nitroform and water from reaction of N-Nitroso compounds and HNF	As Reaction I3	As Reaction I3
K	Direct, low level reaction of pNMA and HNF	No details	Experimental DSC study has suggested that there is a low level reaction that occurs between HNF and pNMA over long contact times.
L	Formation of 2,4-dinitro-pNMA via direct reaction of pNMA with NOx and HNOx species liberated from thermal degradation of HNF	Sammour et al [87] detail that pNMA is reactive against both NO_2 and HNO_2.	Reaction course explains data achieved.

Table 15 – Assessment of Each Reaction Step Within The Proposed Reaction Scheme

As can be seen from Table 15, some aspects of the hypothesis require further study. Stabiliser depletion data is given below for the propellant analysis. Although undertaken, GPC and Infrared studies were inconclusive in elucidating the reaction course and so are not included within this text.

4.5.1 Stabiliser Depletion

4.5.1.1 Introduction

Section 3.5 indicates a number of positions within the reaction scheme that require further study. One of the critical reaction pathways that have been inferred from the test data is that nitration of 2NDPA and pNMA is occurring (and that this removes direct reaction of HNF with HNOx and NOx species). This is generally concerned with reaction pathways E1-E16 of the reaction scheme given in Figure 160. Studies were focussed on this area of the reaction scheme as this was perceived to be the driving reaction for continued propellant degradation.

4.5.1.2 Experimental

After each storage period, samples were removed from storage, 0.2g samples taken and chopped into pieces with dimensions < 850µm. Extraction of stabiliser residues was undertaken by the "cold extraction" technique of extracting the stabiliser residues by washing the propellant sample with 3 x 50ml aliquots of dichloromethane. Once samples had been washed, they were evaporated to dryness and then made up in an eluant of 50:50 acetonitrile : water for introduction into the HPLC. This technique is an accepted method for extraction of stabiliser residues from propellant samples at ROXEL (UK).

The HPLC apparatus consisted of a Thermo-Finnigan CM4000 Quaternary Pump with Gilson 231 auto injector. The detection method was via use of a Waters 996 Photodiode Array (PDA) Detector. Although providing continuous data on the UV spectrum of species passing the detector, quantitative data analysis was extracted at 254nm;this wavelength is commonly used to monitor detection of

denitration stabilisers.   The mobile phase was a 50:50 mixture of acetonitrile : water with a flow rate of 1ml/min. Sample size was set at 20µl at the autoinjector. The column chosen for the analysis was a Waters Nova Pak C18 60A 4µm, with dimensions 3.9mm x 300mm; column temperature was maintained at 23°C.

Post analysis, comparison of retention time (RT) against a range of derivative standards was undertaken. The RT values were taken as the primary indicator that a derivative had been formed. Where any ambiguity or potential confusion arose (eg where unidentified peaks were observed or where thought to overlap with derivative responses), investigation of the UV trace for any peak was compared against the known standards. Quantification of each derivative was taken from the peak area response at 254nm and corrected for initial sample mass.

4.5.1.3 Results and Discussion

Figures 161 to 167 show representative stabiliser depletion and growth of identified nitrated derivatives within samples aged at 40, 60 and 80°C for 2NDPA and pNMA loaded propellants. Assessment of representative chromatograms gives a method for determining nitration patterns of the denitration stabilisers pNMA and 2NDPA. Figure 161 shows the depletion of 2NDPA in formulation STO2 at 80°C. the figure also shows the growth of various nitrated derivatives. It can be observed that no N-NO-2NDPa has been detected in the extract. This non-detection of N-NO-2NDPA was not unexpected due to the demonstrated high reactivity of the derivative with HNF (ie reaction E8 in Figure 160). However, the reaction course as given in reaction E8 would result in the formation of a hydrazone, Nitroform and water. In itself, this would not lead to the formation of higher C-nitrated 2NDPA derivatives. This implies another mechanism may be occurring in the propellant formulation that leads to the formation of the C-nitrated derivatives.

Although the accepted route for nitration of 2NDPA is via N-Nitrosation followed by rearrangement and oxidation to C-nitro derivatives [73-79] , Sammour et al [87] detail an alternative route. He details a series of reactions of stabilisers in acetonitrile for various nitrosating / nitrating reagents. In these studies it is detailed that 2NDPA reacts readily with HNO_3 (liberated from the equilibrium $N_2O_4 \rightleftharpoons NO^+ + NO_3^-$) to form 2 nitrated products without formation of N-Nitroso derivatives as an intermediate step. He states the formation of 2,4-DNDPA and 2,2'-DNDPA as proof of reaction; he also quotes a similar reaction course for pNMA. In the scheme in Figure 160, a similar reaction course via N_2O_4 was suggested (Reaction L) to explain nitration reactions at lower temperatures for pNMA without large-scale loss of HNF (ie not following reaction B). Initially this appears to give a route by

which conflict with the reactions underlying high rate degradation of 2NDPA loaded formulations occurs via N-Nitros-2NDPA / HNF reaction (ie reaction E4). However, the formation of HNO_3 is via the reaction given in Reaction R36

$$RR'NH \quad + \quad NO^+ NO_3^- \longrightarrow RR'NNO + HNO_3$$
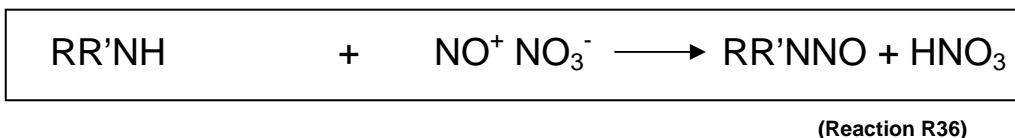
(Reaction R36)

ie producing a mechanism by which N-Nitroso/HNF derivative reactions can occur simultaneously with C-Nitration of the 2NDPA structure. This is proposed to occur at higher temperatures.

Figure 162 shows the progression of nitrated derivatives at 60°C. Comparison against Figure 161 indicates a lower and slower level of conversion of 2NDPA into nitrated derivatives with no derivatives detected above trinitrated products.
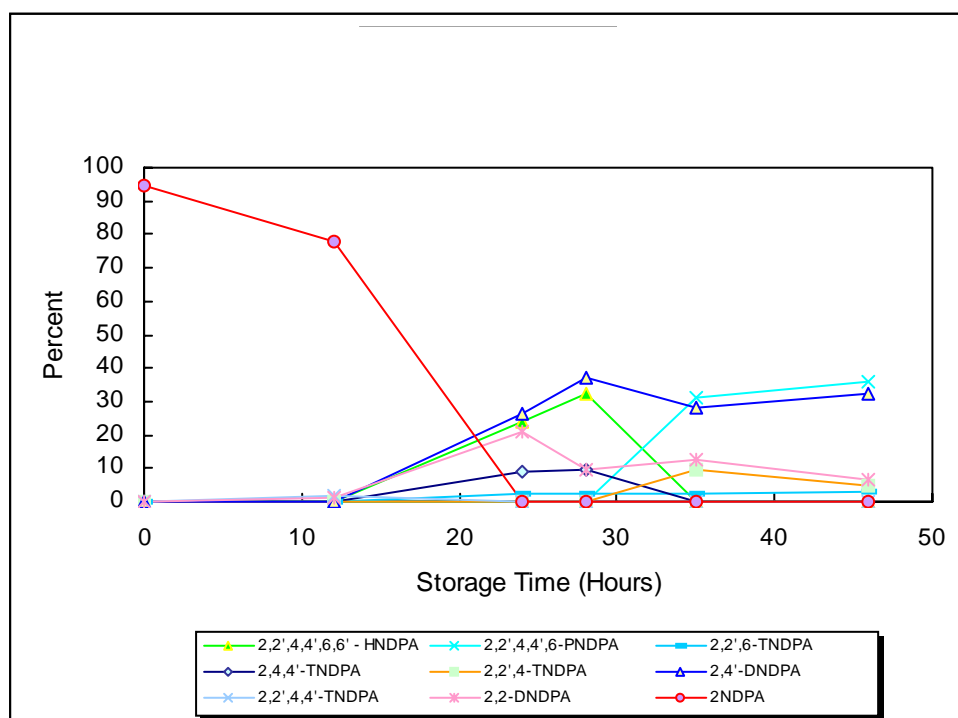
Figure 161 : 2NDPA Depletion in Sample STO2 at 80°C
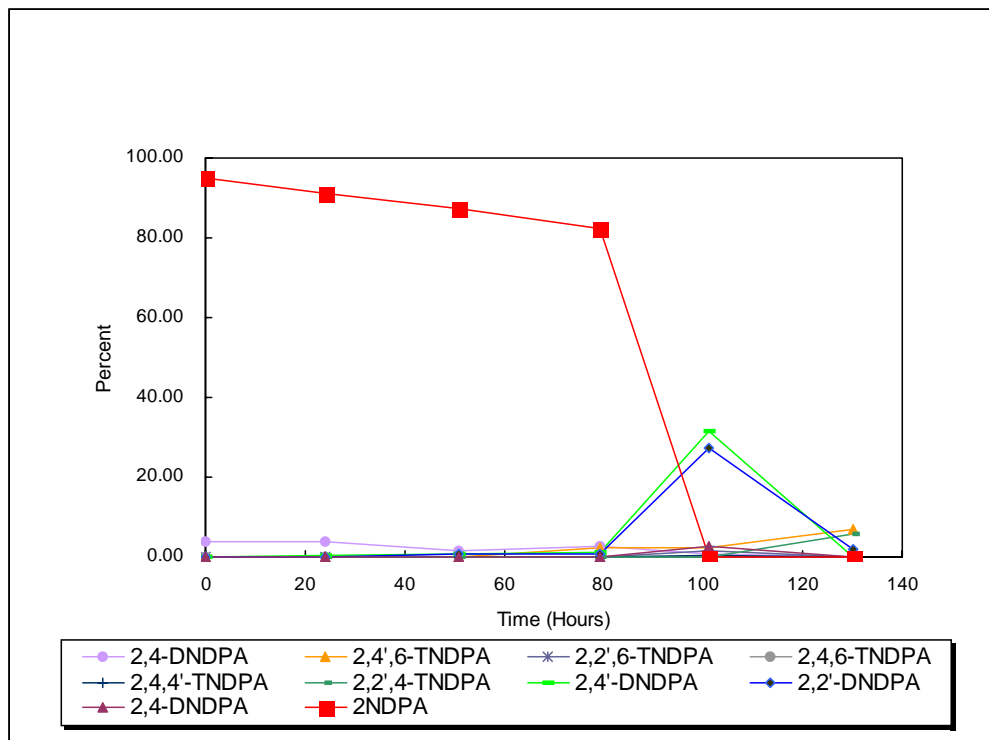
Figure 162 : 2NDPA Depletion in Sample STO2 at 60°C

Figure 161 shows a similar trend with only two nitrated derivatives being detected (Data for storage of STO2 during 40°C storage is not available so results from STO3 (8%) have been included as representative data)
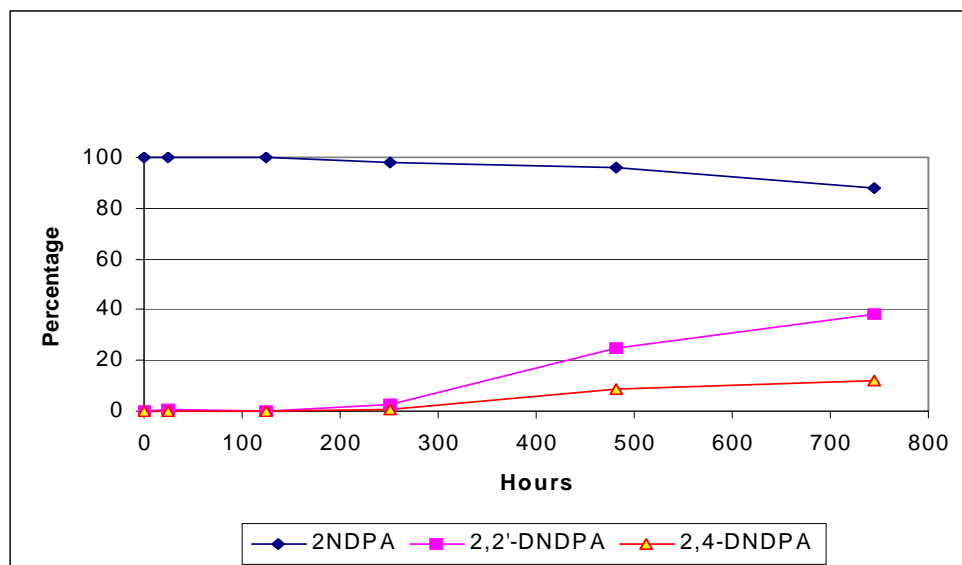
Figure 163 : 2NDPA Depletion in Sample STO3 at 40°C

It is possible to view the nitration patterns in Figures 161-163 as being representative of different sections of the total nitration scheme for the stabiliser. The 40°C data represents the early stages of reaction, the 80°C data the final products and the 60°C data the intermediate

process. Although there are a number of unidentified peaks within the chromatogram (typically eluting at between 2 and 4 minutes), and some co-elution of peaks is also observed, correlation of RT values and UV spectra against standard nitrated derivatives generally indicate that derivative formation follows the stepwise nitration schemes detailed in Section 1.3.2. Sampling frequency of the storage trials is insufficient to capture all steps within the stabiliser degradation mechanism but suggests overall reaction schemes for 2NDPA stabilised polyNIMMO / HNF propellant as given in Figure 164. This appears to confirm that the activity of the dinitro species of 2NDPA to give some degree of added stability until tri- and tetra-nitro derivatives form as was found by Ammann. [133] . A similar analysis for pNMA depletion can be carried out for pNMA stabilised formulations; Figures 165-167 show the data and Figure 168 shows the derivative growth.
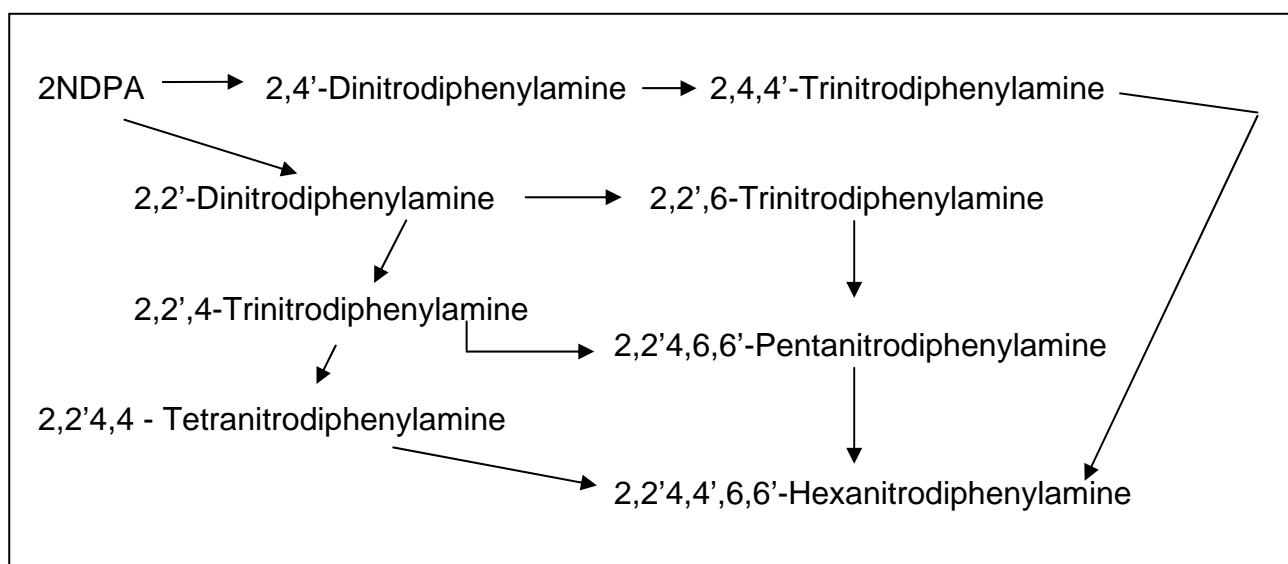
Figure 164 – Nitration Scheme of 2NDPA Within Ageing of HNF / PolyNIMMO Propellant
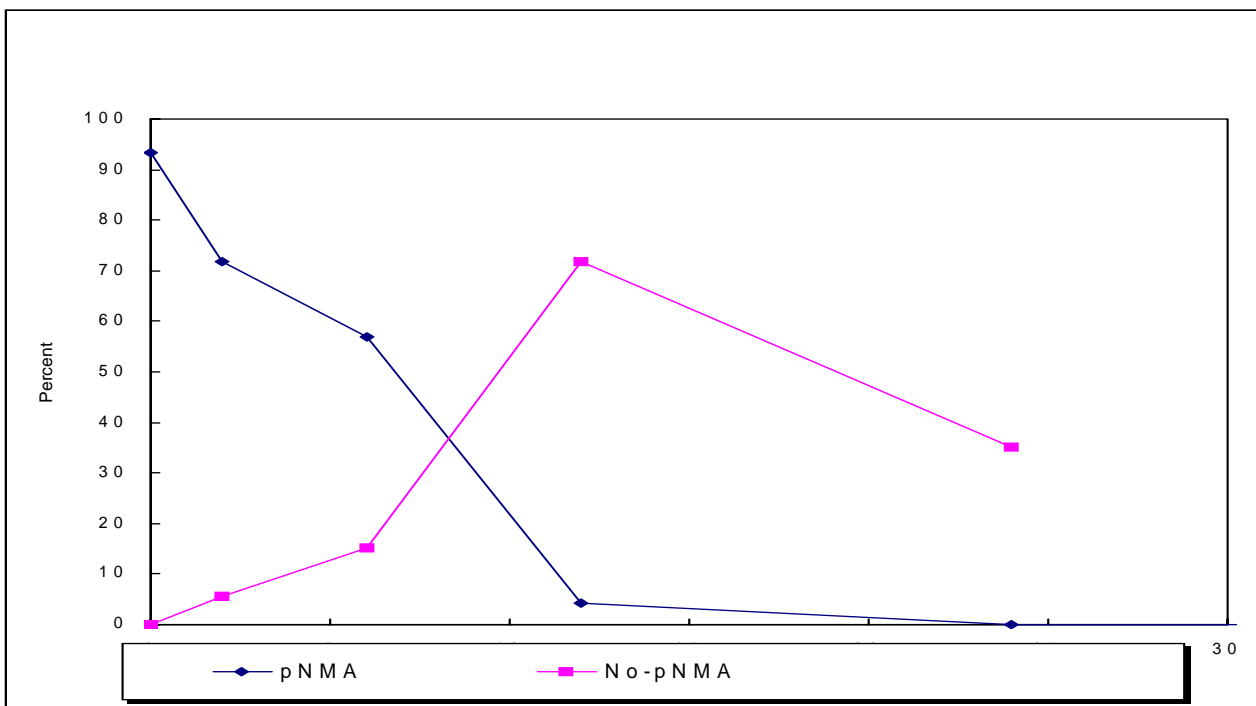
Figure 165 : pNMA Depletion in Sample STO5 at 80°C

Figure 165 shows an interesting trend that is observed solely in the stabiliser data for formulation STO5 at 80°C. The growth of the sample response relating to N-NO-pNMA from pNMA depletion has occurred early within the storage period and then started to decrease. A possible co-elution of Di-NO$_2$ pNMA with N-Nitroso-pNMA (RT 4.95min and 4.84min respectively) might explain this decrease in N-Nitroso concentration with the decrease relating to differences in extinction coefficient at the monitoring wavelength. However, the UV plots of the eluted peak after analysis does not show any evidence of co-elution of the two species N-Nitroso-pNMA (λ max = 211nm, 263nm, 355nm) and 2,4-dinitro-pNMA (λ Max = 218nm, 310nm). This decrease is therefore proposed to be due to removal of N-NO-pNMA by HNF to form a hydrazone (Reaction E7 of Figure 160). It is interesting to observe that the HNF / N-NO-pNMA reaction does not appear to occur until all pNMA has reacted. This likely reflects the low level of reaction that is seen to occur between HNF and N-NO-pNMA (Section 2.4.4.2). This lack of formation of 2,4-dinitro-pNMA during reaction with NOx species was detailed by Sammour et al [76] [80] . This tendency against rearrangement to the 2,4-dinitro derivative plus the lower reactivity of HNF / N-NO-pNMA may also explain why N-NO-pNMA is retained within the propellant formulation until late within the ageing period. It is also apparent that the NOx / pNMA (reaction E5 of Figure 160) is more aggressive / dominant than the NOx / HNF reaction (reaction E4). Only

once pNMA / NOx reactivity has fallen does it "allow" HNF to react with the N-Nitroso derivative.
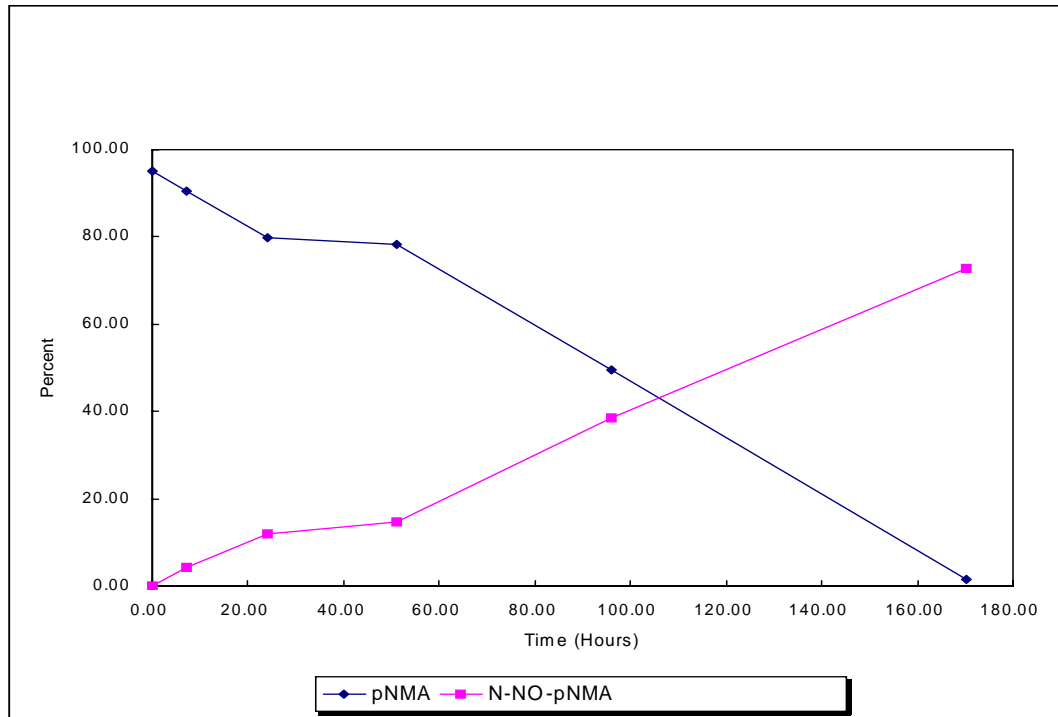
Figure 166 : pNMA Depletion in Sample STO5 at 60°C
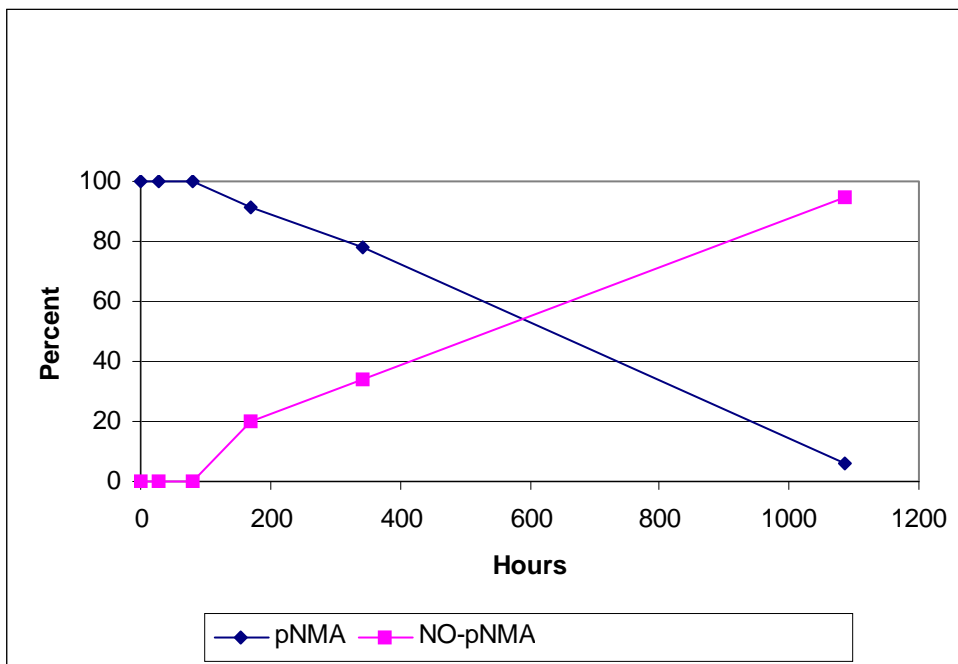
Figure 167 : pNMA Depletion in Sample STO5 at 40°C

$$pNMA \rightarrow N\text{-NO-pNMA} \longrightarrow 2,4 - DiNitromethylaniline$$
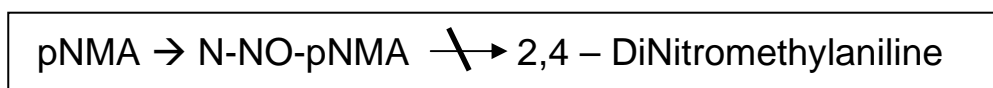
Figure 168 – Nitration Scheme of pNMA Within Ageing of HNF / PolyNIMMO Propellant

Figure 169-171 show stabiliser depletion data from mixed stabiliser systems at 80, 60 and 40°C respectively. The sequential reaction of pNMA followed by 2NDPA is generally evident but there are some deviations. For example, the data for formulation STO10 (8% pNMA / 8% 2NDPA) in Figure 169 shows that the depletion of pNMA and 2NDPA does not occur for up to 12 hours at 80°C. After this time they both appear to start to deplete simultaneously. This apparent simultaneous depletion is likely due to the sampling frequency of the experiment, missing the "between points" data associated with degradation. However, the data at 36 hours storage shows 2NDPA depletion occurs before the activity of pNMA is fully depleted. It is also interesting to note that the rate of 2NDPA depletion is rapid between 36 and 48 hours whereas the rate of depletion of pNMA is near constant. If stabiliser loss was solely via formation of nitrated derivatives, the rate of loss of the dominant stabiliser (pNMA) would be expected to mirror this. This stabiliser depletion profile for formulation STO10 at 80C may be indicative of the transnitrosation reaction proposed by Sammour [84] . Once transnitrosation has been initiated, further reaction occurs rapidly. Where pNMA and 2NDPA levels are not equal (eg formulations STO11 and STO12), the rate of 2NDPA depletion is reduced where

202

the higher pNMA / 2NDPA ratio is present. This again suggests a relationship between 2NDPA and pNMA in their mutual rate of depletion.

At 60°C (Figure 170), the transnitrosation reaction appears to be significantly reduced as depletion of, for example, formulation STO8 (0.5% pNMA / 0.5% 2NDPA) show depletion of pNMA with very little 2NDPA loss. Here sequential reaction appears more evident, indicating pNMA depletion with little (or no) 2NDPA depletion. This appears to confirm that at 60°C, the reaction of NOx species with 2NDPA (reaction E6 in Figure 160) does not occur in the presence of pNMA at 60°C. Combining this with the observation that pNMA reaction with NOx appears more aggressive than HNF / NOx reaction, appears to confirm much of the reaction course after reaction E2 in Figure 160. It also indicates that reaction E5 is dominant over either reaction E4 or E6.

The 60°C data that does show some deviation from the expected sequential reaction is the data for formulation STO12 (2% 2NDPA / 1% pNMA). Figure 170 shows that between the first two sampling periods both stabilisers drop to ~ 60% of their original values. Beyond this 2NDPA content appears to remain constant until pNMA is nearly fully depleted. Once pNMA is fully depleted, the loss of 2NDPA occurs once more and is very rapid. The unusual profile is suggested to relate to the probability of reaction of a "low activity" denitration stabiliser at higher concentration (ie in this sample 2NDPA) compared to one with lower concentration but higher activity (pNMA). The initial drop in 2NDPA level is proposed to be due to the formation of nitrated or nitrosated species (with nitrosated species most likely reacting directly with HNF). This formation of nitrosated / nitrated 2NDPA derivatives reduces the overall concentration of 2NDPA and, eventually, the balance of the relative ratios of

$$\boxed{\frac{\text{activity 2NDPA}}{\text{concentration 2NDPA}}} \quad \text{to} \quad \boxed{\frac{\text{activity pNMA}}{\text{Concentration pNMA}}}$$
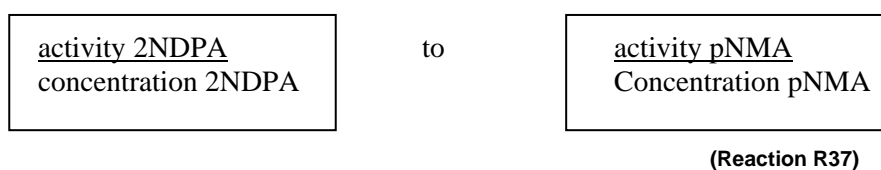
(Reaction R37)

comes to a position where the pNMA side of reaction R37 dominates. At this point, reaction of 2NDPA against NOx species is stopped in favour of NOx reaction with pNMA. Reaction against NOx then continues along the more traditional lines of pNMA depletion eventually followed by 2NDPA depletion once pNMA activity is at zero.

Figures 169 – 17194 show the stabiliser depletion data from mixed stabiliser systems at 80, 60 and 40°C respectively. The sequential reaction of pNMA followed by 2NDPA is evident, being observed most clearly in Figure 170.
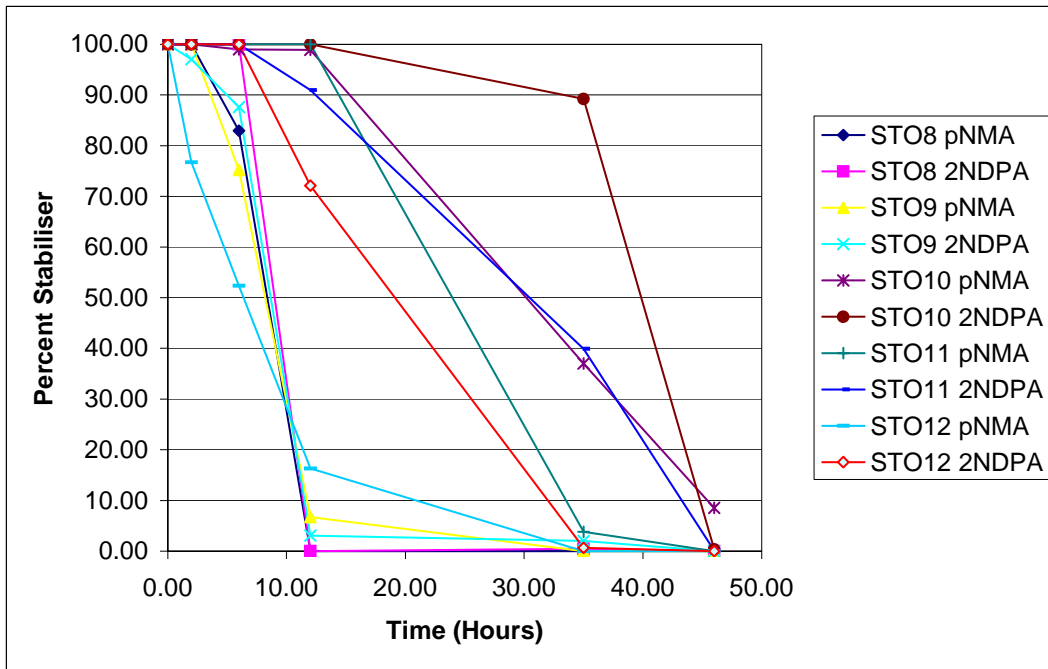
Figure 169 – Mixed Stabiliser Depletion at 80°C
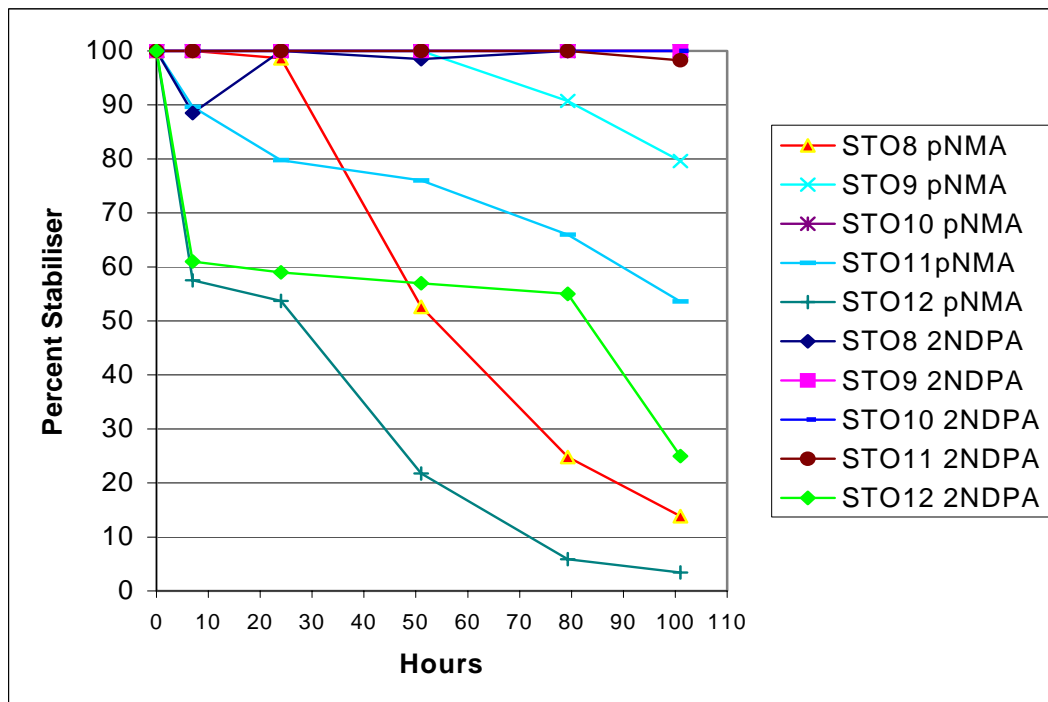
Figure 170 – Mixed Stabiliser Depletion at 60°C

Figure 171 shows the depletion of the denitration stabilisers at 40°C shows a different pattern compared to the 60°C data given in Figure 170. The 60°C data appeared to suggest that the rate of nitration of the stabilisers had reduced compared to the rate at 80°C. Reducing the temperature further to 40°C would have been expected to further reduce this rate of stabiliser nitration. Figure 171 appears to generally agree with this suggestion. At the end of the storage period at 40°C, depletion of the denitration stabilisers has occurred to a level similar to that at 60°C. The general observation of the 2NDPA data in Figure 171 is that (with the exception of formulations STO11 and STO8), some drop in 2NDPA level has occurred with any drop generally coming to a plateau. This suggests that the 2NDPA reactions have also reached an equilibrium within the formulation. In formulation STO8 (0.5% pNMA / 0.5% 2NDPA) , there is shown rapid depletion of 2NDPA without pNMA coming to a minimum; in formulation STO11 (2% pNMA / 1% 2NDPA), pNMA depletion is lower than in other samples with 2NDPA showing little or no reduction in concentration. Comparison of these observations with the data in Table 14 shows that formulations containing 2NDPA show higher mass loss than pNMA analogues with formulation STO12 showing the highest and formulation STO11 the lowest. The data in Figure 171 suggests that 2NDPA in formulation STO11 is protected by the higher ratio of pNMA to 2NDPA. This ratio also gives greater protection when found in formulations with higher overall stabiliser levels in 1:1 pNMA :2NDPA ratio (eg formulation STO8, STO9 and STO10). This implies that the transnitrosation reaction detailed in the hypothesis in Figure 160 has not achieved equilibrium in the formulation STO11. This appears to support the observation for 60°C data for formulation STO12 and suggests that reaction R37 is occurring. This may provide an explanation of the plateau formed in Figure 171. Ammann [133] highlights that the stabiliser activity is encountered for derivatives up to tri- and tetra-nitrated derivatives of 2NDPA. At high concentration of NOx/ HNOx species (eg during ageing at 80°C), the activity / concentration relationship proposed and as detailed in Reaction R37 is less evident. However, as the concentration of NOx and HNOx species decrease at lower temperature, the relationship becomes more important. Figure 172 shows that 2NDPA initially shows depletion and then reaches an equilibrium position. It is proposed that this equilibrium relates to the balance of activity : concentration for 2NDPA and the activity : concentration for a derivative (eg 2,2'-DNDPA or 2,4-DNDPA). This would help explain the plateau regions observed in the 40°C data that are not observed at 80°C and only at higher pNMA / 2NDPA ratios at 60°C.
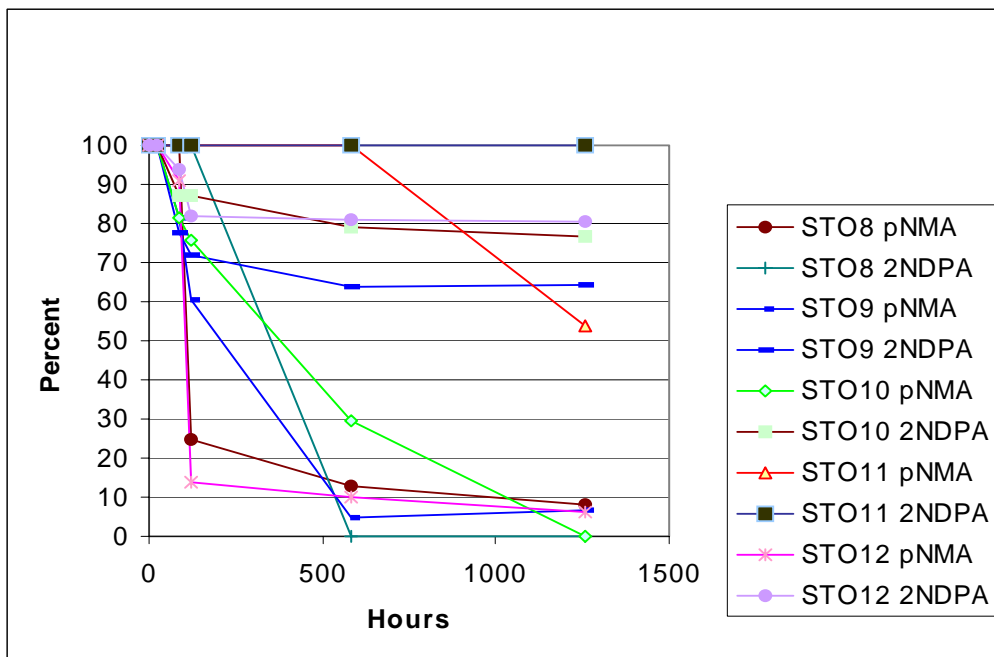
Figure 171 – Mixed Stabiliser Depletion at 40°C
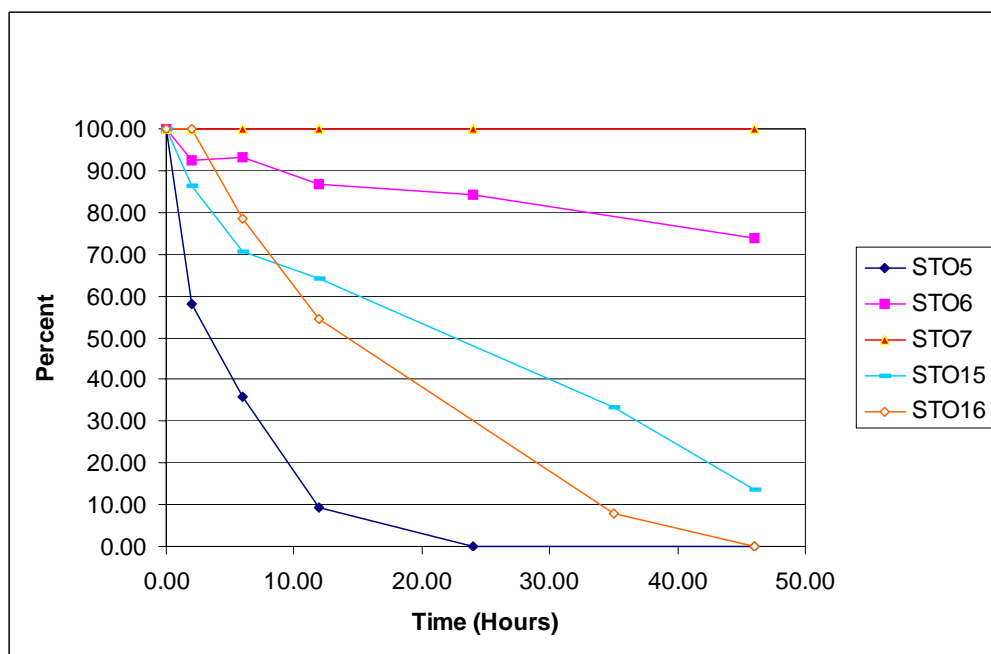
Figure 172 – pNMA Depletion at 80°C

Figures 172 – 175 shows the depletion of pNMA from sample at 80, 60 and 40°C respectively. The result from STO7 indicates that little or no depletion of pNMA has occurred in this formulation. The data in Table 14 confirms the very low level of reaction that has occurred in the sample. From Figure 160 this implies that the presence of pNMA reacts via NOx / HNOx species (Reaction E5) to successfully compete with and dominate Reaction E4 (HNF / NOx). However, the lack of depletion of pNMA in sample STO7 implies that little NOx or HNOx has been liberated at any time during the ageing process. This does not fit with the hypothesis in Figure 160 which implied that at 80°C, reaction D would occur in all

samples at a high rate to liberate NOx and HNOx species (via reaction E1). Although the pNMA / NOx reaction (reaction E5) appears to be occurring in formulations STO6 and STO5, the lack of similarity in STO7 implies an alternative reaction course is present.
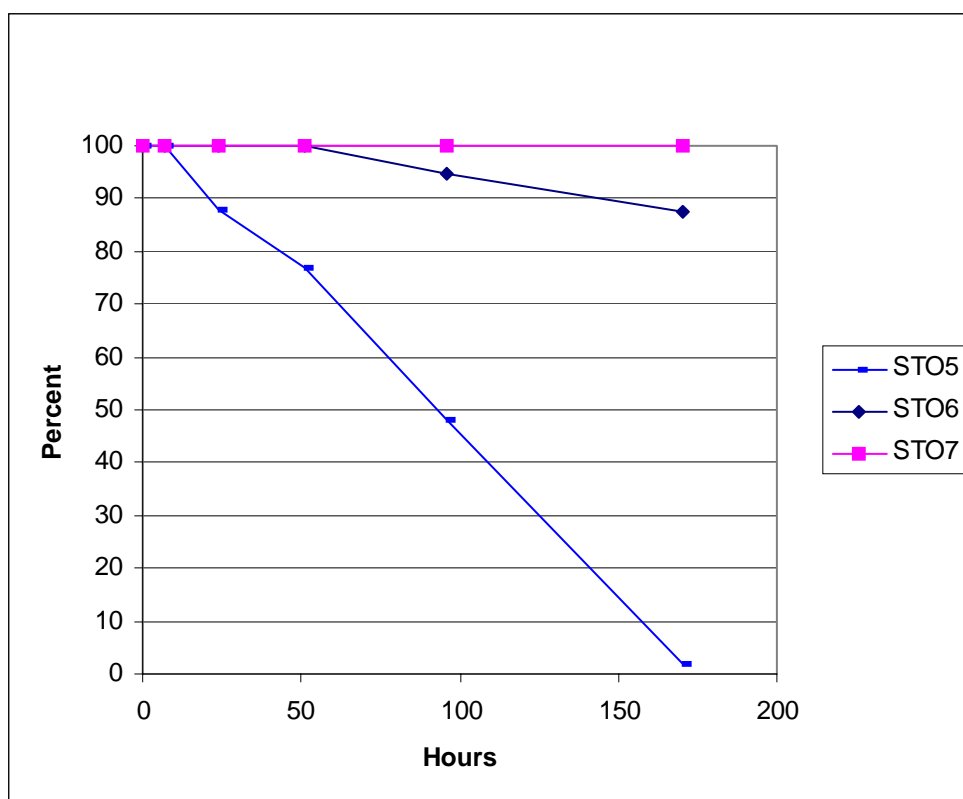
Figure 173 – pNMA Depletion at 60°C

Figure 151B showed the change in pH with ageing of HNF. Bellerby et al [104] have highlighted the production of nitrous acid and the possibility of an hydrazoic acid intermediate (reaction A1) from HNF of Figure 160 to form acidic species. pNMA has a basic pH character and it is possible that the higher concentration of stabiliser in the formulation STO7 serves to inhibit acidic reaction products from being formed at Reaction A. The work of Pai Verneker [109] highlights that liberation of acidic species is a key step in the thermal decomposition of hydrazinium perchlorate and that removing acidic species would be expected to reduce decomposition of the hydrazinium ion. The work of Schoyer [44] has shown that Magnesium Sulphate and Calcium Carbonate help inhibit the initial decomposition of HNF and that this also may be due to the removal of acidic species. This control of low pH initially appears to conflict with the work of Brown et al [107] who advocate addition of phosphoric acid to stabilise HNF. However, the various forms of phosphoric acid give different levels of dehydrating power and overall acidity [136] so in combination my function by modification of reaction B. All the reactions highlight that the control of pH is important and, although unproven, the basicity of pNMA must be considered as an active function of the

stabiliser when in large excess. If true, the pH of the hydrazine scavengers investigated would also be expected to be important.

Figure 173 shows the action of the hydrazine scavengers on pNMA depletion. It can be seen that although ammonium peroxodisulphate (in formulation STO16) initially leads to retention of pNMA, once depletion occurs, the rate of depletion is more rapid than in the Sodium Sulphite analogue (STO15). Comparison with Figures 70 and 97 show the higher rate of reaction of STO16 compared to STO15 following the start of depletion of pNMA. For the hypothesis in Figure 160, this suggests that ammonium peroxodisulphate is a more aggressive reactant at positions B1 and C1 than sodium sulphite but sodium sulphite reacts with more liberated hydrazine / water.

The data at 60°C (Figure 172) shows a similar form to that of the 80°C data although all samples show an induction period prior to commencement of depletion. This induction period is proposed to be due to the low level of thermal decomposition of HNF (ie Figure 160 Reaction A) predicted at this temperature. This reduces the formation of NOx and HNOx species at reaction E1. However, once depletion of stabilisers is initiated, the rate is fairly constant. This implies that, even though not evident from the data in Table 14, that the removal of NOx by the stabiliser does encourage further reaction in the propellant (Possibly encouraging denitration via drawing reaction E to the right).

Figures 174 shows depletion of pNMA at 40°C. The figure shows the greatest deviation of all formulations tested from the predicted reaction course with NOx. Liberation of NOx / HNOx species is predicted to be the lowest at 40°C in all test formulations and samples STO5 and STO6 show similar reaction profiles to the data at 60°C and so do follow the expected pattern of reaction. However, formulation STO7 has inverted its apparent efficiency with STO6, with STO7 now showing a high level of depletion. This implies that the reaction of pNMA in this formulation is not via reaction with NOx / HNOx species but via an alternative route. This reaction appears to confirm reaction K of Figure 160 whilst inferring that the pH benefits observed at 60°C are not evident here (presumably due to the lower level of acidic species liberated via Reaction A at this temperature). The additional reaction does not help to elucidate the reaction products or mechanism of the reaction.
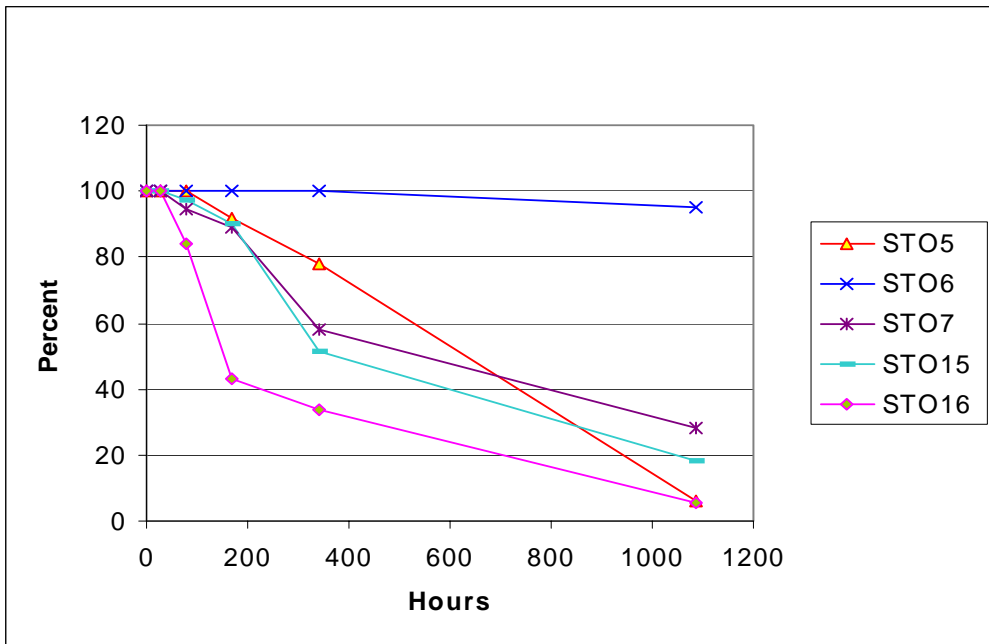
Figure 174 – pNMA Depletion at 40°C

Figures 175, 176 and 177 show 2NDPA depletion at the various test temperatures.
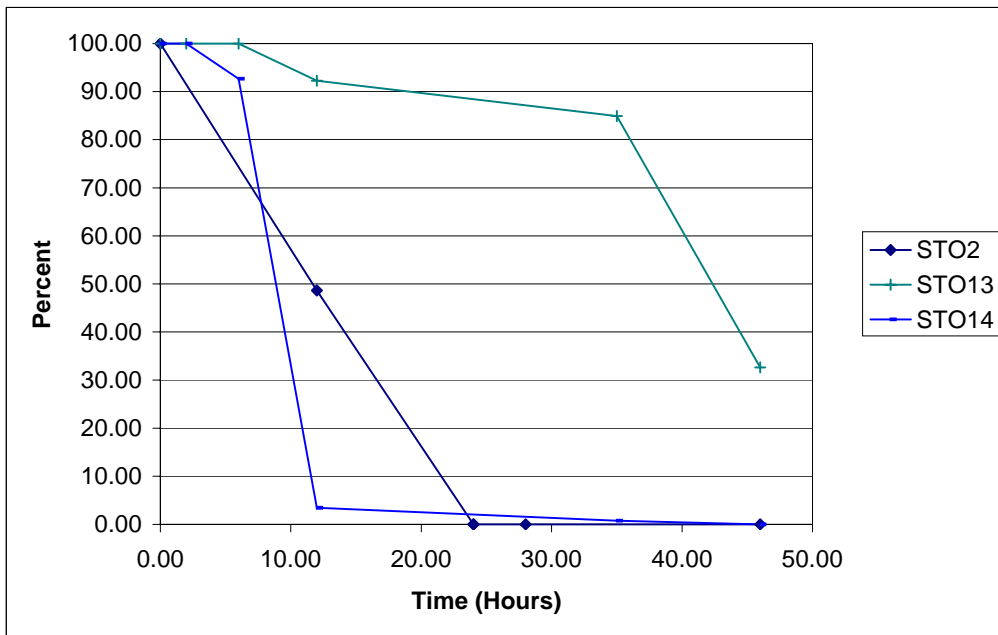
Figure 175 – 2NDPA Depletion at 80°C
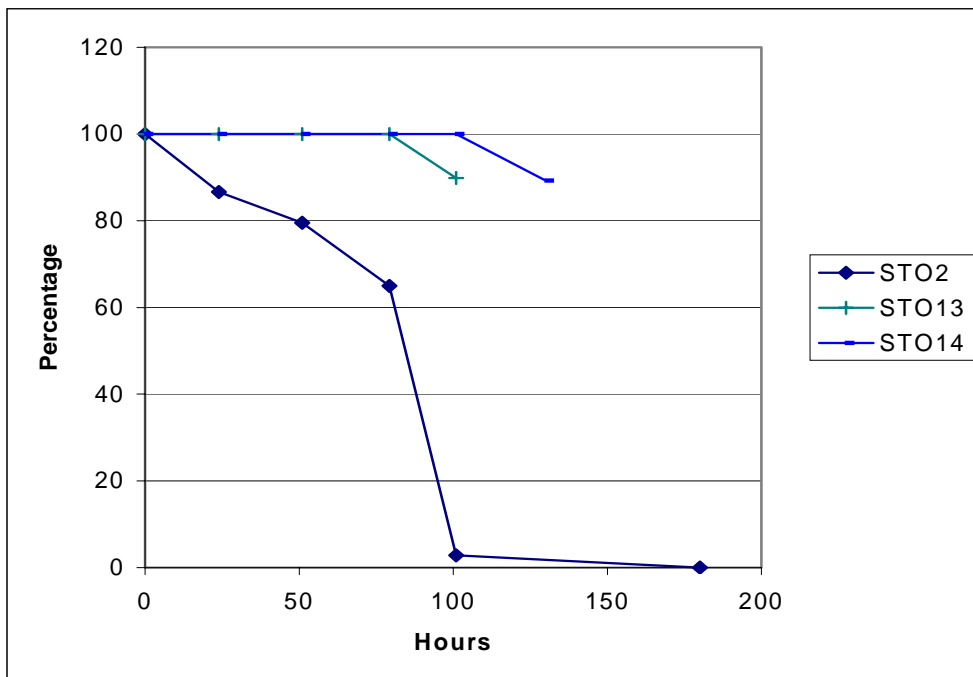
Figure 176 – 2NDPA Depletion at 60°C

Few samples loaded with 2NDPA as a sole stabiliser survived storage at 80°C and as a consequence, comparison of data in Table 14 is difficult. The result from formulation STO2 (1% 2NDPA) at 80°C in Figure 175 does show rapid depletion of 2NDPA but it is not possible to infer whether this is via N-Nitroso formation or not. The results in Figure 175 show that at 80°C a more interesting result are those from formulations STO13 and STO14 incorporating the hydrazine scavengers. From Figure 175, it can be seen that the presence of sodium sulphite has encouraged retention of 2NDPA for far longer during the ageing period compared to Ammonium Peroxodisulphate but there has still been a reduction in the overall concentration of 2NDPA. This does not fit in with the hypothesis given in Figure 160 but again suggests an alternative route to 2NDPA nitration without going via reaction B or C. Introduction of the reaction given in Reaction R36 provides an explanation of this nitration. The more rapid depletion of 2NDPA in STO14 is proposed to occur via exhaustion of reaction B / C leading to extensive denitration of the polyNIMMO chain in addition to reaction R36. The data for 60°C (Figure 176) and 40°C (Figure 177) follow a similar path to that described for the 80°C data for 2NDPA depletion.

210
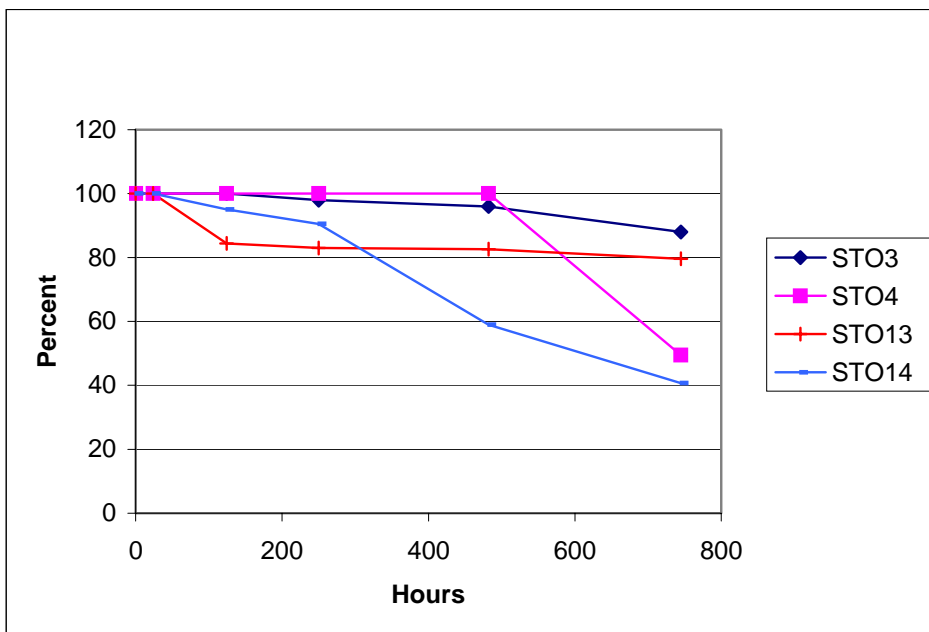
Figure 177 – 2NDPA Depletion at 40°C

4.5.1.4 Conclusions from Stabiliser Depletion Data

Assessment of the stabiliser depletion data indicates that the reaction course of the denitration stabilisers pNMA and 2NDPA follow the expected nitration route for these materials with NOx and HNOx species. The pH of pNMA is thought to be contributing to inhibiting the reaction course when present in excess

Incorporation of the various additional mechanisms identified in the stabiliser depletion data analysis into the overall hypothesis leads to the modified scheme given in Figure 178

211

+ XS pNMA   pH Control   + O$_2$ A2 → **N$_2$O + H$_2$O**   + pNMA or 2NDPA   L
NO$_2$ / N$_2$O$_4$ I2   + (NH$_4$)$_2$S$_2$O$_8$

HNF   A →   N$_2$H$_4$ + HN$_3$ + N$_2$ + ANF + HNO$_2$ I1

B   I3   + PN   ANF

Minor   A1   I4

+ Na$_2$SO$_3$ or (NH$_4$)$_2$S$_2$O$_8$ Polyurethane + NF

C   B1   Trapping / Removal of Water   HO-Z +

Release of Water   + HNF   Y-N-C=O   C(NO$_2$)$_3$

+ Na$_2$SO$_3$ or (NH$_4$)$_2$S$_2$O$_8$ B2   B4   Secondary NF Reactions

C1   Hydration Limit of Scavengers Achieved   I5

+ HNF   Polyurethane Exhausted   I6

Reaction Limit of Scavengers Achieved

J   B3   Support for Ionic Dissociation / Solvation   Polymer Degradation   Hydrazone Formation + Nitroform + Water

+ PN   + PN

HC(NO$_2$)$_3$ +   D   H   H + NO$_2$ →   + H$_2$O   E1   HNO$_2$ ⇌   E2   N$_2$O$_3$ + H$_2$O   Unexplained Reaction

HNF + PN   N   F   E3   + PN

D1   N$_2$O$_4$ NO$^+$ + NO$_2$$^-$ Degraded HNF / pNMA

H   G   H   K   J

O   + HNF

Bridging H-Bonds   C   + HNF   + pNMA   + 2NDPA

polyNIMMO Polymer Backbone   E4   E5   N-NO-pNMA   E6   N-NO-2NDPA

I   + 2NDPA Transnitros   + HNF

H1   + NOx   E7   + HNF   E8   + NOx   E13

E14   E9   E10   E12

E11   + Na$_2$SO$_3$ or (NH$_4$)$_2$S$_2$O$_8$

E15   C-Nitro Derivatives of 2NDPA   E16

H   H   Di-nitro-methyl aniline

+ H$_2$O   H   NO-N—N-H$^+$ $^-$C(NO$_2$)$_3$ XS NOx / HNOx   + NOx / HNOx

HC(NO$_2$)$_3$ + HONNHNH$_2$ + HNO$_2$ + HN$_3$ + NO$^+$ NO-N   N-H   Activity of Denitration Stabilisers Fully Depleted

H   H
(Intermediate)

— = Does not Occur

X = Reference Point for Discussion in Text   X = Modification to Previous Hypothesis

Figure 178 – Overall Proposed Reaction Scheme for HNF / polyNIMMO Propellant Degradation

212

5. Conclusions, Recommendations and Further Work

The reaction of HNF / polyNIMMO propellant systems is intimately linked to the chemical ageing properties of crystalline HNF. Colorimetric studies have shown that the liberation of hydrazine occurs during storage but that this is not detected by GC-MS analysis. This hydrazine liberation is proposed to be one of the driving reactions behind propellant degradation. However, although reaction between hydrazine and HNF has been demonstrated (leading to increased solid degradation), the level of gas / solid autocatalysis in the degradation of crystalline HNF appears very low.

GC-MS analysis suggests that the presence (and eventual release) of the crystal impurity, isopropyl alcohol, contributes to the eventual autocatalytic breakdown of the crystal matrix. This may be related to the chemical compatibility data achieved from functional group analysis that suggested that the alcohol moiety was not chemical detrimental to HNF stability unless encountered in a 1,2-diol form. Functional group analysis also highlighted the high level of reaction between HNF and the carbonyl group that was attributed to hydrazone formation through the hydrazinium ion.

Investigations into the chemical compatibility of HNF with nitrosated and nitrated derivatives of 2NDPA and pNMA indicated that the reaction of HNF is most rapid with N-NO-2NDPA but there is also a lower level (but significant) reaction with N-Nitroso-pNMA.. This direct reaction of HNF with N-Nitroso derivatives of denitration stabilisers has an obvious implication on the use of these stabilisers in the presence of HNF and nitrate ester explosives.

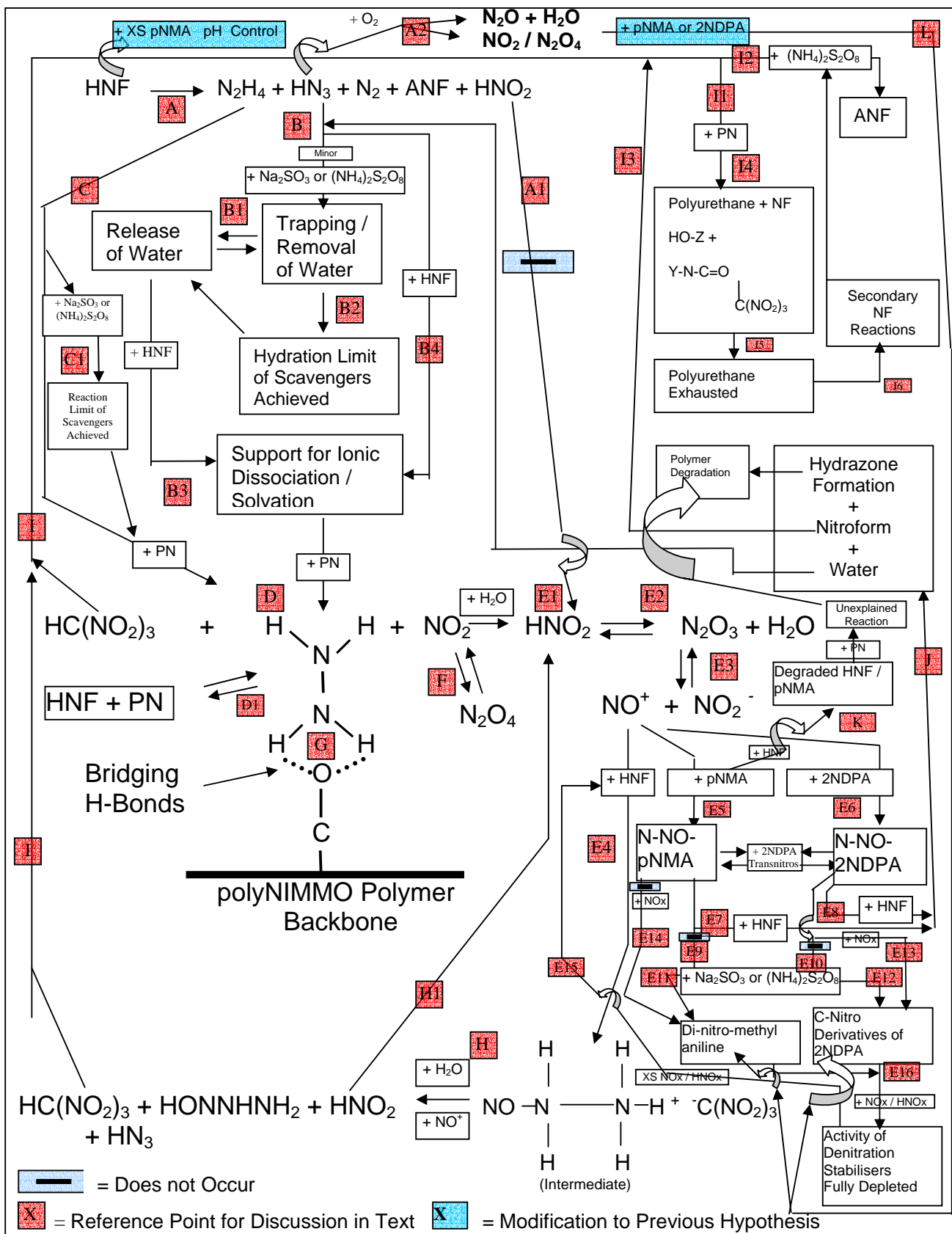Analysis of a range of polyNIMMO / HNF propellants has allowed development of a general hypothesis for propellant decomposition. This hypothesis has been built on the data available within literature with the addition of detailed analysis of analytical results achieved during this program of work; this final hypothesis is given in Figure 178. The data has indicated that the degradation of polyNIMMO / HNF propellants is a complex process involving a number of interrelated and interdependent reactions, some of which suggest autocatalysis will be present if reaction initiation is not controlled. The reactions vary in their relative dominance in the overall reaction scheme with storage temperature and details of this are given in the text.

At 80°C there appears to be a significantly different reaction rate for propellant degradation compared to either 60°C or 40°C suggesting a mechanism change at this temperature. The critical aspects of the reaction mechanism at all temperatures identified are :-

1) Removal of NOx / HNOx species by denitration stabilisers to minimise direct reaction of HNF/NOx

2) Formation of N-NO derivatives of the denitration stabiliser 2NDPA is detrimental to propellant longevity due to high reactivity between this derivative and HNF. The analogous reaction of N-NO-pNMA is significant but has lower direct reactivity with HNF

3) HNF catalyses denitration of polyNIMMO and increase denitration rate possibly via the formation of a polyNIMMO / hydrazine complex.

4) HNF shows decomposition within propellant formulations almost independent of polymer degradation until late within the sample storage period.

5) Control of hydrazine liberation from HNF thermal decomposition by addition of hydrazine scavengers is a second critical degradation mechanism to control

At 80°C, control of reactions (1) and (5) appear to be the most affective at improving propellant longevity; the use of a 1% anhydrous sodium sulphite + 1% pNMA mixed stabiliser system has shown promise for use in propellant formulations up to temperature of 80°C. This type of stabiliser system serves to control propellant degradation by controlling each branch of the degradation so limiting progression of secondary reactions. Some level of success in stabilisation has also been achieved using very high levels of pNMA within the propellant formulation. However, the levels required to achieve the observed improvements in stability would be detrimental to the propellant performance (in terms of overall propellant energy) and so is not as desirable as the use of pNMA + anhydrous sodium sulphite.

At lower temperatures, liberation of NOx and HNOx species appears significantly reduced; this in turn appears to lead to an increase in dominance of reactions (2) (especially in 2NDPA based formulations) and (5).

Overall, results imply that the use of HNF within military tactical missile systems would be difficult due to the apparent change in reaction course at 80°C. However, possible incorporation of HNF into civilian or strategic systems would appear to be a viable goal for future studies.

A number of areas of further investigation remain concerning the decomposition of HNF and HNF based PolyNIMMO propellants. It is suggested that future work be focussed closely on the following :-

1) Interaction of hydrazine scavengers on IPA in the presence of HNF and the mechanism by which this reaction promotes propellant decomposition. Other grades of HNF (eg COOL or Solvent / Non-solvent grade) are likely to be recrystallised in the absence of IPA (or conversely they may have different levels of IPA contamination within the crystal). Investigation of the relationship between initial level of IPA contaminant, time to release of the impurity from the crystal matrix and the degree of acceleration observed following release of the impurity would be beneficial.

2) Assessment of co-precipitation of anhydrous sodium sulphite with HNF to assess the effect of more intimate molecular mixing on stability. If control of hydrazine formation is one of the driving forces for improved HNF stability, the more intimate the contact between crystals of HNF and hydrazine scavengers, the more closely controlled the further reaction of any hydrazine liberated. Co-precipitation of the scavenger with HNF would provide the most intimate of mixing conditions to allow assessment of this possible effect. A similar study could be undertaken with the denitration stabiliser pNMA.

3) Assessment of the direct reaction of HNF with NOx and HNOx species. The direct reaction of NOx and HNOx with HNF has been identified as one of the major drivers towards HNF breakdown within the propellant matrix. However, the driving reagent for this reaction (eg NO_2, NO, N_2O, HNO_2, HNO_3 etc) has not been clearly identified. Investigation into the effect of introduction of each of these potential NOx and HNOx species onto an HNF crystal surface (and study of any reaction products) would help elucidate the extent of chemical incompatibility of the analytes.

4) Determination of the "critical" temperature at which the comparatively benign low temperature mechanism for propellant breakdown changes to the more aggressive / detrimental mechanism observed at 80°C. It has already been proposed that a change in reaction mechanism occurs at some storage temperature between 60°C and 80°C. Further studies at temperatures between these two values would help focus on the temperature dependence of the dominant reactions and would further elucidate the temperature dependence of each reaction course within the propellant systems.

5) Assess the effect of denitration stabiliser ratio on overall stabiliser efficiency and apply the findings to introduction of anhydrous sodium sulphite in propellant systems. There appears to be a relationship between the 2NDPA :pNMA ratio in the HNF / polyNIMMO propellant systems and the efficiency of those stabiliser systems. This ratio effect has been assigned to a relationship between the concentration of a stabiliser and its efficiency at removal of NOx and HNOx species. There is also a likely effect from the overall stabiliser ratio within any optimised ratio. Further studies into the effect of alternative pNMA : 2NDPA ratios on propellant stability, over a range of overall stabiliser concentrations and also the potential effect of other

nitrated derivatives (eg 2,4-DNDPA) or alternative stabilisers (eg Akardites) would be beneficial to investigate this effect further.

6) Further analytical investigation and identification of the polyNIMMO / HNF, polyNIMMO / Hydrazine and, polyurethane / nitroform intermediate structures proposed to be formed during the ageing process. HPLC analysis showed that a range of unidentified products was present within a dicholoromethane extraction, thus suggesting that dichloromethane extraction followed by Thin Layer Chromatography might be a viable route towards separation and identification of the various reaction products.

7) Identification of the chemical effect of hydrazine scavenger addition and the products formed from these scavengers during the ageing process. Although the overall review of test data suggests that the primary function of the hydrazine scavengers is not centred on their oxidising power nor dessicatting power, further study of the products formed from HNF / scavenger reactions would be beneficial to elucidate the reaction course.

References

[1] "Current Strands of Research in DERA on the Chemistry of Energetic Materials and Insensitive Munitions" : S.P.Philbin. Insensitive Munitions and Energetic Materials Technology Symposium NDIA Nov 2000 San Antonio.

[2] "Properties of Hydrazinium Nitroformate" : M.Van Zelst, A.E.D.M van Der Heijden. 31st International Conference Of Ict June 27 June 30 2000 Energetic Materials Analysis Diagnostics And Testing, Karlsruhe, Germany, Poster 8

[3] "New Ingredients and Propellants" : A.Sanderson. American Institute Of Aeronautics And Astronautics, Solid Rocket Technical Committee Lecture Series : Reno, Nevada, USA (1994)

[4] "Energetic Polymers as Binders in Composite Propellants and Explosives" : M.E.Colclough, H.Desai, R.W.Millar, N.C.Paul, M.J.Stewart, P.Golding. Polymers and Advanced Technologies, Vol 5, pp554-560

[5] "Development of HTPB Propellant For Ballistic Missiles" : G.Thompson, E.E. Day Technical Report Air force Rocket Propulsion Laboratory (AFRPL) Report No: AFRPL-TR-75-23, May 1975

[6] "Reality of Environmental Implications of Operational Solid Rocket Propellants" : A.J.McDonald. American Institute Of Aeronautics And Astronautics, Solid Rocket Technical Committee Lecture Series : Reno, Nevada, USA (1994)

[7] "Atmospheric Effects of Chemical Rocket Propulsion" : A.E.Jones. American Institute Of Aeronautics And Astronautics Workshop, Sacramento, June 1991

[8] "Scavenger Propellants" : R.R.Bennett. American Institute Of Aeronautics And Astronautics, Reno, Nevada, USA (1994)

[9] "Solid Rocket Plumes" : A.C.Victor. Tactical Missile Propulsion , American Institute Of Aeronautics And Astronautics, Solid Rocket Technical Committee Lecture Series, Progress in Astronautics and Aeronautics Volume 170, Chapter 8 (1996)

[10] "Stabilisation of Nitroform Salts" : J.A.Brown, C.L.Knapp. US Patent 3,384,674 (1968)

[11] Data generated using RO program CET_PLUS utilising NASA-LEWIS Thermodynamic code CET89.

[12] "Decomposition and Flame Structure of Hydrazinium Nitroformate" : J.Louwers, T.Parr, D.Hanson-Parr. American Institute Of Aeronautics And Astronautics Paper 99-1091, Reno, NV, Jan 1999

[13] "First Experimental Results of an HNF / Al / GAP Solid Rocket propellant" : H.F.R Shoyer, A.J.Schnorhk, P.A.O.G Korting. 33rd AIAA/ASME/SAE/ASEE Joint Propulsion Conference July 1997 Seattle. AIAA Paper 97-3131.

[14] "Hydrazinium Nitroformate Propellant Stabilised with Nitroguanidine" : G.M.Low, V.E.Haury. US Patent 3, 658,608.

[15] "Improvement of Hydrazinium Nitroformate Product Characteristics" : M.J.Rodgers, A.E.D.M van der Heijden, R.M.Geertman, W.Veltmans. International Meeting of ICT (1999) p55

[16] "Hydrogen Peroxide Based Liquid - Solid Fuel Hybrid Propellant Systems for Rockets" : A.J Cesaroni, M.J Dennett. US Patent Application US 2002-44473 20020110

[17] "Development of a Liquid Propellant Microthruster For Small Spacecraft" : R.A Yetter, V.Yang, D.L.Milius, I.A.Aksay, F.L Dryer. Chemical and Physical Processes in Combustion (2001) p377-380.

[18] "Decomposition of Different Monopropellants at Laboratory Level Methodology, Experimental Results and Performance Calculations" : R.Eloirdi, S.Rossignol, D.Duprez, C.Kappenstein, N.Pillet, A.Melchior. Proceedings of the First International Conference on Green Propellants for Space Propulsion. ESA Special Publication SP-484, p148-155

[19] "Liquid Oxidisers and Their Use in Hybrid Propellants for Rockets" : Y.Takishita, H.Shibamoto, T.Onda, T.Kuwahara. Jpn Koka Tokkyo Koho (2002). Japanese patent application JP 2002020191

[20] "Industrial Benefits of Applying HNF in Monopropellant Satellite Propulsion" : M.Fick, P.Schiebener, J.L.P.A Moerel, R.P Van der Berg, H.M Sanders, W.H.M Welland Veltmans. Proceedings of the First International Conference on Green Propellants for Space Propulsion. ESA Special Publication SP-484, p138-147

[21] "Monopropellant Formulations for Gas Generation or Propulsion of Spacecraft, Submarines and Jet Aircraft" : R.P Van Der Berg, J.M Mul, P.J.M.Elands. European Patent Application EP-98-201190.

[22] "On the Dense Packing of Particles : An Introductory Discussion" : C.E.Hermance. Chemical and Physical Processes Combustion 1991 p115-1 to 115-4

[23] "Method of Preparing Hydrazine Nitroform" : F.W.M.Zee. World Patent Reference WO 94/10104

[24] "First Experimental Results of an HNF / AL / Gap Solid Rocket propellant" : H.F.R Shoyer, A.J.Schnorhk, P.A.O.G Korting, P.J.Van Lit , American Institute Of Aeronautics And Astronautics paper 97-3131, Seattle, 1997

[25] "Development of hydrazinium nitroformate Based Solid Propellants" : H.F.R Shoyer, A.J.Schnorhk, P.A.O.G Korting, , American Institute Of Aeronautics And Astronautics paper 95-2864, San Diego, 1995

[26] "New Solid Propellants Based on Energetic Binders and HNF" : G.Gadiot, H.F.R Shoyer, A.J.Schnorhk, P.A.O.G Korting, P.J.Van Lit IAF paper IAF 92-0633, 1992

[27] "HNF Crystallisation" : W.H.M Veltmans, F.J.M Wierckx. World Patent Application 99200592.6

[28] "The Effect of Different Crystallisation Techniques on Morphology and Stability of HNF" : W.H.M Veltmans, A.E.D.M Van der Heijden, J.M.Bellerby, M.I.Rodgers. 31st International Annual Conference of ICT, Karlsruhe (Germany), June 2000 P22.

[29] "Countercurrent Flow Column With Heating and Cooling Zones for Prilling of Explosives" : T.K Highsmith, H.E Johnston US Patent Application US-6610157 Date 26-08-2003

[30] "Liquid Oxidisers and Their Use in Hybrid Propellants for Rockets" : Y.Takishita, H.Shibamoto, T.Onda, T.Kuwahara. Jpn Koka Tokkyo Koho (2002). Japanese patent application JP 2002020191

[31] "Manufacture of Hydrazinium Nitroformate for Propellants" : H.Hatano, T.Onda. Japan Kokai Tokkyo Koho (1995) Japanese Patent JP3508205 (2004)

[32] "Physical and Chemical Properties of HNF" : T.Anan, T.Harada. Kayaku Gakkaishi (1995), 56(3), p99-104.

[33] "Characterisation and Thermal Analysis of Hydrazinium Nitroformate (HNF)" : P.S.Dendage, D.B.Sarwade, A.B.Mandale, S.N.Asthana. J.Energetic Materials (2003), 21(3), 167-183.

[34] "Ecofriendly Energetic Oxidiser – Hydrazinium Nitroformate (HNF) and Propellants Based on HNF" : P.S.Dendage, S.N.Asthana, H.Singh. J.Indian Chemical Society (2003), 80(5), p563-568

[35] "Hydrazinium Nitroformate (HNF) and HNF Based Propellants – A Review" : P.S.Dendage, D.B.Sarwade, S.N.Asthana, H.Singh. J.Energetic Materials (2001), 19(1), p41-78

[36] "Modelling Combustion of Hydrazinium Nitroformate" : K.C.Tang, M.Q. Brewster. Proceedings of the Combustion Institute (2002), 29 (Pt2), p2897-2904

[37] "Window Bomb Burning Rates of BTATZ, DAAT and HNF" : A.I.Atwood, D.T.Dui, P.O.Curran, D.A Ciaramitaro, K.B.Lee. 38th JANNAF Combustion Subcommittee Meeting, 2002 CPIA Publication (2002) 712 p119-127.

[38] "Burning Rate of Solid Propellant Ingredients Part 1 – Pressure and Initial Temperature Effects" : A.I.Atwood, T.L.Boggs, P.O.Curran, T.P.Parr, D.M.Hanson-Parr, C.F.Price, J.Wiknich. J.Propulsion and Power (1999), 15(6), p740-747

[39] "Thermal Properties Measurements of Solid Rocket Propellant Oxidisers and Binder Materials as a Function of Temperature" : D.M.Hanson-Parr, T.P.Parr. J.Energetic Materials (1999), 17(1), p1-48.

[40] "DFT Study of the Intermolecular Interaction of Hydrazinium nitroformate Ion Pair" : J.Xue-Hai, J.J Xiao, H.M.Xiao. Gaodeng Xuexiao Huaxue Xuebao (2003), 24(6), p1067-1071

[41] "Hydrazine Nitroform and Method of Preparation" : J.R Lovett. US Patent 3,378,594 (1968)

[42] "Method of Preparing Hydrazine Nitroformate" : F.W.M.Zee, World Patent Reference WO 9410104, 1998

[43] "Improvement of Hydrazinium Nitroformate Product Characteristics" : W.H.M Veltmans, A.E.D.M Van der Heijden, M.J.Rogers, R.M.Greetman. Proceedings of 30th Annual Conference of ICT (1999) p55.

[44] "Achieving Higher Energy" : H.F.R Schoyer. , American Institute Of Aeronautics And Astronautics, Solid Rocket Technical Committee Lecture Series : Reno, Nevada, USA (1994)

[45] "Improved Length – Diameter Ratio of Ammonium Nitroformate Crystals For Use in Solid Propellants" : J.Louwers, A.E.D.M Van Der Heijden. International Patent WO9958498

[46] "Improved Crystallisation of Oxidisers" : F.Wierckx. European Patent EP1033357

[47] " Sonocrystallisation of Hydrazinium Nitroformate to Improve Product Characteristics" : W.H.M. Veltmans, A.E.D.M Van Der Heijden. Industrial Crystallisation (1999)

[48] Personal Communication, 13/10/00 from Willianne Veltman, APP bv, PO Box 697, Bergen-Op-Zoom, Holland. UN Class 1.1D, UN Number 0475, Proper shipping Name, substances, explosive, NOS, packing wooden box UN 4D/Y18-Z27/S/... Max load 4.5 Kg in 6 inner receptacles.

[49] "Package for Solid Propellant-Fuelled Systems Containing Spaced Arrays of Oxidiser Pellets with Binder" : A.J.Cesaroni, M.J.Dennett, J.Louwers. US Patent 2002157557

[50] "PolyNIMMO, a candidate binder for Solid Fuel Gas Generator Propellants" : P.J.Honey, D.W.Anderson : Challenges in Propellants and Combustion : 100 Years After Nobel Edited K.Kuo P706-718. Published 1998 Begell House Inc

[51] "Preliminary Investigation of the Degradation and Stabilisation of the Energetic Oxetane Binder polyNIMMO" : P. Bunyan, A.V.Cunliffe, A.Davis, F.A. Kirby. National Technical Information Service (NTIS) Report Order No: AD-A247718 (1991)

[52] "Synthesis of Energetic Prepolymers" : R.A.Earl, R.D.Carpenter, M.G.Mangum. Hercules Aerospace Ltd, On Behalf of Office of Naval Research, Contract No: N00014-82-C-0431

[53] "Synthesis of Energetic Compounds" : M.B.Frankel, E.R.Wilson, W.O.Woolery. Proc JANNAF Propulsion meeting Chemical Propulsion Information Agency (CPIA) Publication 340 (1981) p 39

[54] "A New Polymerisation Technique for Preparing Low Molecular Weight Polyether Glycols" : G.E.Manser, J.Guimont, D.L.Ross. Proc 1981 Jannaf Propulsion Meeting New Orleans Louisiana May 1981 (CPIA) Publication 340 (1981) P29

[55] "The Development of Energetic Oxetane Polymers" : G.E.Manser. 21st Annual Conference ICT, Karlsruhe, Germany 1990.

[56] "A Study on the Cationic Polymerisation of Energetic Oxetane Derivatives" : Y.G Cheun, J,S. Kim, B.W Jo. 25th International Annual Conference of ICT, Karlsruhe (Germany), 1994, Poster 71

[57] "Characterisation of polyNIMMO and PolyGLYcidyl Nitrate Energetic Binders" : P.Flower, B.Garaty. International Annual Conference of ICT, Karlsruhe (Germany) Volume 25 (1994) p70.

[58] "Insensitive High Explosives and Propellants - The United Kingdom Approach" : A.S.Cumming. American Defense Preparedness Association (ADPA) Symposium on Insensitive Munitions Technology, ADPA Insensitive Munitions Technology Symposium Williamsburg Virginia June 6-9, 1994.

[59] "Characteristics of Novel United Kingdom Energetic Materials" : A.Cumming. International Symposium on Energetic Material Technology : Insensitive Munitions Technology Symposium, Williamsburg 15-18 June 1992 Meeting 277 p69-74

[60] "Energetic Polymers as Binders in Composite Propellants and Explosives" : M.E.Colclough, H.Desai, R.W.Millar, N.C.Paul, M.J.Stewart, P.Golding. Polymers and Advanced Technologies, Vol 5, pp554-560

[61] "Synthetic Routes to Higher Energy" : R.Miller. , American Institute Of Aeronautics And Astronautics, Solid Rocket Technical Committee Lecture Series : Reno, Nevada, USA (1994)

[62] "Possible Ways of Development of Ecologically Safe Solid Rocket Propellants": B.G.Manelis : AIAA/SAE/ASME/ASEE 29th Joint Propulsion Conference and Exhibition 28-30 June 1993 (Monteray)

[63] Nobel Enterprises (ICI) Datasheet for polyNIMMO (1999)

[64] "Mechanical and Swelling Properties of Copolyurethanes Based on Hydroxy-Terminated Polybutadiene and Its Hydrogenated Analog" : V.Sekkar, V.N Krishnamurthy. Propellants, Explosives , Pyrotechnics 22, 289-295 (1997)

[65] "Characterisation of polyNIMMO and PolyGLYCIDYL Nitrate Energetic Binders" : P.Flower, B.Garaty. 25th International Annual Conference of ICT, Karlsruhe (Germany) 1994. Poster P70

[66] "Factors Affecting the Vulnerability of Composite LOVA Gun Propellants" : C.Leach, D.Debenham, J.Kelly, K.Gillespie. ADPA International Symposium on Energetic Materials Technology. Phoenix 1995 p132- 139.

[67] "Plasticisers In Energetic Materials Formulation - A UK Overview" : C.Leach, P.Flower, R.Hollands, S.Flynn, E.Marshall, J.Kendrick. 29th Annual Conference of ICT, Karlsruhe (Germany), 1998 Poster P2.

[68] "Selection of Energetic Polymer Plasticiser Formulations for Next Generation Research" : D.Wagstaff RO Internal Technical Report 202 587 TR 3 E000 (2000)

[69] "Inert and Energetic Prepolymers Co-cured With Isocyanate" : UK Patent 2,296,248 (1994)

[70] "The Thermal Decomposition of Nitrate Esters – Ethyl Nitrate" : J.B.Levy. J.Amer.Chem.Soc (1954) 76, p3254-3257

[71] "The Thermal Decomposition of Nitrate Esters II – The Effect of Additives" : J.B.Levy. J.Amer.Chem.Soc (1954) 76, p3790-3793

[72] "Considerations Concerning the Service Life, Handling and Storage of Double Base Solid Propellant Rocket Motors" : G.I.Evans, S.Gordon. IMI Technical Report 71/12 (1971)

[73] "Primary Processes of the Nitrate Ester Thermal Decomposition" : G.Amer. 9th Symposium on Chemical Problems Connected with Stability of Explosives, Margaretop, Sweden Aug23-27, 1993. P119-156.

[74] "Contribution a l'etude de la thermolyse des esters nitriques" : A.A.Amer. Propellants, Explosives and Pyrotechnics 8, p149-155 (1983)

[75] "An assessment of the Stability of Nitrate Ester Based Propellants Using Heat Flow Calorimetry" : R.G.Jeffrey, M.McParland, M.Elliot. Proceedings of Workshop on the Microcalorimetry of Energetic Materials, Leeds (UK), TTCP Technical Cooperation Program Title: Proceedings Of The Workshop On The Microcalorimetry Of Energetic Materials 7-9th April, Leeds United Kingdom, Pages J1-J12 (1997)

[76] "Role of Diphenylamine as a Stabiliser in Propellants ; Analytical Chemistry of Diphenylamine in Propellants (A Survey Report)" : J.B.Apatoff, G.Norwitz. Technical Report T73-12-1. Frankford Arsenal, Philadelphia. December 1973

[77] "Determining the Shelf Life of Solid Propellants" : F.Volk. Propellants and Explosives 1, p59-65 (1976)

[78] "Prediction of Life Time of Propellants – Improved Kinetic Description of the Stabilizer Consumption" : M.A.Bohn. Propellants, Explosives, Pyrotechnics 19, p266-269 (1994)

[79] "Isomer Distribution of Nitro Derivatives of Diphenylamine in Gun Propellants : Nitrosamine Chemistry" : N.J.Curtis. Propellants, Explosives, Pyrotechnics 15, p222-230 (1990)

[80] "Analysis of 2-Nitrodiphenylamine and its Major Derivatives in Double and Triple Base Propellants" : L.Kansas. Propellants, Explosives, Pyrotechnics 19, p171-173 (1994)

[81] "Kinetic Modelling of the Stabilizer Consumption and of the Consecutive Products of the Stabilizer in a Gun Propellant" : M.A.Bohn, N.Eisenreich. Propellants, Explosives, Pyrotechnics 22, p125-136 (1997)

[82] "Stabilizer Reactions in Cast Double Base Rocket Propellants. Part I : HPLC Determination of Stabilizers and Their Derivatives in e Propellant Containing the Stabiliser Mixture para-Nitro-N-Methylaniline and 2-Nitrodiphenylamine Aged at 80°C and 90°C"– J.M.Bellerby, M.H.Sammour. Propellants, Explosives, Pyrotechnics 16, p235-239 (1991)

[83] "Stabilizer Reactions in Cast Double Base Rocket Propellants. Part II :Formation and Subsequent Reactions of N-Nitroso Derivatives of para-Nitro-methylaniline and 2-Nitrodiphenylamine in Mixed Stabiliser Propellants Aged at 80°C and 90°C"– J.M.Bellerby, M.H.Sammour. Propellants, Explosives, Pyrotechnics 16, p273-278 (1991)

[84] "Stabilizer Reactions in Cast Double Base Rocket Propellants. Part III : Evidence for Stabiliser Interaction During Extraction of Propellant for HPLC Quantitative Analysis – A.J.Bellamy, M.H.Sammour. Propellants, Explosives, Pyrotechnics 18, p46-50 (1993)

[85] "Stabilizer Reactions in Cast Double Base Rocket Propellants. Part IV : A Comparison of Some Potential Secondary Stabilisers for Use with the Primary Stabilizer 2-Nitrodiphenylamine" – M.H.Sammour. Propellants, Explosives, Pyrotechnics 18, p223-229 (1993)

[86] "Stabilizer Reactions in Cast Double Base Rocket Propellants. Part V : Prediction of Propellant Shelf Life – M.H.Sammour. Propellants, Explosives, Pyrotechnics 19, p82-86 (1994)

[87] "Stabilizer Reactions in Cast Double Base Rocket Propellants. Part VI : Reactions of Propellant Stabilizers with the Known Propellant Decomposition Products NO_2, HNO_2 and HNO_3" – M.H.Sammour, A.J.Bellamy. Propellants, Explosives, Pyrotechnics 20, p126-134 (1995)

[88] "Stabilizer Reactions in Cast Double Base Rocket Propellants. Part VII :Effect of Lead Based Ballistic Modifiers on the Reactions of Propellant Stabilisers During Simulated Ageing of Cast Double Base Solid Propellants "– A.J.Bellamy, J.M.Bellerby, M.H.Sammour. Propellants, Explosives, Pyrotechnics 21, p85-89 (1996)

[89] "Stabilizer Reactions in Cast Double Base Rocket Propellants. Part VIII : Characterisation of Propellant Gassing Properties During Simulated Ageing – M.H.Sammour. Propellants, Explosives, Pyrotechnics 21, p276-283 (1996)

[90] "On the Chemical Reactions of Diphenylamine and Its Derivatives with Nitrogen Dioxide at Normal Storage Temperature Conditions" : L.S.Lussier, H.Gagnon. Propellants, Explosives, Pyrotechnics 25, p117-125 (2000)

[91] "Mechanism of the Thermal Degradation of Prepolymeric Poly(3-Nitratomethyl-3-methyloxetane)" : T.J.Kemp, Z.M.Barton, A.V.Cunliffe. Polymer Vol 40 (1998) p65-93.

[92] "Detection and Monitoring of Gases Evolved During Ageing of New Energetic Materials" : K.M.Pearce. Cranfield University, Explosives Ordnance Engineering Thesis, July 1998.

[93] "Hydrazine Nitroform and Method of Preparation" : J.R.Lovett, N.J.Edison. S Patent 3,378,594 (1968)

[94] "The Crystal Structure of Hydrazine Nitroform" : B.Dickens. Chemical Communications 1967, 246-247

[95] "The Crystal Structure of Hydrazinium Trinitromethide" : B.Dickens. J. Research of the National Bureau of Standards Vol 74A, No:3 May 1970 Pg 309-318

[96] "X-Ray Structure of Investigation of Salts of Trinitromethane" : N.V Grigoer'eva, N.V.Margolis . Z.Struk.Kh 7 278-280 (1966)

[97] "The Crystal Structure of Sodium Tricyanomethanide" : P.Anderson, B.Klewe Acta Chem Scand 21, 1530-1542 (1967)

[98] "Thermal Decomposition of Energetic Materials 67. hydrazinium nitroformate (HNF) Rate and Pathways Under Combustion like Conditions" : G.K.Williams, T.B.Brill. Combustion and Flame 102 : p 418-426 (1995).

[99] Suggestion made by D.Wagstaff to J.Louwers during visit to ESTEC 1998 following preliminary HNF analysis 1998.

[100] "Thermal Decomposition of Energetic Materials 58. Chemistry of Ammonium Nitrate and Ammonium Dinitramide Near the Burning Surface Temperature" : T.B.Brill, P.J.Brush, D.G.Patil. Combustion and Flame 92: 178-186 (1993)

[101] "Combustion of hydrazinium nitroformate Based Compositions" : J.Louwers, G.M.H.J.L Gadiot. , American Institute Of Aeronautics And Astronautics, AIAA Paper 98-3385

[102] "GASTEC Precision Gas Detector System" : GASTEC (DETECTAWL), 2/3 Cochran Close, Crownhill, Milton Keynes, Bucks., MK8 0AJ

[103] "Hydrazine and Its Derivatives – Preparation, Properties, Applications Ed. 2" : E.W Schmidt Wiley Interscience (2004)

[104] "Decomposition of Crystalline Hydrazinium Nitroformate (HNF)" : J.M.Bellerby, P.P.Gill. 35th International Annual Conference of ICT, Karlsruhe, 29th June – 2 July 2004. (Poster)

[105] "Analysis of Hydrazinium Nitroformate" : J.M.Bellerby, C.S. Blackman, M.Van Zelst, A.E.D.M van der Heijden. 31st International Annual Conference of ICT, June 2000. P 104

[106] "Ionisation Constants of Aqueous Monoprotic Acids" J.Plambeck, University of Alberta (1995).

[107] "Stabilisation of Nitroform Salts" : J.A.Brown, J.R.Lovett. US Patent 3,378,595 (1968)

[108] V.A Koroban, T.I Smirnova, T.N Bashirova : Mosk, Khim-Teknol.Inst.Im.DI Mendeleeva, 104: 38-44 (1979)

[109] "Thermal Decomposition of Hydrazinium Diperchlorate" : V.R.Pai Vereker, A.N.Sharma. Propellants and Explosives 1, p107-111 (1976)

[110] RO Data relating to preliminary HNF analysis 1997 (Project N7114)

[111] "Properties of Hydrazine Nitroformate : a "New" Oxidiser for High Performance Solid Propellants " : ICT proceedings 25th Annual Conference (1994). A.C.Hordijk, J.M.Mul, J.J.Meulenbrugge, P.A.O.G Korting, P.L,Van Lit, A.J.Schnorhk, H.F.R Schoyer. P69/1

[112] "Hydrazinium Nitroformate Propellant Stabilised with Nitroguanidine" : G.M.Low, V.E.Haury. US Patent 3658608 (Apr 1972)

[113] "Stabilised propellant Compositions Containing Hydrazine Nitroform and Nitrocellulose" : W.H.Jago. US patent 3,307,85 (1967)

[114] "Nitroform-Hydrazine Co-ordination Compounds" : K.O Groves US Patent 3,140,317 (1964)

[115] "Stabilisation of Nitroform Salts" : J.A.Brown, US Patent 3,384,675 (1968)

[116] "Propellant Comprising Hydrazine Nitroform Stabilised with Dicarboxylic Acid Anhydride" : H.E.Rice US Patent 3,418,183 (1968)

[117] Personal Communication with Eric Marshall, Nobel Enterprises, Ardeer Site, Stevenson, Scotland

[118] "Basic Principles of Organic Chemistry" : John Roberts, Marjorie Cassario (1977) Second Edition

[119] "Overview of the Development of Hydrazinium Nitroformate Based Propellants" – H.F.R Schoyer. W.H.M Welland-Veltmans, J.Louwers, P.A.O.G.Korting, A.E.D.M Van Der Heijden. H.L.J.Keizers, R.P Van Der Berg. J.Propulsion and Power (2002), 18(1) p138-145

[120] "Ageing Behaviour of Propellant Investigated by Heat Generation, Stabiliser Consumption and Molar Mass Degradation" – M. A Bohn, F.Volk. Propellants, Explosives, Pyrotechnics (1992) 17(4), p171-8

[121] "Stability Analyses of Double Base Propellants Containing New Stabilisers. Part II" – J.Petrzilek, S.Wilker, U.Ticmanis, G.Pantel, L.Scottmeister, J.Skladel. International Conference of ICT (2001) 32nd Ed, Karlsruhe (Germany), p 12/1-12/17

[122] "Modelling of the Stability, Ageing and Thermal Decomposition of Energetic Components and Formulations Using Mass Loss and Heat Generation" : M.A Bohn. Proceedings of the International Pyrotechnics Seminar (2000), 27th Ed p751-770.

[123] "Thermal Ageing of Rocket Propellant Formulations Containing HNIW Investigated by Heat Generation Rate and Mass Loss" : M.A.Bohn. Thermochimica Acta Vol 401 Iss 1 May 2003 p27-41

[124] "The Chemistry of Hydrazine" : Audrieth and Ackerson 1951, Wiley Interscience

[125] Merck Chemical Catalogue 2001. Available from Merck Chemicals Limited, Merck House, Poole, Dorset

[126] "GASTEC Precision Gas Detector System-Handbook" : GASTEC (DETECTAWL), 2/3 Cochran Close, Crownhill, Milton Keynes, Bucks., MK8 0AJ

[127] "Hydrazoic Acid Controls and Risks When Processing Plutonium Solutions in HB-Line Phase II" – D.F.Hallman. Document WSRC-TR-2000-00443, NTIS or electronically at http://www.osti.gov/bridge/ (Accessed Sept 2004)

[128] Unpublished Observations - Internal ROXEL Document 201932-TR/3/E000 : M.Adams, D.Wagstaff

[129] "Effect of Intentional Impurities, Ageing, Particle Size and Pre-Irradiation on the Thermal Decomposition of Hydrazinium Diperchlorate" : V.R.Pai Verneker, A.N.Sharma. Propellants and Explosives, 2, p45-48 (1977)

[130] CRC Handbook of Chemistry and Physics – Student Edition 72nd Edition Lide (1992).

[131] "Reactions of Nitrate Esters II Reactions with Hydrazine" – R.T.Merror, R.W. Van Dolah. J.Am.Chem.Soc (1954) 76 p4522-5

[132] "Accelerated Ageing of Plateau Burn Composite Propellant" : Y.Oyumi, E.Kimura, K.Nagayama. Propellants, Explosives, Pyrotechnics 22, 263-268 (1997)

[133] "Is There a Critical Composition of Reaction Products of Diphenylamine Stabilised Nitrocellulose Propellants During Ageing ?" : R.Ammann. Proceedings of Symposium on Chemical Problems Connected with the Stability of Explosives 1976, 4 p9-27

[134] "Is Hydrazoic Acid (HN3) an Intermediate in the Destruction of Hydrazine by Excess Nitrous Acid ?" – A.M.M.Doherty, K.R.Howes, G.Stedman, M.Q.Naji. J.Chem.Soc. Dalton Transactions (1995) p3103 – 3107

[135] "Chemistry and Technology of Explosives – Vol 3" - T.Urbanski (1985) p 245-251 (Pergamon Press)

[136] "Modern Inorganic Chemistry" – G.F. Liptrot 3rd Ed 1981 (Bell and Hyman)

[137] "Oxidation of N-NO-Diphenylamine" : T.Lindblom, L.E.Paulsson, L.G.Svensson. Proceedings of Symposium on Chemical Problems Connected with the Stability of Explosives, Margretetorp, 1993, p157-159